Development and Application of a Regioselective Nickel-Catalyzed Macrocyclization Method; and Development of Bench Stable Sugar Silanes for Use in Copper-Catalyzed Dehydrogenative Silylations

by

Allison Rose Knauff

A dissertation submitted in partial fulfillment
of the requirements for the degree of
Doctor of Philosophy
(Chemistry)
in the University of Michigan
2013

Doctoral Committee:

Professor John Montgomery, Chair
Assistant Professor Anne Jennifer McNeil
Professor David H. Sherman
Professor John P. Wolfe

Dedication

To my parents. Without your love and support, I would not be where I am today.

Acknowledgements

First and foremost, I would like to thank Professor John Montgomery for the opportunity to complete my Ph.D. studies in his group. His knowledge and guidance have helped me to develop into the scientist that I am today. I am also incredibly appreciative of his support in my exploration of opportunities both within and outside of the chemistry department to develop as a teacher. I would also like to thank Prof. Brian Coppola for working with me on a chemical education project that is not covered in this thesis.

I also want to acknowledge all of the students and postdocs I have had the opportunity to work with in the Montgomery lab. I am particularly thankful for the mentorship that Dr. Ryan Baxter and Dr. Zachary Buchan provided as peers throughout my graduate career. Solymar Negretti-Emmanuelli, Aireal Jenkins, and Dr. Katie Partridge also supplied much appreciated camaraderie in lab. Taylor Haynes and Zach Miller were always there for coffee breaks. Working with Dale Lee has introduced me to new challenges and has been incredibly rewarding.

Outside of the Montgomery group, I am grateful to have made many friends who have supported me over the past five years. Thank you so much to Crystal Young, Jenna Welby, Aireal Jenkins (again), Sharon Neufeldt, Joey Braymer, Noah Gardner, Kevin Hartman, Tom Slaney, Eric Majchrzak, Ted Boron, Yuta Suzuki, and Nick Babij. Without your friendships, this time would have been much more strenuous than it already was.

Finally, I need to thank my family for being there for me always. Holidays and gatherings with the Knauff clan and Bartos family are always something I look forward to, and their support is deeply cherished. I love you Mom, Dad, and Erin.

Table of Contents

List of Figures

List of Schemes

List of Tables

List of Abbreviations

Ac	acetyl
Ar	aryl
Bn	benzyl
n-Bu	butyl
t-Bu	*tert*-butyl
°C	temperature in degrees centigrade
cod	1,5-cyclooctadiene
*m*CPBA	*meta*-chloroperoxybenzoic acid
Cy	cyclohexyl
DCC	dicyclohexylcarbodiimide
DDQ	2,3-dichloro-5,6-dicyano-1,4-benzoquinone
DHP	dihydropyran
DMAP	4-dimethylaminopyridine
DMF	*N*,*N*-dimethyl formamide
DMP	Dess Martin periodinane
DMSO	dimethyl sulfoxide
DP-IPr	(rac)-(4*S*,5*S*)-1,3-bis(2,6-diisopropylphenyl)-4,5-diphenylimidazolidin-2-ylidene
dr	diastereomeric ratio
DTBMP	2,6-di-*tert*-butyl-4-methylpyridine
Et	ethyl
equiv.	equivalent
GCMS	gas chromatography mass spectrometry

h	hour(s)
n-Hex	hexyl
IMes	1,3-bis-(1,3,5-trimethylphenyl)imidazol-2-ylidene
IPr	1,3-bis-(2,6-diisopropylphenyl)imidazol-2-ylidene
K_d	dissociation constant
LCMS	liquid chromatography mass spectrometry
LRMS	low resolution mass spectrometry
Me	methyl
Ms	methanesulfonyl (mesyl)
NHC	*N*-heterocyclic carbene
NHK	Nozaki-Hiyama-Kishi
NIS	*N*-iodosuccinimide
PCC	pyridinium chlorochromate
Pd/C	palladium on carbon
PG	protecting group
Ph	phenyl
i-Pr	isopropyl
i-Pr-BAC	2,3-bis(diisopropylamino)cycloprop-2-en-1-ylium
pyr	pyridine
rac	racemic
RCM	ring-closing metathesis
RSM	recovered starting material
rs	regioselectivity

RT	room temperature
SIPr	1,3-bis(2,6-diisopropylphenyl)-imidazolidin-2-ylidene
TBAF	tetrabutylammonium fluoride
TBDPS	tert-butyldiphenylsilyl
TBS	tert-butyldimethylsilyl
Tf	trifluoromethanesulfonate
TMS	trimethylsilyl
THF	tetrahydrofuran
THP	tetrahydropyran
TLC	thin layer chromatography
Ts	*para*-toluenesulfonyl (tosyl)

Abstract

Many pharmaceuticals are derivatives of natural products or are the natural products themselves. Investigating the biosynthesis of natural products and their bioactivity modes of action can lead to the formulation of proposals for new chemical structures that are more potent drugs. Synthesis of these compounds is accomplished through the use of chemical methods, biochemical methods, or a combination thereof. Several different methodological advances have been made in synthetic and biosynthetic areas related to the synthesis of macrolide natural products.

The P450 monooxygenase PikC is utilized in a chemoenzymatic fashion to hydroxylate unnatural substrates. This enzyme is found to be promiscuous in nature, oxidizing two differently sized rings to macrolide natural products. Exploiting this promiscuity, the sugar desosamine was appended to a number of simple aglycones for use as a remote directing group, or anchoring group. Several of these unnatural substrates were oxidized to mono-hydroxylated products by PikC, particularly those substrates containing macrocycles. Through LCMS comparison of the enzymatic products with authentic samples, it was determined that the C-H bonds furthest from the anchoring group were selectively oxidized.

A synthetic macrocyclization technique that allows the synthesis of two different sized rings from the same starting material was also explored. This methodology utilitizes nickel-catalyzed reductive couplings that have previously been shown to switch the regioselectivity of alkyne

addition to an aldehyde by switching the ligand on the metal center. Through application in the synthesis of the macrolide methymycin, both the natural product and its smaller-ringed derivative were formed. Here, the regioselectivities previously only observed in intermolecular reductive couplings or biased intramolecular systems were generalized in the intramolecular nickel-catalyzed reductive coupling of terminal alkynes and aldehydes to yield either the endo or exocyclic product from one substrate.

Finally, a simple procedure that uses bench stable starting materials for the synthesis of tethered carbohydrate-aglycone molecules that are used in intramolecular glycosylation is introduced. The identity of a sugar moiety can play an important role in the biosynthesis of natural products and their modes of action; thus, methodologies to produce glycosides easily and stereospecifically are attractive. Diisopropyl sugar silanes have been shown to be competent substrates in the copper-catalyzed O-H insertion into a variety of alcohol substrates. These user friendly reagents are stable to chromatography and storage, representing an improvement over previously used dimethyl sugar silanes, which decompose readily under standard storage conditions. The products formed have also been shown to participate in the desired intramolecular glycosylation reaction.

Chapter 1

Introduction

Natural products formed in plants, animals, fungi, and bacteria can possess a range of biological activity in humans from beneficial to toxic.[1] Through traditional plant-based medicine and later isolation and derivatization, natural products have been used for many thousands of years to treat diseases and ailments, including infections, nausea, and cancer.[2,3] Studying how these molecules are synthesized in nature and how they function can lead to insights that further drive the development of more potent drugs.

One class of natural products that is of particular pharmaceutical interest is those containing macrocycles.[4–8] Macrocyclic natural products cover a broad range of molecules that display biological functions including antibiotic, antiviral, antifungal, immunosuppressant, and anticancer, among others. Many of these compounds have been used clinically, and many are still in use today. The two main sub-classes are cyclic polypeptides (also known as depsipeptides and non-ribosomal peptides) and macrolides, which typically contain a macrolactone and at least one sugar molecule.

Of particular interest to us are the macrolide natural products, which are synthesized in nature via three stages: polyketide synthesis, glycosylation, and oxidative tailoring.[9] The first stage is catalyzed by enormous polyketide synthases (PKS), which are composed of individual multi-enzyme modules.[10] Each type I PKS module is responsible for the addition of one 2 or 3 carbon unit, derived from the corresponding acyl group attached to coenzyme A via a thioester

linkage. Three enzymes are found in each module because they are required to lengthen the polyketide chain: a ketosynthase, acyltransferase, and acyl carrier protein. Reductive enzymes are often also present within a module and are responsible for the reduction of the ketone to an alcohol, dehydrogenation, or reduction of the enol tautomer of the ketone. Following completion of the linear polyketide chain, a thioesterase catalyzes cyclization to produce the aglycone natural product precursor. The PKS of erythromycin A to produce the aglycone 6-deoxyerythronolide B is shown as an example (Figure 1.1). The biosyntheses of non-ribosomal peptides has also been greatly explored,[11] and will not be discussed here as it does not relate to this thesis.

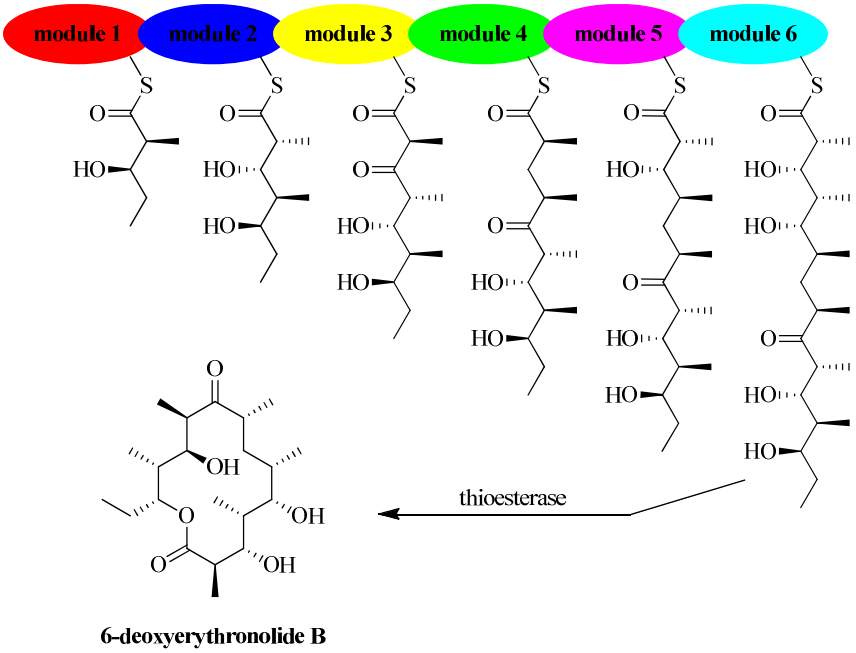

Figure 1.1. PKS of the aglycone of erythromycin A.

The wealth of knowledge gained from the studies into polyketide synthases has led to the development of chemoenzymatic synthesis, where enzymes or multienzyme modules are excised from the PKS and used individually or replaced with other enzymes in order to biosynthesize new molecules.[12] By feeding unnatural substrates to an enzyme, information can be gained

about any substrate specificity these enzymes possess toward their endogenous substrates and preferred conformations within the active site can be assessed by the stereochemical outcome of any new products formed. As more data is collected regarding the function of each individual enzyme, it may be possible to mix and match enzymes with known functions to synthesize new macrocyclic molecules.

Following polyketide synthesis, the next step in the biosynthesis of macrolides is the glycosylation with one or more sugar molecules. These sugars are often important for the bioactivity of these molecules, which have been shown to lose a significant amount, if not all, activity when the sugars are removed.[13] They can also play a role in binding to the enzymes responsible for the oxidative tailoring steps to produce the final product (see section 2.1.2). Similar to work done with PKS, the glycosyltransferase enzymes responsible for glycosylation have been studied in relation to toleration of unnatural glycosyl donors and acceptors.[14,15]

The final biosynthetic step in macrolide synthesis involves oxidative tailoring through stereo- and regioselective hydroxylation and/or epoxidation performed by cytochrome P450 monooxygenases. These enzymes use molecular oxygen, coupled with a redox partner, to oxidize the heme iron center, which in turn oxidizes the substrate. Bioengineering of P450s has led to enzymes that accept exogenous substrates and are self-sufficient (i.e. require no external redox partner).[16–18]

Also of note is the mode of action that these natural products demonstrate in their biological activity. Members of the same family of natural products can have different modes of action that lead to the same end result.[19] For example, while most macrolides inhibit bacterial growth activity through binding near the protein exit tunnel and prevention of peptide chain elongation,[20] the smaller methymycin binds in the peptidyl transferase center, inhibiting bacterial growth

through interference with tRNA and forcing the rearrangement of RNA nucleotides into unproductive orientations.[21]

Small changes in the structure of a natural product can also significantly enhance the biological activity. A common example is the natural product erythromycin and second generation synthetic analogue azithromycin (Figure 1.2). By changing from a 14- to a 15-membered ring and replacing a ketone with an amino group, increased bioavailability and decreased adverse side reactions are achieved. Both of these molecules are used clinically today.

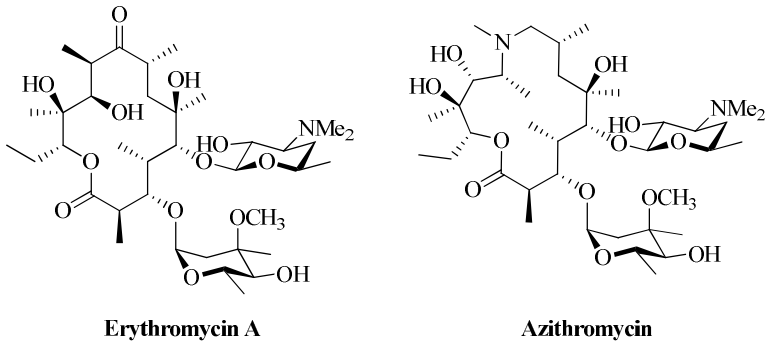

Figure 1.2. Structures of natural product erythromycin A and derivative azithromycin.

Alternatively to chemoenzymatic synthesis, synthetic chemists often try to mimic the powerful biochemistry found in nature with small molecule catalysis. For example, the selective oxidation of a C-H bond, similar to the selective oxidative function of P450s, is a common problem pursued by synthetic chemists (see section 2.1.1 for a detailed discussion). This transformation is commonly achieved by employing metal catalysts, with the ligands used classified as heme-like or non-heme-like types.

In this thesis, several topics inspired by biosynthetic pathways are examined. The chemoenzymatic use of the P450 monooxygenase PikC to hydroxylate unnatural substrates is discussed in chapter 2. This methodology exploits the natural function of the sugar desosamine to form an ionic bond in the active site of the enzyme by attaching it to exogenous aglycones,

which are then evaluated for oxidation by PikC. The use of a functional group tethered to compounds which are not otherwise oxidized by the enzyme is termed an anchoring group.

In chapter 3, a non-enzymatic macrocyclization technique that allows the synthesis of two different sized rings from the same starting material is explored. The generalization of regioselectivities previously only observed in intermolecular reductive couplings is investigated in intramolecular reactions. Through the employment of two sterically different ligands, either endo or exocyclic macrocycles can be obtained in this reaction.

Finally, a simple procedure that uses bench stable starting materials for the synthesis of tethered carbohydrate-aglycones that are used in intramolecular glycosylation is introduced in chapter 4. Dimethyl sugar silanes that behave as reducing agents in hydrosilylation and dehydrogenative silylation reactions are moisture sensitive and require special handling techniques to keep them from decomposing under standard storage conditions. Bulkier diisopropyl sugar silanes are presented as more stable alternatives that readily undergo copper-catalyzed dehydrogenative silylations with a variety of alcohols. The products formed are also shown to participate in the desired intramolecular glycosylation reaction.

Chapter 2

Selective C-H Mono-Oxidation of Unnatural Substrates by an Engineered P450

2.1 Introduction

Macrolides are macrocyclic lactones that contain at least one deoxysugar residue and often have interesting biological activity, such as antibiotic or antifungal activity.[9] These compounds were initially identified as natural products displaying antibiotic activity and are mostly produced by bacteria in the Actinomycete family. They have been in clinical use for more than 50 years and typically contain 12-, 14-, or 16-membered rings. The biosyntheses of many of these macrolides have been carefully studied and are rather well understood. As discussed in chapter 1, the biosynthesis is divided into three distinct steps: polyketide synthesis, sugar synthesis and glycosylation, and oxidative modification steps to produce the final product.

This biosynthesis is exemplified by the biosynthetic pathways to produce the two macrolides methymycin and pikromycin (Figure 2.1).[22] For these two natural products, the four multi-enzyme complexes PikAI, PikAII, PikAIII, and PikAIV are responsible for polyketide synthesis and cyclization to produce 10-deoxymethonolide and narbonolide. These aglycones are glycosylated with the sugar desosamine by the enzymes DesVII and DesVIII,[23,24] and a single

hydroxylation by PikC gives the final products. This final mono-hydroxylation occurs both stereo- and regioselectively (see section 2.1.2 for more detail on this mechanism).

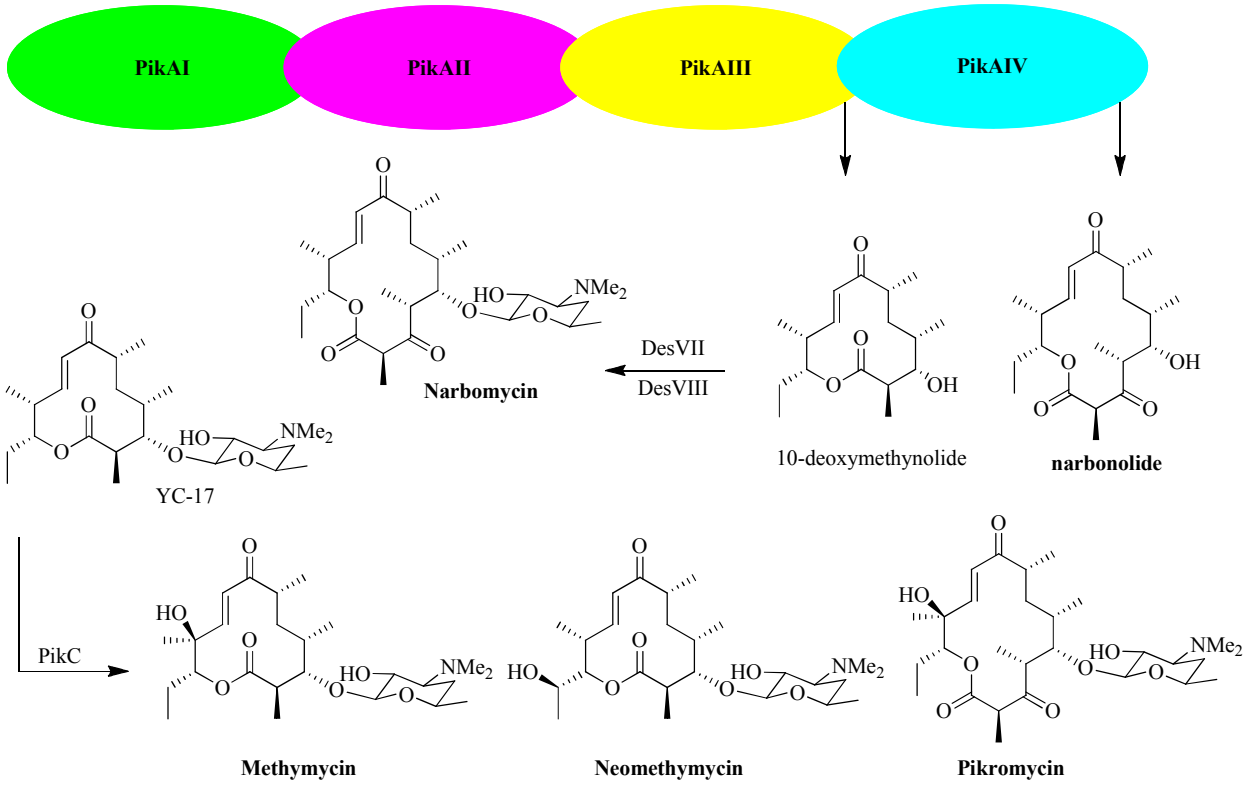

Figure 2.1. Biosynthetic pathways to produce methymycin and pikromycin.

2.1.1 Selective C-H Oxidation Methods by Small Inorganic Complexes

These final C-H oxidation steps in macrolide biosynthesis exemplify a reaction that has been the envy of synthetic chemists.[25,26] The selective oxidation of both sp^2- and sp^3-hybridized C-H bonds is a recently exploding field. One particular challenge is the selective oxidation of less-substituted sp^3-hybridized C-H bonds, as overoxidation and stereochemistry of the product become a concern. Therefore, selectivity is often induced through the use of nearby directing groups or steric and electronic effects.[27]

One of the earliest examples of metal-catalyzed C-H oxidation shows the selectivity of bulky porphyrins bound to manganese or iron for oxidation of *n*-alkanes to primary alcohols over

secondary alcohols.[28] More recently, Sanford and co-workers have developed the use of nitrogen-containing moieties as directing groups for the oxidation of unactivated sp^3-hybridized C-H bonds (Scheme 2.1). The directing groups function by acting as ligands on palladium, positioning the metal center to oxidatively insert into the proximal C-H bond (Scheme 2.1A).[29,30] Reductive elimination affords the acetoxylated product. Further development showed that use of an acetylated oxime as directing group was also facile, resulting in products that could easily be deprotected and hydrolyzed to yield β-hydroxyketones (Scheme 2.1B).[31] Finally, it was shown that the stoichiometric iodosobenzene diacetate oxidant could be replaced with catalytic sodium nitrate in the presence of air or oxygen.[32]

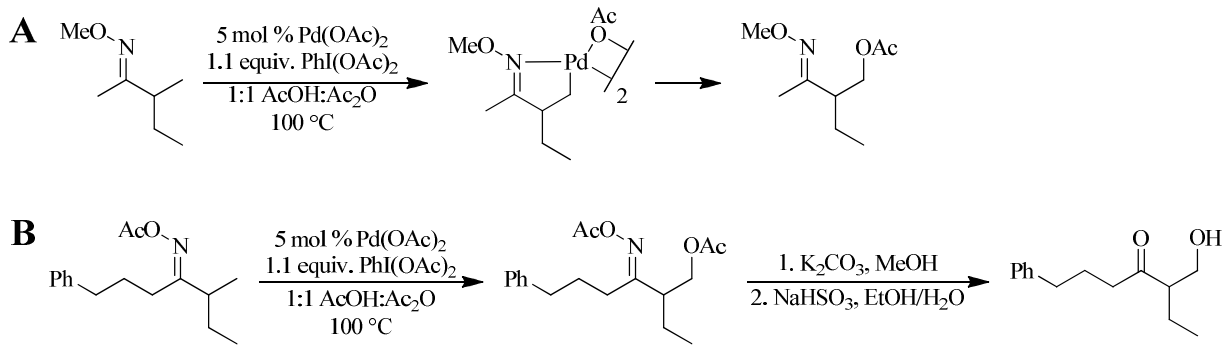

Scheme 2.1. Use of a nitrogen atom directing group to achieve regioselective oxidation of sp^3-hybridized C-H bonds.

The White group has shown that the most electron-rich C-H bond of a molecule is selectively oxidized by an iron (II) catalyst, even in a complex setting such as the natural product artimisinen, where there are multiple potential sites of oxidation with only small electronic biases (Scheme 2.2A).[33] The original protocol required recycling recovered starting material three times to increase the yields to be synthetically useful, but a slow addition procedure was later developed to provide the product in comparable yield.[34] The same catalyst is also capable of the oxidation of methylene groups with "intermediate" reactivity (Scheme 2.2B).[35] This latter case

points out an important limitation to the chemistry, which is that under these conditions methylene groups are doubly oxidized and stopping at the alcohol is not possible. By replacing exogenous acetic acid with a carboxylic acid, directing group activation as described above can be achieved with this catalyst system.[36]

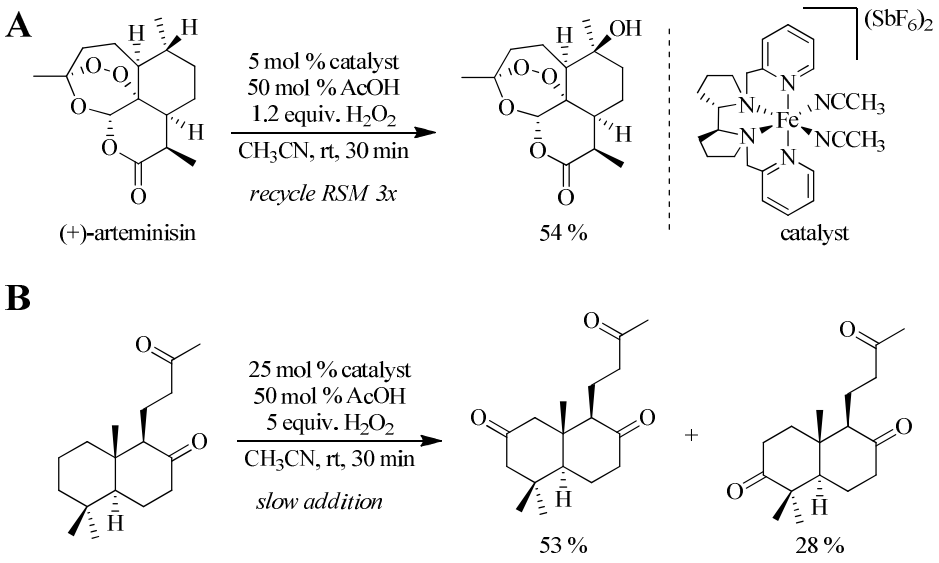

Scheme 2.2. Selective oxidation using an iron catalyst of (A) the most electron-rich tertiary C-H bond of arteminisin and (B) an "intermediate" electron-rich methylene group.

Selective oxidation of a methylene group to a ketone can also be achieved with a manganese catalyst system developed by Crabtree and coworkers. This system uses molecular recognition to direct the oxidation of carboxylic acid-containing substrates (Scheme 2.3).[37,38] A specially designed ligand containing a "U-turn motif" and carboxylic acid is able to hydrogen bond to the carboxylic acid of ibuprofen, positioning one part of the molecule toward the manganese oxide center.

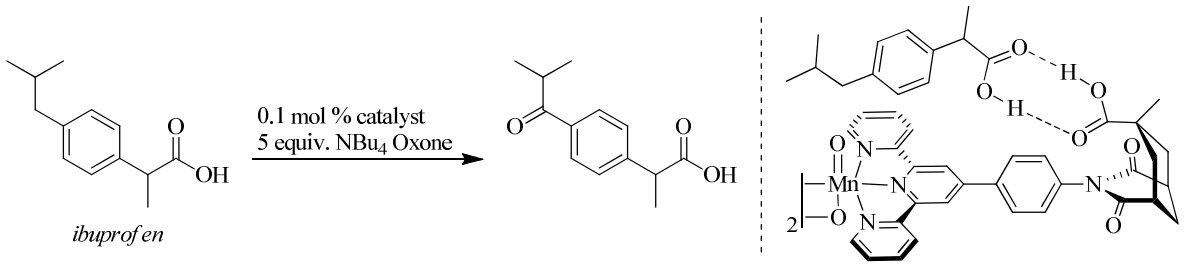

Scheme 2.3. Use of hydrogen bonding between carboxylic acids on the substrate and the ligand as molecular recognition to induce regioselective oxidation.

Other examples of C-H oxidation include utilizing stoichiometric or catalytic Cr (VI) oxidants,[39] a catalytic oxaziridine with hydrogen peroxide as the stoichiometric oxidant,[40] or a manganese system where the substrate is tethered to the ligand and later hydrolyzed.[41]

2.1.2 The Enzyme PikC

The cytochrome P450 monooxygenase PikC is responsible for the hydroxylation step in the synthesis of two differently sized macrolides (Scheme 2.4).[22] The compound YC-17, a 12-membered macrolide, is mono-oxidized by PikC to regioisomeric products methymycin and neomethymycin in a 1:1 ratio.[42] A 14-membered compound, narbomycin, is oxidized primarily to pikromycin. PikC also oxidizes narbomycin to neopikromycin, albeit in a much lower yield.

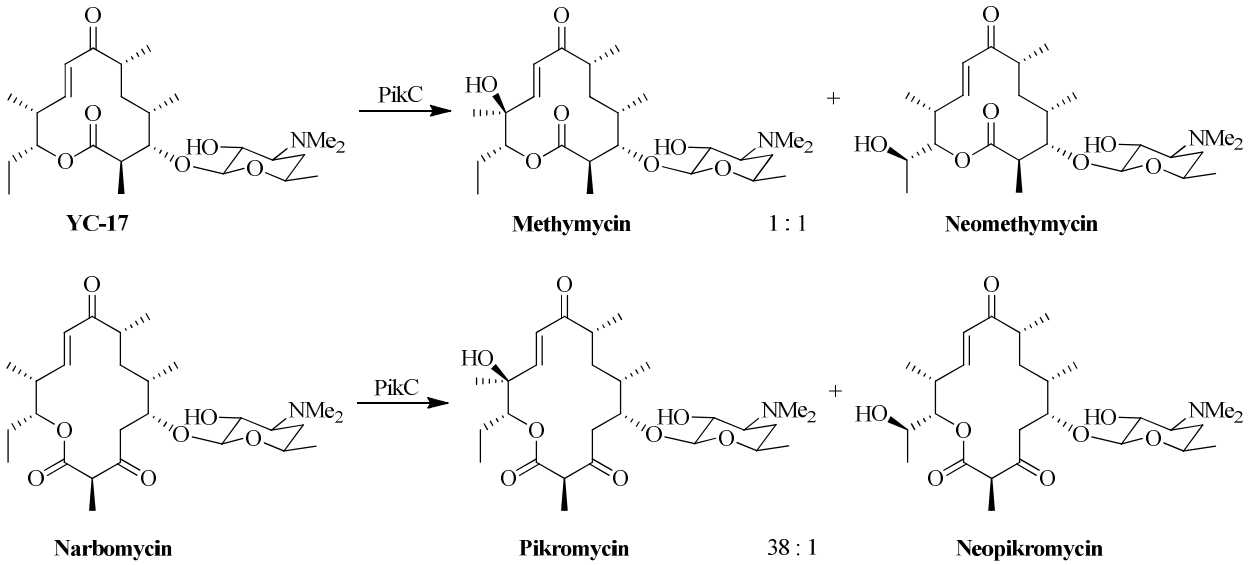

Scheme 2.4. Regioselective oxidation of YC-17 and narbomycin by PikC.

Co-crystal structures of YC-17 or narbomycin bound to the active site of PikC both show that a salt bridge is formed between the protonated dimethylamino group of the desosaminyl sugar residue and the nearby deprotonated carboxylate residues of the protein (Figure 2.2).[42] However, the interaction of the aglycone and the enzyme within the binding pocket is mainly comprised of hydrophobic interactions, and no ionic or hydrogen bonds are observed. These non-specific interactions may account for the ability of the protein to accept substrates of different sizes, as well as allow substrate flexibility within the binding pocket, which explains the formation of multiple products from a single substrate.

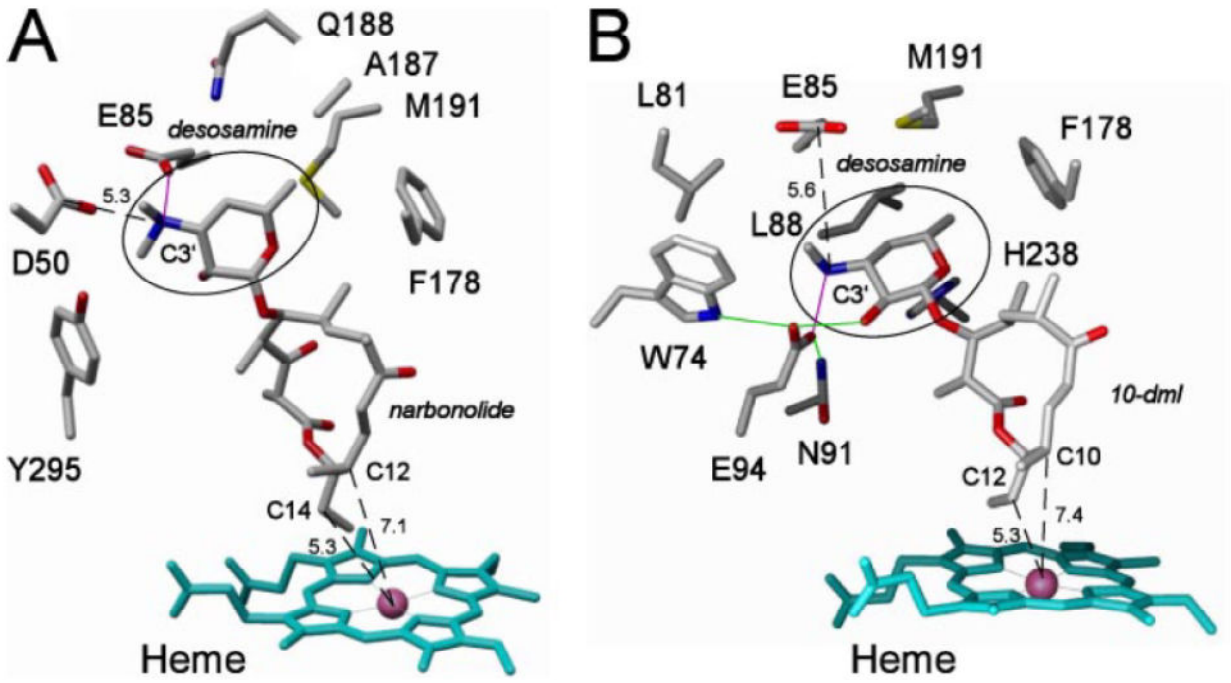

Figure 2.2. Co-crystal structures of (A) narbomycin and (B) YC-17 bound within the active site of PikC.[42] The labeled desosamine moiety forms a salt bridge between its protonated dimethylamino group and the deprotonated carboxylate moieties of the nearby amino acid residues.

The regioselectivity of oxidation can be rationalized through a combination of electronic and proximity effects. The tertiary allylic positions (C12 for narbomycin and C10 for YC-17) are located slightly further from the heme center than the less activated ethyl side chains (C14 for narbomycin and C12 for YC-17) for both molecules. The conformation of the ethyl group near the active site provides better alignment for methylene oxidation in the YC-17 substrate versus the narbomycin substrate, resulting in the more regioselective oxidation to pikromycin compared to the oxidation of YC-17 to equivalent amounts of methymycin and neomethymycin.

2.1.3 Development of a More Efficient PikC Derivative

Studies in the Sherman lab have shown that significant rate enhancement for oxidation of both YC-17 and narbomycin occurs with the mutation of an aspartate to an asparagine residue at

the 50-position located within the active site of PikC.[42] While this was not understood at the time, further studies suggested that substrate binding to the enzyme is a two-step process, where the desosaminyl dimethylamino group first interacts with the surface-exposed D50, where it can then be shuttled to the buried pocket to bind with E85 (YC-17) or E94 (narbomycin).[43] Replacement of the aspartate with the non-ionic asparagine allows single-step binding to the buried pocket, increasing the efficiency of this mutant compared with the wild-type enzyme.

In order to re-oxidize the iron heme center to start the catalytic cycle, an exogenous oxidant or redox partner is often used, such as spinach ferredoxin reductase/ferredoxin. However, a new biosynthetic P450 was discovered which contains a covalently linked reductase domain known as RhFRED. A fusion protein to covalently link this reductase to PikC was synthesized.[44] This chimeric protein shows similar binding affinity to wt-PikC for the endogenous PikC substrates YC-17 and narbomycin, as would be expected since the PikC domain is unchanged. However, the rate of the oxidation reaction is enhanced approximately four-fold, presumably due to the involvement of a covalently linked redox partner in place of undergoing an intermolecular redox reaction. This engineered PikC derivative is more efficient and cheaper to use, as it does not require the use of an expensive exogenous redox partner. The enzyme used for the experiments described below was the $PikC_{D50N}$-RhFRED fusion protein.

2.2 Synthesis of Unnatural Substrates and their Interactions with PikC

This project examined the use of the sugar unit desosamine as a remote directing group (termed anchoring group) for the oxidation of C-H bonds without the use of molecular bias near the oxidation site.[45] By attaching desosamine to simple molecules and feeding these molecules to the PikC mutant enzyme, the C-H bonds closest to the iron heme center (and therefore furthest from desosamine, see section 2.1.2) are expected to be selectively oxidized.

2.2.1 Unnatural Substrates Oxidized by PikC

With this in mind, several different alcohols were glycosylated with desosamine fluoride (harvested and prepared from erythromycin) and subjected to the $PikC_{D50N}$-RhFRED enzyme (Figure 2.3). Biochemical experiments were conducted by Dr. Shengying Li in Prof. David Sherman's group. The reaction extract was analyzed by LCMS to determine both the extent of substrate conversion and the number of mono-oxidized products produced from each substrate ().

Not surprisingly, macrocylic aliphatic substrates **1**, **2**, **3**, and **4** were oxidized by the enzyme, albeit multiple products were formed in each case. Unexpectedly, linear substrates **8** and **9** were also oxidized, although the conversion was not as high as for the macrocyclic compounds. Pyrene derivative **10** was only oxidized in a 4 % yield, but a single peak was observed in the LCMS trace. Smaller rings (**5** and **6**) and several other substrates (linear derivative **7** and steroid derivative **11**) were not oxidized. The analysis of product formation was performed using single ion monitoring so that only molecules with the mass of the mono-oxidized product produced signals. Products resulting from multiple oxidations on the same molecule were not observed. The binding affinity of each substrate to PikC was also evaluated to provide more information regarding the conversion of the reactions (Table 2.1). A general trend was observed that the lower the dissociation constant (K_d), the higher the yield of the reaction, as would be expected.

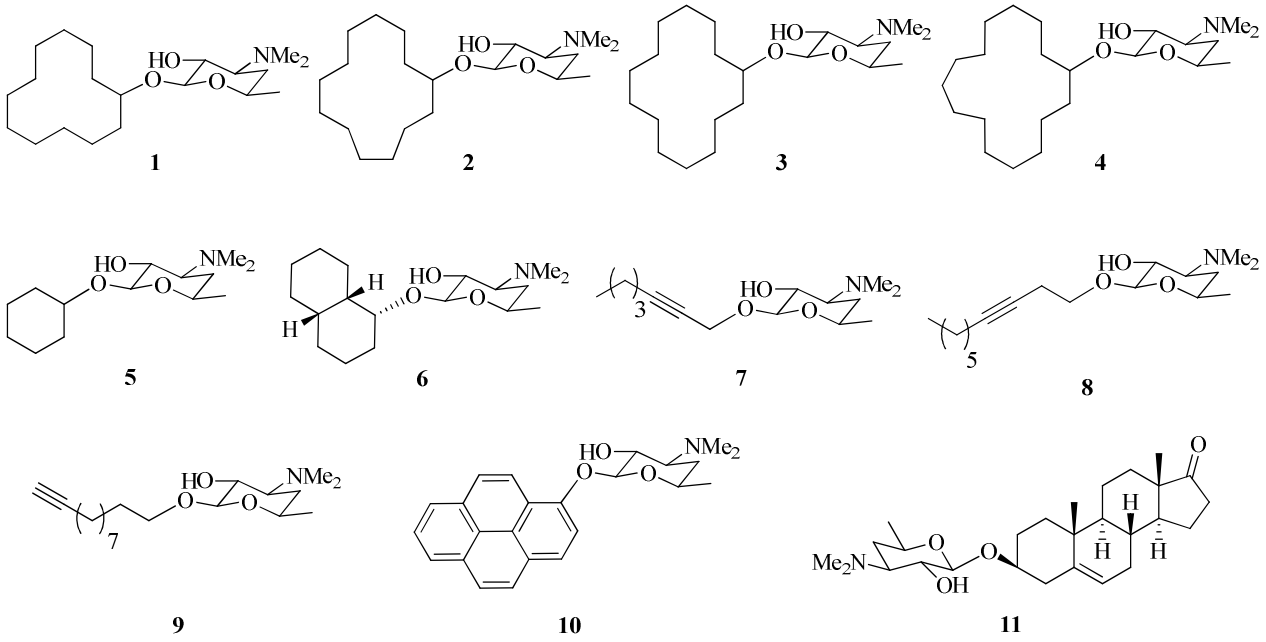

Figure 2.3. Different glycosides subjected to P450 oxidation conditions. In collaboration with Dr. Mani Chaulagain.

Table 2.1. Dissociation constant of binding to PikC, percent conversion, and number of product peaks for each substrate. In collaboration with Dr. Shengying Li.

Compound	K_d (μM)	Conversion (%)	Number of Peaks in LCMS Trace
Methymycin	19	>99	2
1	309	47	7
2	218	65	6
3	289	63	6
4	243	35	9
5	NB*	0	0
6	NB*	0	0
7	NB*	0	0
8	2900	8	5
9	2300	14	7
10	>5000	4	1
11	NB*	<1	0

*NB, no binding

2.2.2 Co-Crystal Structures of Some Unnatural Substrates Bound to PikC

To provide further evidence that desosamine would position the methylene groups furthest from the glycosidic bond toward the heme center, co-crystal structures of the 12-, 13-, and 14-membered carbolides **1**, **2**, and **3** bound to PikC were attempted. Both **1** and **2** gave good crystal structures, while **3** did not give a solvable crystal structure. As was the case with YC-17 and narbomycin,[42] two different PikC chains crystallized with the substrates, represented as Chain A and Chain B (Figure 2.4). This gives two different orientations of the substrates in the PikC active site for each molecule; furthermore, 12-membered substrate **1** showed two different conformations in Chain B.

For the 12-membered ring, the two Chain B conformers both position carbons 6, 7, and 8 closest to the heme iron center, while the Chain A conformation positions carbons 5, 6 and 7 near the iron atom (Figure 2.4, A and B). Throughout this chapter, diastereotopic carbons are numbered differently for ease in analysis and discussion. For the 13-membered ring, the carbons at positions 6, 7, and 8 are also closest to the heme iron center site for oxidation (Figure 2.4, C and D). The two different conformations for the two different chains of the protein show opposite faces of the macrocycle being pointed toward the heme center, indicating that oxidation of both C-H bonds of the methylene groups at these positions is possible. The reason for this non-specificity appears to be the dynamic interactions of the substrates with PikC within the active site (Figure 2.5). There is enough room for flexibility of the substrates, and the salt bridge contact of desosamine is not consistent. In comparison, the more rigid endogenous substrates narbomycin and YC-17 both display only one conformation in each PikC chain. It is also important to note that there are fewer conformations found for the larger 13-membered ring **2**

than for the smaller 12-membered ring **1**, indicating that **2** has less conformational freedom within the active site.

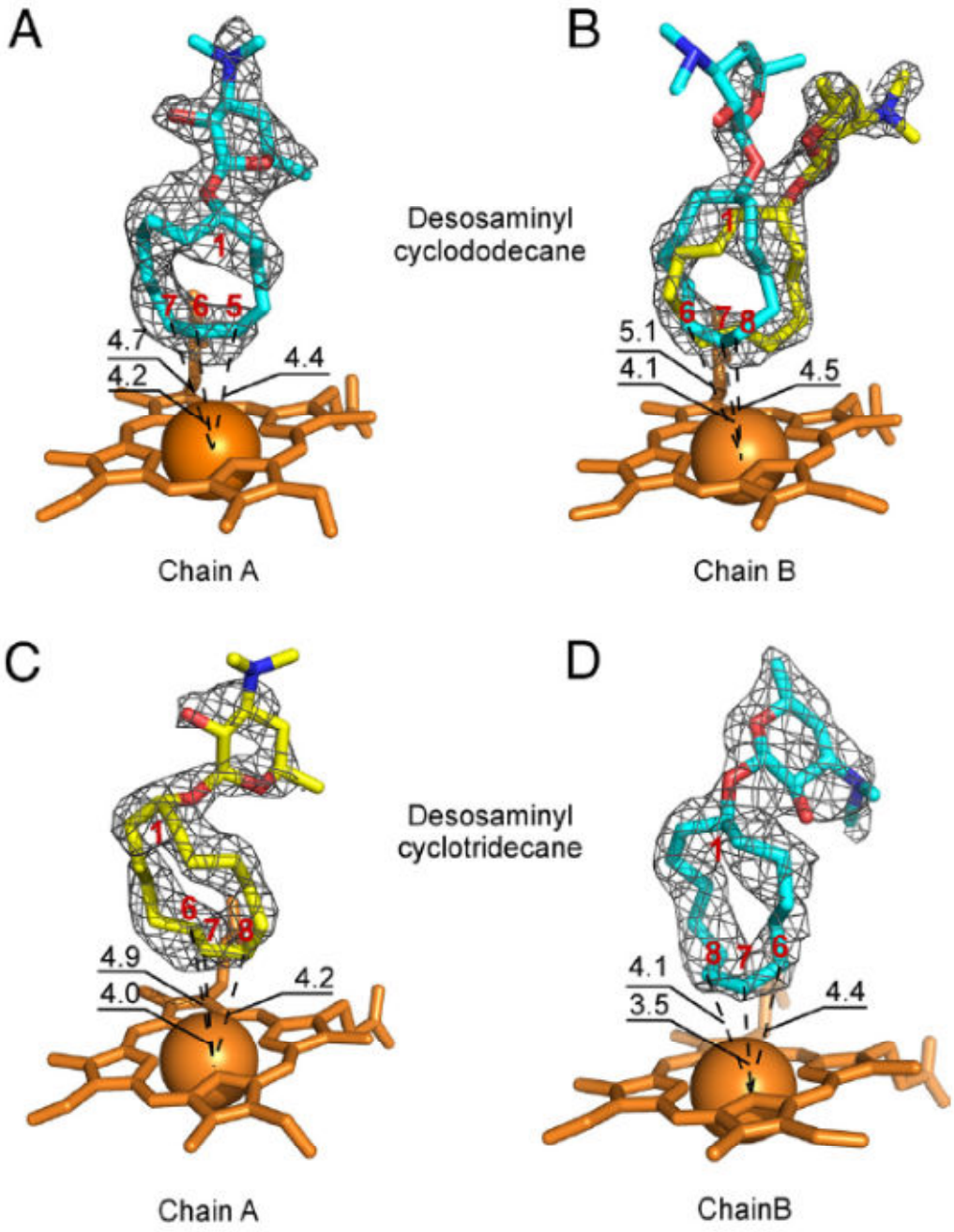

Figure 2.4. Co-crystal structures of different chains of PikC with (A and B) 12-membered macrolide substrate **1**, and (C and D), 13-membered macrolide substrate **2**. In collaboration with Dr. Larissa Podust.

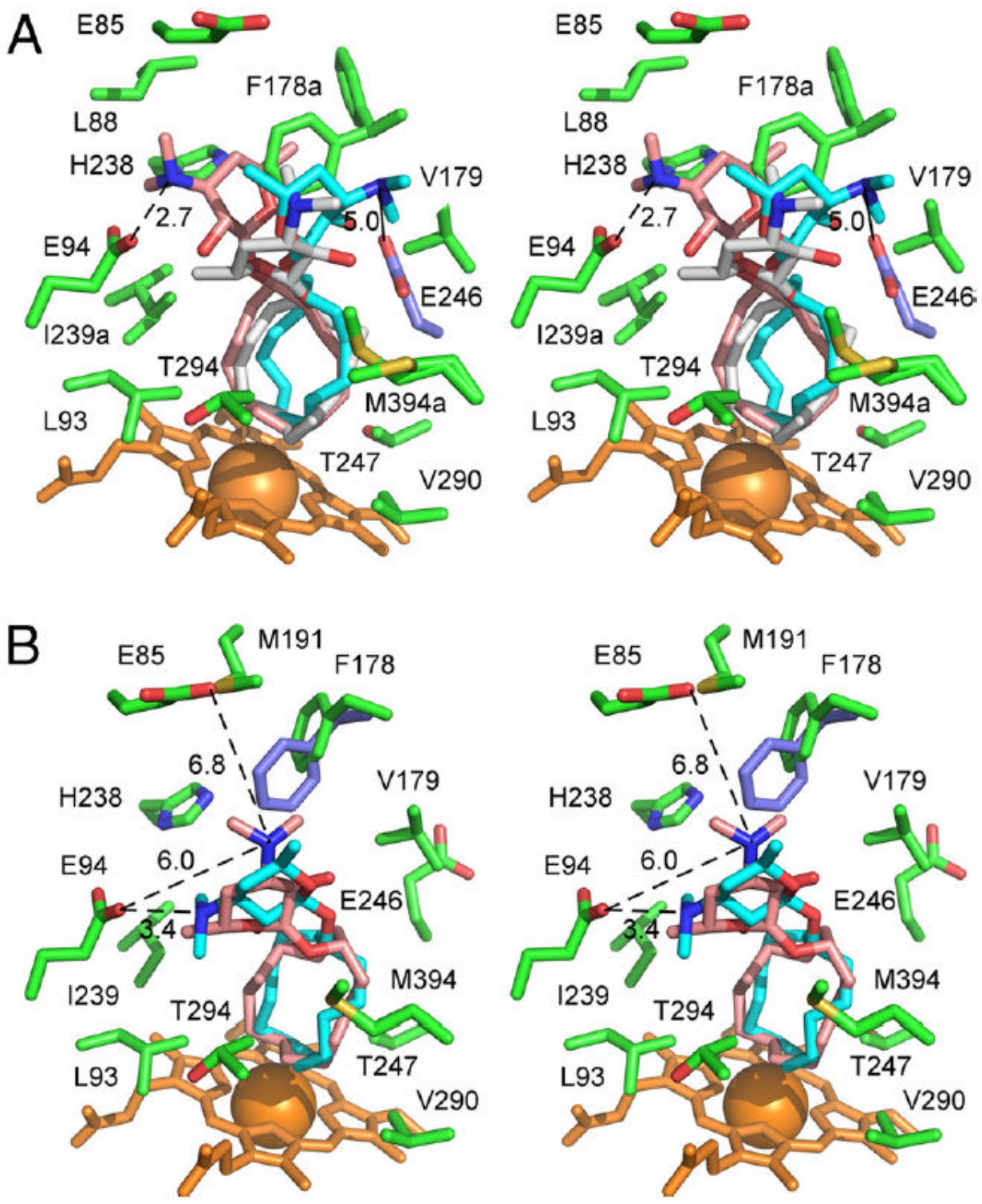

Figure 2.5. Overlays of the several lowest energy conformations within the active site of PikC for (A) 12-membered macrolide substrate **1**, and (B) 13-membered macrolide substrate **2**. In collaboration with Dr. Larissa Podust.

2.3 Synthesis and Comparison of Authentic Standards with Enzymatic Products

Because the likely hydroxylated compounds are structurally very similar to one another, analysis and differentiation by standard analytical techniques is very difficult. Therefore, it was decided that the proposed hydroxylated products would be independently synthesized for comparison with the products from the enzymatic reaction.

2.3.1 Synthesis of Authentic Hydroxylated Standards for the 12-Membered Ring

Authentic standards of the proposed hydroxylated products for 12-membered ring substrate **1** were first synthesized. Based on the co-crystal structure shown in section 2.2.2 (Figure 2.4, Figure 2.5), positions 6, 7, and 8 on the ring are closest to the heme center in the active site of the enzyme, and therefore most likely to be oxidized. These compounds were synthesized as sets of two diastereomers, shown in Figure 2.6.

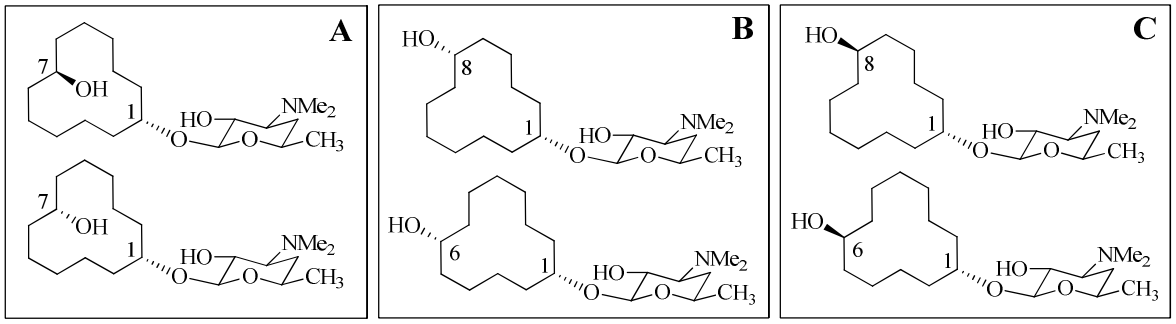

Figure 2.6. Authentic samples from the 12-membered ring series, synthesized as sets of diasteromers: (A) *cis*- and *trans*-C7-hydroxylated products; (B) *cis*-C6 and C8-hydroxylated products; and (C) *trans*-C6 and C8-hydroxylated products. In collaboration with Dr. Mani Chaulagain.

2.3.2 Synthesis of Authentic Hydroxylated Standards for the 13-Membered Ring

Based on the crystal structure of the 13-membered ring bound to PikC and the LCMS trace indicating four major hydroxylated products from the enzymatic reaction, the four possible

diastereomers that would result from oxidation at the C7 and C8 positions were first synthesized (Figure 2.7). As before, these diastereomers were synthesized as sets of two.

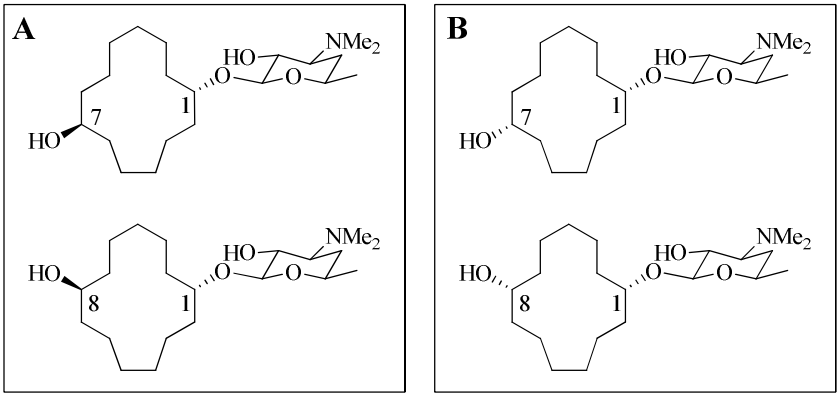

Figure 2.7. Authentic hydroxylated samples from the 13-membered ring series, synthesized as sets of diastereomers: (A) *trans*-C7 and C8-hydroxylated standards; and (B) *cis*-C7 and C8-hydroxylated standards.

Synthesis of the C7/C8 sets of diastereomers began with the Grignard reaction of silyl ether **12** and silyl protected alkyne **13** to generate the 13-carbon chain **14**, which contains the requisite alcohol in the correct position (Scheme 2.5). Protection of the secondary alcohol with an acetate group and subsequent deprotection of the silyl groups, followed by oxidation of the resulting primary alcohol, provided ynal **15**, the macrocyclization precursor. Cyclization using Ni-IMes as the active catalyst and Et_3SiH as the reducing agent gave the *endo* product exclusively in 46 % yield and 1:1 diastereoselectivity of *cis*:*trans* isomers (with respect to the silyloxy and acetoxy substituents, not the alkene, which is formed exclusively as the *trans* isomer). The two isomers were separated at this point, and each was carried on individually for the remaining synthetic transformations. Removal of the silane and hydrogenation of the alkene gave the aglycone **16**, which was glycosylated with desosamine fluoride. At this point, each set of *cis* and *trans* isomers existed as a set of two diastereomers from the glycosylation of each enantiomer with the chiral sugar moiety. Global acetate deprotection gave the final authentic standards **17**, each as a set of two products (Figure 2.7).

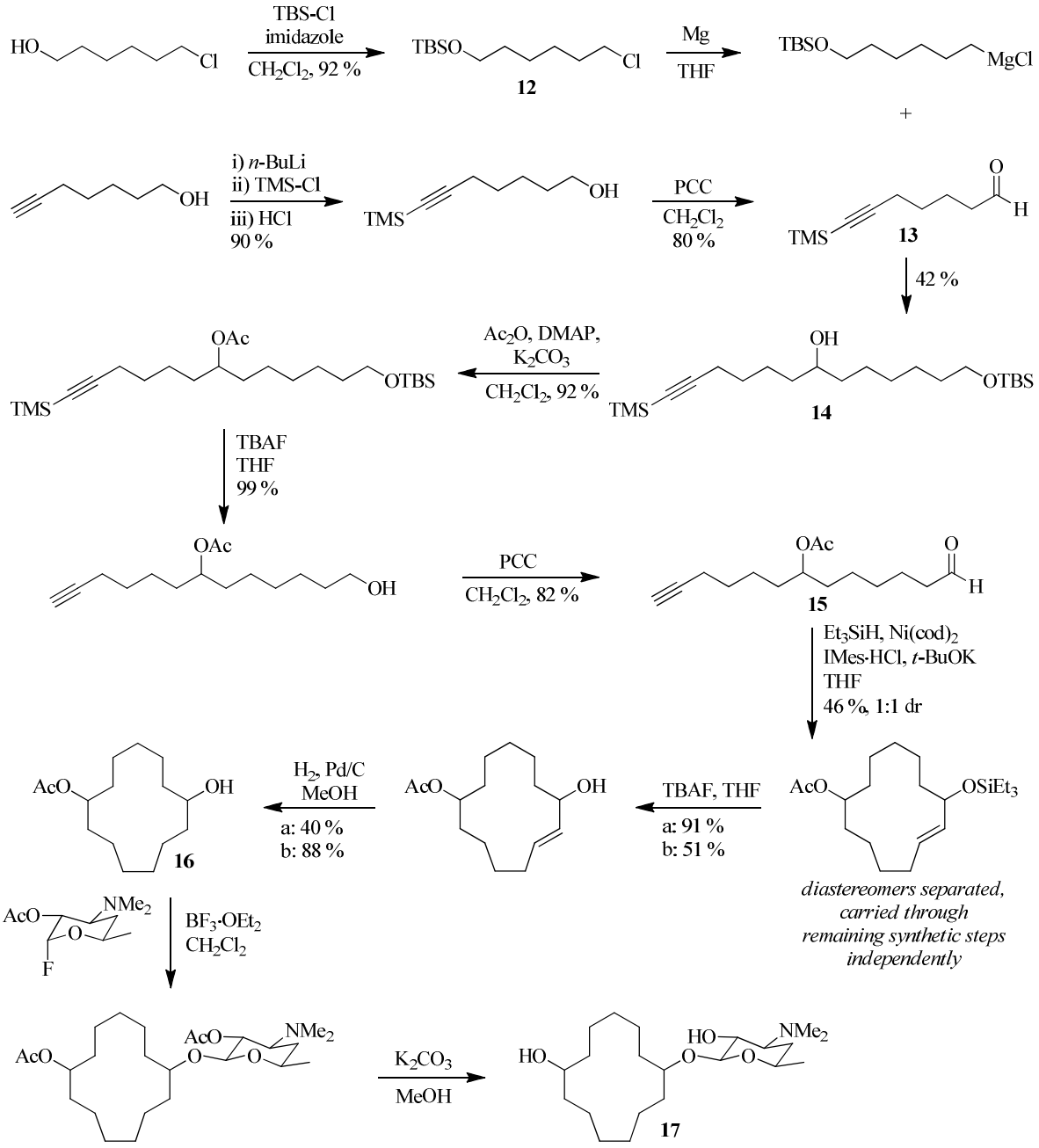

Scheme 2.5. Synthesis of the C7/C8 authentic hydroxylated samples. A total of four compounds were synthesized, as shown in Figure 2.7. Letters *a* and *b* correspond to the separated diastereomers.

Because the C7/C8 authentic hydroxylated standards did not account for all of the major products in the enzymatic reaction (see section 2.3.4), the C6/C9 hydroxylated compounds were also synthesized (Figure 2.8). A similar strategy was followed to synthesize the C6 and C9

authentic hydroxylated standards (Scheme 2.6). In this case, the 8-carbon bromo-alcohol **18** and 5-carbon ynol **19** were used to introduce the alcohol in the correct position in the end product. Protected alkynol **20** was be oxidized via the Parikh-Doering method since the resulting aldehyde **21** has a relatively low boiling point and was not isolable under standard PCC workup conditions. Standard protecting group manipulations and oxidation led to macrocyclization precursor **22**, which, upon Ni-catalyzed macrocyclization, led to the desired product **23** in a 24 % yield and 2.5:1 diastereomeric ratio. Presumably, the closer relationship of the acetate group to the forming alkene led to this change in diastereoselectivity from what was observed in the synthesis of the C7/C8 series. The two diastereomers were separated at this point and each was carried on through the remaining synthetic steps individually. Silane deprotection and olefin hydrogenation led to compounds **24**, which were each glycosylated with desosamine fluoride under Lewis-acid mediated conditions. Acetate deprotection gave the desired products **25**, which were synthesized as two sets of two products each, as shown in Figure 2.8.

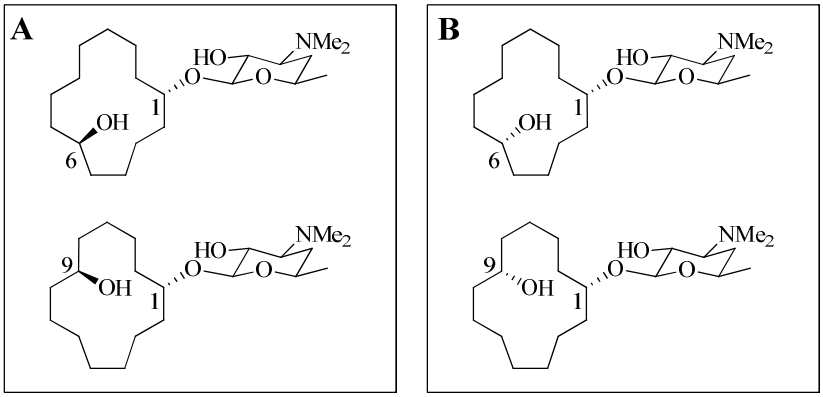

Figure 2.8. Authentic hydroxylated samples from the 13-membered ring series, synthesized as sets of diastereomers: (A) *trans*-C6 and C9-hydroxylated standards; and (B) *cis*-C6 and C9-hydroxylated standards.

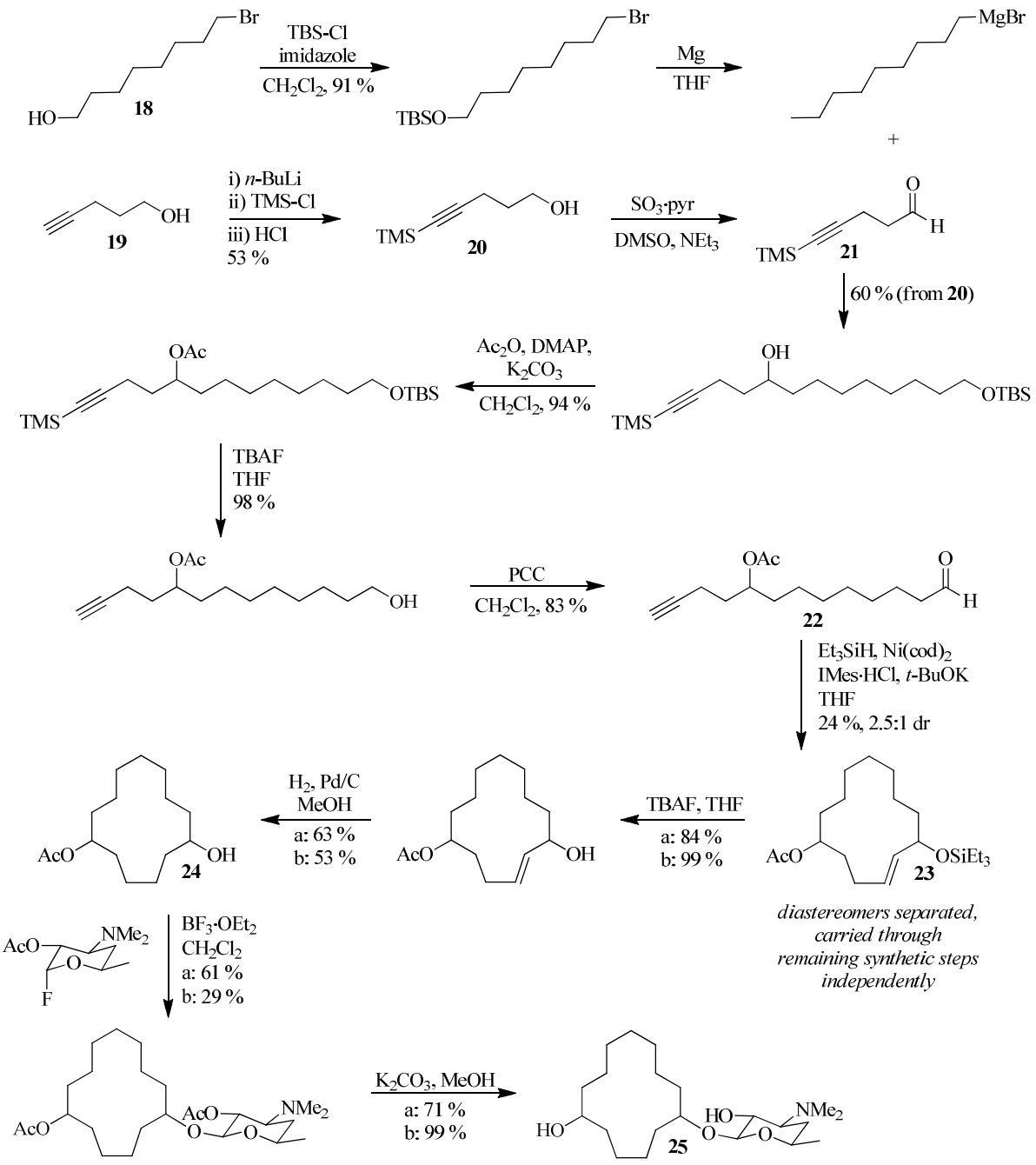

Scheme 2.6. Synthesis of the C6/C9 authentic hydroxylated standards. Four compounds were synthesized, as shown in Figure 2.8. Letters *a* and *b* correspond to the separated diastereomers.

2.3.3 Synthesis of Authentic Propargyl Alcohol Standard

Although the aliphatic macrocyclic substrates were oxidized in the highest yields by PikC, we noticed that linear substrate **9** produced one major product when submitted to enzymatic

oxidation (Figure 2.9). Because PikC oxidation favors C-H bonds that are both close to the heme center and electronically activated, we hypothesized that the propargylic position was the most likely to have been oxidized. Therefore, authentic standard **26** was synthesized for comparison with the enzymatic products (Scheme 2.7).

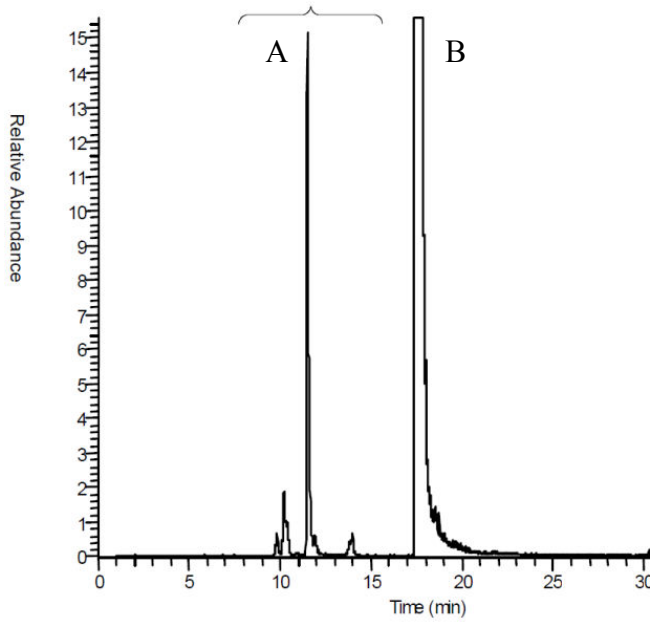

Figure 2.9. Enzymatic mono-oxidized products from the reaction of **9** (peak B). There is one major product (peak A).

Mono-protected diol **27** was obtained and subjected to oxidation. PCC oxidation proved to be too harsh, leading to silyl deprotection and bis-oxidation of the resulting diol (equivalent to a double oxidation of diol **28**). Therefore, Dess-Martin periodinane was used as a milder reagent. Acetylide addition to the resulting aldehyde gave product **29**, which was acetylated and deprotected with TBAF to give aglycone **30**. Glycosylation and global acetate deprotection led to the desired product **26**.

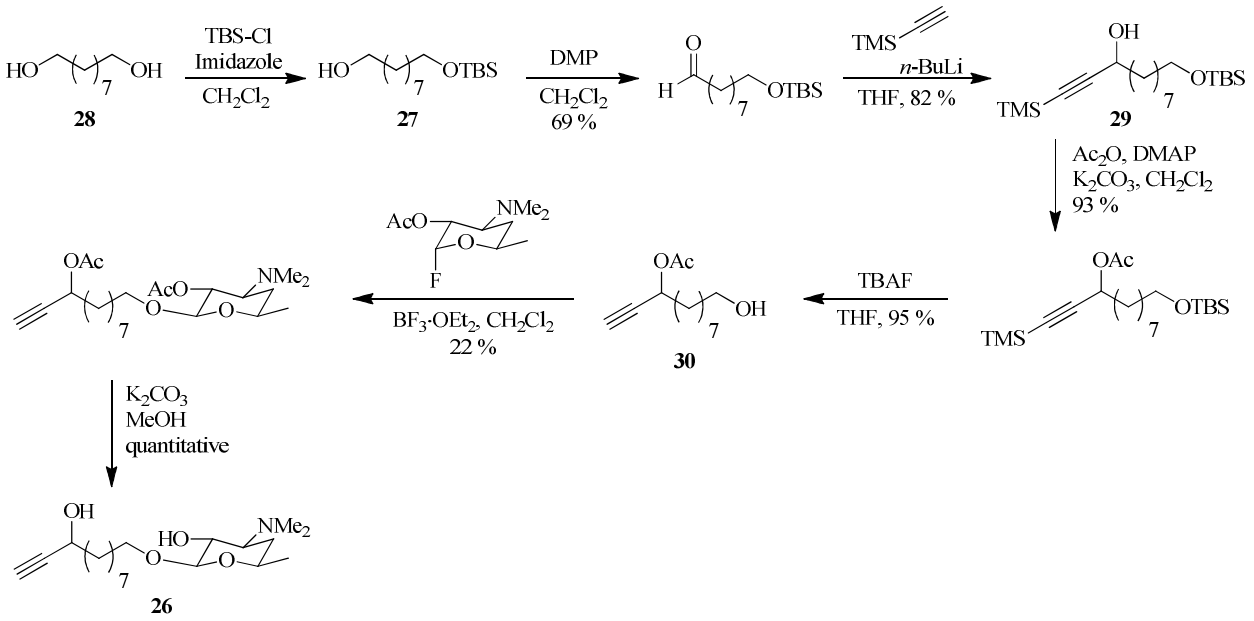

Scheme 2.7. Synthesis of authentic propargyl alcohol standard.

2.3.4 Comparison of Enzymatic Products with Authentic Standards

The authentic standards for 12-membered ring **1** were first compared to the hydroxylated products from the enzymatic reaction via LCMS analysis (Figure 2.10). The two sets of two C6/C8 diastereomers (traces B and C) correspond to four of the five major products (peaks a, c, e, and g) from the enzymatic reaction, while the set of C7 diastereomers (trace D) corresponds to one of the five major products (peak f) and one of the minor products (peak b). The smallest product peak (d) from the enzymatic reaction does not correspond to oxidation at C6, C7, or C8, but C5 is also positioned near the active site of the enzyme in one of the three conformations of substrate **1** bound to PikC (Figure 2.4). It is therefore postulated that a minor amount of oxidation at this position accounts for the final product in the enzymatic oxidation reaction.

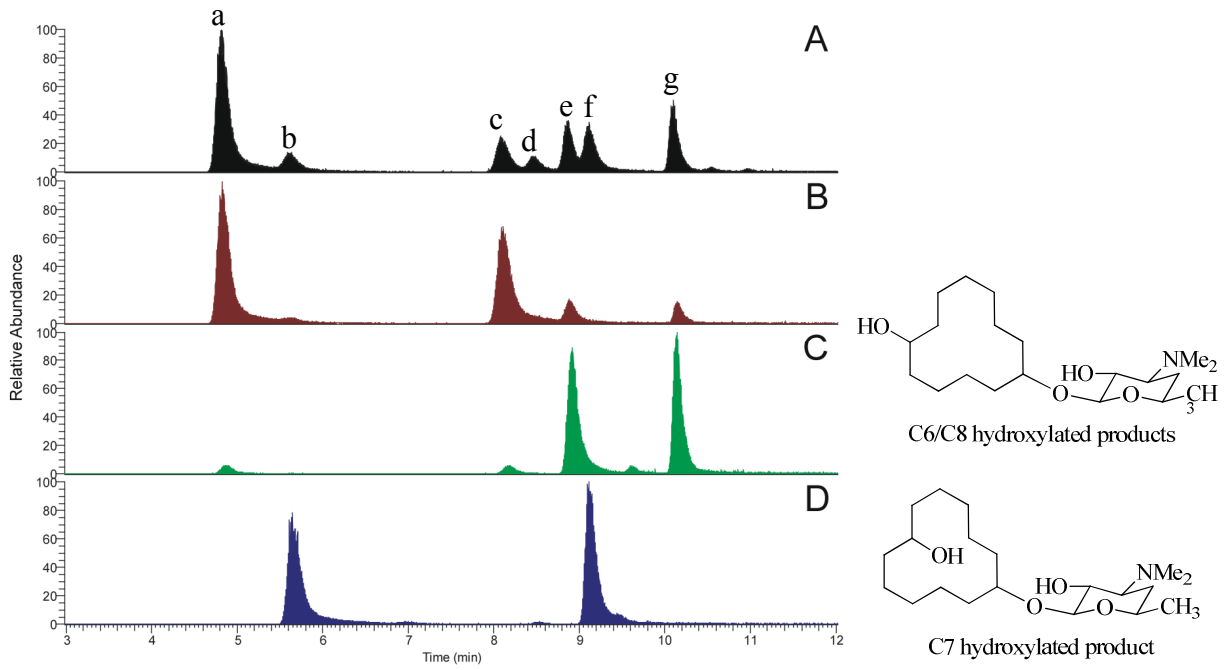

Figure 2.10. LCMS traces of (A) all products from the PikC-catalyzed oxidation of **1**, (B) diastereomers A of C6/C8 hydroxylated sample (C) diastereomers B of C6/C8 hydroxylated sample, and (D) authentic C7 hydroxylated sample. In collaboration with Dr. Mani Chaulagain and Dr. Shengying Li.

A similar analysis to that described above was performed for 13-membered substrate **2** (Figure 2.11). The enzymatic reaction produced four major peaks (a-d) with two very minor products (e-f). Because of the proximity of C7 and C8 to the heme center (Figure 2.4), it was hypothesized that the four major products formed in the enzymatic reaction are the four diastereomers corresponding to the oxidation of each of the four C-H bonds present in these two methylenes. However, synthesis of the authentic samples corresponding to these four products and analysis by LCMS showed that the two sets of diastereomers co-elute (traces D and E). Attempts to separate the four products through method modification were unsuccessful. Because the four C7 and C8 hydroxylated compounds did not account for the four major products formed in the enzymatic reaction, the two sets of diastereomers corresponding to oxidation at C6 and C9 were also synthesized. These compounds correspond to peaks a, d, and f from the enzymatic reaction, although it is important to note that one of the diastereomers also overlaps with peak c.

Because some of the resolved diastereomers correspond to smaller peaks in the enzymatic trace (e.g. peak f and trace C), it seems likely that diastereoselectivity is imparted in the active site, although this cannot be confirmed due to the poor LCMS resolution of the different oxidized isomers. Peak e most likely arises from a very minor amount of oxidation at C5 or C9.

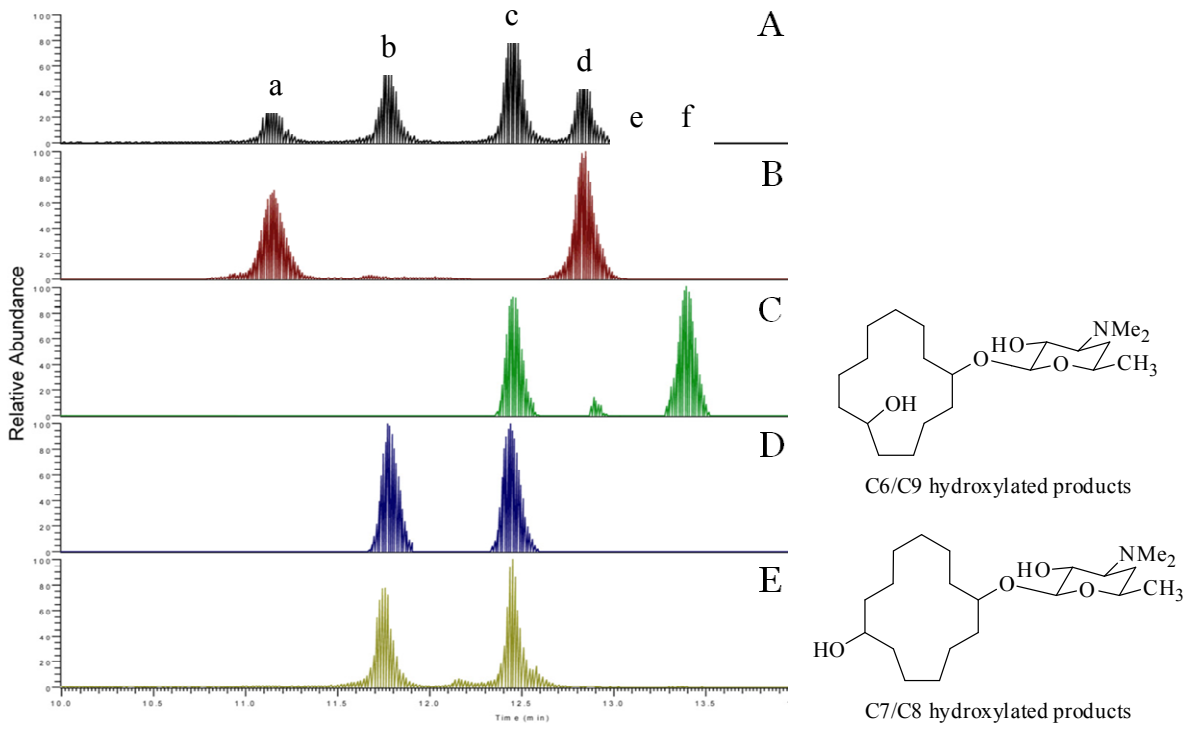

Figure 2.11. LCMS traces of (A) all products from the PikC-catalyzed oxidation of **2**, (B) major diastereomers of C6/C9 hydroxylated standards, (C) minor diastereomers of C6/C9 hydroxylated standards, (D) diastereomers A of C7/C8 hydroxylated standards, and (E) diastereomers B of C7/C8 hydroxylated standards. In collaboration with Dr. Shengying Li.

The propargylic position of linear substrate **9** is most likely to be oxidized by PikC because it is electronically activated and likely to be positioned near the heme iron center (away from desosamine) within the active site of the enzyme. Therefore, the two propargylic alcohol diastereomers were synthesized and compared with the enzymatic products (Figure 2.12). The two diastereomers co-eluted, but this peak corresponded to the major enzymatic product, confirming our hypothesis.

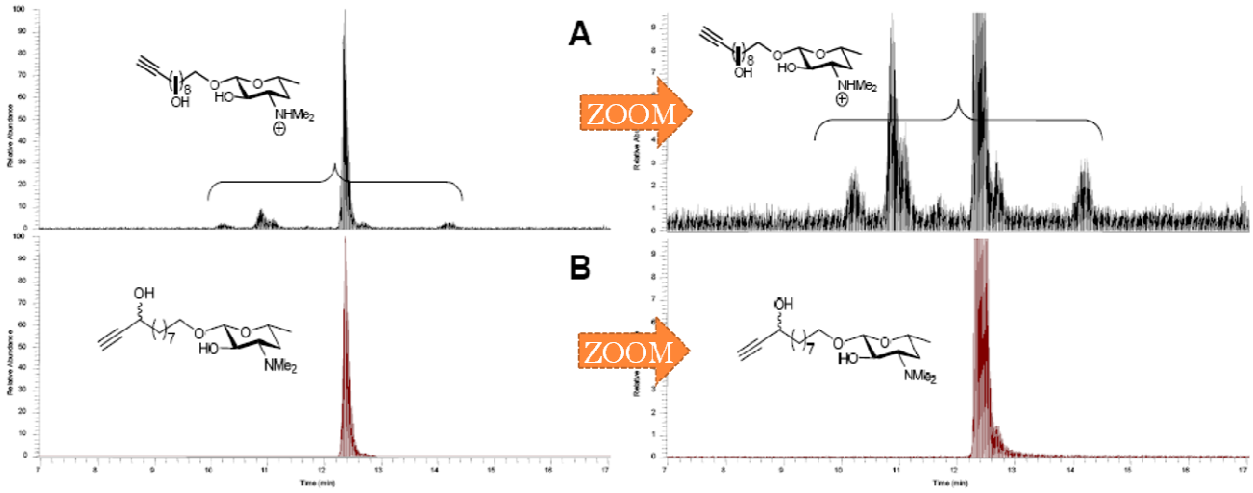

Figure 2.12. LCMS traces of (A) all products from the PikC-catalyzed oxidation of **9**, and (B) authentic propargylic alcohol product. Full spectra are shown on the left and spectra zoomed in on the baseline are shown on the right.

2.4 Antibiotic Activity of Unnatural Substrates and Some Authentic Standards

Because desosamine has been shown play an important role in the antibiotic mode of action of macrolides,[20] the synthesized substrates were also assayed for bioactivity against eight different bacterial strains (Table 2.2). Natural products erythromycin A, methymycin, and pikromycin were used as comparisons, although erythromycin is the only one of these compounds to be used clinically. YC-17, narbomycin, and authentic hydroxylated standards **17** and **25** were also compared to provide information regarding the change in bioactivity (or lack thereof) between hydroxylated and non-hydroxylated compounds.

While most of the synthetic substrates did not show significant antibiotic activity, compounds **1**, **2**, **3**, **4** and **10** showed promising activity, with minimal inhibitory concentrations (MICs) at or below those of pikromycin for the eight bacteria studied. Their corresponding aglycones (cyclododecanol, cyclotridecanol, and cyclotetradecanol) were also examined and found to have no bioactivity, indicating the importance of the desosamine residue. Hydroxylated substrates **17** and **25** did not show significant bioactivity against any of the bacterial strains. This

observation is in alignment with the endogenous substrates, where the final hydroxylation also raises the MIC values (YC-17 vs. methymycin and narbomycin vs. pikromycin).

2.5 Conclusions and Outlook

This work has shown that the naturally promiscuous P450 PikC accepts unnatural substrates bound to desosamine into its active site for oxidation. The use of desosamine as a remote anchoring group provides access to a new method of organic molecule C-H oxidation which differs in approach from the typical means of using inherent steric or electronic biases or directing groups near the location of oxidation (see section 2.1.1).

Mono-hydroxylation is observed in the positions located closest to the heme iron center within the active site of the enzyme, as confirmed by co-crystallizations of macrocyclic substrates **1** and **2** with PikC. Although the same selectivity as for the endogenous substrates YC-17 and narbomycin was not achieved, significant regioselectivity is observed for the simple substrates. These results indicate that there may be synergistic effects of both desosamine binding and macrolactone conformation that are promoting more selective oxidation of the natural products.

Because the co-crystal structures of both the endogenous and unnatural substrates bound to PikC indicate that the strongest substrate-enzyme interaction is the salt bridge that is formed between the dimethylamino functionality on desosamine and the glutamate residues within the active site, analogous linkers could be envisioned that are much simpler than the entire desosamine sugar. For example, compound **31** was synthesized, which contains a three-carbon linear linker with a dimethylamino group at the end (Scheme 2.8). Synthesis of the linker is a single step process, although the installation step still needs optimization. Commercially available amino alcohol **32** was first mesylated, and a displacement reaction led to the product.

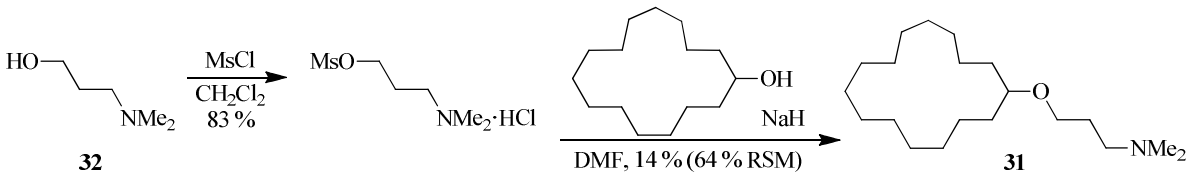

32 **31**

Scheme 2.8. Synthesis of 15-membered carbocycle attached to a simple linker.

This compound was subjected to oxidation by PikC, and a 30 % conversion was observed, resulting in 6 peaks in the LCMS. This conversion is similar to that seen for the 15-membered carbocycle attached to desosamine (35 %, Figure 2.3), but appears to be more selective (6 peaks vs. 9 peaks observed). Current work in the Montgomery lab is focused on learning more about what types of linkers are allowed by the enzyme, give good selectivity, and are easily cleaved. Linkers being studied include terminal dimethylamino groups containing various length carbon tethers, such as the 3-membered tether show in compound **31**, as well as esters, silyl-acetal, and aromatic ring-containing linkers. Work is also being conducted in the area of synthesis of YC-17 analogues for more concrete determination of the roles of the different functional groups in producing regio- and stereoselective oxidation.

This project was a collaborative effort that involved contributions from a variety of people. Dr. Mani Chaulagain was responsible for the original synthesis of the compounds shown in Figure 2.3 and the hydroxylated standards shown in Figure 2.6. Dr. Shengying Li performed all biochemical experiments presented in this chapter. Prof. Larissa Podust solved the co-crystal structures of the ligands bound to PikC shown in Figure 2.4 and Figure 2.5.

Table 2.2. Antibiotic activities of synthesized compounds against eight different bacteria.

Compound	Minimal Inhibitory Concentration (MIC, μM)							
	Kocuria rhizophila ATCC9341[a]	*Staphylococcus aureus* ATCC6538P	*Bacillus subtillis* DHS5333	*Deinococcus radiodurans*[b]	*Escherichia coli*TolC[c]	*S. aureus* NorA[d]	*Acinetobacter baumannii*	Multidrug resistant *S. aureus* (MRSA)
Erythromycin A	< 0.8	< 0.8	< 0.8	6.2	< 0.8	< 0.8	25	> 100
YC-17	100	100	100	400	100	100	> 400	> 400
Methymycin	50	100	100	200	50	100	> 400	> 400
Narbomycin	< 3.1	6.2	< 3.1	100	25	3.1	> 400	> 400
Pikromycin	6.2	25	12.5	100	100	12.5	> 400	> 400
1	50	> 400	200	100	50	200	> 400	400
2	50	400	200	100	50	200	> 400	200
3	50	>400	200	50	50	400	> 400	400
4	50	200	100	50	50	100	> 400	100
5	> 400	> 400	> 400	> 400	> 400	> 400	> 400	> 400
6	> 400	> 400	> 400	> 400	> 400	> 400	> 400	> 400
7								
8	> 400	> 400	> 400	> 400	> 400	> 400	> 400	> 400
9	> 400	> 400	> 400	> 400	400	> 400	> 400	> 400
10	25	25	6.2	25	25	25	100	25
11	> 400	> 400	> 400	> 400	> 400	> 400	> 400	> 400
17-a[e]	> 400	> 400	> 400	400	> 400	> 400	> 400	> 400
17-b[e]	> 400	> 400	> 400	100	400	> 400	> 400	> 400
25-a[e]	> 400	> 400	> 400	> 400	> 400	> 400	> 400	> 400
25-b[e]	> 400	> 400	> 400	400	> 400	> 400	> 400	> 400
Cyclododecanol	> 400	> 400	> 400	> 400	> 400	> 400	> 400	> 400
Cyclotridecanol	> 400	> 400	> 400	> 400	> 400	> 400	> 400	> 400
Cyclopentadecanol	> 400	> 400	> 400	> 400	> 400	> 400	> 400	> 400

[a] Previously known as *Micrococcus luteus* ATCC 9341, which is sensitive to macrolides antibiotics

[b] A gift from Prof. Ada E. Yonath (Structural Biology Department, Weizmann Institute of Science, Rehovot, Israel)

[c] *E. coli* W3110 TolC disruption mutant that is more sensitive to antibiotics

[d] *S. aureus* 8325 NorA disruption mutant that is more sensitive to antibiotics

[e] **17-a**, **17-b**, **25-a**, and **25-b** correspond to the separated diastereomers of the hydroxylated products of **2**, shown in Figure 2.7and Figure 2.8.

Chapter 3

Nickel-Catalyzed Ligand-Dependent Regioselective Macrocyclizations of Ynals

3.1 Introduction

3.1.1 Macrocycle-Containing Natural Products

As discussed in chapter 1 and section 2.1, many biologically active natural products contain a macrocyclic core. Oftentimes, the biological activity of these compounds can be altered by changing the ring size. For example, erythromycin is a 14-membered ring containing natural product that has found use clinically as an antibiotic for a number of bacterial infections, including skin and respiratory infections, as well as syphilis.[9] Bitter taste and stomach cramps were common side effects of this drug, so second-generation derivatives of the natural product have also been pursued. Azithromycin is a 15-membered ring variant that is synthesized from erythromycin and exhibits enhanced bioactivity, including alleviation of the side effects mentioned above and increased oral bioavailability so that it only has to be taken once a day (Figure 3.1). Synthesis of natural products and derivatives thereof can lead to the development of molecules with more interesting biological activity.

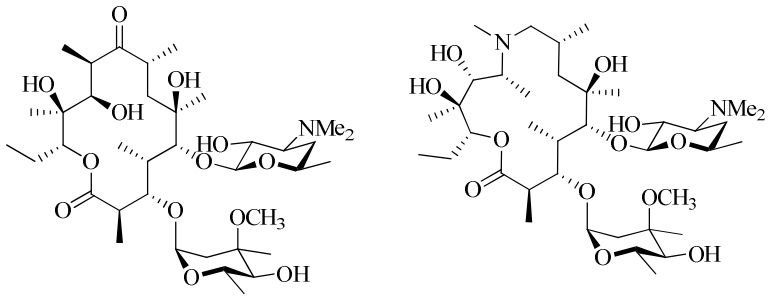

Erythromycin A **Azithromycin**

Figure 3.1. Structures of natural product erythromycin and derivative azithromycin.

3.1.2 Metal-Catalyzed Macrocyclizations

One of the most common techniques used in the total syntheses of macrolides is macrolactonization.[46,47] However, several examples of transition-metal catalyzed carbon-carbon bond forming processes have also been developed. One such reaction is the Nozaki-Hiyama-Kishi (NHK) reaction, which involves the nickel-catalyzed formation of a vinyl or allyl chromium species that adds to an aldehyde to form an allylic or homoallylic alcohol (Scheme 3.1).[48] The nickel (II) catalyst is reduced by chromium (II) to nickel (0), which can oxidatively insert into the starting halide. Transmetallation leads to the chromium adduct, which adds to the aldehyde to give the final product. Alternatively, the reaction can be made catalytic in chromium through the addition of manganese (0) as a terminal reducing agent to regenerate chromium (II).

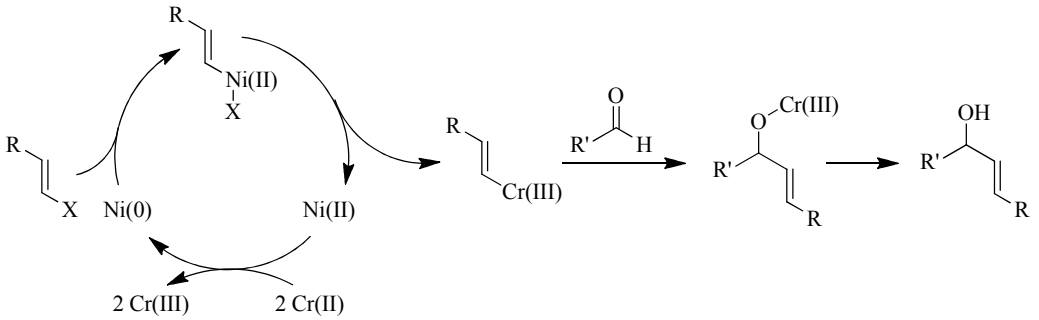

Scheme 3.1. Mechanism of the NHK reaction.

The NHK reaction has been used as the key macrocycle-forming step in a number of natural product syntheses, including (-)-bipinnatin J,[49,50] (-)-dictyostatin and analogues,[51] and amphidinolactone A (Figure 3.2).[52] The aglycone narbonolide was also synthesized using an intramolecular NHK reaction, which provided improved yields over previous macrolactonization and Horner-Wadsworth-Emmons approaches.[53] This work was furthered through the biosynthetic conversion of narbonolide to pikromycin (see chapter 2 for a discussion describing the biosynthesis and biological activity of these two compounds).[54]

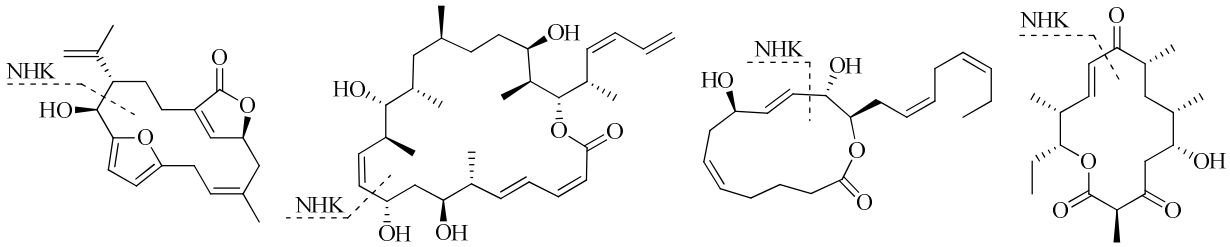

Figure 3.2. Natural products synthesized through an NHK coupling to form the macrocycle.

Ring-closing metathesis (RCM) is another common way to form alkene-containing macrocycles.[55,56] Anti-tumor agents pladienolides A and D[57] and several resorcylic acid macrolactones[58,59] have been synthesized using this method (Figure 3.3A). Recently, Hoveyda, Schrock, and co-workers applied their tungsten metathesis catalyst to the synthesis of macrocyclic *Z*-alkenes epothilone C and nakadomarin A (Figure 3.3B).[60]

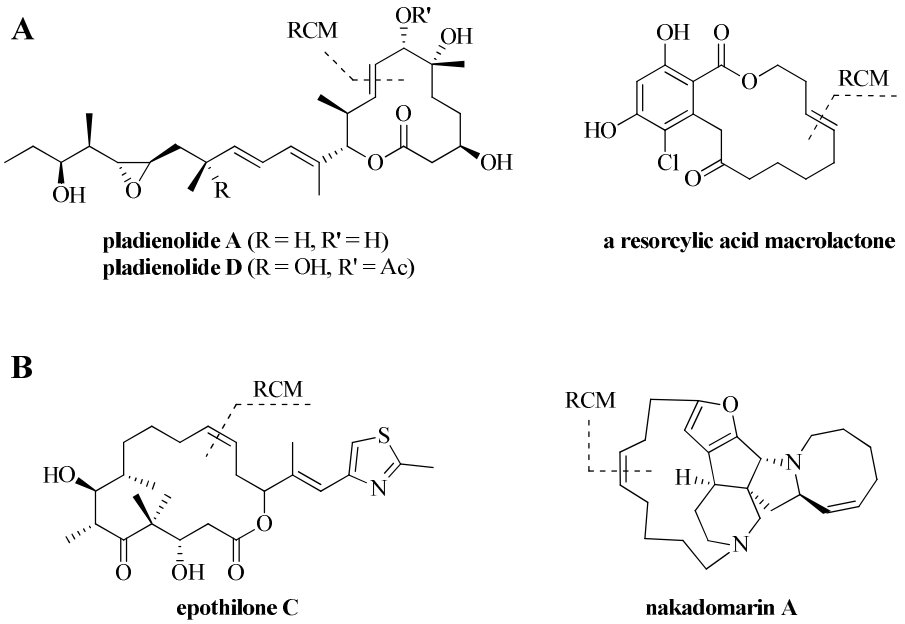

Figure 3.3. Macrocyclic products synthesized utilizing ring-closing metathesis to form (A) *E*-olefins and (B) *Z*-olefins.

An early example of a carbon-carbon bond-forming macrocyclization by the metal-promoted coupling of a tethered aldehyde and alkyne was presented in the synthesis of (-)-muscone (Scheme 3.2A).[61] The alkyne first undergoes hydroboration followed by metallation with Et_2Zn. Addition to the aldehyde occurs stereospecifically through use of a chiral ligand. The total syntheses of amphidinolides T1 and T4 through nickel-phosphine catalyzed macrocyclizations has also been reported (Scheme 3.2, B and C).[62] These reactions occur in high (>10:1) diastereoselectivity and produce the exocyclic product exclusively.

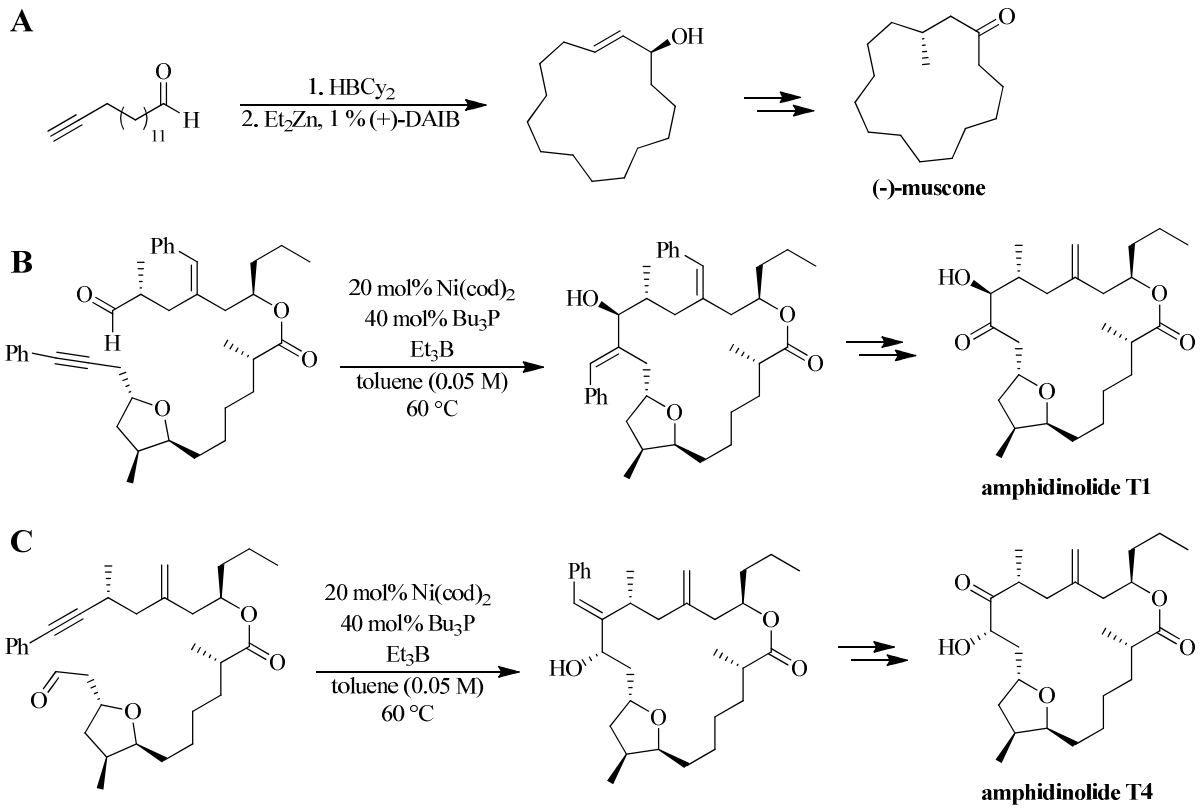

Scheme 3.2. Macrocyclizations utilizing metal-promoted couplings of aldehydes and alkynes in the synthesis of natural products.

Work in our lab elaborated on the examples of intramolecular aldehyde/alkyne coupling presented above by expanding it to include terminal alkynes (Figure 3.4).[63] By using a similar procedure to the previously developed intermolecular nickel-catalyzed three component reductive coupling reactions,[64] a variety of rings ranging in size from 11-22 membered were able to be synthesized in good yields favoring the monomeric endocyclic product. The smaller 9-membered chain gave the macrocyclic dimer exclusively. This methodology was applied to the total synthesis of aigialomycin D, a resorcylic macrolactone.[65]

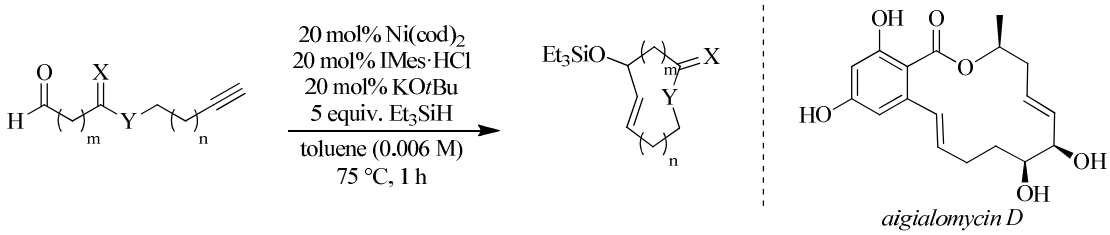

Figure 3.4. Nickel-catalyzed macrocyclization of terminal alkynes to yield endo products.

The regioselectivity of the reaction utilizing internal alkynes was also examined, and it was determined that by switching from NHC to phosphine ligands, the exocyclic product **33** could be favored over the endocyclic product **34** (Figure 3.5). However, this regioselectivity switch was only observed in substrates containing methyl-substituted internal alkynes; phenyl-capped alkynes gave the exocyclic product exclusively, while terminal alkynes only yielded the endocyclic product under all conditions.

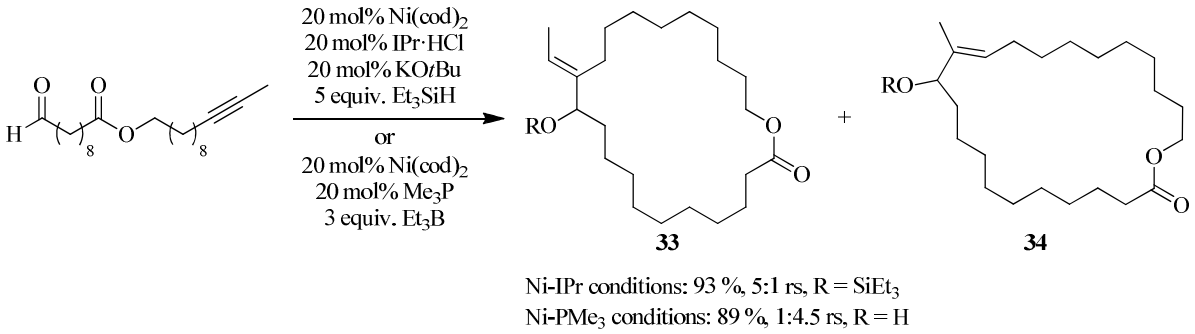

Figure 3.5. Nickel-catalyzed ynal macrocyclization of methyl-alkynes, which can be regioselectively diverged.

3.1.3 Ligand-Dependent Regioselective Intermolecular Three-Component Couplings

A breakthrough in our lab revealed that specialized ligands could override substrate-controlled regioselectivity in the nickel-catalyzed intermolecular three-component couplings of aldehydes, alkynes, and silanes (Table 3.1).[66] Under these conditions, similar alkyl groups, such as methyl and propyl groups, could be differentiated to give high selectivity for either isomer by simply switching the ligand on the metal center (entry 1). The high substrate control

demonstrated previously with phenyl alkynes[67] (entry 2), terminal alkynes[67] (entry 3), and propargyl silyl ethers[68] (entry 4) was overcome in this methodology.

Table 3.1. Ligand Dependent Regioselectivity in Nickel-Catalyzed Reductive Couplings

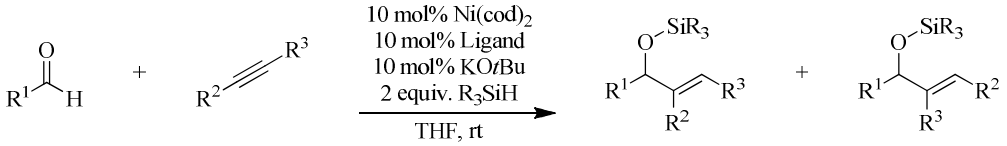

Entry	R^1	R^2	R^3	Ligand	Yield (rs)	Ligand	Yield (rs)
1	*n*-Hex	Me	*i*-Pr	*i*-Pr-BAC	78 % (88:12)	SIPr	85 % (7:93)
2	Ph	Me	Ph	IMes	84 % (>98:2)	SIPr	99 % (19:81)
3	Ph	H	*n*-Hex	IMes	82 % (97:3)	DP-IPr	71 % (12:88)
4	Ph	H	CH_2OTBS	IMes	88 % (93:7)	DP-IPr	86 % (15:85)

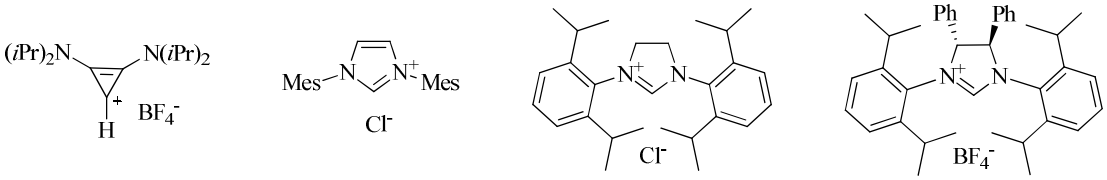

***i*-Pr-BAC·HBF$_4$** **IMes·HCl** **SIPr·HCl** **(rac)-DP-IPr·HBF$_4$**

The proposed mechanism for this reaction begins with coordination and of the aldehyde and alkyne substrates to the nickel-NHC complex (Scheme 3.3A). Oxidative cyclization gives the 5-membered metallacycle, which can undergo σ-bond metathesis with the silane to generate a nickel-hydride intermediate. Reductive elimination leads to the product and reforms the active nickel (0) catalyst.

Computational work has shown that the regioselectivity results from interactions between the aldehyde, alkyne, and ligand (Scheme 3.3B). [69] When a small ligand (*i*-Pr-BAC or IMes) is used, aldehyde-alkyne interactions dominate, directing the largest alkyne substituent away from the aldehyde. With large ligands (SIPr or DP-IPr), ligand-alkyne interactions govern the regioselectivity of the reaction, so that the largest substituent on the alkyne is positioned away

from the ligand. The calculations performed in this study also predicted similar regioselectivities to those observed experimentally, lending further support to the proposed interactions described.

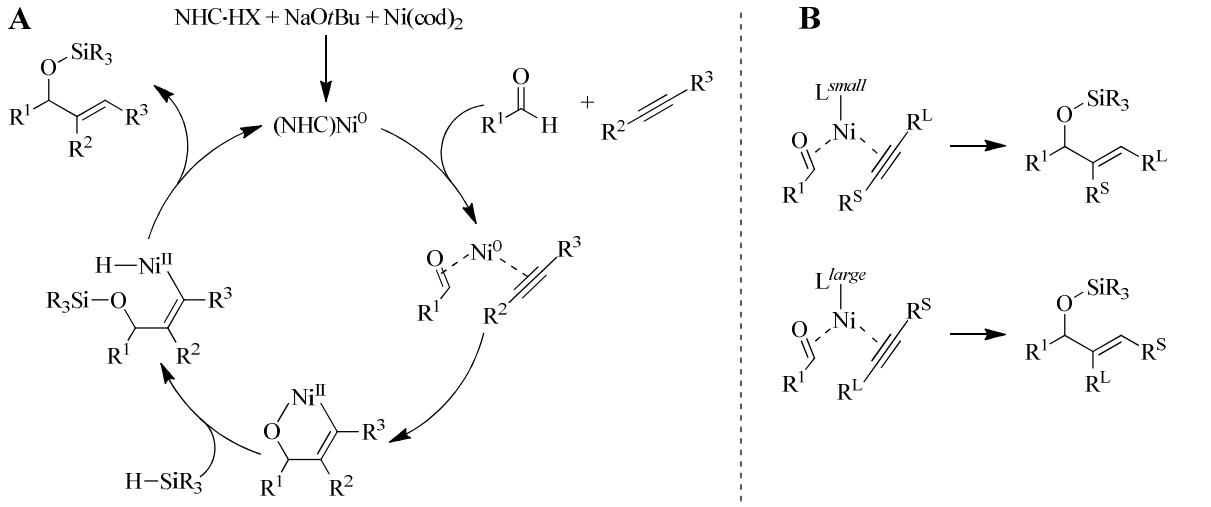

Scheme 3.3. (A) Proposed mechanism of nickel-catalyzed reductive couplings of aldehydes and alkynes and (B) rationale for observed regioselectivity.

This methodology was applied to the total synthesis of 10-deoxymethonolide, the aglycone of methymycin, and the analogue derived from the opposite regioisomer (Scheme 3.4).[70] By using the ligand IMes, the natural product core **35** can be obtained, while use of DP-IPr leads to the smaller 11-membered ring **36**. This finding represents a unique manner to access two differently sized macrocycles from a common intermediate. See chapter 1 and section 3.1.1 for further discussion regarding the role of ring size in biological activity of natural products and their derivatives.

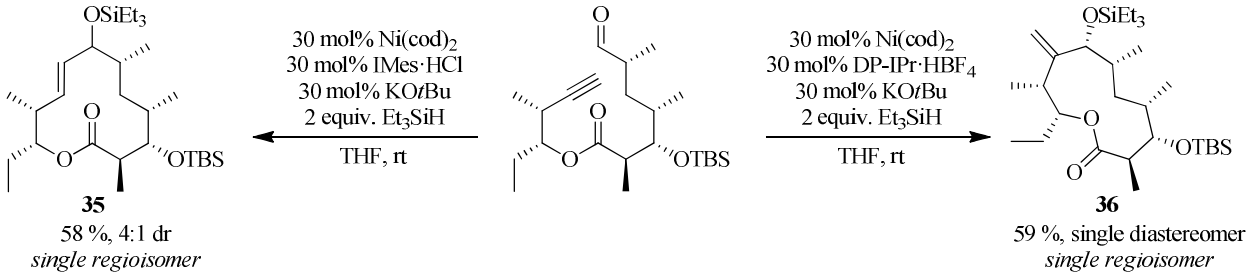

Scheme 3.4. Synthesis of 10-deoxymethonolide and its exocyclic regioisomer via regioselective nickel-catalyzed macrocyclizations.

3.2 Results and Discussion

Encouraged by the results presented above (section 3.1.3), we sought to expand the generality of nickel-catalyzed regioselective macrocyclizations to include substrates that have proven problematic, namely terminal alkynes and aryl alkynes.

3.2.1 Synthesis of Substrates

Several linear aliphatic substrates containing terminal alkynes were synthesized to test in the macrocyclization reaction, as well as substrates containing an ester linkage. 12- and 14-carbon chains **39** and **40** were synthesized from 1,10-decanediol and 1,12-dodecanediol, respectively (Scheme 3.5). The diol was mono-brominated,[71] followed by THP-protection of the remaining alcohol. Although previous syntheses of these and similar molecules used a lithium-acetylide/ethylenediamine complex for the alkyne addition reaction,[72,73] *in situ* formation of TMS-acetylide, addition to the bromide, and subsequent deprotection of the alkyne in the same pot led to more reproducible yields of **37** and **38**. Deprotection of the THP group gave the free alcohols in high yields, which could be oxidized to the corresponding ynal and used the same day in a macrocyclization reaction.

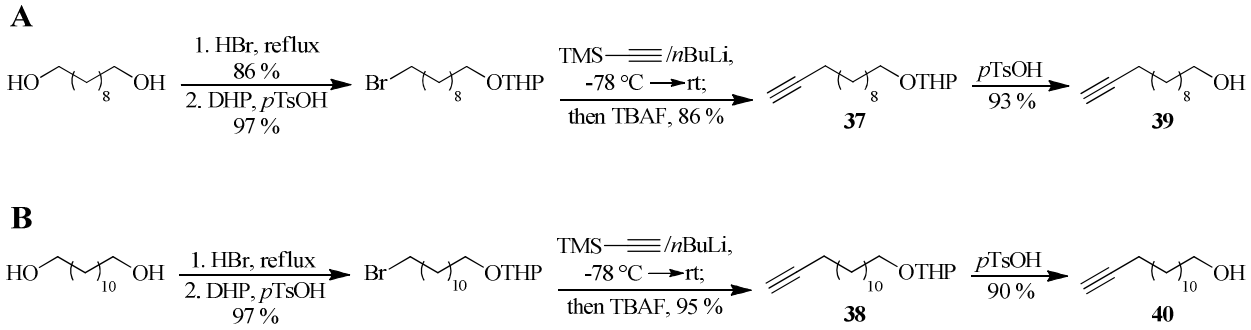

Scheme 3.5. Synthesis of linear (A) 12-carbon and (B) 14-carbon substrates.

Several longer chain substrates bearing esters were also synthesized as previously described (Scheme 3.6).[63] Silane protection and saponification of commercially available methyl 10-

hydroxydecanoate gave the carboxylic acid **41**, which was coupled with ynols of differing carbon chain length. Deprotection led to the alcohol substrates **42** and **43**, which were later oxidized before submission to macrocyclization conditions.

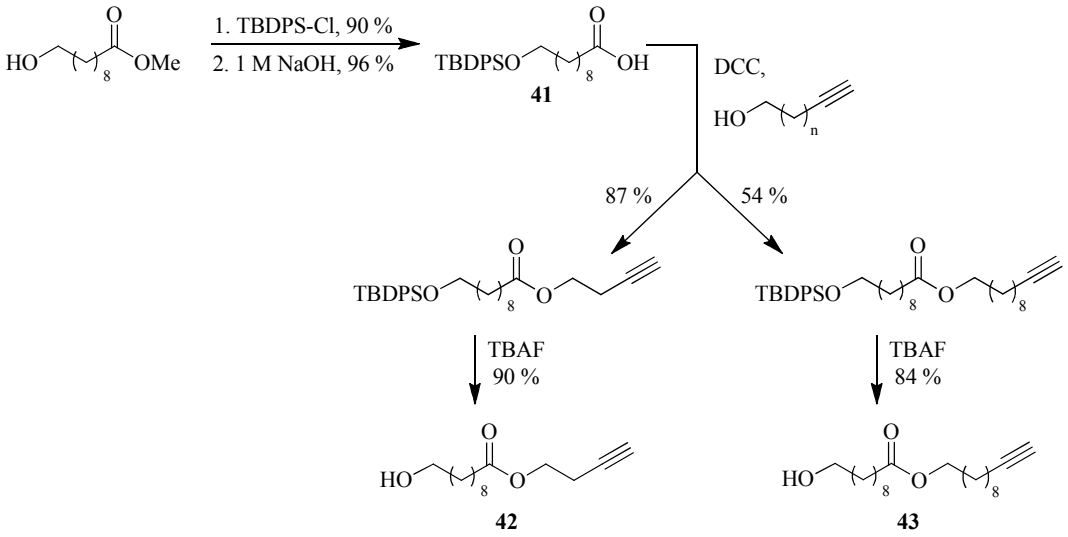

41 **42** **43**

Scheme 3.6. Synthesis of ester-bearing substrates.

3.2.2 Reaction Optimization Studies

Optimization of reaction conditions for the macrocyclization of aliphatic ynals began with the commercially available 10-undecyn-1-ol, which, after oxidation to the aldehyde, can yield 10- and 11-membered rings upon cyclization. However, it became apparent that this substrate is less than ideal to perform optimization studies on because of its low yield (<30 %) of product under all conditions studied. Therefore, the 12- and 14-carbon substrates prepared from oxidation of **39** and **40** were used for most of the optimization studies (Table 3.2).

Table 3.2. Optimization studies of nickel-catalyzed macrocyclizations.

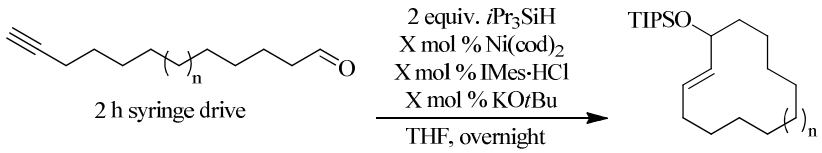

Entry	X	n	Final [ynal] (M)	Yield
1	10	0	0.006	28 %
2	20[a]	0	0.006	27 %
3	10	1	0.01	20 %
4	20	1	0.01	40 %
5	20	1	0.02	36 %
6	20[a]	1	0.01	38 %
7	20[b]	3	0.01	42 %
8	20[a]	3	0.01	38 %
9	20[a]	3	0.005	43 %
10	20[a]	3	0.001	17 %
11	20[a,c]	3	0.005	37 %
12	30[b]	3	0.01	42 %

[a]catalyst split into two equal portions; second aliquot was added after the completion of the syringe drive
[b]Et_3SiH used instead of iPr_3SiH
[c]4 h syringe drive of ynal to catalyst instead of 2 h

Several different parameters were varied, including the final concentration of the ynal in solution, amount of catalyst, adding the catalyst in one or two aliquots, silane reducing agent, and length of syringe drive. Switching from 10 to 20 mol% catalyst loading doubled the yield for the 12-membered macrocycle (entries 3 and 4), while the same experiment showed no change in the 11-membered product yield (entries 1 and 2). The final concentration of the ynal in solution did not significantly change the yield of the reaction, except when it was diluted to 0.001 M (entry 10). This low yield likely has more to do with low concentration of catalyst in solution with this procedure. Because the ynal is added to the reaction via syringe drive, it is not surprising that the final concentration of the substrate in solution does not affect the product yield. Both iPr_3SiH and Et_3SiH (entries 7 and 12) are tolerated as the reducing agent in the

reaction, which fits with our mechanistic hypothesis that the silane is not part of the rate-limiting step of this reaction.[74] In all of these reactions, the endocyclic product shown is the only observed product.

3.2.3 Substrate Scope and Regioselectivity Dependence on Ring Size

The five different substrates were subjected to the simplest reaction conditions from the optimization studies, i.e. 20 mol% catalyst loading (added in one aliquot) and a 2 hour syringe addition of the ynal to the catalyst solution (Table 3.3). A general trend was recognized that the larger the macrocycle being formed, the higher the yield of the reaction. This trend is often observed in macrocyclization reactions due to increased ring strain associated with smaller-sized rings,[75–78] and has recently been observed in ring-closing enyne metathesis[79] and the oxidative coupling of furans with β-ketoesters.[80]

Table 3.3. Substrate scope of nickel-catalyzed macrocyclizations.

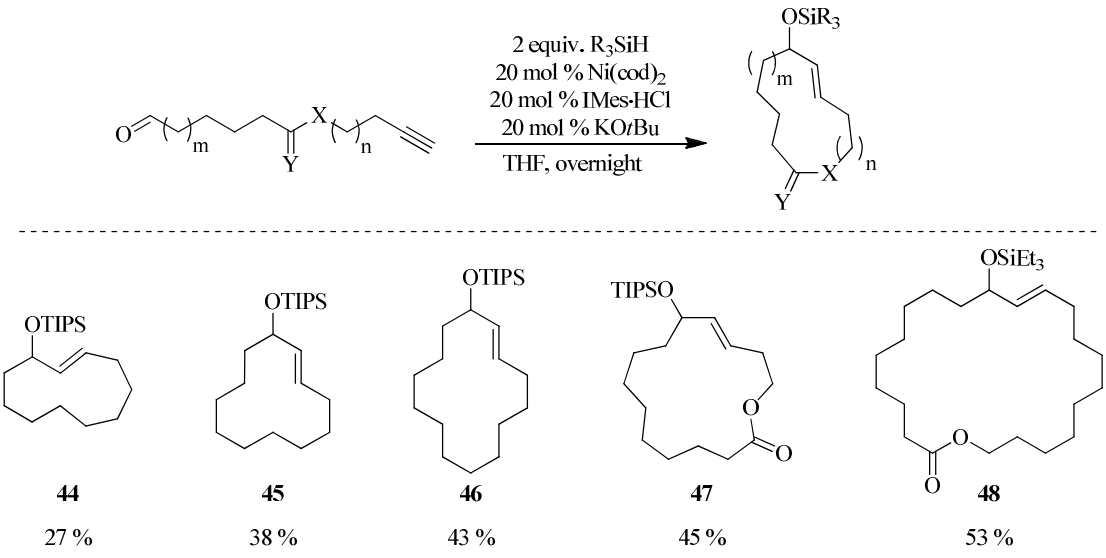

The effect of changing the ligand on the nickel catalyst center was also examined (Table 3.4). Although SIPr did not lead to a dramatic change in regioselectivity compared with IMes,

switching to DP-IPr led to the exo isomer **49** being favored over endo isomer **46**, albeit in about a 1.4:1 manner. This small regioselectivity was surprising, seeing how this large ligand dramatically switches the regioselectivity in the intermolecular cases.[66] Apparently, the ring strain associated with forming the 13-membered ring dictates the outcome of the reaction more than the sterics associated with using the large DP-IPr ligand (see Table 3.1 for ligand structures).

Table 3.4. Effect of NHC ligand on regioselectivity of the macrocyclization of a 14-membered substrate.

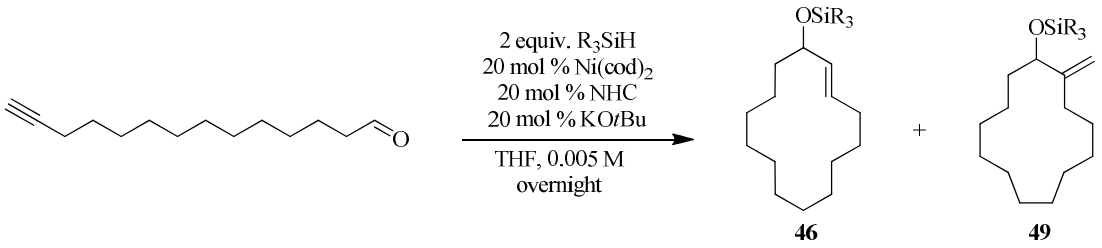

Ligand	Silane	Yield	Regioselectivity (46:49)[a]
IMes·HCl	*i*Pr$_3$SiH	43 %	> 98:2
SIPr·HCl	Et$_3$SiH	44 %	93:7
DP-IPr·HBF$_4$	Et$_3$SiH	45 %	42:58

[a]determined by crude GCMS ratios

Because of the greater ring strain associated with smaller rings, a 22-membered substrate was next subjected to the macrocyclization with different ligands (Table 3.5). As expected, exo isomer **50** was favored in a 2.6:1 ratio over endo isomer **48** when using DP-IPr as a ligand. These results represent a significant improvement over the previously reported macrocyclization studies, which were unable to produce the exo product when terminal alkynes were employed.[63]

Table 3.5. Ligand effects on the nickel-catalyzed macrocyclization of a 22-membered substrate.

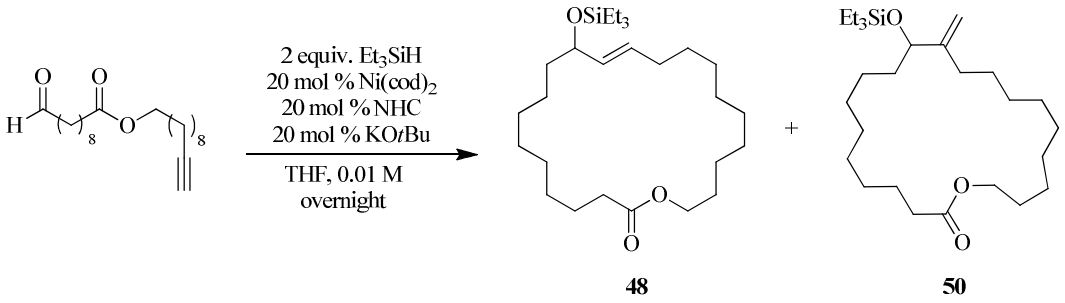

Ligand	Yield	Regioselectivity (48:50)[a]
IMes·HCl	53 %	> 98:2
DP-IPr·HBF_4	40 %	28:72

[a]determined by crude GCMS ratios

3.3 Conclusions and Outlook

Preliminary data has been obtained regarding the effects of different NHC ligands on the regioselectivity of nickel-catalyzed reductive macrocyclizations of terminal alkynes and aldehydes. A reversal in regioselectivity with terminal alkynes from the endocyclic to the exocyclic product can be obtained by using the bulky DP-IPr ligand, which had previously been observed for intermolecular couplings but had not been generalized for macrocyclizations. However, ring strain associated with the product formation causes the regioselectivity ratios to be modest.

Ring strain has been shown previously to play an important role in the rate of different macrocyclization reactions. Energy calculation of the transition states leading to the two different regioisomers could lead to more insight into the role of ring strain in the nickel-catalyzed reductive macrocyclizations presented here. Expansion of the substrate scope to include other substrates which have shown to be problematic in the regioselective reversal of macrocyclizations, such as phenyl alkynes, will lead to a general method for access to either the

endo or exo macrocycle from a single substrate, broadening the toolbox of the synthetic chemist for synthesis of macrocyclic compounds.[5]

Chapter 4

Development of Bench Stable Sugar Silanes for Use in Copper-Catalyzed Dehydrogenative Silylations

4.1 Introduction

4.1.1 Sugars in Nature

Sugars are found in many different areas of nature in the forms of oligo- and polysaccharides, glycolipids, glycoproteins, and other glycoconjugates. They can play many roles; for example, cellulose composes the cell walls in most plants and sucrose is used as table sugar. Glycolipids and glycoproteins are often found in mammalian cell walls, where they function as molecular markers to mediate cell growth, fertilization, and inflammation, among a plethora of other processes.[81] These molecules play an important role in biological functions, and changes in the structure of the sugar moiety can lead to significant alterations in the molecule's activity.

One example is the difference in one of the sugar monomers of the oligosaccharide attached to red blood cells distinguishing between blood types A, B, and O (Figure 4.1). Blood types A and B differ only the *N*-acetylgalactosamine versus galactose monomers, while blood type O lacks this fourth sugar monomer completely. Because these oligosaccharides are involved in red blood cell recognition of antibodies in the blood stream, such a small change in structure can

have drastic effects when it comes to molecular recognition by the body in events such as blood transfusions.

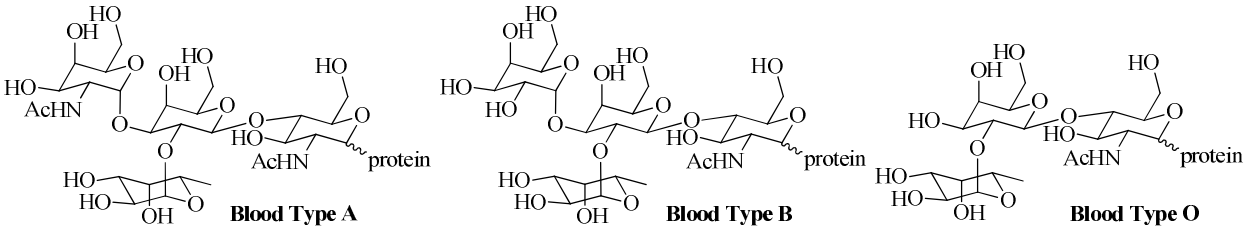

Figure 4.1. Oligosaccharides attached to red blood cells, which determine blood type.

4.1.2 Importance of Sugar Moieties for Biological Activity

The presence or absence of a sugar appendage can also be important for a molecule's therapeutic function. As described in section 2.1, the antibiotic activity of erythromycin disappears if the desosamine sugar molecule is removed. This reliance on the desosamine sugar for biological activity was also seen with the antibiotic activity of synthetic desosaminyl glycosides tested in our previous experiments (see section 2.4). Although unnatural substrates **1**, **2**, and **3** are not as potent antibiotics as erythromycin, they do exhibit measurable activity, while the corresponding free alcohols did not show any measurable antibiotic activity against the eight bacterial strains tested (Table 2.2).

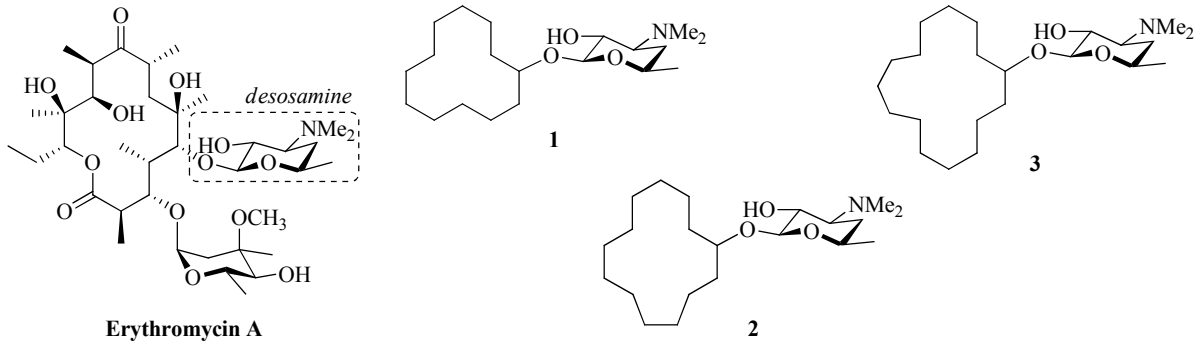

Figure 4.2. Structures of erythromycin A and other less functionalized substrates containing a desosamine residue. The desosamine sugar moiety labeled is required for the antibiotic activity of all compounds shown.

The structure of the sugar molecule has also been shown to change the biological activity of a compound.[13] In an effort to develop new molecules with interesting biological activity, Thorson and coworkers have developed glycorandomization and neoglycorandomization strategies to synthesize libraries of glycosylated compounds.[15,82] The former approach utilizes promiscuous glycosyltransferases to attach a variety of sugars to either the natural compounds associated with the enzymes or aglycones fed to the system. One example exploited the DesVII/DesVIII pathway described in section 2.1 to glycosylate 10-deoxymethynolide and narbomycin with several exogenous sugar moieties.[83]

On the other hand, neoglycorandomization uses chemical means to glycosylate secondary alkoxylamines with unprotected sugar molecules (Scheme 4.1).[84] The aglycone is easily synthesized by condensation of the alkoxylamine with a ketone and subsequent reduction. It then condenses with the open chain aldehyde form of the starting sugar to form the iminium ion intermediate, which re-cyclizes, yielding the product. This strategy is advantageous over glycorandomization in that the glycosyl donors do not need to be protected and any glycosyl donors may be used, not just those that are accepted by the glycosyl transferases. Neoglycorandomization has been employed in the glycosylation of the digitoxin aglycone with a variety of different carbohydrates, and the resultant products were analyzed for anticancer activity against a variety of cancer cell lines. Several of the products were found to have similar properties to the natural product, while two were found to be either more selective for one type of cancer cell or more active across all cell lines.

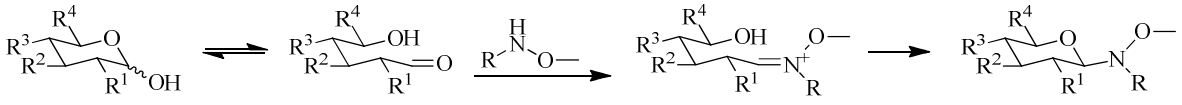

Scheme 4.1. Chemical neoglycorandomization strategy.

4.2 Development of Sugar Silanes

4.2.1 Glycosylation Methods and Challenges

Synthetic chemists have long been interested in synthesizing new glycosides, which is typically accomplished by activation of a leaving group in the anomeric position, forming an oxocarbenium intermediate (Scheme 4.2). The incoming glycosyl acceptor can then add into the oxocarbenium to give the desired product. Common leaving groups include halides, thiols, sulfoxides, acyloxy groups, trichloroimidates, and phosphates, among others.[85] When no directing effect is utilized, a mixture of the α- and β-anomers shown is commonly produced because the incoming nucleophile can add to either face of the oxocarbenium ion. In the glucose series, the β-anomer is the kinetic product due to sterics from the equatorial group in the 2-position and resultant formation of an all-equatorial chair conformation. However, the α-product is the thermodynamic product due to the anomeric effect, or donation of electron density from the axial lone pair on the pyranose oxygen into the σ^* orbital of the axial C-O bond in the anomeric position. For the mannose series, the α-anomer is both the kinetic and thermodynamic product, making synthesis of the β-anomer much more difficult.

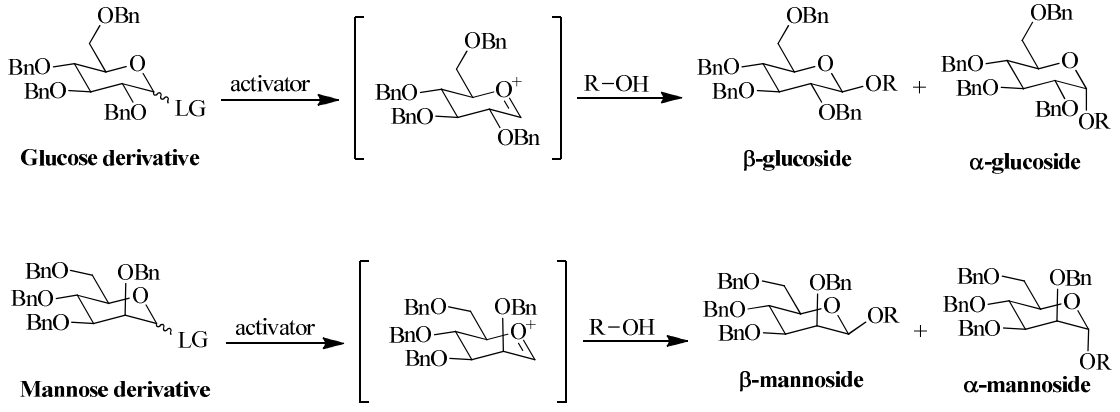

Scheme 4.2. Typical reaction sequence for synthesis of glucosides.

A common method to produce 1,2-*trans*-glycosides is the Koenigs-Knorr reaction, which utilizes halides as the anomeric leaving group (Scheme 4.3).[86] An acyl group in the 2-position then provides anchimeric assistance to block one face of the sugar, so that the nucleophile must approach from the opposite face. This neighboring group effect results in high diastereoselectivity of the desired product.

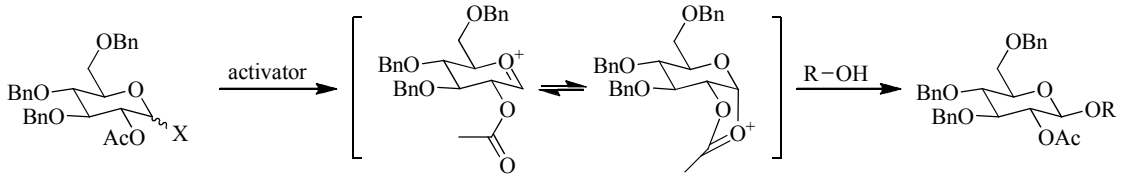

Scheme 4.3. Neighboring-group participation to form 1,2-*trans*-glycosides.

While the Koenigs-Knorr method works well for the synthesis of 1,2-*trans*-glycosides, 1,2-*cis*-glycosides are more challenging to produce. The most common method for synthesis of β-mannosides is the Crich method (Scheme 4.4).[87] In this case, the anomeric sulfoxide leaving group is first activated with triflic acid using the Kahne protocol. The triflate anion then adds in to the oxocarbenium to form the α-triflate exclusively.[88] S_N2-like displacement with the incoming nucleophile yields the β-mannoside in up to 20:1 anomeric selectivity. For many substrates, adding benzene or 1,4-dimethoxybenzene to the reaction increased the selectivity for the β-anomer, although the reason for this trend is unclear.

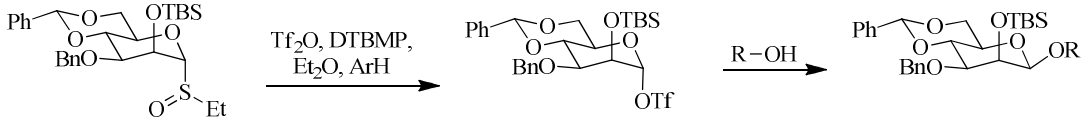

Scheme 4.4. Crich method for synthesis of β-mannosides, which proceeds via the α-triflate.

4.2.2 Intramolecular Glycosylations for Selective Synthesis of 1,2-cis-Glycosides

Many methods have been developed for the synthesis of glycoconjugates through the use of tethered aglycones to improve the stereo- and regioselectivity of the reaction.[89] The first example of intramolecular glycosylation using tethering at the C2 position employed isopropylidene ketals, which form acetals upon reaction with the aglycone under acidic conditions (Scheme 4.5).[90] The thioethyl leaving group was then activated using N-iodosuccinimide (NIS), and further studies showed that the addition of the base 2,6-di-*t*-butyl-4-methylpyridine (2,6-DTBMP) led to better glycosylation yields.[91] Several disaccharides containing β-mannoside linkages have been synthesized in this fashion.

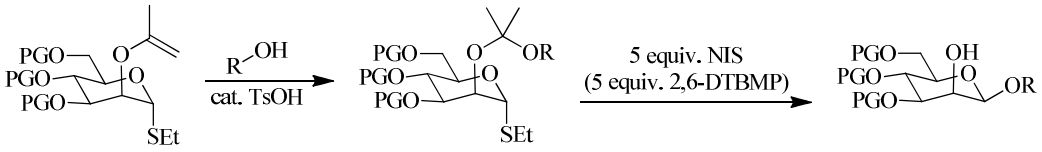

Scheme 4.5. Intramolecular glycosylation using isopropylidine-linked aglycones.

A similar strategy was developed using 4-methoxybenzilidene acetals, which are synthesized by activation of the benzyl ether with DDQ and addition of the glycosyl acceptor (Scheme 4.6).[92] The intermediate acetal can be formed as a mixture of diastereomers, although one is usually formed as the major isomer and both have been shown to undergo the glycosylation step effectively. This method allows for the use of bulkier glycosyl acceptors than the isopropylidene approach.

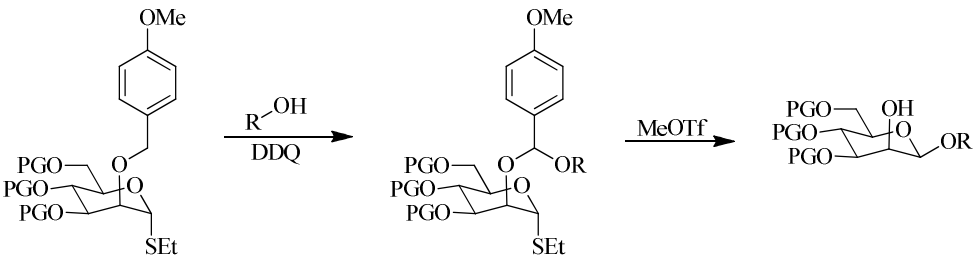

Scheme 4.6. Use of 4-methoxybenzilidene acetals for intramolecular glycosylation.

Inspired by the anchimeric assistance from the 2-acetate group in the Koenigs-Knorr reaction, Bols developed a method for the synthesis of silyl-tethered aglycones, which are formed from the reaction of the 2-hydroxy sugar and aglycone with dichlorodimethylsilane (Scheme 4.7).[93,94] The tethered aglycone adds in to the oxocarbenium intermediate from the same face as the substituent in the 2-position, and cleavage of the silane results in exclusive production of the 1,2-*cis*-product. This methodology has been applied to the synthesis of α-gluco disaccharides[95,96] and the trisaccharide kojitriose.[97]

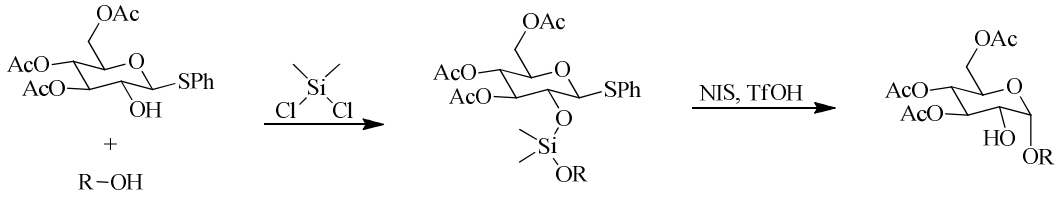

Scheme 4.7. Use of silyl-tethered aglycone to deliver aglycone from same face as the 2-substituent.

Concurrently, similar work was developed in the Stork lab for the synthesis of disaccharides (Scheme 4.8).[98,99] By using the sulfoxide leaving group in the synthesis of the silyl linked disaccharide, simply mixing a 1:1 mixture of the glycosyl donor and acceptor with the dichlorodimethylsilane gives the mixed silyl acetal in good yield without significant homodimerization of either alcohol reagent. This procedure is an important improvement over previous syntheses which required a two-step process, used an excess of one alcohol reagent and

the silane, and involved the difficult isolation of the intermediate chlorosilane, resulting in moderate yields.

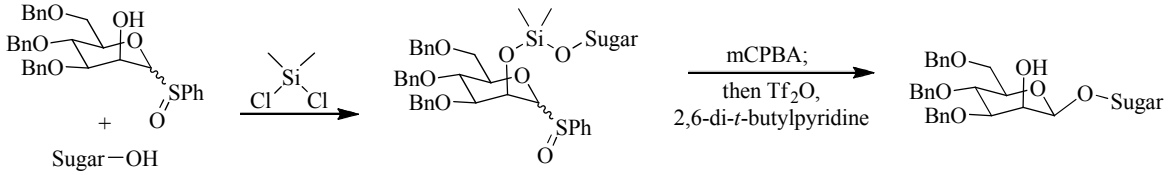

Scheme 4.8. Synthesis of disaccharides via silyl-linked intramolecular aglycone delivery.

4.2.3 Sugar Silanes as Reducing Agents in the Nickel-Catalyzed Hydrosilylation of Ketones

To ease the synthesis of the silyl ether linked aglycone, commercially available chlorodimethylsilane was utilized to develop a sugar substrate containing a dimethyl silyl hydride in the 2-position. This molecule was termed a sugar silane and can be utilized as the reducing agent in the nickel-catalyzed hydrosilylation of ketones (Scheme 4.9). A variety of ketones were efficient electrophiles in the reaction, although the chirality of the sugar did not transfer to give high diastereomeric ratios of the products formed. Substrate-controlled diastereoselectivity was observed in the hydrosilylation of biased ketones. The less reactive menthone substrate required the use of a copper catalyst system, which has previously been shown to tolerate more sterically hindered substrates (see section 4.3.2), in replacement of the nickel catalyst to achieve good yields. All of the substrates underwent intramolecular glycoslation as previously described to give the 1,2-*cis*-glycoside as the only observed product. Both glucosyl and mannosyl sugar silanes were employed. This methodology represents an orthogonal entry to silyl ether tethered aglycones through the ketone oxidation state instead of the alcohol functional group.

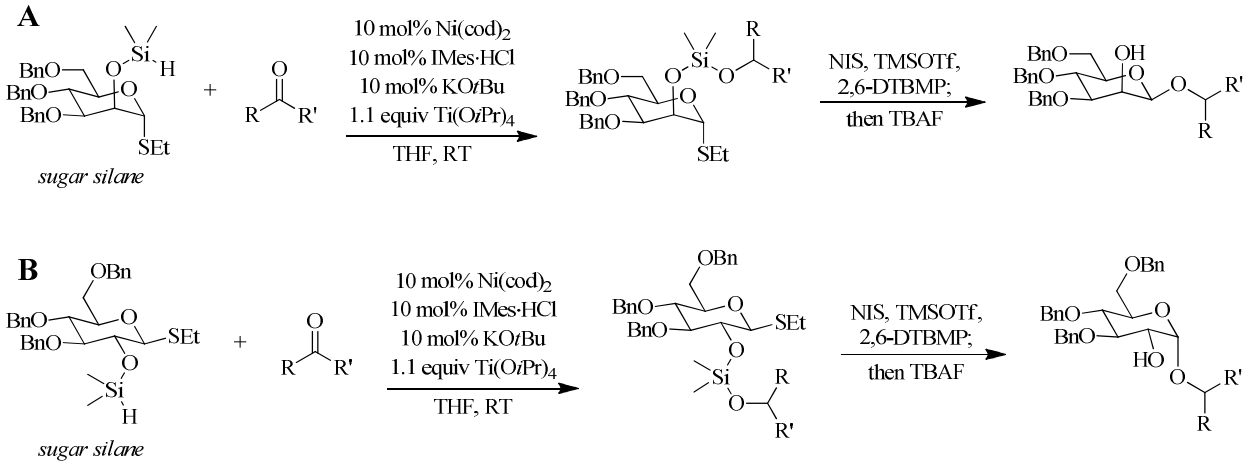

Scheme 4.9. Use of (A) mannosyl and (B) glucosyl sugar silanes in hydrosilylations of ketones followed by glycosylation.

The sugar silanes were also shown to be useful reagents in copper-catalyzed dehydrogenative silylation reactions. In fact, both this reaction and the nickel-catalyzed hydrosilylation reaction can be performed independently on a substrate containing both alcohol and ketone moieties without the use of protecting groups (Scheme 4.10). Treatment of substrate **51** with the sugar silane under nickel catalysis conditions led only to the hydrosilylation product (Scheme 4.10A), while treatment of the same substrate with the same sugar silane under copper catalysis conditions primarily produced the dehydrogenative silylation product (Scheme 4.10B).

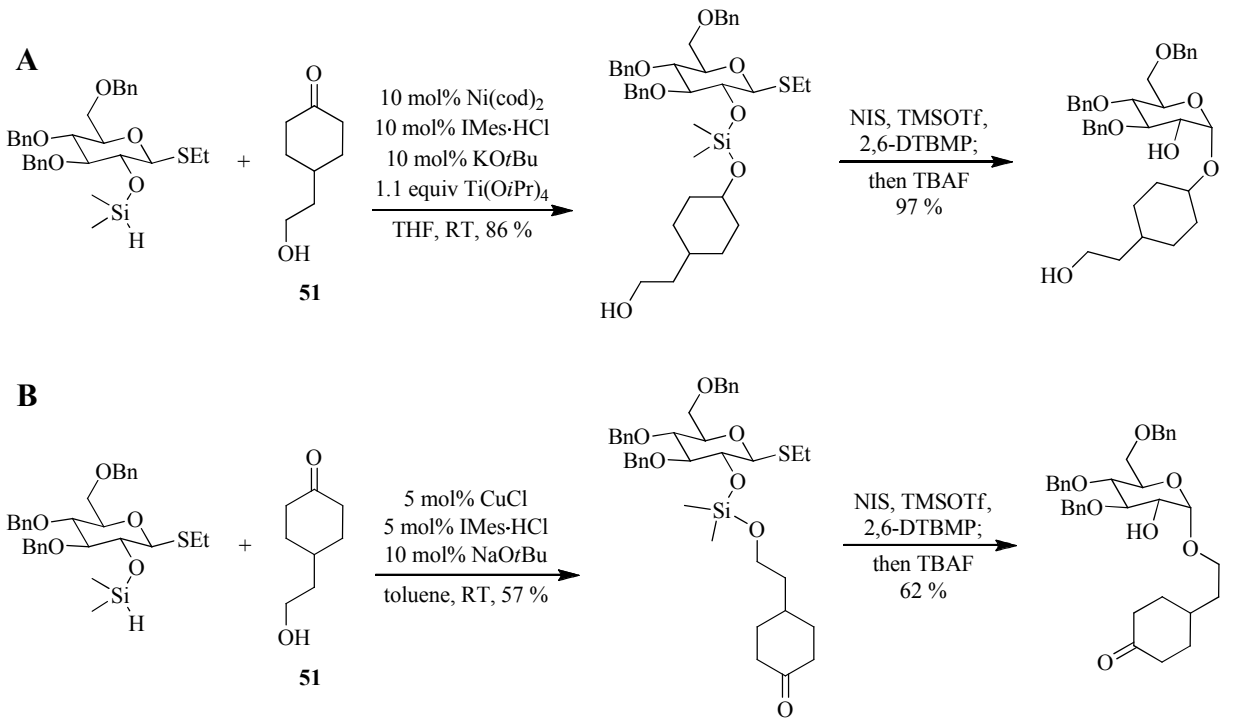

Scheme 4.10. (A) Nickel-catalyzed hydrosilyation and (B) copper-catalyzed dehydrogenative silylation of a keto-alcohol without the use of protecting groups.

4.3 Copper-Hydride Catalysis Using Simple Silanes

The dehydrogenative silylation reaction of alcohols with silyl hydrides is known to proceed under mild conditions with hydrogen gas being the only stoichiometric side product evolved. As mentioned above (section 4.2.3), the copper-based catalyst tends to be more reactive with more sterically hindered ketones and alcohols, and was therefore chosen for further exploration.

4.3.1 Copper-Phosphine Catalyzed Processes

The original report of utilizing a copper-hydride species to produce silyl ethers from alcohols used Stryker's catalyst, $(PPh_3CuH)_6$.[100] This seminal report presented the silylation of primary, secondary, and tertiary alcohols with a variety of silanes, including less reactive trialkyl silanes (Scheme 4.11). Dehydrogenative silylation occurred in the presence of alkenes and alkynes, which are known to undergo hydrosilylation reactions catalyzed by more reactive transition

metal catalysts. The scope of this reaction was later expanded through the use of a Cu-Xantphos catalyst system, prepared *in situ* from Cu-O*t*Bu and the ligand.[101]

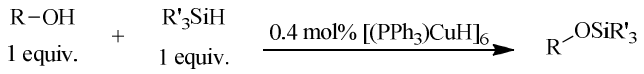

Scheme 4.11. Dehydrogenative silylation of alcohols using Stryker's catalyst.

Copper-hydride species with large "bowl-shaped" phosphine ligands have been utilized in the hydrosilylation of ketones, particularly the hydrosilylation of sterically hindered ketones in the presence of less sterically hindered ketones or the more reactive aldehyde functional group.[102] Furthermore, a variety of chiral ligands have been shown to promote the asymmetric hydrosilylation of ketones utilizing polymethylhydrosiloxane (PMHS) as the reducing agent.[103] These reactions involve cleavage of the silyl ether in the workup to yield the chiral alcohol product directly. Chiral phosphine ligands have also been used to facilitiate the asymmetric hydride addition to α,β-unsaturated esters.[104]

4.3.2 Copper-NHC Catalyzed Processes

Buchwald and co-workers expanded the use of copper-hydride catalysis with the development of copper-NHC complexes.[105] This catalyst system was able to promote the hydride addition to a wider range of α,β-unsaturated carbonyl compounds beyond esters. These reactions are proposed to proceed via the (NHC)CuH species, which has been characterized *in situ*.[106]

Nolan and co-workers pioneered the hydrosilylation of carbonyl functionalities using copper-NHC catalysts.[107] A variety of alkyl and aryl ketones can be reduced using the defined (IPr)CuCl complex and NaO*t*Bu to form the active catalyst (Scheme 4.12).[108] Sterically hindered ketones are also well tolerated in the reaction. Further studies showed that CuCl,

IPr·HCl, and NaO*t*Bu could be mixed to generate the active catalyst in solution without synthesizing an NHC-copper complex.[109]

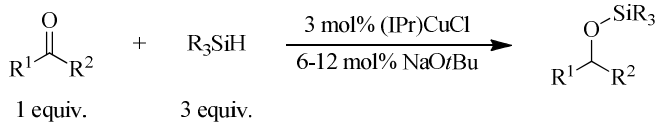

Scheme 4.12. Hydrosilylation of ketones catalyzed by (IPr)CuCl and NaO*t*Bu.

The proposed mechanism for this reaction begins with generation of the active copper hydride catalyst (Scheme 4.13A). The NHC·HX compound is deprotonated by NaO*t*Bu to produce (NHC)CuCl, which can then undergo ligand exchange with a second equivalent of NaO*t*Bu to generate (NHC)CuO*t*Bu. This copper alkoxide undergoes σ-bond metathesis with a sacrificial amount of silane to product the copper hydride complex. The ketone then coordinates, where hydride addition to the carbonyl carbon leads to a copper alkoxide, which undergoes σ-bond metathesis to produce the product and regenerate the active catalyst.

Cationic copper (I) complexes with two NHC ligands bound to the metal center were later shown to be more reactive than the single NHC ligand.[110] Detailed mechanistic studies indicate that the proposed active catalyst is the same for both catalytic systems; however, one NHC molecule is released upon production of the copper *t*-butoxide in the latter reaction (Scheme 4.13B). This nucleophilic free carbene promotes the final σ-bond metathesis between the copper alkoxide and the silane reducing agent to produce the product, increasing the rate of the reaction.[111]

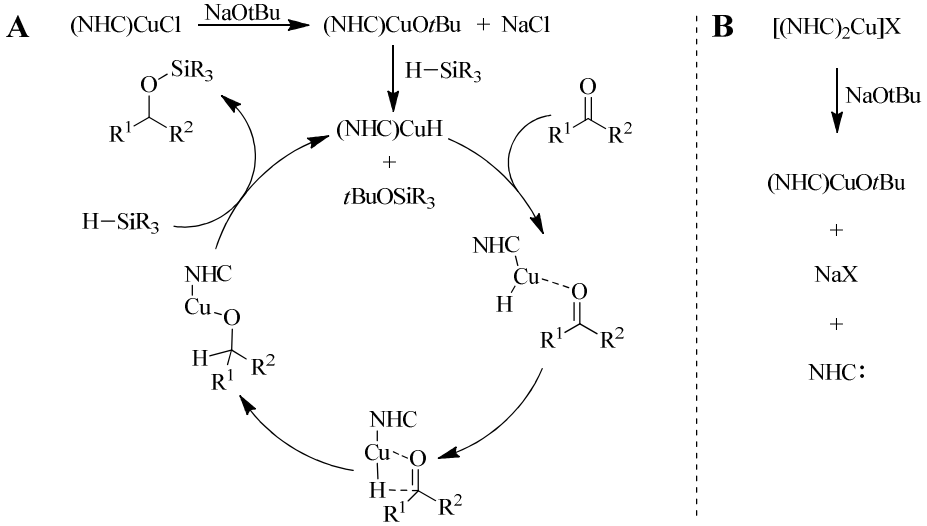

Scheme 4.13. Proposed catalytic cycle for hydrosilylation of ketones with an (NHC)CuH active catalyst. The catalyst can be formed from an (NHC)CuCl or $[(NHC)_2Cu]X$ precatalyst.

The copper-catalyzed O-H insertion is proposed to proceed through a similar pathway as the copper-catalyzed hydrosilylation reaction (Scheme 4.14). The active copper-hydride species is formed in the same manner as described above, and the alcohol then coordinates to this complex. σ-Bond metathesis generates hydrogen gas and a copper alkoxide, which can undergo another σ-bond metathesis to release the product and regenerate the active catalyst.

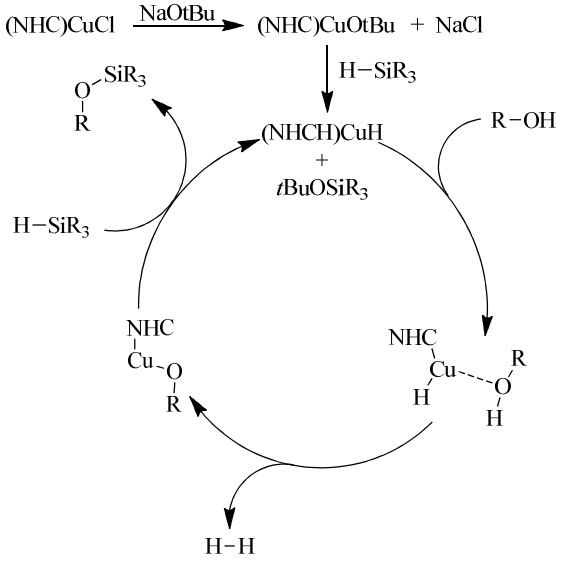

Scheme 4.14. Proposed catalytic cycle for the copper-catalyzed dehydrogenative silylation reaction.

4.4 Results and Discussion

Although the dimethyl sugar silanes function as effective reducing agents in the reactions presented above, they are unfortunately unstable to typical storage conditions. To prevent decomposition to the 2-hydroxy sugar, presumably by water, the substrate must either be stored under vacuum or frozen as a solution in benzene. This instability causes significant drawbacks in the ease of use, and a bench stable sugar silane is therefore desirable. Thus, the purpose of the following studies was to develop a more user friendly reagent for use as a reducing agent in the synthesis of silyl ether linked aglycones that can undergo intramolecular glycosylation.

4.4.1 Synthesis of Sugar Silane Reducing Agents

To increase the stability of the sugar silanes, bulkier alkyl groups on the silane itself were explored. These sugar silanes were synthesized in the same manner as the dimethyl sugar silanes from the reaction of 2-hydroxy sugar **52** or **53** with commercially available chlorodialkylsilanes. Both glucosyl and mannosyl sugar silanes were prepared (Table 4.1). Diisopropyl and diisobutyl groups were explored with the expectation that the increased bulk would increase their stability compared to the dimethyl sugar silanes. The diisobutyl groups are less sterically demanding around the silicon-hydride bond than the diisopropyl substitutents, which are anticipated to lead to enhanced reactivity for the diisobutyl over the diisopropyl sugar silanes. Both the diisopropyl and diisobutyl sugar silanes are chromatographable and bench stable for several months when stored in a dessicator.

Table 4.1. Synthesis of dialkyl sugar silanes.

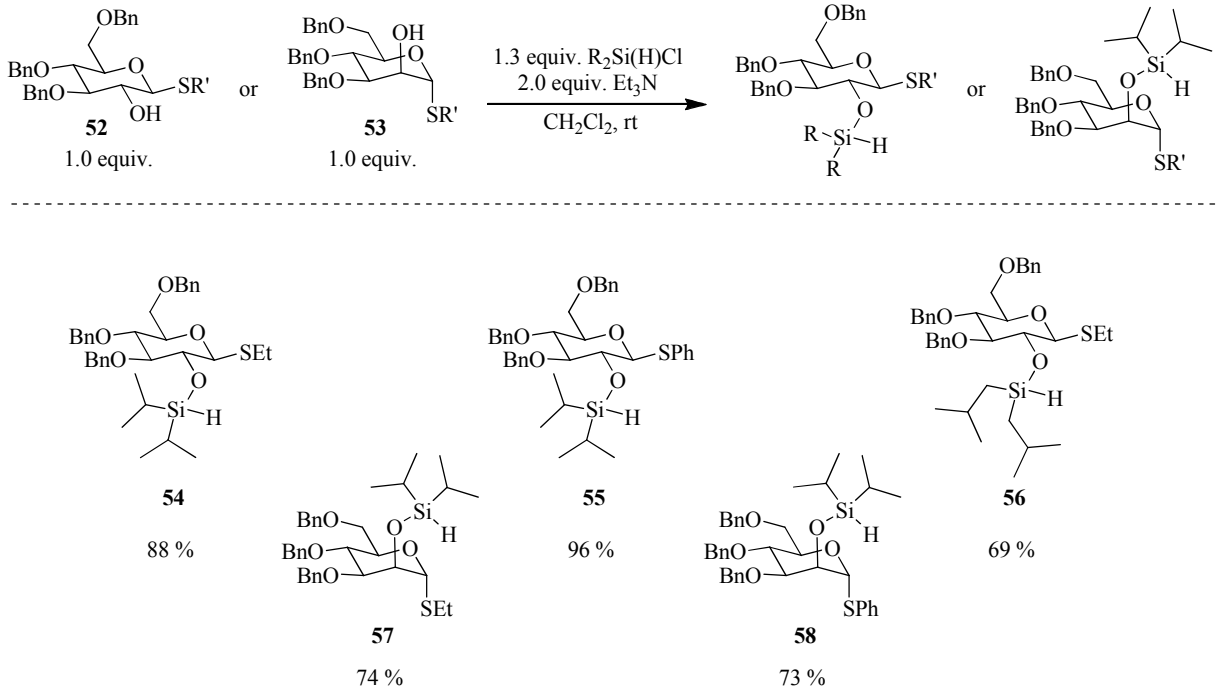

4.4.2 Copper-Catalyzed Dehydrogenative Silylation

When subjected to the copper-IMes catalyzed dehydrogenative silylation reaction at room temperature, both the diisopropyl and diisobutyl sugar silanes **54** and **56** gave lower yields of the products **59** and **60** than typical yields using the dimethyl sugar silane (Scheme 4.15). These lower yields are due to a significant amount of decomposition of the starting material to the 2-hydroxy sugar **52**. The diisopropyl sugar silane continued to be explored further over the diisobutyl sugar silane as it is a more cost effective approach.

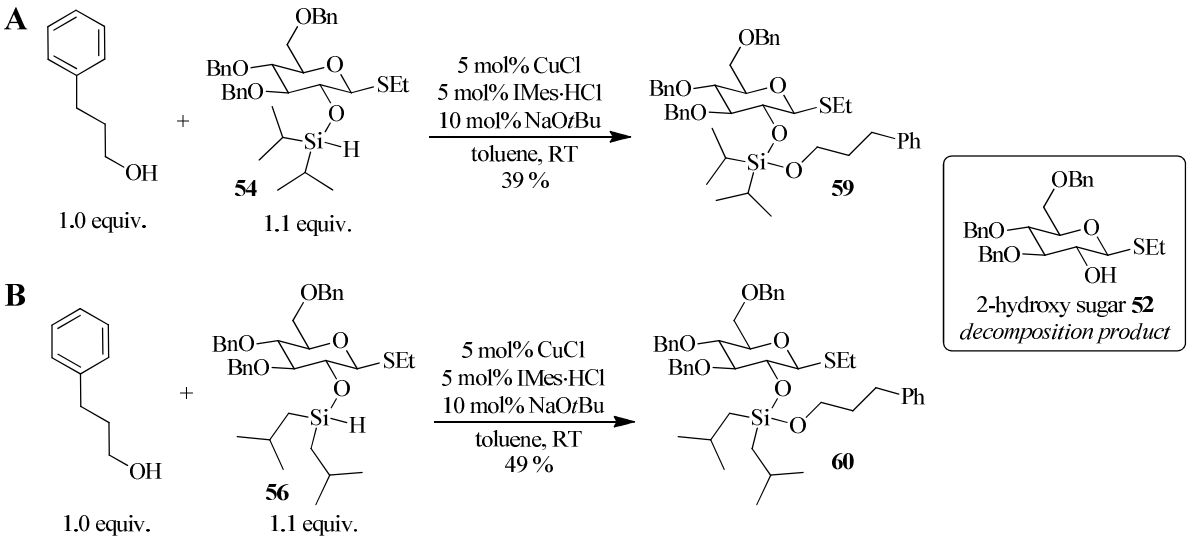

Scheme 4.15. Copper-catalyzed O-H insertion of (A) diisopropyl sugar silane X and (B) diisobutyl sugar silane X with 3-phenylpropan-1-ol.

4.4.2.1 Temperature Screen

A temperature screen was then run to determine whether or not synthetically useful yields could be achieved with diisopropyl sugar silane **54** (Table 4.2). It appears that even a slight increase in temperature significantly enhances the rate of the desired reaction over that of the detrimental decomposition. The optimal temperature of 60 °C was chosen, and this is the temperature at which the remaining optimization reactions were performed. In all cases, the remainder of the mass balance was observed as the decomposed side product **52**.

Table 4.2. Temperature screen.

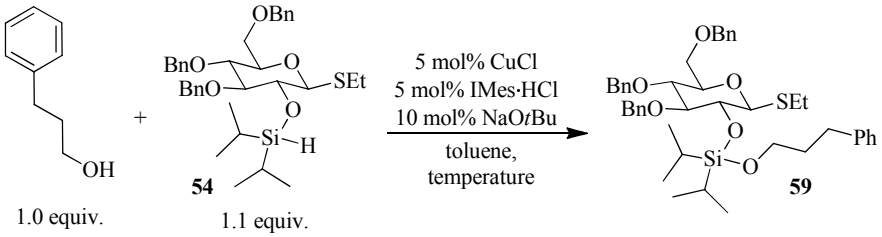

Temperature (˚C)	Yield
RT	39 %
40	58 %
50	58 %
60	67 %
70	61 %

4.4.2.2 NHC Ligand Screen

To further probe the possibility of increasing the yield of this reaction, a variety of NHC ligands were screened (Table 4.3). The ratio of ligand to metal was also altered, as this was shown to have an effect on the yield of hydrosilylation reactions when discreet NHC-copper catalysts were employed.[111] Changing the ligand to metal ratio from 1:1 to 2:1 decreased the yield of the product when using IMes. The more electron rich ligand SIMes did not enhance the yield, but the bulkier IPr ligand gave a yield similar to IMes when used in a 1:1 ratio with the copper. It should be noted that the reaction with IPr did not go to completion, and the sugar silane starting material and product are inseparable via column chromatography. This result indicates that IPr has the ability to suppress decomposition to the 2-hydroxy sugar, as the sugar silane starting material remains in the reaction mixture even after a prolonged reaction time. Switching to a 2:1 ratio of ligand to metal with IPr led to a sluggish reaction that proceeded to < 50 % conversion even after 24 h.

Table 4.3. NHC ligand screen.

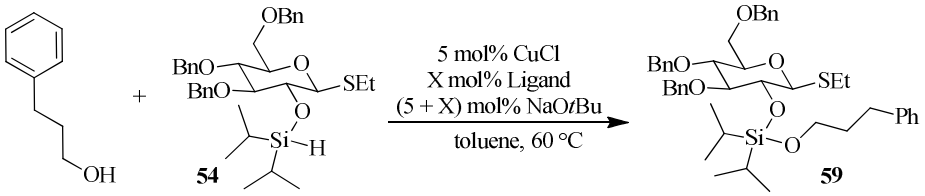

1.0 equiv. 1.1 equiv.

Ligand	X	Yield
IMes·HCl	5	67
IMes·HCl	10	45
SIMes·HCl	5	51
IPr·HCl	5	69
IPr·HCl	10	--*

*Reaction was not at 50 % conversion after 24 h, yield not determined

A screen of IMes and IPr was also performed using the secondary alcohol cyclohexanol (Table 4.4). A 1:1 ligand to metal ratio was used in both cases, as this ratio proved to be best with the primary alcohol shown above. For the secondary alcohol, IMes gave an increased yield of product **61** when compared to the primary alcohol. However, using IPr as the ligand led to minimal product, even after 24 h. Therefore, IMes was determined to be the best NHC ligand for the general reaction, as optimum yields were obtained for both primary and secondary alcohols.

Table 4.4. NHC ligand screen with a secondary alcohol substrate.

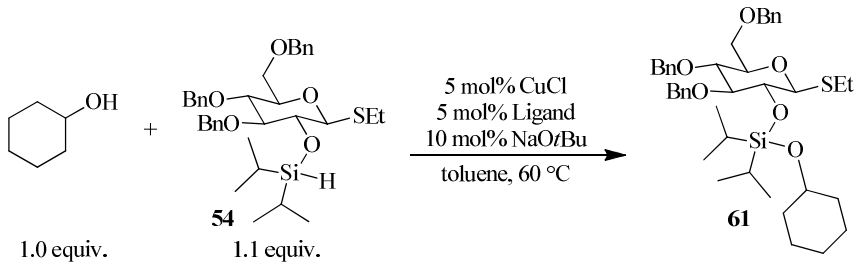

1.0 equiv. 1.1 equiv.

Ligand	Yield
IMes·HCl	85 %
IPr·HCl	NR*

*minimal product was observed after 24 h.

A number of control reactions were performed to discern the pathway leading to decomposition of the starting material (Table 4.5). Subjecting the starting material **54** to catalytic amounts of CuCl or IMes·HCl for a period of time longer than the typical productive reaction did not lead to any decomposition (entries 1 and 2). Similarly, HO*t*Bu and NaCl, which could both be produced under the reaction conditions, only led to recovered starting material (RSM, entries 3 and 4). Heating the starting material in toluene also did not lead to decomposition (entry 5).

Stirring the sugar silane starting material with 10 % NaO*t*Bu led to decomposition of approximately half of the original material in 4 h, as analyzed by ^{1}H NMR (entry 6). Subjection to 40 % NaO*t*Bu overnight led to complete decomposition to the 2-hydroxy sugar **52** overnight, and one equivalent of base led to faster decomposition (entries 7 and 8). Typical reaction conditions with exclusion of the alcohol led to a mixture of decomposition, recovered starting material, and silanol **62**, presumably formed from the successful dehydrogenative silylation reaction with trace water (entry 9).

Based on these control reactions, the source of decomposition seems to be related to *t*-butoxide in the reaction, as sodium *t*-butoxide catalyzes the desilylation reaction of the sugar silane starting material to the 2-hydroxy sugar. Unreacted sodium *t*-butoxide may be responsible for the decomposition that occurs under reaction conditions. Careful control of the amounts of the individual catalyst components added to the reaction leads to higher yields, faster reaction times, and suppression of decomposition of the starting material.

Table 4.5. Control reactions to determine source of decomposition of the starting material.

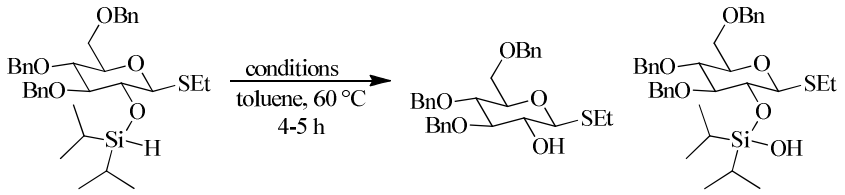

54 **52** **62**

Entry	Conditions	Results
1	5 % CuCl	RSM **54**
2	5 % IMes·HCl	RSM **54**
3	5 % HO*t*Bu	RSM **54**
4	10 % NaCl	RSM **54**
5	--	RSM **54**
6	10 % NaO*t*Bu	1:1 RSM **54**:**52**
7	40 % NaO*t*Bu (overnight)	**52**
8	1 equiv. NaO*t*Bu	**52**
9	5% CuCl, 5% IMes·HCl, 10% NaO*t*Bu	RSM **54**, **52**, **62**

The product **59** was also subjected to the catalyst system without either the sugar silane or alcohol starting material present (Scheme 4.16A). In a separate experiment, the catalyst was also formed in the presence of triethylsilane to generate the copper-hydride species that is the active catalyst in the O-H insertion reaction (Scheme 4.16B). Neither of these conditions led to any decomposition of the product, which appears to be stable under standard reaction conditions.

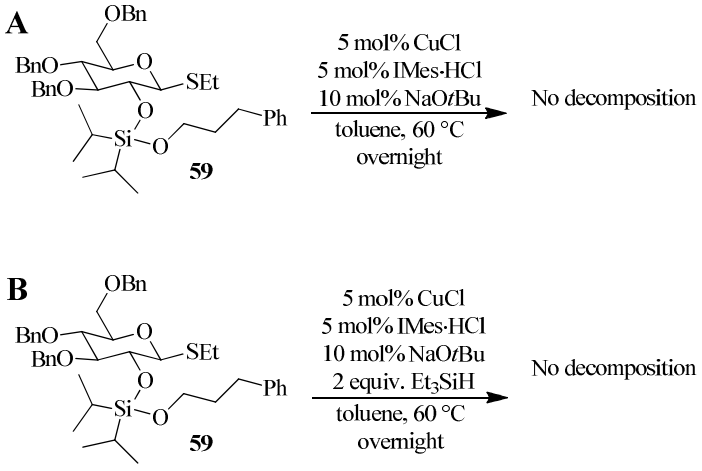

Scheme 4.16. Control reactions to test the stability of the product under reaction conditions.

Development of a discreet pre-catalyst or a different ligand scaffold that obviates the need for the addition of sodium *t*-butoxide to the reaction could also lead to better reactivity. Indeed, substitution of the NHC·HCl compounds with commercially available (NHC)CuCl complexes is viable (Table 4.6). These pre-formed catalysts still require the use of sodium *t*-butoxide to form the reactive copper *t*-butoxide complex, which undergoes σ-bond metathesis to yield the active copper hydride catalyst. While the two IMes ligand systems gave comparable yields (entries 1 and 2), a significant increase in yield was observed when switching from the IPr·HCl/CuCl system to the pre-formed (IPr)CuCl (entries 3 and 4). The latter reaction also went to completion in a similar time frame as the IMes reactions, whereas the three-component catalyst system never gave complete conversion of the starting material, even after an extended reaction time.

Table 4.6. Comparison of pre-formed (NHC)CuCl complexes and NHC·HCl/CuCl as pre-catalysts in dehydrogenative silylations.

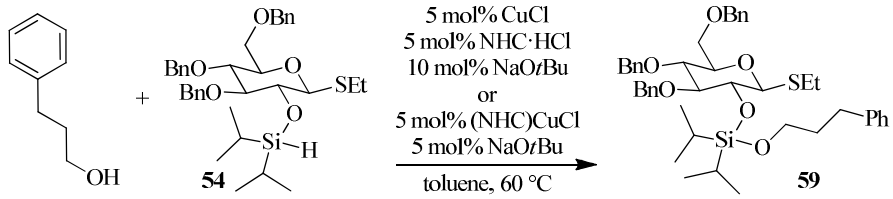

Entry	Pre-catalyst	Yield
1	IMes·HCl/CuCl	67 %
2	(IMes)CuCl	72 %
3	IPr·HCl/CuCl	69 %
4	(IPr)CuCl	81 %

4.4.2.3 Phosphine Ligand Screen

Because phosphine ligands have previously been utilized in forming copper hydride species, these were also screened in the dehydrogenative silylation reaction of diisopropyl sugar silanes with 3-phenylpropan-1-ol (Table 4.7). Monodentate ligand PPh_3 gave a 53 % yield after 3 h,

which was improved to 64 % by allowing the reaction to go to completion overnight. Bidentate ligand dppf gave a 52 % yield after 3 h, similar to that when PPh_3 is employed. However, PCy_3 and BINAP did not give any observable product. Although a clear trend was not observed among the different phosphine ligands, it is obvious that they are viable for this transformation.

Table 4.7. Screening of phosphine ligands

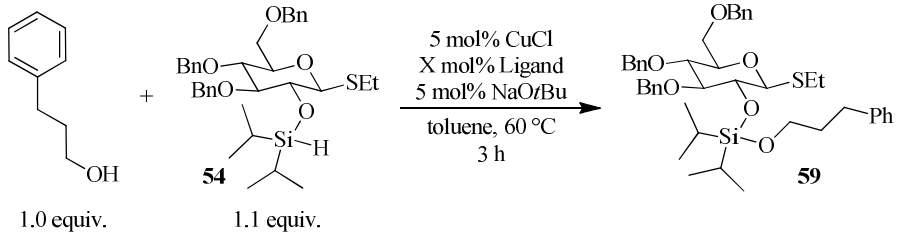

Ligand	X	Yield
PPh_3	10	53 %
PCy_3	10	NR[a]
dppf	5	52 %
(rac)-BINAP	5	NR[a]
Xantphos	5	45 %
PPh_3[b]	10	64 %

[a]NR = no reaction observed
[b]reaction run to full conversion (20h)

4.4.2.4 Substrate Scope

The scope of the reaction was then explored using the optimized procedure (Table 4.8). Both glucosyl and mannosyl sugar silanes were utilized in combination with primary and secondary alcohols. Simple alcohols such as 3-phenylpropan-1-ol and cyclohexanol were well tolerated in the reaction, forming products **59**, **61**, **64**, and **69**. The more complex steroid was also tolerated to form **63**, and no products resulting from hydrosilylation of the ketone were observed. Menthol also underwent the reaction to give the products **65**, **66**, **67**, and **68**, which include both glucose and mannose sugar silanes as well as thioethyl and thiophenyl leaving groups (*vida*

infra). A general trend was recognized that secondary alcohols give better yields in the reaction than primary alcohols.

Table 4.8. Scope of the O-H insertion reaction with glucose and mannose sugar silanes.

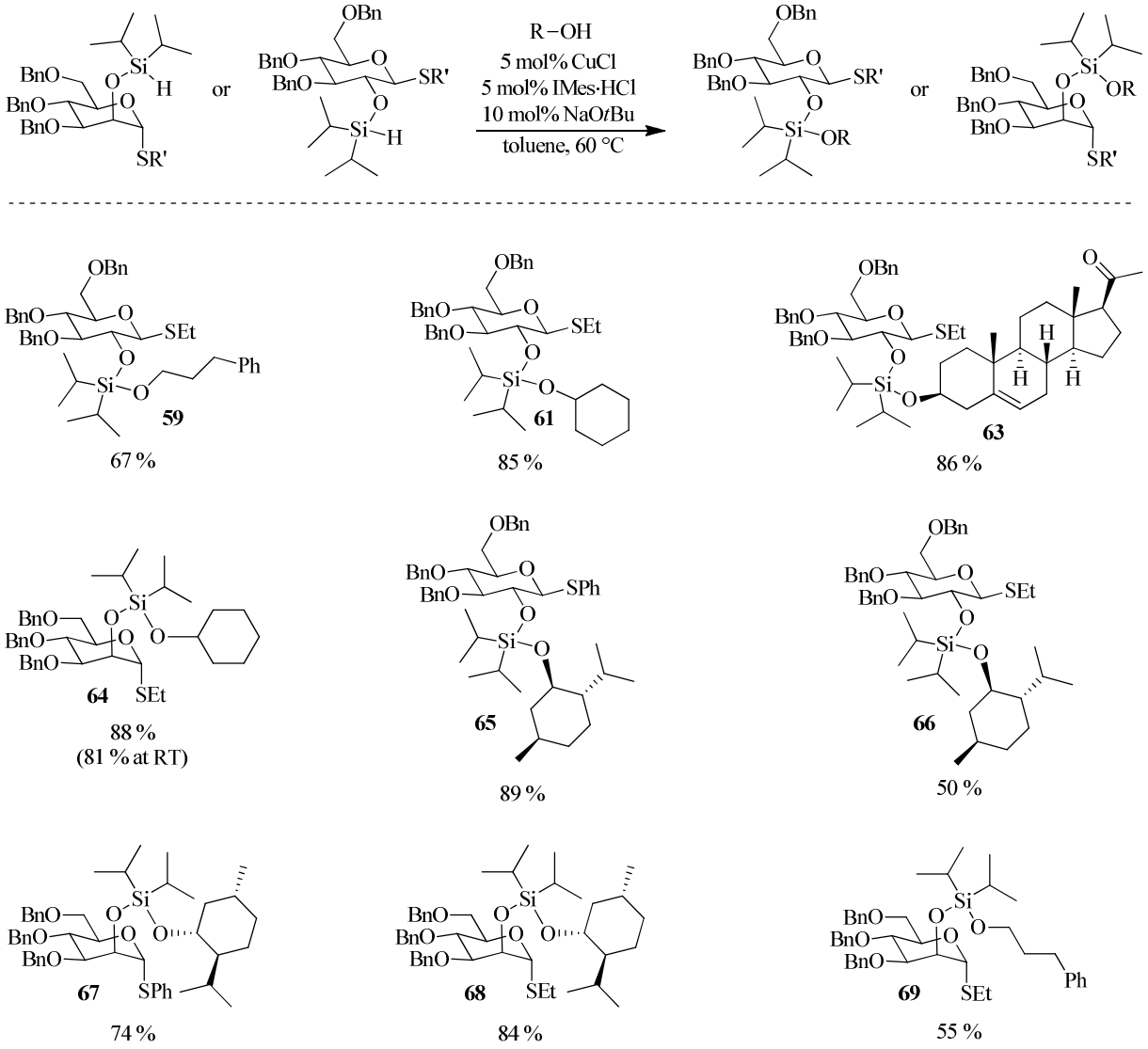

4.4.2.5 Screening of Other Catalysts

Following the development of a bench stable sugar silane reagent, several air stable copper pre-catalysts were screened for efficiency in dehydrogenative silylations. All of these catalysts have been shown previously to form copper-hydride species in solution and have been used for

hydride addition reactions. Unfortunately, CuF_2[112] and $CuCl_2 \cdot 2H_2O$[105] did not exhibit reactivity under the same conditions employed in previous studies. Development of a bench stable catalyst or pre-catalyst will significantly enhance the utility of this reaction.

4.4.3 Glycosylations

The products described above were also subjected to glycosylation conditions to ensure that the more sterically hindered diisopropyl groups did not hinder this important step (Scheme 4.17). All substrates performed similarly to those containing the dimethyl silane moiety. Both primary and unhindered secondary alcohols give good yields of glycosylated products **70** and **71** in the glucose case, with the cyclohexanol group also undergoing glycosylation in excellent yield to give **72** in the mannose series.

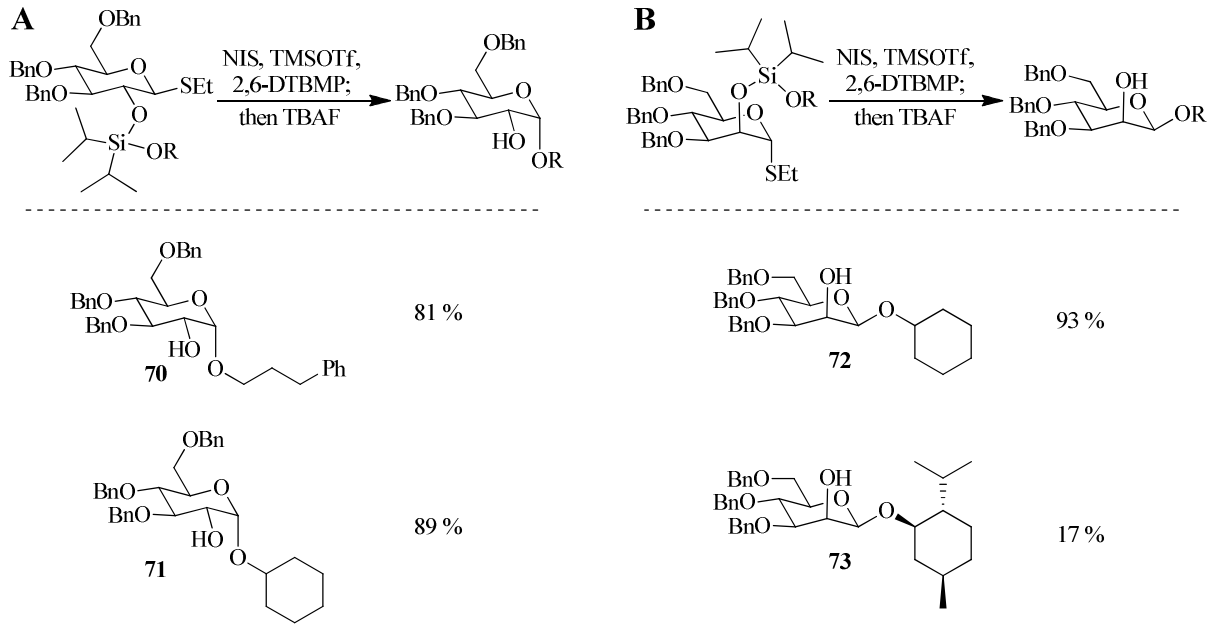

Scheme 4.17. Glycosylation of (A) glucose series and (B) mannose series substrates.

However, the hindered secondary alcohol menthol gave a poor yield of **73** in the glycosylation step. As seen with the dimethyl sugar silanes, switching the leaving group from

thioethyl to the more activated thiophenyl led to an improved glycosylation yield (Scheme 4.18). This improved yield was observed for both the glucose and mannose series to give α-glucoside **74** and β-mannoside **73**.

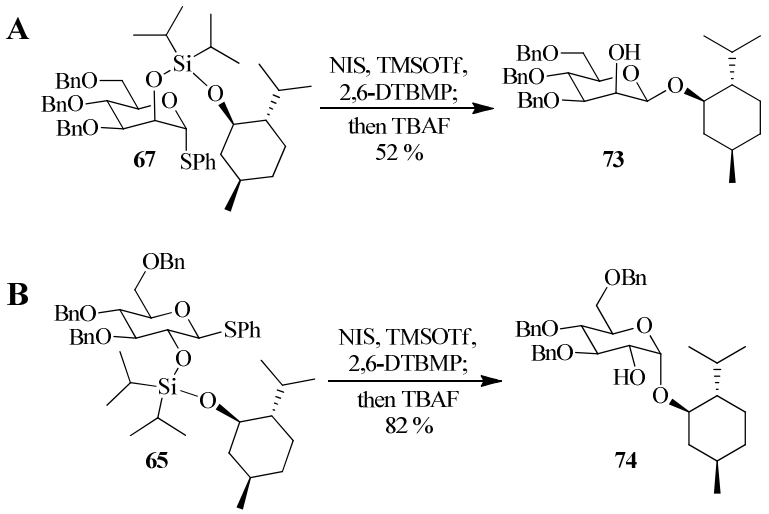

Scheme 4.18. Glycosylation of (A) glucose and (B) mannose with the menthol aglycone and thiophenyl leaving group.

4.5 Conclusions and Outlook

A bench stable sugar silane has been developed that is stable to storage in air for several months without noticeable decomposition to the 2-hydroxysugar. This substrate undergoes copper-catalyzed O-H insertion with a variety of primary and secondary alcohols, and the intramolecular glycosylation of the resulting silyl-linked aglycones also proceeds in excellent yields. Dehydrogenative silylation proceeds selectively in the presence of a ketone, which has been demonstrated to undergo hydrosilylation in previous studies with the copper catalyst system used.

While this new diisopropyl sugar silane is more stable and easier to handle than the previously developed dimethyl sugar silane, the catalyst components decompose in air and therefore must be stored under an inert atmosphere. An improvement of the current system

would be the development of a catalyst that can be stored in an open atmosphere and is simpler to use. Commercially available (NHC)CuCl complexes have been shown to be viable in the reaction, laying the foundation for the development of a more user-friendly catalyst system.

Another direction for this project is to utilize the copper catalyst for the hydrosilylation of carbonyl groups. Use of chiral phosphines would promote the diasteroselective reduction of ketones, a transformation that has yet to be realized with the sugar silane reducing agent as the chirality present in the sugar moiety does not induce significant diastereoselectivity (see section 4.2.3).

Chapter 5

Conclusions

The development of new and more streamlined synthetic organic methodologies leads to the more efficient synthesis of known and novel compounds. Many molecules of interest are natural products or derivatives thereof, owing to their fascinating roles in the organisms in which they are produced. A significant amount of research has been dedicated to the study of how these molecules are made in nature, what their bioactivities are, how they function, and the development of new ways to make them synthetically. Inspired by the biosynthesis of macrolide natural products, three methodologies have been investigated in this thesis.

The first reaction that was explored involved the use of the P450 monooxygenase PikC in a chemoenzymatic fashion, where selective oxidation of simple unnatural substrates was exhibited. The sugar desosamine was introduced as an anchoring group in this technique, based on previous work which had shown that the protonated dimethylamino group forms a salt bridge in the active site of the enzyme, positioning the remote parts of the aglycone closest to the heme center.

Macrocyclic ring containing unnatural substrates, which were the substrates tested that are most similar to the enzyme's endogenous substrates, led to the highest conversion to mono-hydroxylated products. Several carbolides containing smaller-sized rings and linear aglycones were not oxidized by PikC, presumably because none of the C-H bonds were near enough to the iron-oxide center to be activated. However, an 11-carbon terminal alkyne substrate was oxidized

in low yield to give predominantly the product resulting from oxidation of the most electronically activated propargylic position, mirroring the enzyme's natural function.

PikC was able to oxidize these unnatural substrates with moderate yields and selectivities. Co-crystal structures of two of the macrocycle-containing substrates bound to the enzyme revealed that desosamine is performing as the anchoring group, and that the C-H bonds located nearest the heme iron are the ones being oxidized, as assessed through synthesis of the authentic hydroxylated standards. Research currently being conducted in this area is looking at simpler tethers that can function as removable anchoring groups.

Secondly, a general procedure for regioselective nickel-catalyzed reductive macrocyclization of terminal alkynes tethered to aldehydes was explored. By switching the ligand on the nickel catalyst, both the endo and exocyclic products could be favored, allowing for the formation of two differently sized macrocycles from the same starting material. Ring strain associated with the products is difficult to overcome, and only modest selectivities for the exocyclic products were observed. However, the regioselectivity reversal that had previously been observed in intermolecular reactions with terminal alkynes is shown for the first time in macrocyclizations.

The final project discusses the development of a more bench stable reagent for use as a reducing agent in metal-catalyzed reactions. While the dimethyl sugar silanes previously developed participated satisfactorily in hydrosilylation and O-H insertion reactions, they were found to be sensitive to air, moisture, and column chromatography, rapidly decomposing back to the starting alcohol. Diisopropyl sugar silanes were therefore developed, which are bench stable for several months before decomposition is observed.

These newly developed substrates undergo dehydrogenative silylation at elevated temperatures with a variety of alcohols. Simple, complex, and sterically hindered alcohols are

all tolerated under reaction conditions. The resultant products containing diisopropyl silyl acetals proceed in the intramolecular glycosylation step with good yields, providing exclusively 1,2-*cis*-glycosides. This project improves upon the existing methodology by incorporation of more user-friendly reagents. Future directions should include development of a bench stable catalyst for this reaction so that all reagents can be stored and handled with ease.

The three projects described in this thesis are all related to the overall goal of improving synthetic chemists' toolboxes. Particularly, they are all derived from the natural bioactivity and biosynthesis of macrolide natural products. Utilization of these techniques to synthesize derivatives of known compounds can lead to the development of more potent drugs, a never-ending pharmaceutical battle.

Chapter 6

Experimental Procedures

6.1 General Statement

All reagents were used as received unless otherwise noted. Solvents were purified under nitrogen using a solvent purification system (Innovative Technology, Inc., Model # SPS400-3 and PS-400-3). $Ni(cod)_2$, IMes·HCl, IPr·HCl were purchased from Strem Chemicals, Inc. CuCl, IMesCuCl, and IPrCuCl were purchased from Sigma Aldrich. These chemicals, sodium *tert*-butoxide, and potassium *tert*-butoxide were stored and weighed in an inert atmosphere glovebox. All reactions were conducted in flame- or oven-dried glassware under a nitrogen atmosphere unless otherwise noted. ^{1}H and ^{13}C NMR spectra were obtained in $CDCl_3$ at room temperature, unless otherwise noted, on a Varian vnmrs 700 MHz, Varian vnmrs 500 MHz, Varian Inova 500 MHz, Varian MR 400 MHz, or Varian Inova 400 MHz instrument. Chemical shifts of ^{1}H NMR spectra were recorded in parts per million (ppm) on the δ scale from an internal standard of residual chloroform (7.27 ppm). Chemical shifts of ^{13}C NMR spectra were recorded in ppm from the central peak of $CDCl_3$ (77.0 ppm) on the δ scale. Low resolution electrospray mass spectra were obtained on a Micromass LCT spectrometer and high resolution electrospray mass spectra were obtained on a Micromass AutoSpec Ultima spectrometer at the University of Michigan Mass Spectrometry Laboratory.

6.2 Chapter 2 Experimental

General procedure for glycosylation with desosamine[113]

A suspension of alcohol (1.0 equiv), 4-(dimethylamino)-2-fluoro-6-methyltetrahydro-2*H*-pyran-3-yl acetate (2.0 equiv) and molecular sieves (4Å) in dichloromethane was stirred for 30 min. $BF_3.OEt_2$ (4.0 equiv, freshly distilled from CaH_2) was added to the ice cooled reaction mixture and stirred for 1 h at 0 °C. The reaction mixture was neutralized with saturated sodium bicarbonate solution and extracted with ethyl acetate. The combined organic layers were dried with $MgSO_4$, filtered, concentrated, and purified by column chromatography (SiO_2, 5 % MeOH/ EtOAc).

General procedure for acetate deprotection

To the solution of the acetate obtained above (1 equiv) in methanol (20 mL/mmol), K_2CO_3 (4 equiv) was added as a solid and stirred at rt until the starting material was consumed as judged by TLC analysis. The reaction mixture was diluted with brine and extracted with ethyl acetate. The combined organic layers were dried with $MgSO_4$, filtered, and concentrated to afford the deprotected desosamine conjugate.

6.2.1 Synthesis of Unnatural Substrates

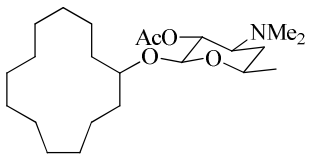

2-(Cyclotridecyloxy)-4-(dimethylamino)-6-methyltetrahydro-2*H*-pyran-3-yl acetate.

Following the general procedure, cyclotridecanol (21 mg, 0.11 mmol, prepared by $NaBH_4$ reduction of cyclotridecanone), 4-(dimethylamino)-2-fluoro-6-methyltetrahydro-2*H*-pyran-3-yl

acetate (30 mg, 0.14 mmol), molecular sieves (150 mg) and $BF_3 \cdot OEt_2$ (28 μL, 2.8 mmol) were employed to obtain 2-(cyclotridecyloxy)-4-(dimethylamino)-6-methyltetrahydro-2*H*-pyran-3-yl acetate (28 mg, 0.07 mmol, 64 %) after column chromatography (SiO_2, ethyl acetate) as a white solid. ^{1}H NMR (400 MHz): δ 4.80 (dd, *J* = 10.4, 7.6 Hz, 1H) 4.33 (d, *J* = 7.6 Hz, 1H) 3.62 (quint, *J* = 6.0 Hz, 1H) 3.52 (dqd, *J* = 10.8, 6.0, 2.0 Hz, 1H) 2.74 (ddd, *J* = 12.8, 10.4, 4.4 Hz, 1H) 2.27 (s, 6H) 2.05 (s, 3H) 1.72 (ddd, *J* = 13.2, 4.4, 2.0 Hz, 1H) 1.66-1.32 (m, 25H), 1.25 (d, *J* = 6.0 Hz, 3H); ^{13}C NMR (100 MHz): δ 169.9, 101.5, 79.0, 71.1, 69.0, 63.2, 40.6, 32.7, 31.5, 30.9, 26.6, 26.5, 26.1, 26.0, 25.80, 25.78, 25.6, 22.7, 22.4, 21.3, 21.2; HRMS (ESI) *m/z* calculated for $[M+H]^+$ 398.3270 found 398.3260.

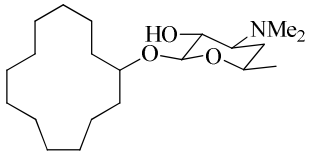

2-(Cyclotridecyloxy)-4-(dimethylamino)-6-methyltetrahydro-2*H*-pyran-3-ol. Following the general procedure, 2-(cyclotridecyloxy)-4-(dimethylamino)-6-methyltetrahydro-2*H*-pyran-3-yl acetate (16 mg, 0.04 mmol), K_2CO_3 (50 mg, 0.36 mmol), and methanol (2 mL) were employed to afford 2-(cyclotridecyloxy)-4-(dimethylamino)-6-methyltetrahydro-2*H*-pyran-3-ol (13 mg, 0.037 mmol, 91 % yield) as a white solid. ^{1}H NMR (400 MHz): δ 4.28 (d, *J* = 6.8 Hz, 1H) 3.73 (quint, *J* = 5.8 Hz, 1H) 3.53 (dqd, *J* = 10.4, 6.4, 2.0 Hz, 1H) 3.26 (dd, *J* = 10.0, 6.8 Hz, 1H) 3.09 (br s, 1H) 2.53 (ddd, *J* = 12.0, 10.0, 3.8 Hz, 1H) 2.28 (s, 6H) 1.61-1.52 (m, 5H) 1.36-1.17 (m, 21H) 1.18 (d, *J* = 6.4 Hz, 3H); ^{13}C NMR (100 MHz): δ 102.8, 78.3, 70.0, 69.4, 65.4, 40.4, 32.8, 31.7, 28.9, 26.59, 26.57, 26.1, 26.0, 25.9, 25.7, 25.6, 22.7, 22.6, 21.4; HRMS (ESI) *m/z* calculated for $[M+H]^+$ 356.3165 found 356.3164.

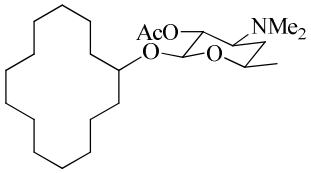

2-(Cyclotetradecyloxy)-4-(dimethylamino)-6-methyltetrahydro-2*H*-pyran-3-yl acetate. Following the general procedure, cyclotetradecanol (8 mg, 0.038 mmol), 4-(dimethylamino)-2-fluoro-6-methyltetrahydro-2H-pyran-3-yl acetate (10 mg, 0.045 mmol), molecular sieves (100 mg) and $BF_3{\cdot}OEt_2$ (10 μL, 0.1 mmol) were employed to obtain 2-(cyclotetradecyloxy)-4-(dimethylamino)-6-methyltetrahydro-2*H*-pyran-3-yl acetate (10 mg, 0.024 mmol, 64 %) after column chromatography (SiO2, ethyl acetate) as a white solid. ^{1}H NMR (400 MHz): δ 4.80 (dd, *J* = 10.6, 7.4 Hz, 1H) 4.33 (d, *J* = 7.2 Hz, 1H) 3.69 (quint, *J* = 5.8 Hz, 1H) 3.52 (dqd, *J* = 10.8, 6.0, 1.8 Hz, 1H) 2.73 (ddd, *J* = 12.0, 10.4, 4.4 Hz, 1H) 2.27 (s, 6H) 2.05 (s, 3H) 1.72 (ddd, *J* = 13.2, 4.6, 2.0 Hz, 1H) 1.59-1.51 (m, 4H) 1.46-1.25 (m, 23 H) 1.25 (d, *J* = 6.0 Hz, 3H); ^{13}C NMR (100 MHz): δ 169.8, 101.5, 78.1, 71.2, 69.0, 63.2, 40.6, 31.8, 31.0, 30.4, 26.0, 25.8, 25.61, 25.57, 24.61, 24.59, 24.5, 24.4, 21.7, 21.3, 21.2, 21.1; HRMS (ESI) *m/z* calculated for $[M+H]^+$ 412.3427, found 412.3436.

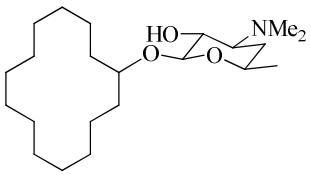

2-(Cyclotetradecyloxy)-4-(dimethylamino)-6-methyltetrahydro-2*H*-pyran-3-ol. Following the general procedure, 2-(cyclotetradecyloxy)-4-(dimethylamino)-6-methyltetrahydro-2*H*-pyran-3-yl acetate (8 mg, 0.019 mmol), K_2CO_3 (15 mg, 0.11 mmol), and methanol (2 ml) were employed to afford 2-(cyclotetradecyloxy)-4-(dimethylamino)-6-methyltetrahydro-2*H*-pyran-3-ol (6 mg, 0.016 mmol, 86 % yield) as a white solid. ^{1}H NMR (400 MHz): δ 4.29 (d, *J* = 7.2 Hz, 1H) 3.81 (quint, *J* = 5.7 Hz, 1H) 3.54 (dqd, *J* = 10.4, 6.4, 2.0 Hz, 1H) 3.28 (dd, *J* = 10.0, 7.6 Hz)

3.00 (br s, 1H) 2.58 (ddd, *J* = 12.4, 10.0, 4.0 Hz, 1H) 2.32 (s, 6H) 1.72-1.25 (m, 28H) 1.25 (d, *J* = 5.6 Hz, 3H); ^{13}C NMR (100 MHz): δ 102.7, 77.6, 70.1, 69.4, 65.4, 40.4, 31.8, 30.4, 29.2, 25.9, 25.8, 25.67, 25.65, 25.5, 24.64, 24.59, 24.4, 24.3, 21.6, 21.4, 21.3; HRMS (ESI) *m/z* calculated for $[M+H]^+$ 370.3321 found 370.3307.

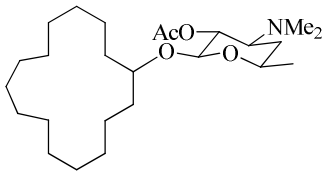

2-(Cyclopentadecyloxy)-4-(dimethylamino)-6-methyltetrahydro-2*H*-pyran-3-yl acetate. Following the general procedure, cyclopentadecanol (35 mg, 0.15 mmol), 4-(dimethylamino)-2-fluoro-6-methyltetrahydro-2H-pyran-3-yl acetate (22 mg, 0.10 mmol), molecular sieves (200 mg) and $BF_3{\cdot}OEt_2$ (20 μL, 0.20 mmol) were employed to obtain 2-(cyclopentadecyloxy)-4-(dimethylamino)-6-methyltetrahydro-2*H*-pyran-3-yl acetate (19 mg, 0.045 mmol, 45 %) after column chromatography (SiO2, ethyl acetate) as a white solid. ^{1}H NMR (400 MHz): δ 4.76 (dd, *J* = 10.8, 7.6 Hz, 1H) 4.29 (d, *J* = 7.6 Hz, 1H) 3.53-3.60 (m, 1H) 3.48 (dqd, *J* = 12.4, 6.4, 2.0 Hz, 1H) 2.70 (ddd, *J* = 12.4, 10.8, 4.4 Hz, 1H) 2.23 (s, 6H) 2.01 (s, 3H) 1.69 (ddd, *J* = 13.2, 4.4, 2.0 Hz, 1H) 1.23-1.60 (m, 29 H) 1.21 (d, *J* = 6.4 Hz, 3H); ^{13}C NMR (100 MHz): δ 169.8, 101.3, 78.8, 71.0, 68.9, 63.1, 40.5, 33.1, 31.7, 30.9, 27.3, 27.2, 26.8, 26.7, 26.6, 26.5, 23.1, 22.5, 21.2, 21.1; LRMS (ESI) *m/z* calculated for $[M+H]^+$ 426.3 found 426.3.

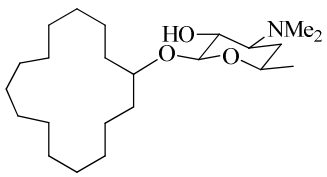

2-(Cyclopentadecyloxy)-4-(dimethylamino)-6-methyltetrahydro-2*H*-pyran-3-ol. Following the general procedure, 2-(cyclopentadecyloxy)-4-(dimethylamino)-6- methyltetrahydro-2*H*-pyran-3-yl acetate (10 mg, 0.023 mmol), K_2CO_3 (15 mg, 0.10 mmol), and methanol (2ml) were

employed to afford 2-(cyclopentadecyloxy)-4-(dimethylamino)-6-methyltetrahydro-2*H*-pyran-3-ol (8 mg, 0.021 mmol, 91 % yield) as a white solid. ^{1}H NMR (500 MHz): δ 4.30 (d, *J* = 7.0 Hz, 1H) 3.72 (quint, *J* = 6.0 Hz, 1H) 3.55 (dqd, *J* = 12.5, 6.0, 2.0 Hz, 1H) 3.32 (dd, *J* = 10.0, 7.5 Hz, 1H) 2.70 (ddd, *J* = 12.5, 10.5, 4.0 Hz, 1H) 1.75 (ddd, *J* = 12.5, 4.5, 2.0 Hz, 1H) 1.54-1.68 (m, 4H) 1.28- 1.45 (m, 25H) 1.27 (d, *J* = 6.0 Hz, 3H); ^{13}C NMR (100 MHz): δ 102,6, 78.5, 70.0, 69.1, 65.0, 45.0, 40.1, 33.2, 32.0, 29.6, 27.3, 27.2, 26.9, 26.8, 26.7, 26.6, 26.5, 23.1, 22.9, 21.2; LRMS (ESI) *m/z* calculated for $[M+H]^+$ 384.3 found 384.3.

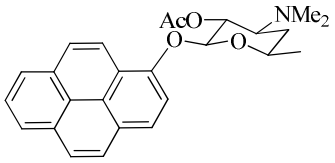

4-(Dimethylamino)-6-methyl-2-(pyren-1-yloxy)tetrahydro-2H-pyran-3-yl acetate. Following the general procedure, 1-hydroxypyrene (20 mg, 0.091 mmol), 4-(dimethylamino)-2-fluoro-6-methyltetrahydro-2H-pyran-3-yl acetate (25 mg, 0.114 mmol), molecular sieves (200 mg) and $BF_3 \cdot OEt_2$ (25 μL, 0.25 mmol) were employed to obtain 4-(dimethylamino)-6-methyl-2-(pyren-1-yloxy)tetrahydro-2H-pyran-3-yl acetate (23 mg, 0.055 mmol, 61 %) after column chromatography (SiO2, ethyl acetate) as a white solid. ^{1}H NMR (400 MHz): δ 8.32 (d, *J* = 9.2 H, 1H) 7.99-8.11 (m, 4H) 7.88-7.96 (m, 3H) 7.69 (d, *J* = 8.4 Hz, 1H) 5.39 (dd, *J* = 10.4, 8.0 Hz, 1H) 5.19 (d, *J* = 7.6 Hz, 1H) 3.82 (dqd, *J* = 12.0, 6.0, 1.6 Hz, 1H) 2.91 (ddd, *J* = 12.0, 10.8, 4.4 Hz, 1H) 2.35 (s, 6H) 2.03 (s, 3H) 1.86 (ddd, *J* = 13.2, 4.4, 1.6 Hz, 1H) 1.55 (q, *J* = 12.4 H, 1H) 1.37 (d, *J* = 6.4 Hz, 3H); ^{13}C NMR (100 MHz): δ 170.3, 151.4, 131.4, 127.0, 126.9, 126.5, 126.1, 125.6, 125.5, 125.2, 124.6, 124.5, 124.4, 121.0, 112.2, 101.7, 70.6, 69.8, 62.9, 40.7, 30.8, 21.3, 21.2; HRMS (ESI MS) *m/z* calculated for $[M+H]^+$ 418.2018 found 418.2008.

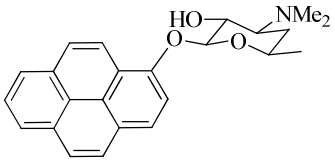

4-(Dimethyl amino)-6-methyl-2-(pyren-1-yloxy)tetrahydro-2*H*-pyran-3-ol. Following the general procedure, 4-(dimethyl amino)-6-methyl-2-(pyren-1-yloxy)tetrahydro-2*H*-pyran-3-yl acetate (23 mg, 0.055 mmol), K_2CO_3 (30 mg, 0.22 mmol), and methanol were employed to afford 4-(dimethyl amino)-6-methyl-2-(pyren-1-yloxy)tetrahydro-2*H*-pyran-3-ol (14 mg, 0.037 mmol, 68 % yield) as a white solid. ^{1}H NMR (400 MHz): δ 8.59 (d, *J* = 9.2 Hz, 1H) 8.00-8.14 (m, 4H) 7.88- 7.99 (m, 3H) 7.76 (d, *J* = 8.4 Hz, 1H) 5.14 (d, *J* = 7.2 Hz, 1H) 3.80 (dd, *J* = 10.4, 7.6 Hz, 1H) 3.72 (dqd, *J* = 12.4, 10.0, 1.6 Hz, 1H) 3.59 (br s, 1H) 2.71 (ddd, *J* = 12.4, 10.4, 4.0 Hz, 1H) 2.38 (s, 6H) 1.78 (ddd, *J* = 12.8, 4.0, 2.0 Hz, 1H) 1.42 (q, *J* = 12.4 Hz, 1H) 1.31 (d, *J* = 6.0 Hz, 3H); ^{13}C NMR (100 MHz): δ 158.6, 151.3, 131.5, 131.4, 127.0, 126.7, 126.0, 125.6, 125.2, 124.7, 124.5, 124.4, 121.7, 121.6, 113.8, 103.7, 70.1, 69.8, 65.5, 40.3, 28.6, 21.3; HRMS (ESI MS) *m/z* calculated for $[M+H]^+$ 376.1913 found 376.1907.

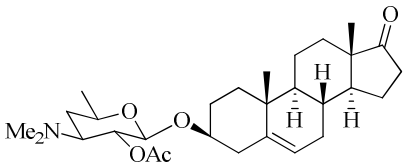

(2*S*,3*R*,4*S*,6*R*)-2-((3*S*,8*R*,9*S*,10*R*,13*S*,14*S*)-10,13-dimethyl-17-oxo-2,3,4,7,8,9,10,11,12,13,14,15,16,17-tetradecahydro-1H-cyclopenta[α]phenanthren-3-yloxy)-4-(dimethylamino)-6-methyltetrahydro-2H-pyran-3-yl acetate. Following the general procedure, *trans*-dehydroandrosterone (57 mg, 0.26 mmol), 4-(dimethylamino)-2-fluoro-6-methyltetrahydro-2*H*-pyran-3-yl acetate (57 mg, 0.26 mmol), molecular sieves (100 mg), and $BF_3{\cdot}OEt_2$ (110 μL, 0.87 mmol) were employed to obtain (2*S*,3*R*,4*S*,6*R*)-2-((3*S*,8*R*,9*S*,10*R*,13*S*,14*S*)-10,13-dimethyl-17-oxo-2,3,4,7,8,9,10,11,12,13,14,15,16,17-

tetradecahydro-1H-cyclopenta[α]phenanthren-3-yloxy)-4-(dimethylamino)-6-methyltetrahydro-2H-pyran-3-yl acetate (19 mg, 38 %) as a white solid after column chromatography (1:19 methanol: ethyl acetate). ^{1}H NMR (400 MHz): δ 5.37 (d, *J* = 5.2 Hz, 1H) 4.79 (dd, *J* = 10.6, 7.8 Hz, 1H) 4.38 (d, *J* = 7.2 Hz, 1H) 3.51 (dqd, *J* = 10.8, 6.0, 1.6 Hz, 1H) 3.45 (tt, *J* = 11.2, 4.8 Hz, 1H) 2.74 (ddd, *J* = 12.8, 10.8, 4.0 Hz, 1H) 2.45 (dd, *J* = 19.0, 8.6 Hz, 1H) 2.31-2.27 (m, 1H) 2.27 (s, 6H) 2.20-2.02 (m, 3H) 2.07 (s, 3H) 1.95-1.90 (m, 2H) 1.84 (dq, *J* = 12.8, 3.6 Hz, 2H) 1.72 (ddd, *J* = 12.8, 4.4, 2.0 Hz, 1H) 1.69-1.27 (m, 10H) 1.05 (dt, *J* = 3.6, 14.0 Hz, 1H) 1.24 (d, *J* = 6.4 Hz, 3H) 1.00 (s, 3H) 0.97 (m, 1H) 0.87 (s, 3H); ^{13}C NMR (100 MHz): δ 221.0, 169.9, 141.1, 120.9, 101.0, 78.8, 77.3, 71.0, 69.2, 63.1, 51.8, 50.3, 47.5, 40.6, 39.1, 37.2, 36.9, 35.8, 31.5, 31.4, 30.9, 30.8, 29.5, 21.9, 21.4, 21.2, 20.3, 19.4, 13.5; HRMS (ESI) *m/z* calculated for $[M+H]^+$ 488.3376, found 488.3380.

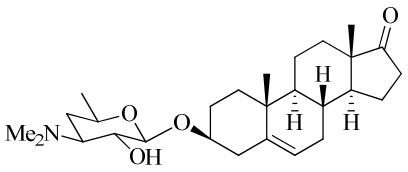

(3*S*,8*R*,9*S*,10*R*,13*S*,14*S*)-3-((2*S*,3*R*,4*S*,6*R*)-4-(dimethylamino)-3-hydroxy-6-methyltetrahydro-2H-pyran-2-yloxy)-10,13-dimethyl-3,4,7,8,9,10,11,12,13,14,15,16-dodecahydro-1H-cyclopenta[α]phenanthren-17(2*H*)-one (15). Following the general procedure, (2*S*,3*R*,4*S*,6*R*)-2-((3*S*,8*R*,9*S*,10*R*,13*S*,14*S*)-10,13-dimethyl-17-oxo-2,3,4,7,8,9,10,11,12,13,14,15,16,17-tetradecahydro-1H-cyclopenta[α]phenanthren-3-yloxy)-4-(dimethylamino)-6-methyltetrahydro-2H-pyran-3-yl acetate (11 mg, 0.022 mmol), K_2CO_3 (9 mg, 0.066 mmol), and methanol (3 mL) were employed to obtain (3*S*,8*R*,9*S*,10*R*,13*S*,14*S*)-3-((2*S*,3*R*,4*S*,6*R*)-4-(dimethylamino)-3-hydroxy-6-methyltetrahydro-2H-pyran-2-yloxy)-10,13-dimethyl-3,4,7,8,9,10,11,12,13,14,15,16-dodecahydro-1H-cyclopenta[α]phenanthren-17(2*H*)-one (14 mg, quantitative) as a white solid. ^{1}H NMR (400 MHz): δ 5.38 (d, *J* = 5.2 Hz, 1H) 4.36 (d, *J*

= 7.2 Hz, 1H) 3.59 (tt, *J* = 11.2, 4.4 Hz, 1H) 3.54 (dqd, *J* = 16.8, 6.4, 2.0 Hz, 1H) 3.26 (dd, *J* = 10.2, 7.0 Hz, 1H) 2.54 (ddd, *J* = 12.0, 10.2, 4.0 Hz, 1H) 2.48-2.42 (m, 2H) 2.36-2.29 (m, 1H) 2.29 (s, 6H) 2.14-1.81 (m, 6H) 1.72-1.42 (m, 7H) 1.32-1.23 (m, 3H) 1.25 (d, *J* = 5.6 Hz, 3H) 1.08 (dt, *J* = 4.0, 13.6 Hz, 1H) 1.03 (s, 3H) 1.01-0.96 (m, 1H) 0.88 (s, 3H); ^{13}C NMR (100 MHz): δ 221.1, 141.1, 120.9, 102.3, 78.2, 69.8, 69.5, 65.4, 51.8, 50.3, 47.5, 40.3, 38.9, 37.3, 36.9, 35.8, 31.5, 31.4, 30.8, 29.6, 28.7, 21.9, 21.3, 20.3, 19.4, 13.5; HRMS (ESI) *m/z* calculated for $[M+H]^+$ 446.3270, found 446.3276.

6.2.2 Synthesis of C7/C8 Authentic Hydroxylation Standards

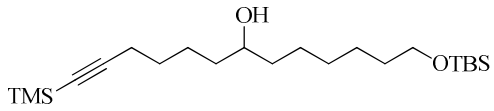

13-(*tert*-Butyldimethylsilyloxy)-1-(trimethylsilyl)tridec-1-yn-7-ol. Razor scraped Mg turnings (161 mg, 6.6 mmol) were added and a reflux condenser was attached. *tert*-Butyl(6-chlorohexyloxy)dimethylsilane[114] (553 mg, 2.2 mmol) was added as a solution in THF (2 mL). Several drops of 1,2-dibromoethane were added and the reaction mixture was heated to reflux for 1 h. Several more drops of 1,2-dibromoethane were added. (Trimethylsilyl)-hept-6-ynal[115] (268 mg, 1.5 mmol) was then added dropwise over 20 min to the refluxing mixture as a solution in THF (2 mL). This was allowed to reflux overnight and was then removed from heat. The reaction mixture was quenched with saturated NH_4Cl and extracted with ethyl acetate. The combined organic layers were washed with brine, dried over $MgSO_4$, and filtered. Flash column chromatography (5 % ethyl acetate/ hexanes) afforded 13-(*tert*-butyldimethylsilyloxy)-1-(trimethylsilyl)tridec1-yn-7-ol (245 mg, 42 %) as a colorless oil. ^{1}H NMR (400 MHz): δ 3.56 (t, *J* = 6.8 Hz, 3H), 2.20 (t, *J* = 6.8 Hz, 2H), 1.55-1.29 (m, 16H), 0.86 (s, 9H), 0.11 (s, 9H), 0.01 (s, 6H); ^{13}C NMR (100 MHz): δ 107.4, 84.5, 71.8, 63.2, 37.4, 36.9, 32.8, 29.5, 28.6, 26.0, 25.8,

25.6, 24.8, 19.8, 18.4, 0.2, -5.3 ppm; HRMS (ESI) *m/z* calculated for $[M+Na]^+$ 421.2934, found 421.2917.

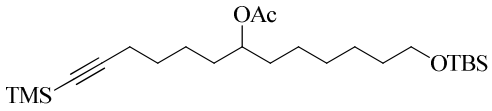

13-((tert-butyldimethylsilyl)oxy)-1-(trimethylsilyl)tridec-1-yn-7-yl acetate. Following the procedure used to synthesize 7-(triethylsilyloxy)cyclododecyl acetate, 13-(*tert*-butyldimethylsilyloxy)-1-(trimethylsilyl)tridec-1-yn-7-ol (200 mg, 0.50 mmol), K_2CO_3 (97 mg, 0.70 mmol), 4-dimethylamino pyridine (6 mg, 0.050 mmol), and acetic anhydride (0.5 mL, 5.0 mmol) were employed to obtain 13-(*tert*-butyldimethylsilyloxy)1-(trimethylsilyl)tridec-1-yn-7-yl acetate (203 mg, 92 %) as a clear oil after flash column chromatography (SiO_2, 5 % ethyl acetate/ hexanes). ^{1}H NMR (400 MHz): δ 4.86 (quint, *J* = 6.1 Hz, 1H), 3.58 (t, *J* = 6.8 Hz, 2H), 2.21 (t, *J* = 7.2 Hz, 2H), 2.03 (s, 3H), 1.53-1.29 (m, 16H), 0.88 (s, 9H), 0.14 (s, 9H), 0.04 (s, 6H); ^{13}C NMR (100 MHz): δ 170.9, 107.2, 84.6, 74.1, 63.2, 34.0, 33.5, 32.8, 29.3, 28.4, 25.8, 25.7, 25.3, 24.4, 21.3, 19.7, 18.4, 0.2, -5.3 ppm; HRMS (ESI) *m/z* calculated for $[M+Na]^+$ 463.3040, found 463.3042.

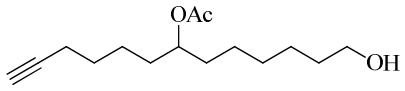

13-Hydroxytridec-1-yn-7-yl acetate. Following the procedure used to prepare dodecy11-yne-1,7-diol, 13-(*tert*-butyldimethylsilyloxy)-1-(trimethylsilyl)tridec-1-yn-7-yl acetate (190 mg, 0.43 mmol) and TBAF (1 M in THF, 0.86 mL, 0.86 mmol) were employed to obtain 13-hydroxytridec-1-yn-7-yl acetate (109 mg, 99 %) after flash column chromatography (SiO_2, 30 % ethyl acetate/ hexanes). ^{1}H NMR (400 MHz): δ 4.81 (quint, *J* = 6.1 Hz, 1H), 3.56 (t, *J* = 6.4 Hz, 2H), 2.13 (dt, *J* = 6.8, 3.5 Hz, 2H), 1.99 (s, 3H), 1.90 (t, *J* = 3.5, 1H), 1.53-1.20 (m, 16H); ^{13}C

NMR (100 MHz): δ 171.0, 84.2, 74.0, 68.3, 62.7, 33.9, 33.5, 32.6, 29.2, 28.2, 25.6, 25.2, 24.3, 21.2, 18.2 ppm; HRMS (ESI) *m/z* calculated for $[M+Na]^+$ 277.1780, found 277.1776.

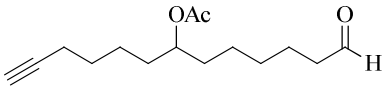

13-Oxotridec-1-yn-7-yl acetate. To a stirring solution of 13-hydroxytridec-1-yn-7-yl acetate (100 mg, 0.39 mmol) in CH_2Cl_2 (3 mL) was added PCC (170 mg, 0.78 mmol). The reaction was allowed to stir for 4 h and was then filtered through a plug of silica gel to afford 13-oxotridec-1-yn-7-yl acetate (81 mg, 82 %) after flash column chromatography (SiO_2, 25 % ethyl acetate/ hexanes). ^{1}H NMR (400 MHz): δ 9.73 (t, *J* = 1.6 Hz, 1H), 4.84 (quint, *J* = 5.6 Hz, 1H), 2.40 (d.t., *J* = 7.3, 1.7 Hz, 2H), 2.156 (d.t., *J* = 7.0, 2.5 Hz, 2H), 2.02 (s, 3H), 1.92 (t, *J* = 2.6 Hz, 1H), 1.63-1.24 (m, 12H); ^{13}C NMR (100 MHz): δ 202.5, 170.8, 84.1, 73.7, 68.3, 42.7, 33.7, 33.4, 28.9, 28.1, 25.0, 24.2, 21.8, 21.1, 18.2 ppm.

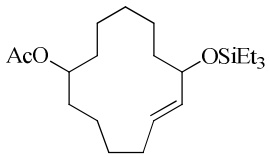

8-(Triethylsilyloxy)cyclotridec-6-enyl acetate. A flame dried round bottom flask was charged with $Ni(cod)_2$ (5 mg, 0.018 mmol), IMes·HCl (6 mg, 0.018 mmol), and *t*-BuOK (2 mg, 0.018 mmol) in the glove box. To this was added THF (5 mL) and the catalyst was allowed to form for 10 min. The catalyst system was then diluted with THF (10 mL) and a solution of 13-oxotridec-1-yn-7-yl acetate (46 mg, 0.18 mmol) and Et_3SiH (58 μL, 0.36 mmol) in THF (15 mL) was added over 2 h via syringe pump. Another flask was charged with $Ni(cod)_2$ (5 mg, 0.018 mmol), IMes·HCl (6 mg, 0.018 mmol), and *t*-BuOK (2 mg, 0.018 mmol), THF (3 mL) was added, and the catalyst was allowed to form over 10 min. This second batch of catalyst was added dropwise to the first flask after addition of the ynal had completed. The reaction was stirred for 1 h, then

opened to air and stirred for 30 min. The reaction mixture was poured through a plug column and then purified via flash column chromatography (SiO_2, 1.5 % ethyl acetate/ hexanes) to afford 8-(triethylsilyloxy)cyclotridec-6-enyl acetate as a 1:1 mixture of diastereomer A (16 mg, 24 %) and diastereomer B (15 mg, 22 %), both as colorless oils.

Diastereomer A

^{1}H NMR (400 MHz): δ 5.44 (ddd, *J* = 15.2, 9.2, 4.0 Hz, 1H), 5.35 (dd, *J* = 15.2, 7.6 Hz, 1H), 4.70 (dq, *J* = 5.2, 8.0 Hz, 1H), 4.06 (dt, *J* = 3.6, 8.4 Hz, 1H), 2.22 (m, 1H), 2.01 (s, 3H), 1.89 (m, 1H), 1.66-1.07 (m, 16H), 0.93 (t, *J* = 8.0 Hz, 9H), 0.57 (q, *J* = 7.7 Hz, 6H); ^{13}C NMR (100 MHz): δ 170.9, 134.7, 131.6, 73.4, 73.0, 37.1, 31.7, 31.0, 30.0, 26.5, 25.6, 22.2, 22.2, 21.9, 21.4, 6.8, 4.9 ppm; HRMS (ESI) *m/z* calculated for $[M+Na]^+$ 391.2644, found 391.2635.

Diastereomer B

^{1}H NMR (400 MHz): δ 5.48 (td, *J* = 15.6, 6.8 Hz, 1H), 5.39 (dd, *J* = 15.6, 6.8 Hz, 1H), 4.79 (dq *J* = 6.4, 4.8 Hz, 1H), 4.00 (ddd, *J* = 9.4, 7.0, 2.8 Hz, 1H), 2.08 (q, *J* = 6.1 Hz, 2H), 2.00 (s, 3H), 1.70-1.07 (m, 16H), 0.93 (t, *J* = 11.8 Hz, 9H), 0.57 (q, *J* = 7.9 Hz, 6H); ^{13}C NMR (100 MHz): δ 170.7, 135.5, 130.3, 73.6, 73.5, 37.6, 30.8, 30.4, 29.9, 27.4, 27.0, 22.0, 21.5, 21.4, 21.1, 6.8, 4.9 ppm; HRMS (ESI) *m/z* calculated for $[M+Na]^+$ 391.2644, found 391.2644.

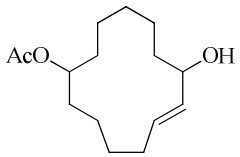

8-Hydroxycyclohex-6-enyl acetate.

Diastereomer A

Following the procedure to make dodec-11-yne-1,7-diol, 8-(triethylsilyloxy)cyclotridec6-enyl acetate (24 mg, 0.065 mmol) and TBAF (1 M, 0.1 mL, 0.098 mmol) afforded 8-hydroxycyclohex-6-enyl acetate (15 mg, 91 %) as a colorless oil after purification by flash

column chromatography (SiO_2, 15 % ethyl acetate/ hexanes). ^{1}H NMR (400 MHz): δ 5.57 (ddd; *J* = 15.6, 9.6, 4.4 Hz, 1H), 5.40 (ddd, *J* = 13.6, 10.0, 1.2 Hz, 1H), 4.70 (sextet, *J* = 4.4 Hz, 1H), 4.11 (d.t., *J* = 3.6, 9.2 Hz, 1H), 2.25 (m, 1H), 2.01 (s, 3H), 1.92 (m, 1H), 1.77-0.69 (m, 16H); ^{13}C NMR (100 MHz): δ 170.9, 134.1, 133.5, 73.2, 72.9, 35.6, 31.7, 31.1, 30.0, 26.3, 25.4, 22.5, 22.2, 22.0, 21.4.

Diastereomer B

Following the procedure to make dodec-11-yne-1,7-diol, 8-(triethylsilyloxy)cyclotridec6-enyl acetate (23 mg, 0.061 mmol) and TBAF (1 M, 0.1 mL, 0.092 mmol) afforded 8-hydroxycyclohex-6-enyl acetate (8 mg, 51 %) as a colorless oil after purification by flash column chromatography (SiO_2, 15% ethyl acetate/ hexanes). ^{1}H NMR (400 MHz): δ 5.60 (d.t., *J* = 15.6, 7.6 Hz, 1H), 5.44 (d.d., *J* = 15.2, 7.6 Hz, 1H), 4.79 (quint, *J* = 5.6 Hz, 1H), 4.04 (d.t., *J* = 10.0, 3.2 Hz, 1H), 2.12 (q, *J* = 6.4 Hz, 2H), 2.01 (s, 3H), 1.77 (m, 1H), 1.63-0.69 (m, 16H); ^{13}C NMR (100 MHz): δ 170.7, 134.8, 132.3, 73.5, 73.3, 36.2, 30.8, 30.4, 30.0, 27.2, 27.1, 22.3, 21.8, 21.4, 21.0.

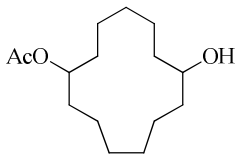

7-Hydroxycyclotridecyl acetate.

Diastereomer A

To a solution of 8-hydroxycyclohex-6-enyl acetate (15 mg, 0.059 mmol) in methanol (10 mL) was added 10 % Pd/C (5 mg). The system was purged with a H_2 balloon for 20 min. The balloon was then refilled and the reaction was allowed to react at rt under a H_2 atmosphere overnight. The reaction mixture was run through a plug of silica gel and flushed with 1:1 ethyl acetate: hexanes to afford 7-hydroxycyclotridecyl acetate (6 mg, 40 %) after flash column

chromatography (15% ethyl acetate/ hexanes). ^{1}H NMR (400 MHz): δ 4.90 (quint, *J* = 5.9 Hz, 1H), 3.79 (quint, *J* = 6.0 Hz, 1H), 1.95 (s, 3H), 1.60-1.25 (m, 21H) 1.18 (s, 1H); ^{13}C NMR (100 MHz): δ 170.8, 73.3, 70.5, 34.9, 34.2, 31.4, 30.9, 25.5, 26.4, 25.9, 22.7, 22.7, 22.40, 22.36, 21.4 ppm; HRMS (ESI) *m/z* calculated for $[M+Na]^+$ 279.1936, found 279.1928.

Diastereomer B

Following the procedure used for diastereomer A, 8-hydroxycyclohex-6-enyl acetate (8 mg, 0.031 mmol) and 10 % Pd/C (5 mg) in methanol (10 mL) afforded 7-hydroxycyclotridecyl acetate (7 mg, 88 %). ^{1}H NMR (400 MHz): δ 4.84 (quint, *J* = 6.0 Hz, 1H), 3.72 (quint, *J* = 5.6 Hz, 1H), 2.02 (s, 3H), 1.62-1.37 (m, 21H) 1.25 (s, 1H); ^{13}C NMR (100 MHz): δ 170.8, 73.5, 70.9, 34.8, 34.7, 31.4, 31.1, 27.1, 25.4, 25.4, 22.64, 22.61, 22.5, 22.3, 21.4 ppm; HRMS (ESI) *m/z* calculated for $[M+Na]^+$ 279.1936, found 279.1941.

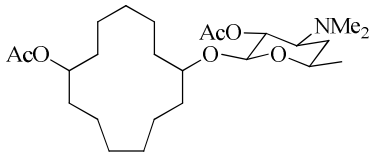

(2S,3R,4S,6R)-4-(dimethylamino)-6-methyl-2-(7-(triethylsilyloxy)cyclotridecyloxy)tetrahydro-2H-pyran-3-yl acetate.

Diastereomer A

Following the general procedure, 7-hydroxycyclotridecyl acetate (6 mg, 0.023 mmol), (2S,3R,4S,6R)-4-(dimethylamino)-6-methyltetrahydro-2*H*-pyran-3-yl acetate (8 mg, 0.035 mmol), 4Å molecular sieves (~100 mg), and $BF_3 \cdot OEt_2$ (14 μL, 0.12 mmol) were employed to afford the product after column chromatography (SiO_2, 1 % Et_3N / ethyl acetate). A trace amount of product (1-2 mg) was obtained and was carried on to the next step without characterization.

Diastereomer B

Following the general procedure, 7-hydroxycyclotridecyl acetate (1 mg, 0.0039 mmol), (2S,3R,4S,6R)-4-(dimethylamino)-6-methyltetrahydro-2H-pyran-3-yl acetate (1 mg, 0.0046 mmol), 4Å molecular sieves (~20 mg), and $BF_3 \cdot OEt_2$ (3 μL, 0.024 mmol) were used to obtain the product, which was carried on to the next step without further purification.

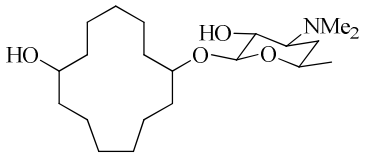

(2S,3R,4S,6R)-4-(dimethylamino)-2-(7-hydroxycyclotridecyloxy)-6-methyltetrahydro-2H-pyran-3-ol. The four diastereomers were obtained as one pair with the 1,7-*trans* relationship and one pair with the 1,7-*cis* relationship. The pairs were not stereochemically characterized.

Diastereomers A (peaks b and c in LCMS trace A, synthetic sample shown as trace D, see Figure 2.11) Following the general procedure, (2S,3R,4S,6R)-4-(dimethylamino)-6-methyl-2-(7(triethylsilyloxy)cyclotridecyloxy)tetrahydro-2H-pyran-3-yl acetate and K_2CO_3 were used to afford the crude product, which was analyzed without purification. LRMS (ESI) *m/z* calculated for $[M+H]^+$ 372.3, found 372.3.

Diastereomers B (peaks b and c in LCMS trace A, synthetic sample shown as trace E, see Figure 2.11) Following the general procedure, (2S,3R,4S,6R)-4-(dimethylamino)-6-methyl-2-(7(triethylsilyloxy)cyclotridecyloxy)tetrahydro-2H-pyran-3-yl acetate and K_2CO_3 were used to afford the crude product, which was analyzed without purification. LRMS (ESI) *m/z* calculated for $[M+H]^+$ 372.3, found 372.3.

6.2.3 Synthesis of C6/C9 Authentic Hydroxylated Standards

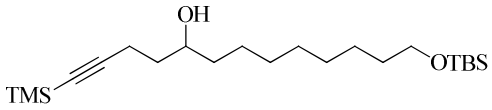

13-(*tert*-Butyldimethylsilyloxy)-1-(trimethylsilyl)tridec-1-yn-5-ol. Following the procedure used to synthesize 13-(*tert*-butyldimethylsilyloxy)-1-(trimethylsilyl)tridec-1-yn-7-ol, (8-bromooctyloxy)(*tert*-butyl)dimethylsilane (1.0 g, 3.1 mmol), Mg turnings (376 mg, 15.5 mmol), and 5-(trimethylsilyl)-pent-4-ynal (370 mg, 2.5 mmol) were employed to yield the product (577 mg, 60 %) as a colorless oil after flash column chromatography (SiO_2, 5 % ethyl acetate/ hexanes). ^{1}H NMR (400 MHz): δ 3.73 (m, 1H) 3.59 (t, *J* = 6.8 Hz, 2H) 2.36 (t, *J* = 7.0 Hz, 2H) 1.78 (d, *J* = 4.8 Hz, 1H) 1.70 (quint of d, *J* = 7.1, 3.4 Hz, 1H) 1.60 (quint of d, *J* = 7.5, 6.9 Hz, 1H) 1.52-1.41 (m, 4H) 1.29 (s, 10H) 0.90 (s, 9H) 0.14 (s, 9H) 0.04 (s, 6H); ^{13}C NMR (100 MHz): δ 107.1, 85.3, 71.2, 63.3, 37.3, 35.7, 32.9, 29.58, 29.56, 29.4, 26.0, 25.8, 25.6, 18.4, 16.6, 0.0, -5.3; HRMS (ESI) *m/z* calculated for $[M+Na]^+$ 421.2934, found 421.2933.

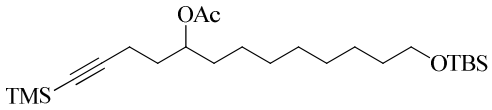

13-(*tert*-Butyldimethylsilyloxy)-1-(trimethylsilyl)tridec-1-yn-5-yl acetate. Following the procedure used to synthesize 7-(triethylsilyloxy)cyclododecyl acetate, 13-(*tert*-butyldimethylsilyloxy)-1-(trimethylsilyl)tridec-1-yn-5-ol (219 mg, 0.55 mmol), acetic anhydride (0.5 mL, 5.5 mmol), K_2CO_3 (106 mg, 0.77 mmol), and 4-dimethylaminopyridine (7 mg, 0.06 mmol) were employed to obtain the product (227 mg, 94%) as a colorless oil after flash column chromatography (SiO_2, 5% ethyl acetate/ hexanes). ^{1}H NMR (400 MHz): δ 4.90 (quint, *J* = 6.4 Hz, 1H) 3.58 (t, *J* = 6.4 Hz, 2H) 2.23 (dt, *J* = 3.6, 7.6 Hz, 2H) 2.02 (s, 3H) 1.77 (t, *J* = 7.6 Hz, 1H) 1.76 (td, *J* = 7.6, 2.8 Hz, 1H) 1.54-1.45 (m, 4H) 1.27 (m, 10H) 0.88 (s, 9H) 0.13 (s, 9H) 0.03 (s, 6H); ^{13}C NMR (100 MHz): δ 170.6, 106.4, 84.8, 73.3, 63.3, 33.8, 33.0, 32.8, 29.5, 29.4, 29.3,

26.0, 25.8, 25.2, 21.2, 18.3, 16.1, 0.1, -5.3; HRMS (ESI) *m/z* calculated for $[M+Na]^+$ 463.3040, found 463.3044.

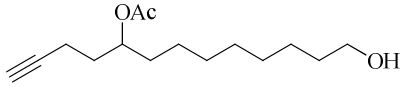

13-hydroxytridec-1-yn-5-yl acetate. Following the procedure used to prepare dodec-11-yne-1,7-diol, 13-(*tert*-butyldimethylsilyloxy)-1-(trimethylsilyl)tridec-1-yn-5-yl acetate (227 mg, 0.51 mmol) and 1 M TBAF (1.03 mL, 1.03 mmol) were employed to obtain 13-hydroxytridec-1-yn-5-yl acetate (128 mg, 98%) as a light yellow oil after column chromatography (SiO_2, 40% ethyl acetate/ hexanes). ^{1}H NMR (400 MHz): δ 4.91 (quint, *J* = 6.2 Hz, 1H) 3.58 (t, *J* = 7.0 Hz, 2H) 2.17 (tt, *J* = 7.4, 2.8 Hz, 2H) 2.01 (s, 3H) 1.92 (t, *J* = 2.6 Hz, 1H) 1.75 (t, *J* = 7.4 Hz, 1H) 1.74 (td, *J* = 7.2, 2.0 Hz, 1H) 1.51 (m, 4H) 1.25 (m, 10H); ^{13}C NMR (100 MHz): δ 170.8, 83.5, 73.1, 68.6, 63.0, 33.9, 32.9, 32.7, 29.4, 29.31, 29.25, 25.7, 25.1, 21.2, 14.8; HRMS (ESI) *m/z* calculated for $[M+Na]^+$ 277.1780, found 277.1775.

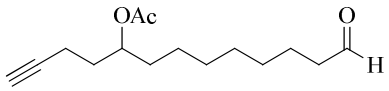

13-oxotridec-1-yn-5-yl acetate. Following the procedure used to synthesize 13-oxotridec-1-yl-7-yl acetate, 13-hydroxytridec-1-yn-5-yl acetate (102 mg, 0.4 mmol) and PCC (173 mg, 0.8 mmol) were employed to yield the product (84 mg, 83 %) as a colorless oil after flash column chromatography (SiO_2, 40% ethyl acetate/ hexanes). ^{1}H NMR (400 MHz): δ 9.70 (t, *J* = 1.8 Hz, 1H) 4.89 (qd, *J* = 5.6, 3.2 Hz, 1H) 2.36 (td, *J* = 7.4, 2.0 Hz, 2H) 2.15 (tt, *J* = 7.4, 2.8 Hz, 2H) 1.99 (s, 3H) 1.90 (t, *J* = 2.6 Hz, 1H) 1.73 (t, *J* = 7.4 Hz, 1H) 1.71 (td, *J* = 7.2, 1.6 Hz, 1H) 1.58-1.45 (m, 4H) 1.24 (m, 8H); ^{13}NMR (100 MHz): δ 202.7, 170.6, 83.4, 73.0, 68.6, 43.8, 33.8, 32.8, 29.1, 29.0, 25.0, 21.9, 21.1, 14.7.

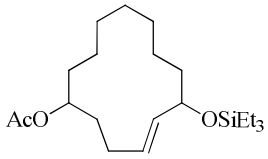

(*E*)-6-(triethylsilyloxy)cyclotridec-4-enyl acetate. Using the procedure to synthesize 8-(triethylsilyloxy)cyclotridec-6-enyl acetate, 13-oxotridec-1-yn-5-yl acetate (150 mg, 0.59 mmol), $Ni(cod)_2$ (16 mg, 0.06 mmol), IMes·HCl (20 mg, 0.06 mmol), *t*-BuOK (7 mg, 0.06 mmol), and triethylsilane (190 μL, 1.2 mmol) were employed to yield a 2.7:1 mixture of diastereomers, which were separated by column chromatography (1.5 % ethyl acetate/hexanes) to obtain diastereomer A (27 mg, 17 %) and diastereomer B (10 mg, 7 %), both as colorless oils. The 1,6-stereochemical relationship of the diastereomers was not established.

Diastereomer A (major)

^{1}H NMR (400 MHz): δ 5.60 (dt, *J* = 15.2, 7.2 Hz, 1H) 5.42 (dd, *J* = 15.6, 8.0 Hz, 1H) 4.93 (quint, *J* = 6.4 Hz, 1H) 3.93 (td, *J* = 8.8, 3.0 Hz, 1H) 2.11 (q, *J* = 6.4 Hz, 2H) 2.03 (s, 3H) 1.79 (quint, *J* = 6.4 Hz, 1H) 1.75 (m, 1H) 1.66-1.53 (m, 2H) 1.43-1.08 (m, 12H) 0.93 (t, *J* = 8.0 Hz, 9H) 0.56 (q, *J* = 8.0 Hz, 6H); ^{13}C NMR (100 MHz): δ 170.8, 135.8, 130.3, 74.0, 71.8, 37.5, 33.4, 31.0, 27.5, 26.8, 25.4, 24.8, 22.5, 22.3, 21.3, 6.8, 4.9; HRMS (ESI) *m/z* calculated for $[M+Na]^+$ 391.2644, found 391.2646.

Diastereomer B (minor)

^{1}H NMR (400 MHz): δ 5.42 (m, 2H) 4.71 (tt, *J* = 7.4, 3.9 Hz, 1H) 4.12 (ddd, *J* = 8.4, 6.8, 4.8 Hz, 1H) 2.21 (ddt, *J* = 14.4, 7.2, 2.4 Hz, 1H) 2.03 (s, 3H) 1.98 (m, 1H) 1.80 (dtd, *J* = 14.8, 7.2, 2.0 Hz, 1H) 1.63-1.16 (m, 15H) 0.93 (t, *J* = 8.0 Hz, 9H) 0.56 (q, *J* = 8.0 Hz, 6H); ^{13}C NMR (100 MHz): δ 170.8, 134.8, 131.4, 73.5, 73.1, 36.6, 33.2, 33.1, 28.9, 26.6, 24.82, 24.80, 22.8, 22.0, 21.4, 6.8, 5.0; HRMS (ESI) *m/z* calculated for $[M+Na]^+$ 391.2644, found 391.2635.

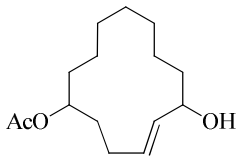

(*E*)-6-hydroxycyclotridec-4-enyl acetate.

Diastereomer A (major diastereomer)

Following the procedure used to synthesize dodec-11-yne-1,7-diol, (*E*)-6-(triethylsilyloxy)cyclotridec-4-enyl acetate (27 mg, 0.07 mmol) and 1 M TBAF (80 µL, 0.08 mmol) were employed to afford (*E*)-6-hydroxycyclotridec-4-enyl acetate (16 mg, 84 %) as a clear oil. ^{1}H NMR (400 MHz): δ 5.71 (dt, *J* = 15.2, 7.2 Hz, 1H) 5.47 (dd, *J* = 15.2, 8.4 Hz, 1H) 4.91 (quint, *J* = 6.4 Hz), 4.00 (td, *J* = 7.4, 3.2 Hz, 1H) 2.15 (q, *J* = 6.5 Hz, 2H), 2.03 (s, 3H) 1.81 (m, 2H) 1.61 (m, 2H) 1.50 (s, 1H) 1.43-1.16 (m, 11H); ^{13}C NMR (100 MHz): δ 170.8, 135.1, 132.1, 73.7, 71.8, 36.2, 32.9, 30.8, 27.5, 26.8, 25.3, 24.8, 22.7, 22.3, 21.3; HRMS (ESI) *m/z* calculated for $[M+Na]^{+}$ 277.1789, found 277.1794.

Diastereomer B (minor diastereomer)

Following the procedure used to synthesize (*E*)-cyclotetradec-2-enol, (*E*)-6-(triethylsilyloxy)cyclotridec-4-enyl acetate (23 mg, 0.06 mmol) and 1 M TBAF (90 µL, 0.09 mmol) were employed to afford (*E*)-6-hydroxycyclotridec-4-enyl acetate (16 mg, 99 %) as a clear oil. ^{1}H NMR (400 MHz): δ 5.55 (ddd, *J* = 15.2, 9.2, 4.4 Hz, 1H) 5.46 (ddd, *J* = 15.2, 7.6, 1.2 Hz, 1H) 4.71 (tt, *J* = 7.6, 4.0 Hz, 1H) 4.17 (br s, 1H) 2.23 (m, 1H) 2.03 (s, 3H) 1.98 (m, 1H) 1.80 (dtd, *J* = 10.4, 7.2, 2.0 Hz, 1H) 1.75-1.15 (m, 15 H); ^{13}C NMR (100 MHz): δ 170.9, 134.1, 133.2, 73.4, 72.8, 35.3, 33.2, 33.1, 28.9, 26.7, 24.7, 24.5, 22.9, 21.8, 21.4; HRMS (ESI) calculated for $[M+Na]^{+}$ 277.1780, found 277.1782.

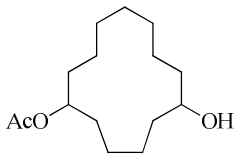

6-hydroxycyclotridecyl acetate.

Diastereomer A (major diastereomer)

Following the procedure used to synthesize 7-hydroxycyclotridecyl acetate, *(E)*-6hydroxycyclotridec-4-enyl acetate (16 mg, 0.06 mmol), Pd/C (10 % Pd) and hydrogen gas were employed to afford 6-hydroxycyclotridecyl acetate (10 mg, 63 %) as a colorless oil. ^{1}H NMR (400 MHz): δ 4.83 (quint, *J* = 6.0 Hz, 1H) 3.70 (quint, *J* = 5.6 Hz, 1H) 2.02 (s, 3H) 1.64-1.36 (m, 22H) 1.25 (br s, 1H); ^{13}C NMR (100 MHz): δ 170.8, 73.3, 70.6, 35.1, 34.6, 31.7, 31.4, 26.0, 25.7, 25.4, 23.5, 23.3, 22.78, 22.76, 21.3; HRMS (ESI) *m/z* calculated for $[M+Na]^+$ 279.1936, found 279.1924.

Diastereomer B (minor diastereomer)

Following the procedure used to synthesize 7-hydroxycyclotridecyl acetate, *(E)*-6hydroxycyclotridec-4-enyl acetate (15 mg, 0.06 mmol), Pd/C (10 % Pd) and hydrogen gas were employed to afford 6-hydroxycyclotridecyl acetate (8 mg, 53 %) as a colorless oil. ^{1}H NMR (400 MHz): δ 4.94 (quint, *J* = 6.4 Hz, 1H) 3.79 (m, 1H) 2.02 (s, 3H) 1.63-1.30 (m, 22H) 1.25 (br s, 1H); ^{13}C NMR (100 MHz): δ 170.8, 73.1, 70.1, 34.8, 34.7, 31.4, 31.2, 26.3, 26.2, 25.9, 23.1, 22.9, 22.8, 22.7, 21.4; HRMS (ESI) *m/z* calculated for $[M+Na]^+$ 279.1936, found 279.1941.

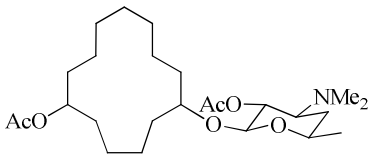

6-((2S,3R,4S,6R)-3-acetoxy-4-(dimethylamino)-6-methyltetrahydro-2*H*-pyran-2-yloxy)cyclotridecyl acetate.

Diastereomer A (major diastereomer)

Following the general procedure, 7-hydroxycyclotridecyl acetate (10 mg, 0.04 mmol), (2S,3R,4S,6R)-4-(dimethylamino)-6-methyltetrahydro-2*H*-pyran-3-yl acetate (19 mg, 0.09 mmol), 4Å MS (100 mg), and $BF_3 \cdot OEt_2$ (24 μL, 0.20 mmol) were employed to obtain the product (11 mg, 61 %, as a mixture of two diastereomers) after flash column chromatography (SiO_2, 1 % NEt_3, 5 % MeOH/ ethyl acetate). ^{1}H NMR (500 MHz): δ 4.84 (q, *J* = 6.0 Hz, 1H) 4.79 (dd, *J* = 10.0, 8.0 Hz, 1H) 4.31 (dd, *J* = 7.5, 2.0 Hz, 1H) 3.54 (m, 2H) 2.74 (m, 1H) 2.27 (s, 6H) 2.05 (s, 3H) 2.02 (s, 3H) 1.75-1.25 (m, 27H); ^{13}C NMR (100 MHz): δ 170.9, 169.9, 101.8, 101.6, 79.3, 78.9, 73.3, 73.2, 71.1, 69.0, 63.2, 40.7, 40.6, 32.8, 32.4, 31.80, 31.77, 31.7, 31.6, 31.5, 31.2, 30.9, 29.7, 29.3, 26.3, 26.0, 25.6, 25.5, 25.4, 25.2, 23.9, 23.6, 23.12, 23.08, 23.0, 22.9, 22.7, 22.4, 21.4, 21.3, 21.2, 14.1; HRMS (ESI) *m/z* calculated for $[M+Na]^+$ 478.3145, found 478.3144.

Diastereomer B (minor diastereomer)

Following the general procedure, 7-hydroxycyclotridecyl acetate (5 mg, 0.02 mmol), (2S,3R,4S,6R)-4-(dimethylamino)-6-methyltetrahydro-2*H*-pyran-3-yl acetate (8 mg, 0.04 mmol), 4Å MS (100 mg), and $BF_3 \cdot OEt_2$ (12 μL, 0.09 mmol) were employed to obtain the product (2.5 mg, 29 %, as a mixture of two diastereomers) after flash column chromatography (SiO_2, 1 % NEt_3, 5 % MeOH/ ethyl acetate). ^{1}H NMR (500 MHz): δ 4.31 (d, *J* = 7.5 Hz, 1H) 3.64 (quint, *J*

= 5.0 Hz, 1H) 3.51 (ddt, *J* = 11.0, 6.0, 5.0 Hz, 1H) 2.74 (m, 1H) 2.27 (s, 6H) 2.06 (s, 3H) 2.02 (s, 3H) 1.72 (m, 1H) 1.66-1.17 (m, 26H).

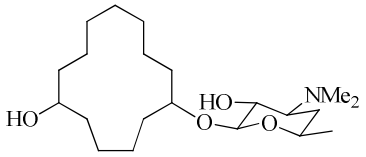

(2*S*,3*R*,4*S*,6*R*)-4-(dimethylamino)-2-(6-hydroxycyclotridecyloxy)-6-methyltetrahydro-2*H*-pyran-3-ol.

Diastereomers A (major) (peaks a and d in LCMS trace A, synthetic sample shown as trace B, see Figure 2.11) Following the general procedure, the diastereomeric mixture of 6-((2*S*,3*R*,4*S*,6*R*)-3acetoxy-4-(dimethylamino)-6-methyltetrahydro-2*H*-pyran-2-yloxy)cyclotridecyl acetate (10 mg, 0.02 mmol) and K_2CO_3 (13 mg, 0.09 mmol) were used to afford the product (6 mg, 71 %, as a mixture of two diastereomers) as a pale yellow solid. ^{1}H NMR (**X** MHz): δ 4.27 (d, *J* = 7.6 Hz, 1H) 3.72-3.63 (m, 2H) 3.53 (dq, *J* = 9.6, 7.0 Hz, 1H) 3.26 (dd, *J* = 10.0, 7.6 Hz, 1H) 2.55 (m, 1H) 2.29 (s, 6H) 1.69-1.17 (m, 26 H); ^{13}C NMR (100 MHz): δ 103.1, 102.7, 78.5, 77.9, 70.6, 70.4, 70.00, 69.99, 69.4, 65.4, 40.3, 35.3, 35.1, 34.8, 34.5, 33.0, 32.5, 32.0, 31.9, 29.7, 28.9, 26.2, 26.1, 25.9, 25.8, 25.7, 25.3, 23.8, 23.7, 23.3, 23.0, 22.9, 22.72, 22.68, 21.3; HRMS (ESI) *m/z* calculated for $[M+Na]^+$ 394.2933, found 394.2917.

Diastereomers B (minor) (peaks c and f in LCMS trace A, synthetic sample shown as trace C, see Figure 2.11) Following the general procedure, the diastereomeric mixture of 6-((2*S*,3*R*,4*S*,6R)-3acetoxy-4-(dimethylamino)-6-methyltetrahydro-2*H*-pyran-2-yloxy)cyclotridecyl acetate (2.5 mg, 0.005 mmol) and K_2CO_3 (4 mg, 0.03 mmol) were used to afford the product (2 mg, 99 %, as a mixture of two diastereomers). HRMS (ESI) *m/z* calculated for $[M+H]^+$ 372.3114, found 372.3107.

6.2.4 Synthesis of Propargyl Alcohol Authentic Standard

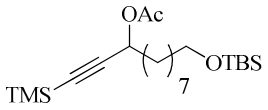

11-(*tert*-butyldimethylsilyloxy)-1-(trimethylsilyl)undec-1-yn-3-yl acetate. Following the procedure used to synthesize 7-(triethylsilyloxy)cyclododecyl acetate, 5-(*tert*butyldimethylsilyloxy)-1-(trimethylsilyl)pent-1-yn-3-ol (77 mg, 0.21 mmol), acetic anhydride (0.2 mL, 2.1 mmol), K_2CO_3 (40 mg, 0.29 mmol), and DMAP (3 mg, 0.02 mmol) were employed to obtain the product (80 mg, 93%) as a pale yellow oil after flash column chromatography (SiO_2, 5% ethyl acetate/ hexanes). ^{1}H NMR (400 MHz): δ 5.38 (t, *J* = 6.8 Hz, 1H) 3.60 (t, *J* = 6.8 Hz, 2H) 2.09 (s, 3H) 1.74 (dtd, *J* = 8.4, 6.6, 2.4 Hz, 2H) 1.51 (quint, *J* = 6.4 Hz, 2H) 1.42 (quint, *J* = 7.2 Hz, 2H) 1.30 (m, 8H) 0.90 (s, 9H) 0.18 (s, 9H) 0.05 (s, 6H); ^{13}C NMR (100 MHz): δ 169.9, 102.8, 90.2, 64.4, 63.3, 34.8, 32.8, 29.4, 29.3, 29.0, 26.0, 25.8, 24.3, 21.1, 18.4, -0.2, -5.3; HRMS (ESI) *m/z* calculated for $[M+Na]^+$ 435.2727, found 435.2724.

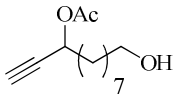

5-hydroxypent-1-yn-3-yl acetate. Following the procedure used to prepare dodec-11yne-1,7-diol, 11-(*tert*-butyldimethylsilyloxy)-1-(trimethylsilyl)undec-1-yn-3-yl acetate (72 mg, 0.17 mmol) and 1 M TBAF (0.35 mL, 0.35 mmol) were employed to obtain 5-hydroxypent-1-yn-3-yl acetate (37 mg, 95%) as a light yellow oil after column chromatography (SiO_2, 20% ethyl acetate/ hexanes). ^{1}H NMR (400 MHz): δ 5.34 (td, *J* = 6.8, 2.1 Hz, 1H) 3.64 (t, *J* = 6.6 Hz, 2H) 2.45 (d, *J* = 2.0 Hz, 1H) 2.09 (s, 3H) 1.80-1.74 (m, 2H) 1.57 (quint, *J* = 7.0 Hz, 2H) 1.46-1.40 (m, 2H) 1.37-1.32 (m, 8H); ^{13}C NMR (100 MHz): δ 170.0, 81.3, 73.4, 63.8, 63.0, 34.5, 29.3, 29.2, 29.0, 25.7, 24.8, 21.0; HRMS (ESI) *m/z* calculated for $[M+Na]^+$ 249.1467, found 249.1463.

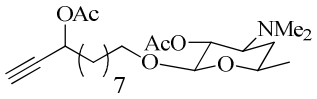

5-((2*R*,3*R*,4*S*,6*R*)-3-acetoxy-4-(dimethylamino)-6-methyltetrahydro-2*H*-pyran-2yloxy)pent-1-yn-3-yl acetate. Following the general procedure, 5-hydroxypent-1-yn-3yl acetate (31 mg, 0.14 mmol), (2*S*,3*R*,4*S*,6*R*)-4-(dimethylamino)-6-methyltetrahydro-2*H*-pyran-3-yl acetate (45 mg, 0.21 mmol), 4Å molecular sieves (~150 mg), and $BF_3 \cdot OEt_2$ (85 µL, 0.68 mmol) were employed to afford the product (13 mg, 22 %) after column chromatography (SiO_2, ethyl acetate). ^{1}H NMR (400 MHz): δ 5.34 (td, *J* = 6.6, 1.9 Hz, 1H) 4.82 (dd, *J* = 10.4, 7.6 Hz, 1H) 4.29 (d, *J* = 7.6 Hz, 1H) 3.84 (dt, *J* = 9.6, 6.2 Hz, 1H) 3.55 (dqd, *J* = 11.2, 6.3, 1.8 Hz, 1H) 3.42 (dt, *J* = 9.6, 6.8 Hz, 1H) 2.75 (ddd, *J* = 12.4, 10.6, 4.2 Hz, 1H) 2.45 (d, *J* = 2.0 Hz, 1H) 2.28 (s, 6H) 2.09 (s, 3H) 2.07 (s, 3H) 1.79-1.72 (m, 3H) 1.59-1.49 (m, 2H) 1.45-1.27 (m, 10H) 1.27 (d, *J* = 6.4 Hz, 3H); ^{13}C NMR (100 MHz) δ 170.0, 169.9, 102.2, 81.3, 73.4, 70.9, 69.4, 69.2, 63.8, 63.1, 40.6, 34.5, 30.9, 29.6, 29.3, 29.2, 29.0, 25.9, 24.8, 22.0, 21.1, 21.0; HRMS (ESI) *m/z* calculated for $[M+H]^+$ 426.2856, found 426.2853.

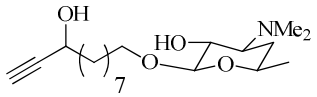

(2*R*,3*R*,4*S*,6*R*)-4-(dimethylamino)-2-(3-hydroxypent-4-ynyloxy)-6-methyltetrahydro-2*H*-pyran-3-ol. Following the general procedure, 5-((2*R*,3*R*,4*S*,6*R*)-3-acetoxy-4-(dimethylamino)-6-methyltetrahydro-2*H*-pyran-2-yloxy)pent-1-yn-3-yl acetate (6 mg,0.014 mmol) and K_2CO_3 (10 mg, 0.070 mmol) were employed to afford the product (5 mg, quantitative). ^{1}H NMR (400 MHz): δ 4.37 (td, *J* = 6.4, 1.2 Hz, 1H) 4.26 (d, *J* = 7.2 Hz, 1H) 3.89 (dt, *J* = 9.2, 6.8 Hz, 1H) 3.60-3.51 (m, 2H) 3.32 (dd, *J* = 10.2, 7.4 Hz, 1H) 2.65 (m, 1H) 2.47 (d, *J* = 1.6 Hz, 1H) 2.37 (s, 6H) 1.81-1.63 (m, 3H) 1.59-1.49 (m, 2H) 1.46-1.26 (m, 15H); ^{13}C NMR (100 MHz): δ 103.8,

85.0, 72.8, 69.9, 69.7, 69.4, 65.3, 62.3, 40.3, 37.6, 29.7, 29.6, 29.3, 29.2, 29.0, 25.9, 24.9, 21.2; HRMS (ESI) *m/z* calculated for $[M+H]^+$ 342.2644, found 342.2636.

6.2.5 Synthesis of 3-dimethylaminopropanol-linked substrate

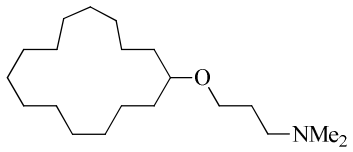

3-(cyclopentadecyloxy)-*N,N*-dimethylpropan-1-amine (31). Cyclopentadecanol (100 mg, 0.44 mmol) and NaH (60 %, 53 mg, 1.3 mmol) were dissolved in DMF (2 mL) and cooled to 0 ˚C. 3-(dimethylamino)propyl methanesulfonate hydrochloride (96 mg, 0.44 mmol) was added in three equivalent portions every 20 min. The reaction was allowed to stir until determined to be complete by TLC. It was then diluted with CH_2Cl_2, quenched with H_2O, extracted with CH_2Cl_2, dried over $MgSO_4$, and filtered. The product was purified via column chromatography (SiO_2, 20 % ethyl acetate/ hexanes followed by 100 % ethyl acetate) to yield 20 mg of the desired product (14 %) and 65 mg of starting material cyclopentadecanol (64 %). ^{1}H NMR (400 MHz): δ 3.45 (t, J = 6.6 Hz, 2H) 3.27 (quint, J = 5.6 Hz, 1H) 2.35 (t, J = 7.2 Hz, 2 H) 2.23 (s, 6H) 1.73 (quint, J = 7.0 Hz, 2H) 1.57-1.47 (m, 4H) 1.35-1.33 (m, 24H); ^{13}C NMR (100 MHz): δ 78.7, 66.8, 56.9, 45.6, 32.0, 28.4, 27.3, 26.9, 26.8, 26.64, 26.62, 23.2.

6.3 Chapter 3 Experimental

6.3.1 Synthesis of Starting Materials

General PCC oxidation procedure.

The ynol (1 equiv.) was dissolved in CH_2Cl_2 (0.3 M). A 1:1 w:w mixture of PCC and SiO_2 (1.2 equiv. PCC) was added to the solution, and the reaction was allowed to stir until complete by TLC analysis. It was then diluted with ether and filtered through a celite pad topped with a layer of silica gel, eluting with 20 % ethyl acetate/ hexanes. This was concentrated and the product was purified by column chromatography.

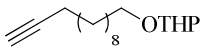

Acetylide 37. TMS-acetylene (5 mL, 35.0 mmol) was dissolved in THF (65 mL) and cooled to -78 °C. *n*BuLi (1.5 M in hexanes, 21 mL) was added dropwise and this solution was allowed to stir for ~10 min. DMPU (12.5 mL) was then added. 2-((10-Bromodecyl)oxy)tetrahydro-2H-pyran[116] (5.7 g, 17.7 mmol) was dissolved in THF (10 mL) and added dropwise to the lithium TMS-acetylide solution. The reaction was allowed to warm to room temperature and stirred overnight, after which it was quenched with methanol. TBAF (1 M in THF, 19.5 mmol) was then added and this was allowed to stir for ~90 min. The reaction was then quenched with sat. aq. $NaHCO_3$, extracted with ethyl acetate, washed with brine, dried over $MgSO_4$, filtered, and concentrated. The product was purified by column chromatography (SiO_2, 5 % ethyl acetate/ hexanes) to yield 4.21 g (89 %) of the terminal alkyne product. Spectral data match those previously reported.[116]

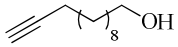

11-dodecyn-1-ol (39). THP-protected alcohol **37** (4.21 g) was dissolved in MeOH (53 mL) and *p*TsOH·H_2O was added to the solution, which was allowed to stir until completion, as determined by TLC analysis. The reaction was then quenched with 75 mg solid $NaHCO_3$, filtered through a celite pad, rinsing with methanol, and concentrated. The residue was taken up in 25 mL H_2O, extracted with ethyl acetate, washed with sat. aq. $NaHCO_3$, dried over $MgSO_4$, filtered, and concentrated. Purification by column chromatography (SiO_2, 20 % ethyl acetate/ hexanes) gave 2.70 g (94 %) of the alcohol product. Spectral data match those previously reported.[117]

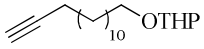

Acetylide 38. Following the procedure to synthesize **37**, TMS-acetylide (9.4 mL), *n*BuLi (29 mL, 2.1 M in hexanes), a THF solution of 2-((12-bromododecyl)oxy)tetrahydro-2H-pyran[118] (9.72 g in 14 mL), THF (112 mL total), DMPU (28 mL), and TBAF (30.5 mL, 1 M in THF) were employed to give 7.81 g (95 %) of the desired product. Spectral data match those previously reported.[118]

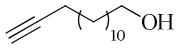

13-tetradecyn-1-ol (40). Following the procedure to synthesize 11-dodecyn-1-ol, THP-protected alcohol **38** (7.81 g), *p*TsOH·H_2O (504 mg), and MeOH (88 mL) were employed to give 5.04 g (90 %) of the alcohol product. Spectral data match those previously reported.[118]

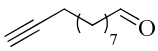

10-undecyn-1-al. Following the general procedure, 10-undecyn-1-ol (115 μL), PCC (155 mg), SiO_2 (155 mg), and CH_2Cl_2 (2 mL) were employed to give 68 mg (68 %) of the ynal product

after column chromatography (SiO_2, 5 % ethyl acetate/ hexanes). Spectral data match those previously reported.[119]

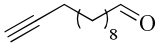

11-dodecyn-1-al. Following the general procedure, 11-dodecyn-1-ol (91 mg), PCC (129 mg), SiO_2 (129 mg), and CH_2Cl_2 (2 mL) were employed to give 71 mg (79 %) of the ynal product after column chromatography (SiO_2, 5 % ethyl acetate/ hexanes). Spectral data match those previously reported.[120]

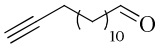

13-tetradecyn-1-al. Following the general procedure, 13-tetradecyn-1-ol (105 mg), PCC (162 mg), SiO_2 (162 mg), and CH_2Cl_2 (2 mL) were employed to give 82 mg (79 %) of the ynal product after column chromatography (SiO_2, 5 % ethyl acetate/ hexanes). Spectral data match those previously reported.[117]

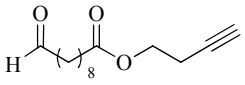

But-3-yn-1-yl 10-oxodecanoate. Following the general procedure, ynol **41** (88 mg), PCC (118 mg), SiO_2 (118 mg), and CH_2Cl_2 (2 mL) were employed to give 51 mg (59 %) of the ynal product after column chromatography (SiO_2, 5 % ethyl acetate/ hexanes). Spectral data match those previously reported.[63]

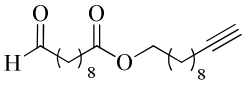

Undec-10-yn-1-yl 10-oxodecanoate. Following the general procedure, ynol **43** (100 mg), PCC (96 mg), SiO_2 (96 mg), and CH_2Cl_2 (2 mL) were employed to give 84 mg (85 %) of the ynal product after column chromatography (SiO_2, 5 % ethyl acetate/ hexanes). Spectral data match those previously reported.[63]

6.3.2 Macrocyclizations

General macrocyclization procedure.

$Ni(cod)_2$ (20 mol%), NHC·HX (20 mol%), and NaO*t*Bu (20 mol%) were charged to a flame- or oven-dried flask in the glovebox. The flask was then sealed with a rubber septum, removed from the glovebox, and put under N_2. Dry THF (5-10 mL) was added and the catalyst was allowed to form over 10-20 min while stirring at room temperature. Meanwhile, the ynal and silane were dissolved in dry THF (half the total volume of the reaction). After the catalyst had formed, it was diluted to half the total volume with dry THF, and the ynal solution was added via syringe drive. Upon completion of the reaction by TLC analysis, it was opened to air and allowed to stir for several minutes. It was then diluted with hexanes and run through a silica gel plug, eluting with 50 % ethyl acetate/ hexanes. Concentration followed by immediate purification via column chromatography gave the product.

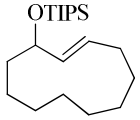

Macrocycle 44. Following the general procedure, 11-undecyn-1-al (63 mg), TIPS-H (150 μL), $Ni(cod)_2$ (10.5 mg), IMes·HCl (13 mg), KO*t*Bu (4.5 mg), and THF (63 mL) were employed to give 33 mg (27 %) of the desired product after column chromatography (0.5 % ethyl acetate/ hexanes). ^{1}H NMR (400 MHz): δ 5.58 (ddd, *J* = 15.1, 8.9, 6.1 Hz, 1H) 5.40 (dd, *J* = 15.6, 7.2 Hz, 1H) 4.17-4.12 (m, 1H) 2.20-2.14 (m, 1H) 2.08-1.99 (m, 1H) 1.78-1.71 (m, 1H) 1.62-1.53 (m, 1H) 1.50-1.12 (m, 12H) 1.10-1.00 (m, 21H).

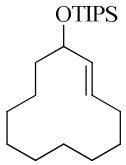

Macrocycle 45. Following the general procedure, 12-dodecyn-1-al (61 mg), TIPS-H (140 μL), $Ni(cod)_2$ (19 mg), IMes·HCl (23 mg), KO*t*Bu (8 mg), and THF (34 mL) were employed to give 46 mg (40 %) of the desired product after column chromatography (0.5 % ethyl acetate/ hexanes). ^{1}H NMR (500 MHz): δ 5.47 (ddd, *J* = 15.5,8.8, 4.8 Hz, 1H) 5.40 (dd, *J* = 16.0, 7.0 Hz, 1H) 4.16 (ddd, *J* = 8.3, 7.0, 3.3 Hz, 1H) 2.21-2.16 (m, 1H) 2.04-1.97 (m, 1H) 1.75-1.69 (m, 1H) 1.55-1.47 (m, 3H) 1.40-1.23 (m, 12H) 1.14-1.03 (m, 21H).

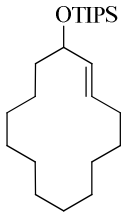

Macrocycle 46. Following the general procedure, 13-tetradecyn-1-al (77 mg), TIPS-H (150 μL), $Ni(cod)_2$ (20 mg), IMes·HCl (25 mg), KO*t*Bu (8 mg), and THF (74 mL) were employed to give 59 mg (43 %) of the desired product after column chromatography (hexanes). ^{1}H NMR (400 MHz): δ 5.42-5.31 (m, 2H) 4.13 (ddd, *J* = 11.8, 7.8, 3.8 Hz, 1H) 2.20-2.14 (m, 1H) 2.02-1.94 (m, 1H) 1.63-1.55 (m, 1H) 1.51-1.17 (m, 19H) 1.09-0.97 (m, 21H).

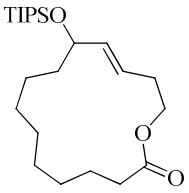

Macrocycle 47. Following the general procedure, but-3-yn-1-yl 10-oxodecanoate (50 mg), TIPS-H (90 μL), $Ni(cod)_2$ (12 mg), IMes·HCl (14 mg), KO*t*Bu (5 mg), and THF (42 mL) were employed to give 37 mg (45 %) of the desired product after column chromatography (3 % ethyl

acetate/ hexanes). ^{1}H NMR (400 MHz): δ 5.50-5.49 (m, 2H) 4.26-4.21 (m, 1H) 4.18-4.15 (m, 1H) 4.12-4.07 (m, 1H) 2.41-2.39 (m, 2H) 2.37-2.32 (m, 2H) 1.71-1.49 (m, 5H) 1.36-1.21 (m, 14H) 1.05-0.97 (m, 16H).

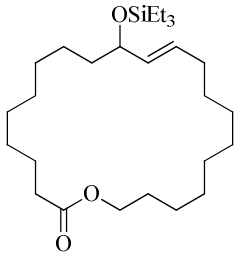

Macrocycle 48. Following the general procedure, undec-10-yn-1-yl 10-oxodecanoate (89 mg), TES-H (85 μL), Ni(cod)$_2$ (14.5 mg), IMes·HCl (18 mg), KO*t*Bu (7.5 mg), and THF (26 mL) were employed to give 63 mg (53 %) of the desired product after column chromatography (0.5 % ethyl acetate/ hexanes). Spectral data match those previously reported.[63]

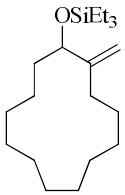

Macrocycle 49. Following the general procedure, 13-tetradecyn-1-al (74 mg), TES-H (110 μL), Ni(cod)$_2$ (20 mg), DP-IPr·BF$_4$ (44 mg), KO*t*Bu (8 mg), and THF (71 mL) were employed to give 52 mg (45 %) of a 1.4:1 mixture of exo:endo regioisomers, which were easily separated by column chromatography (hexanes to 1 % ethyl acetate hexanes) to give 32 mg of the desired product and 20 mg of the endo product. ^{1}H NMR (500 MHz): δ 4.99 (d, *J* = 1.0 Hz, 1H) 4.84 (d, *J* = 1.5 Hz, 1H) 4.05 (dd, *J* = 7.8, 4.8 Hz, 1H) 2.20-2.14 (m, 1H) 2.01-1.95 (m, 1H) 1.72-1.64 (m, 1H) 1.57-1.55 (m, 1H) 1.41-1.27 (m, 18H) 0.95 (t, *J* = 8.0 Hz, 9H) 0.59 (q, *J* = 8.0 Hz, 6H).

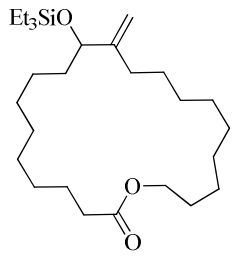

Macrocycle 50. Following the general procedure, undec-10-yn-1-yl 10-oxodecanoate (75 mg), TES-H (70 μL), $Ni(cod)_2$ (12 mg), DP-IPr·BF_4 (28 mg), KO*t*Bu (6 mg), and THF (22 mL) were employed to give a 2.6:1 crude ratio of exo:endo regioisomers, and 40 mg (40 %) of a 2.8:1 mixture of exo:endo regioisomers were isolated after purification by column chromatography (2.5 % ethyl acetate hexanes). **Exo isomer:** ^{1}H NMR (500 MHz): δ 4.94 (s, 1H) 4.80 (d, *J* = 1.5 Hz, 1H) 4.16-4.08 (m, 2H) 4.03 (t, *J* =6.5 Hz, 1H) 2.31 (t, *J* = 7.0 Hz, 2H) 2.13-2.06 (m, 1H) 1.98-1.90 (m, 1H) 1.63-1.29 (m, 28H) 0.94 (t, *J* = 7.8 Hz, 9H) 0.58 (q, *J* = 8.0 Hz, 6H).

6.4 Chapter 4 Experimental

6.4.1 Synthesis of Sugar Silanes

General procedure for sugar silane synthesis.

The 2-hydroxy sugars containing thiol leaving groups in the anomeric positions were synthesized as previously reported.[121,122] The sugar (1 equiv.) was dissolved in CH_2Cl_2 (0.2 M). Et_3N (2 equiv.) was added and allowed to stir for ~3 min, at which point $R_2Si(H)Cl$ (1.3 equiv.) was added. The reaction was stirred at rt until complete by TLC analysis. It was then quenched with sat. aq. $NaHCO_3$, extracted with ethyl acetate, washed with water, washed with brine, dried over $MgSO_4$, filtered, concentrated, and purified by column chromatography.

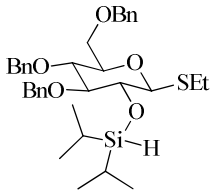

Diisopropyl sugar silane 54. Following the general procedure, 2-hydroxy sugar (1.0 g), triethylamine (0.55 mL), and chlorodiisopropylsilane (0.45 mL) were employed, followed by purification by column chromatography (SiO_2, 7.5 % ethyl acetate/ hexanes) to give 1.08 g (88 %) of the desired product as a colorless oil. ^{1}H NMR (500 MHz): δ 7.37-7.26 (m, 8H) 7.30-7.26 (m, 5H) 7.13-7.11 (m, 2H) 4.93 (d, *J* = 11.0 Hz, 1H) 4.88 (d, *J* = 10.5 Hz, 1H) 4.61 (d, *J* = 12.0 Hz, 1H) 4.56 (d, *J* = 12.0 Hz, 1H) 4.55 (d, *J* = 11.0 Hz, 1H) 4.41 (s, 1H) 4.36 (d, *J* = 9.5 Hz, 1H) 3.76 (dd, *J* = 11.0, 2.0 Hz, 1H) 3.71-3.66 (m, 2H) 3.62 (t, *J* = 9.3 Hz, 1H) 3.55 (t, *J* = 8.5 Hz, 1H) 3.50 (ddd, *J* = 9.8, 4.8, 1.8 Hz, 1H) 2.78 (dq, *J* = 12.6, 7.4 Hz, 1H) 2.71 (dq, *J* = 12.8, 7.4 Hz, 1H) 1.32 (t, *J* = 7.5 Hz, 3H) 1.22-1.15 (m, 1H) 1.10-1.00 (m, 13 H); ^{13}C NMR (125 MHz): δ 138.6, 138.2, 138.0, 128.32, 128.30, 128.2, 127.8, 127.72, 127.70, 127.5, 127.3, 87.4, 86.4, 79.1, 78.2, 75.4, 75.3, 74.9, 73.4, 69.1, 24.7, 17.8, 17.6, 17.5, 17.3, 15.0, 12.6, 12.1; IR (thin film, cm^{-1}) 3031, 2941, 2865, 2112; HRMS (ESI) *m/z* calculated for $[M+NH_4]^+$ 626.3330, found 626.3338, *m/z* calculated for $[M+Na]^+$ 631.2884, found 631.2888.

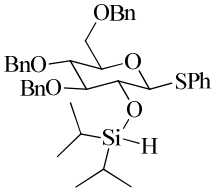

Diisopropyl sugar silane 55. Following the general procedure, 2-hydroxy sugar (975 mg), triethylamine (0.5 mL), and chlorodiisopropylsilane (0.4 mL) were employed, followed by column chromatography (SiO_2, 7.5 % ethyl acetate/ hexanes) to give 1.12 g (96 %) of the desired product as a colorless oil. ^{1}H NMR (700 MHz) δ 7.57-7.55 (m, 2H) 7.36-7.24 (m, 16H) 7.15-

7.14 (m, 2H) 4.92 (d, *J* = 11.2 Hz, 1H) 4.89 (d, *J* = 11.2 Hz, 1H) 4.77 (d, *J* = 10.5 Hz, 1H) 4.61 (d, *J* = 9.1 Hz, 1H) 4.60 (d, *J* = 11.9 Hz, 1H) 4.57 (d, *J* = 10.5 Hz, 1H) 4.54 (d, *J* = 11.9 Hz, 1H) 4.45 (s, 1H) 3.79-3.76 (m, 2H) 3.71 (dd, *J* = 11.2, 4.2 Hz, 1H) 3.65 (t, *J* = 9.5 Hz, 1H) 3.57 (t, *J* = 8.8 Hz, 1H) 3.54 (ddd, *J* = 9.6, 5.1, 1.9 Hz, 1H) 1.23-1.18 (m, 1H) 1.10-1.05 (m, 10H) 1.01-1.00 (m, 3H); ^{13}C NMR (175 MHz) δ 138.5, 138.2, 138.0, 134.7, 131.2, 128.8, 128.4, 128.3, 128.2, 127.8, 127.74, 127.71, 127.5, 127.4, 127.1, 89.4, 87.4, 79.0, 78.1, 75.4, 74.91, 74.86, 73.4, 69.0, 17.8, 17.6, 17.5, 17.3, 12.6, 12.1; IR (thin film, cm^{-1}) 3031, 2941, 2864, 2112; HRMS (ESI) *m/z* calculated for $[M+NH_4]^+$ 674.3330, found 674.3330.

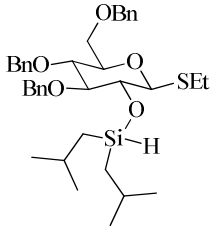

Diisobutyl sugar silane 56. Following the general procedure, 2-hydroxy sugar (210 mg), triethylamine (120 μL), and chlorodiisobutylsilane (120 μL) were employed, followed by column chromatography (SiO_2, 5 % ethyl acetate/ hexanes) to give 1.76 g (69 %) of the desired product as a colorless oil. ^{1}H NMR (700 MHz) δ 7.37-7.31 (m, 8H) 7.29-7.26 (m, 5H) 7.14-7.12 (m, 2H) 4.90 (d, *J* = 11.2 Hz, 1H) 4.86 (d, *J* = 11.2 Hz, 1H) 4.81 (quint, *J* = 2.6 Hz, 1H) 4.77 (d, *J* = 10.5 Hz, 1H) 4.60 (d, *J* = 11.9 Hz, 1H) 4.55 (d, *J* = 10.5 Hz, 1H) 4.54 (d, *J* = 10.5 Hz, 1H) 4.33 (d, *J* = 9.1 Hz, 1H) 3.75 (dd, *J* = 11.2, 2.1 Hz, 1H) 3.69 (dd, *J* = 10.9, 5.3 Hz, 1H) 3.61-3.57 (m, 2H) 3.52 (t, *J* = 8.8 Hz, 1H) 3.48 (ddd, *J* = 9.8, 4.9, 1.4 Hz, 1H) 2.76 (dq, *J* = 12.6, 7.5 Hz, 1H) 2.71 (dq, *J* = 12.6, 7.5 Hz, 1H) 1.89 (septet, *J* = 6.7 Hz, 1H) 1.84 (septet, *J* = 6.8 Hz, 1H) 1.32 (t, *J* = 7.7 Hz, 3H) 0.97 (d, *J* = 7.0 Hz, 3H) 0.96 (d, *J* = 6.3 Hz, 3H) 0.91 (d, *J* = 7.0 Hz, 3H) 0.90 (d, *J* = 6.3 Hz, 3H) 0.85 (ddd, *J* = 14.9, 6.8, 2.3 Hz, 1H) 0.80 (ddd, *J* = 14.7, 7.0, 2.1 Hz, 1H) 0.72 (ddd, *J* = 14.7, 7.0, 2.8 Hz, 1H) 0.62 (ddd, *J* = 14.9, 7.2, 3.3 Hz, 1H); ^{13}C NMR (175 MHz) δ 138.6,

138.2, 138.1, 128.4, 128.3, 128.2, 127.9, 127.72, 127.70, 127.5, 127.45, 127.38, 87.4, 86.3, 79.2, 78.0, 75.6, 75.5, 74.9, 73.4, 69.1, 26.01, 25.95, 25.92, 25.85, 25.3, 24.84, 24.76, 24.4, 24.3, 15.0; IR (thin film, cm^{-1}) 3031, 2953, 2867, 2122; HRMS (ESI) *m/z* calculated for $[M+NH_4]^+$ 654.3643, found 654.3637.

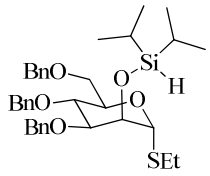

Diisopropyl sugar silane 57. Following the general procedure, 2-hydroxy sugar (500 mg), triethylamine (0.3 mL), and chlorodiisopropylsilane (0.25 mL) were employed, followed by purification by column chromatography (SiO_2, 7.5 % ethyl acetate/ hexanes) to give 436 mg (74 %) of the desired product as a colorless oil. ^{1}H NMR (500 MHz): δ 7.40-7.25 (m, 13H) 7.19-7.17 (m, 2H) 5.33 (d, *J* = 1.5 Hz, 1H) 4.85 (d, *J* = 11.0 Hz, 1H) 4.76 (d, *J* = 11.5 Hz, 1H) 4.67 (d, *J* = 12.0 Hz, 1H) 4.61 (d, *J* = 11.5 Hz, 1H) 4.52 (d, *J* = 12.0 Hz, 1H) 4.50 (d, *J* = 10.5 Hz, 1H) 4.32 (s, 1H) 4.25 (app. t, *J* = 2.0 Hz, 1H) 4.14 (ddd, *J* = 9.6, 4.4, 1.6 Hz, 1H) 4.01 (t, *J* = 9.8 Hz, 1H) 3.81 (dd, *J* = 11.0, 4.5 Hz, 1H) 3.79 (dd, *J* = 9.0, 3.0 Hz, 1H) 3.73 (dd, *J* = 11.0, 2.0 Hz, 1H) 2.69 (dq, *J* = 13.0, 7.3 Hz, 1H) 2.61 (dq, *J* = 13.0, 7.5 Hz, 1H) 1.30 (t, *J* = 7.3 Hz, 3H) 1.08-1.02 (m, 14H); ^{13}C NMR (125 MHz): δ 138.5, 138.4, 138.2, 128.25, 128.20, 128.17, 128.0, 127.8, 127.51, 127.47, 127.3, 85.1, 80.9, 75.0, 74.4, 73.1, 73.0, 72.1, 71.9, 69.1, 25.3, 17.5, 17.45, 17.43, 17.3, 15.0, 12.7, 12.6; HRMS (ESI) *m/z* calculated for $[M+NH_4]^+$ 626.3330, found 626.3341, *m/z* calculated for $[M+Na]^+$ 631.2884, found 631.2890.

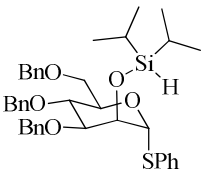

Diisopropyl sugar silane 58. Following the general procedure, 2-hydroxy sugar (2.0 g), triethylamine (1 mL), and chlorodiisopropylsilane (0.8 mL) were employed, followed by column chromatography (SiO_2, 5 % ethyl acetate/ hexanes) to give 1.76 g (73 %) of the desired product as a colorless oil. ^{1}H NMR (700 MHz) δ 7.51-7.49 (m, 2H) 7.41-7.40 (m, 2H) 7.36-7.24 (m, 14H) 7.21-7.20 (m, 2H) 5.52 (d, *J* = 1.4 Hz, 1H) 4.87 (d, *J* = 10.5 Hz, 1H) 4.79 (d, *J* = 11.2 Hz, 1H) 4.65 (d, *J* =11.9 Hz, 1H) 4.64 (d, *J* = 11.9 Hz, 1H) 4.53 (d, *J* = 11.2 Hz, 1H) 4.48 (d, *J* = 12.6 Hz, 1H) 4.40 (app. t, *J* = 2.1 Hz, 1H) 4.32 (s, 1H) 4.29 (ddd, *J* = 9.5, 4.9, 1.8 Hz, 1H) 4.04 (t, *J* = 9.8 Hz, 1H) 3.84-3.81 (m, 2H) 3.75 (dd, *J* = 10.9, 1.8 Hz, 1H) 1.09-0.98 (m, 14H); ^{13}C NMR (175 MHz) δ 138.5, 138.3, 138.1, 134.4, 131.6, 128.6, 129.0, 128.30, 128.27, 128.2, 128.1, 127.9, 127.61, 127.56, 127.55, 127.33, 127.28, 88.7, 80.8, 75.1, 74.4, 73.1, 72.9, 72.8, 72.1, 69.1, 17.5, 17.42, 17.41, 17.3, 12.7, 12.6; IR (thin film cm^{-1}) 3031, 2943, 2864, 2100; HRMS (ESI) *m/z* calculated for $[M+NH_4]^+$ 674.3330, found 674.3335.

6.4.2 Copper-Catalyzed O-H Insertions

General procedure for O-H insertion with NHC·HX, CuCl, and KO*t*Bu.

An oven-dried vial was charged with CuCl (15 mol%), NHC·HX (15 mol%), and KO*t*Bu (30 mol%) in the glovebox and sealed with a rubber septum. This vial was removed from the glovebox and put under N_2. Dry toluene (1 mL) was added and the catalyst was allowed to form over 15-20 min. Meanwhile, the alcohol (1 equiv.) and sugar silane (1.1 equiv.) were weighed out in a separate vial and put under N_2. They were dissolved in dry toluene (0.1 M) and heated to the reaction temperature, when appropriate. One third of the catalyst solution (5 mol%) was

then added to the substrate solution via syringe, and the reaction was allowed to stir until complete as judged by LRMS analysis. It was then cooled, diluted with hexanes and run through a silica plug, eluting with 50 % ethyl acetate/ hexanes. Concentration and purification by column chromatography provided the product.

General procedure for O-H insertion with (NHC)CuCl and KO*t*Bu.

An oven-dried vial was charged with (NHC)CuCl (15 mol%) and KO*t*Bu (15 mol%) in the glovebox and sealed with a rubber septum. This vial was removed and put under N_2. Dry toluene (1 mL) was added and the catalyst was allowed to form over 15-20 min. Meanwhile, the alcohol (1 equiv.) and sugar silane (1.1 equiv.) were weighed out in a separate vial and put under N_2. They were dissolved in dry toluene (0.1 M) and heated to 60 °C. One third of the catalyst solution (5 mol%) was then added to the substrate solution via syringe, and the reaction was allowed to stir until complete as judged by LRMS analysis. It was then cooled, diluted with hexanes and run through a silica plug, eluting with 50 % ethyl acetate/ hexanes. Concentration and purification by column chromatography provided the product.

General procedure for O-H insertion with PR_3, CuCl, and KO*t*Bu.

An oven-dried vial was charged with CuCl (15 mol%), PR_3 (15 mol% for bidentate, 30 mol% for monodentate), and KO*t*Bu (15 mol%) in the glovebox and sealed with a rubber septum. This vial was removed from the glovebox and put under N_2. Dry toluene (1 mL) was added and the catalyst was allowed to form over 15-20 min. Meanwhile, the alcohol (1 equiv.) and sugar silane (1.1 equiv.) were weighed out in a separate vial and put under N_2. They were dissolved in dry toluene (0.1 M) and heated to 60 °C. One third of the catalyst solution (5 mol%) was then added

to the substrate solution via syringe, and the reaction was allowed to stir until complete as judged by LRMS analysis. It was then cooled, diluted with hexanes and run through a silica plug, eluting with 50 % ethyl acetate/ hexanes. Concentration and purification by column chromatography provided the product.

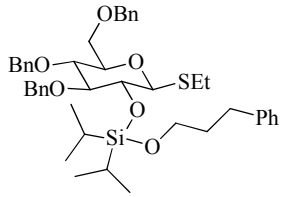

Sugar silane 54 and 3-phenylpropan-1-ol (compound 59). Following the general procedure, diisopropyl sugar silane **54** (60 mg, 0.09 mmol), 3-phenylpropan-1-ol (12 μL, 0.09 mmol), and one third of the catalyst solution prepared from CuCl (1.3 mg, 0.0014 mmol), IMes·HCl (4.5 mg, 0.014 mmol), and NaO*t*Bu (2.5 mg, 0.027 mmol) were used. Column chromatography (SiO_2, 10 % ethyl acetate/ hexanes to 20 % ethyl acetate/ hexanes) gave 44 mg (67 %) of the desired product as a colorless oil, along with 16 mg (32 %) of the decomposition product. ^{1}H NMR (500 MHz) δ 7.36-7.24 (m, 15H) 7.18-7.14 (m, 3H) 7.11-7.09 (m, 2H) 4.94 (d, *J* = 11.5 Hz, 1H) 4.88 (d, *J* = 11.5 Hz, 1H) 4.70 (d, *J* = 11.5 Hz, 1H) 4.62 (d, *J* = 12.0 Hz, 1H) 4.57 (d, *J* = 12.0 Hz, 1H) 4.54 (d, *J* = 11.0 Hz, 1H) 4.41 (d, *J* = 9.5 Hz, 1H) 3.82-3.78 (m, 3H) 3.76 (dd, *J* = 11.0, 2.0 Hz, 1H) 3.69 (dd, *J* = 11.0, 5.0 Hz, 1H) 3.63 (t, *J* = 9.3 Hz, 1H) 3.55 (t, *J* = 8.5 Hz, 1H) 3.51 (ddd, *J* = 9.8, 4.8, 2.0 Hz, 1H) 2.76 (dq, *J* = 12.6, 7.5 Hz, 1H) 2.71 (dq, *J* = 12.8, 7.5 Hz, 1H) 2.64 (app. t, *J* = 7.8 Hz, 2H) 1.84-1.78 (m, 2H) 1.31 (t, *J* = 7.5 Hz, 3H) 1.16-1.04 (m, 14H); ^{13}C NMR (175 MHz) δ 142.4, 138.8, 138.2, 137.9, 128.4, 128.34, 128.32, 128.2, 128.1, 127.8, 127.75, 127.70, 127.6, 127.2, 127.0, 125.6, 87.1, 86.4, 78.9, 78.6, 74.8, 74.7, 74.1, 73.4, 69.1, 62.5, 34.3, 32.0, 24.8, 17.8, 17.7, 17.6, 15.1, 12.8, 12.6; IR (thin film, cm^{-1}) 3029, 2943, 2866; HRMS (ESI) *m/z* calculated for $[M+NH_4]^+$ 760.4062, found 760.4071.

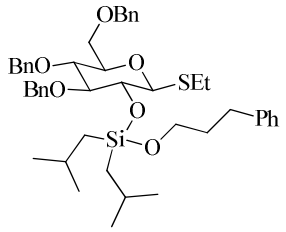

Sugar silane 56 and 3-phenylpropan-1-ol (compound 60). Following the general procedure, diisobutyl sugar silane **56** (64 mg, 0.1 mmol), 3-phenylpropan-1-ol (12 μL, 0.09 mmol), and one third of the catalyst solution prepared from CuCl (1.5 mg, 0.0014 mmol), IMes·HCl (4.5 mg, 0.014 mmol), and NaO*t*Bu (2.5 mg, 0.027 mmol) were used. Column chromatography (SiO_2, 5 % ethyl acetate/ hexanes to 30 % ethyl acetate/ hexanes) gave 34 mg (49 %) of the desired product as a colorless oil, along with 14 mg (28 %) of the decomposition product. ^{1}H NMR (700 MHz) δ 7.38-7.32 (m, 8H) 7.31-7.26 (m, 7H) 7.19-7.15 (m, 3H) 7.12-7.11 (m, 2H) 4.98 (d, *J* = 11.2 Hz, 1H) 4.89 (d, *J* = 11.9 Hz, 1H) 4.73 (d, *J* = 10.5 Hz, 1H) 4.63 (d, *J* = 11.9 Hz, 1H) 4.58 (d, *J* = 12.6 Hz, 1H) 4.56 (d, *J* = 11.2 Hz, 1H) 4.38 (d, *J* = 8.4 Hz, 1H) 3.79-3.75 (m, 4H) 3.71 (dd, *J* = 11.2, 4.9 Hz, 1H) 3.64 (t, *J* = 9.5 Hz, 1H) 3.54 (t, *J* = 8.4 Hz, 1H) 3.51 (ddd, *J* = 9.8, 4.9, 1.4 Hz, 1H) 2.77 (dq, *J* = 12.6, 7.2 Hz, 1H) 2.72 (dq, *J* = 12.6, 7.4 Hz, 1H) 2.63 (app. t, *J* = 8.1 Hz, 2H) 1.93-1.85 (m, 2H) 1.83-1.79 (m, 2H) 1.32 (t, *J* = 7.4 Hz, 3H) 0.96 (d, *J* = 7.0 Hz, 3H) 0.95 (d, *J* = 6.3 Hz, 3H) 0.93 (d, *J* = 6.3 Hz, 3H) 0.92 (d, *J* = 7.0 Hz, 3H) 0.74-0.65 (m, 4H); ^{13}C NMR (175 MHz) δ 142.4, 138.8, 138.2, 137.9, 128.4, 128.35, 128.32, 128.20, 128.15, 127.9, 127.75, 127.72, 127.6, 127.2, 126.9, 125.6, 87.0, 86.4, 79.0, 78.5, 74.8, 74.0, 73.4, 69.1, 62.1, 34.2, 32.1, 26.42, 26.39, 26.1, 26.0, 24.7, 24.4, 24.3, 23.9, 23.8, 15.0; IR (thin film, cm^{-1}) 3030, 2952, 2926, 2867; HRMS (ESI) *m/z* calculated for $[M+NH_4]^+$ 788.4375, found 788.4376.

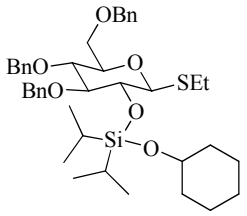

Sugar silane 54 and cyclohexanol (compound 61). Following the general procedure, diisopropyl sugar silane **54** (64 mg, 0.105 mmol), cyclohexanol (10 mg, 0.1 mmol), and one third of the catalyst solution prepared from CuCl (1.5 mg, 0.015 mmol), IMes·HCl (5 mg, 0.015 mmol), and NaO*t*Bu (3 mg, 0.03 mmol) were used. Column chromatography (SiO_2, 5 % ethyl acetate/ hexanes) gave 60 mg (86 %) of the desired product as a colorless oil. ^{1}H NMR (500 MHz) δ 7.37-7.25 (m, 13H) 7.12-7.10 (m, 2H) 4.97 (d, *J* = 11.0 Hz, 1H) 4.88 (d, *J* = 11.0 Hz, 1H) 4.70 (d, *J* = 10.5 Hz, 1H) 4.62 (d, *J* = 12.5 Hz, 1H) 4.58 (d, *J* = 12.0 Hz, 1H) 4.55 (d, *J* = 10.5 Hz, 1H) 4.43 (d, *J* =10.5 Hz, 1H) 3.90 (septet, *J* = 4.3 Hz, 1H) 3.83 (dd, *J* = 9.0, 8.0 Hz, 1H) 3.77 (dd, *J* =11.0, 2.0 Hz, 1H) 3.70 (dd, *J* = 11.0, 5.0 Hz, 1H) 3.64 (t, *J* = 9.5 Hz, 1H) 3.57 (t, *J* = 8.0 Hz, 1H) 3.53 (ddd, *J* = 9.5, 5.0, 2.0 Hz, 1H) 2.80 (dq, *J* = 13.0, 7.5 Hz, 1H) 2.72 (dq, *J* = 13.0, 7.5 Hz, 1H) 1.84 (m, 2H) 1.70-1.69 (m, 2H) 1.48-1.45 (m, 1H) 1.37-1.29 (m, 2H) 1.33 (t, *J* = 7.5 Hz, 3H) 1.24-1.14 (m, 3H) 1.10-1.02 (m, 14H); ^{13}C NMR (125 MHz) δ 138.9, 138.2, 137.9, 128.33, 128.31, 128.1, 127.8, 127.74, 127.68, 127.5, 127.1, 126.9, 86.9, 86.5, 78.74, 78.71, 74.6, 74.5, 73.9, 73.4, 70.5, 69.2, 35.9, 35.8, 25.6, 24.8, 24.1, 17.79, 17.76, 17.74, 17.70, 15.0, 13.2, 13.0; IR (thin film, cm^{-1}) 3031, 2931, 2864; HRMS (ESI) *m/z* calculated for $[M+NH_4]^+$ 724.4062, found 724.4073.

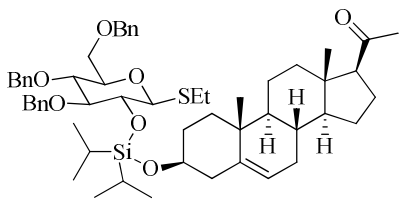

Sugar silane 54 and steroid (compound 63). Following the general procedure, diisopropyl sugar silane **54** (67 mg, 0.11 mmol), (3β)-3-hydroxypregn-5-en-20-one (32 mg, 0.1 mmol), and one third of the catalyst solution prepared from CuCl (1.5 mg, 0.015 mmol), IMes·HCl (5 mg, 0.015 mmol), and NaO*t*Bu (3 mg, 0.03 mmol) were used. Column chromatography (SiO_2, 10 % ethyl acetate/ hexanes) gave 79 mg (86 %) of the desired product as a colorless oil. ^{1}H NMR (700 MHz) δ 7.36-7.24 (m, 13H) 7.10-7.09 (m, 2H) 5.29-5.28 (m, 1H) 4.95 (d, *J* = 11.2 Hz, 1H) 4.89 (d, *J* = 11.2 Hz, 1H) 4.69 (d, *J* = 11.2 Hz, 1H) 4.61 (d, *J* = 11.9 Hz, 1H) 4.57 (d, *J* = 12.6 Hz, 1H) 4.54 (d, *J* = 10.5 Hz, 1H) 4.42 (d, *J* = 9.8 Hz, 1H) 3.84 (t, *J* = 8.8 Hz, 1H) 3.79-3.75 (m, 2H) 3.70 (dd, *J* = 11.2, 4.9 Hz, 1H) 3.64 (t, *J* = 9.5 Hz, 1H) 3.55 (t, *J* = 8.4 Hz, 1H) 3. 52 (ddd, *J* = 9.5, 5.1, 1.9 Hz, 1H) 2.77 (dq, *J* = 12.6, 7.6 Hz, 1H) 2.72 (dq, *J* = 12.6, 7.4 Hz, 1H) 2.54 (t, *J* = 8.8 Hz, 1H) 2.33 (ddd, *J* = 13.5, 4.9, 2.1 Hz, 1H) 2.29-2.17 (m, 3H) 2.13 (s, 3H) 2.08-2.04 (m, 1H) 1.99 (dtd, *J* = 17.2, 5.1, 2.6 Hz, 1H) 1.84-1.82 (m, 1H) 1.77 (dt, *J* = 6.3, 3.5 Hz, 1H) 1.72-1.42 (m, 9H) 1.31 (t, *J* = 7.4 Hz, 3H) 1.27-1.22 (m, 2H) 1.17-0.93 (m, 14H) 0.96 (s, 3H) 0.64 (s, 3H); ^{13}C NMR (175 MHz) δ 209.6, 141.5, 138.9, 138.2, 138.0, 128.35, 128.33, 128.1, 127.9, 127.75, 127.70, 127.6, 127.1, 126.9, 120.8, 86.9, 86.5, 78.80, 78.75, 74.6, 74.5, 73.9, 73.5, 72.1, 69.2, 63.7, 57.0, 50.1, 44.0, 42.7, 38.9, 37.3, 36.5, 31.93, 31.88, 31.85, 31.5, 24.8, 24.5, 22.8, 21.1, 19.4, 17.8, 17.73, 17.71, 17.68, 15.1, 13.2, 13.1, 13.0; IR (thin film, cm^{-1}) 3031, 2934, 2866, 1704; HRMS (ESI) *m/z* calculated for $[M+NH_4]^+$ 940.5576, found 940.5569.

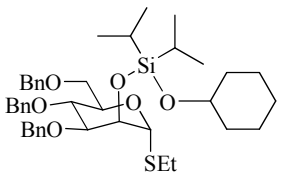

Sugar silane 57 and cyclohexanol (compound 64). Following the general procedure, diisopropyl sugar silane **57** (64 mg, 0.105 mmol), cyclohexanol (10 mg, 0.1 mmol), and one third of the catalyst solution prepared from CuCl (1.5 mg, 0.015 mmol), IMes·HCl (5 mg, 0.015 mmol), and NaO*t*Bu (3 mg, 0.03 mmol) were used. Column chromatography (SiO_2, 5 % ethyl acetate/ hexanes) gave 62 mg (89 %) of the desired product as a colorless oil. ^{1}H NMR (500 MHz) δ 7.37-7.25 (m, 13H) 7.20-7.18 (m, 2H) 5.31 (s, 1H) 4.85 (d, *J* = 11.0 Hz, 1H) 4.75 (d, *J* = 11.5 Hz, 1H) 4.66 (d, *J* = 12.0 Hz, 1H) 4.63 (d, *J* = 11.0 Hz, 1H) 4.53 (d, *J* = 12.5 Hz, 1H) 4.52 (d, *J* = 10.5 Hz, 1H) 4.41 (t, *J* =1.8 Hz, 1H) 4.13 (dd, *J* = 9.5, 3.5 Hz, 1H) 4.01 (t, *J* = 9.5 Hz, 1H) 3.87 (septet, *J* = 4.3 Hz, 1H) 3.80 (dd, *J* = 10.5, 4.8 Hz, 1H) 3.78 (dd, *J* = 9.0, 3.3 Hz, 1H) 3.73 (dd, *J* = 11.0, 1.0 Hz, 1H) 2.67 (dq, *J* = 13.0, 7.4 Hz, 1H) 2.59 (dq, *J* = 13.0, 7.5 Hz, 1H) 1.81-1.78 (m, 2H) 1.71-1.67 (m, 2H) 1.46-1.45 (m, 1H) 1.39-1.32 (m, 2H) 1.29 (t, *J* = 7.5 Hz, 3H) 1.25-1.17 (m, 3H) 1.10-0.96 (m, 14H); ^{13}C NMR (125 MHz) δ 138.7, 138.5, 128.25, 128.16, 128.0, 127.7, 127.5, 127.4, 127.34, 127.27, 85.6, 80.7, 75.0, 74.8, 73.0, 72.4, 72.1, 71.0, 70.5, 69.4, 35.9, 35.8, 25.6, 25.2, 23.9, 17.42, 17.40, 15.1, 13.1, 12.9; IR (thin film, cm^{-1}) 3031, 2931, 2865; HRMS (ESI) *m/z* calculated for $[M+NH_4]^+$ 724.4062, found 724.4067.

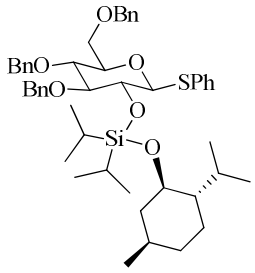

Sugar silane 55 and menthol (compound 65). Following the general procedure, diisopropyl sugar silane **55** (60 mg, 0.1 mmol), (1*R*, 2*S*, 5*R*)-menthol (13 mg, 0.09 mmol), and one third of the catalyst solution prepared from CuCl (1.3 mg, 0.014 mmol), IMes·HCl (4.5 mg, 0.014 mmol), and NaO*t*Bu (3 mg, 0.027 mmol) were used. Column chromatography (SiO_2, 7.5 % ethyl acetate/ hexanes) gave 60 mg (90 %) of the desired product as a colorless oil. ^{1}H NMR (700 MHz) δ 7.56-7.55 (m, 2H) 7.42-7.41 (m, 2H) 7.35-7.27 (m, 11H) 7.25-7.22 (m, 3H) 7.20-7.18 (m, 2H) 5.02 (d, *J* = 10.5 Hz, 1H) 4.93 (d, *J* = 10.5 Hz, 1H) 4.78 (d, *J* = 11.2 Hz, 1H) 4.68 (d, *J* = 9.1 Hz, 1H) 4.604 (d, *J* = 11.9 Hz, 1H) 4.602 (d, *J* = 9.8 Hz, 1H) 4.56 (d, *J* = 11.9 Hz, 1H) 3.90 (dd, *J* = 9.5, 8.1 Hz, 1H) 3.80 (dd, *J* = 10.9, 1.8 Hz, 1H) 3.74-3.67 (m, 3H) 3.61-3.58 (m, 2H) 2.40 (septet of d, *J* = 7.0, 2.1 Hz, 1H) 2.13-2.11 (m, 1H) 1.60-1.52 (m, 2H) 1.30-1.24 (m, 1H) 1.24-1.56 (m, 2H) 1.15-1.10 (m, 1H) 1.13 (d, *J* = 7.7 Hz, 3H) 1.12 (d, *J* = 7.7 Hz, 3H) 1.08-1.02 (m, 1H) 1.06 (d, *J* = 7.7 Hz, 3H) 1.02 (d, *J* = 7.7 Hz, 3H) 0.91 (qd, *J* = 13.0, 3.0 Hz, 1H) 0.85 (d, *J* = 6.3 Hz, 3H) 0.84 (d, *J* = 7.0 Hz, 3H) 0.78-0.72 (m, 1H) 0.77 (d, *J* = 7.0 Hz, 1H); ^{13}C NMR (175 MHz) δ 138.6, 138.2, 137.9, 135.2, 130.7, 128.8, 128.4, 128.3, 128.1, 127.8, 127.69, 127.66, 127.5, 127.4, 126.9, 89.3, 86.8, 78.8, 78.7, 74.8, 74.7, 73.8, 73.43, 73.41, 69.1, 50.3, 45.7, 34.6, 31.7, 24.9, 22.6, 22.4, 21.3, 18.1, 17.95, 17.88, 15.9, 13.4, 12.6; IR (thin film, cm^{-1}) 2951, 2923, 2867; HRMS (ESI) *m/z* calculated for $[M+NH_4]^+$ 828.4688, found 828.4692.

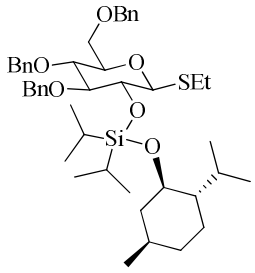

Sugar silane 54 and menthol (compound 66). Following the general procedure, diisopropyl sugar silane **54** (64 mg, 0.105 mmol), (1*R*, 2*S*, 5*R*)-menthol (16 mg, 0.1 mmol), and one third of the catalyst solution prepared from CuCl (1.5 mg, 0.015 mmol), IMes·HCl (5 mg, 0.015 mmol), and NaO*t*Bu (3 mg, 0.03 mmol) were used. Column chromatography (SiO_2, 10 % ethyl acetate/ hexanes) gave 40 mg (50 %) of the desired product as a colorless oil. ^{1}H NMR (700 MHz) δ 7.41-7.40 (m, 2H) 7.36-7.26 (m, 11H) 7.16-7.15 (m, 2H) 4.99 (d, *J* = 10.5 Hz, 1H) 4.92 (d, *J* = 10.5 Hz, 1H) 4.75 (d, *J* = 11.2 Hz, 1H) 4.62 (d, *J* = 11.9 Hz, 1H) 4.673 (d, *J* = 12.6 Hz, 1H) 4.669 (d, *J* = 11.2 Hz, 1H) 4.41 (d, *J* = 9.8 Hz, 1H) 3.79 (dd, *J* = 9.1, 8.4 Hz, 1H) 3.77 (dd, *J* = 10.9, 1.8 Hz, 1H) 3.74-3.69 (m, 2H) 3.63 (t, *J* = 9.1 Hz, 1H) 3.56 (t, *J* = 8.4 Hz, 1H) 3.54 (ddd, *J* = 9.6, 4.9, 1.9 Hz, 1H) 2.78 (dq, *J* = 12.6, 7.2 Hz, 1H) 2.73 (dq, *J* = 12.4, 7.4 Hz, 1H) 2.38 (septet of d, *J* = 7.0, 2.1 Hz, 1H) 2.15-2.13 (m, 1H) 1.62-1.60 (m, 1H) 1.56-1.53 (m, 1H) 1.36-1.30 (m, 1H) 1.32 (t, *J* = 7.4 Hz, 3H) 1.19-1.10 (m, 10H) 1.05 (d, *J* = 7.7 Hz, 3H) 1.03 (d, *J* = 7.7 Hz, 3H) 0.96-0.89 (m, 1H) 0.89 (d, *J* = 6.3 Hz, 3H) 0.85 (d, *J* = 7.0 Hz, 3H) 0.80-0.75 (m, 1H) 0.77 (d, *J* = 7.0 Hz, 3H); ^{13}C NMR (175 MHz) δ 138.8, 138.2, 138.0, 128.4, 128.3, 128.1, 127.8, 127.74, 127.70, 127.53, 127.52, 127.3, 86.8, 86.6, 78.9, 78.8, 74.72, 74.69, 74.3, 73.4, 73.3, 69.2, 50.4, 45.8, 34.6, 31.7, 24.9, 24.8, 22.7, 22.4, 21.3, 18.1, 17.92, 17.89, 15.9, 15.0, 13.4, 12.7; IR (thin film, cm^{-1}) 3031, 2925, 2867; HRMS (ESI) *m/z* calculated for $[M+NH_4]^+$ 780.4688, found 780.4691.

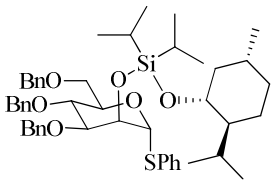

Sugar silane 58 and menthol (compound 67). Following the general procedure, diisopropyl sugar silane **58** (60 mg, 0.09 mmol), (1*R*, 2*S*, 5*R*)-menthol (13 mg, 0.08 mmol), and one third of the catalyst solution prepared from CuCl (1.2 mg, 0.012 mmol), IMes·HCl (4 mg, 0.012 mmol), and NaO*t*Bu (2.5 mg, 0.025 mmol) were used. Column chromatography (SiO_2, 5 % ethyl acetate/ hexanes) gave 50 mg (75 %) of the desired product as a light yellow oil. ^{1}H NMR (700 MHz) δ 7.50-7.49 (m, 2H) 7.40-7.39 (m, 2H) 7.34-7.23 (m, 16H) 5.53 (s, 1H) 4.89 (d, *J* = 10.5 Hz, 1H) 4.79 (d, *J* = 11.9 Hz, 1H) 4.68 (d, *J* = 11.9 Hz, 1H) 4.63 (d, *J* = 12.6 Hz, 1H) 4.60 (s, 1H) 4.57 (d, *J* = 11.2 Hz, 1H) 4.51 (d, *J* = 11.9 Hz, 1H) 4.30 (dd, *J* = 10.2, 5.3 Hz, 1H) 4.03 (t, *J* = 9.8 Hz, 1H) 3.82-3.80 (m, 2H) 3.77 (d, *J* = 11.2 Hz, 1H) 3.65 (td, *J* = 10.2, 4.0 Hz, 1H) 2.30 (septet of d, *J* = 7.0, 2.1 Hz, 1H) 2.01-2.00 (m, 1H) 1.61-1.55 (m, 2H) 1.31-1.27 (m, 1H) 1.14-1.10 (m, 1H) 1.08-0.96 (m, 15H) 0.92-0.86 (m, 1H) 0.86 (d, *J* = 7.0 Hz, 3H) 0.82 (d, *J* = 6.3 Hz, 3H) 0.82-0.76 (m, 1H) 0.74 (d, *J* = 7.0 Hz, 3H); ^{13}C NMR (175 MHz) δ 138.6, 138.44, 138.37, 134.8, 131.5, 128.9, 128.3, 128.21, 128.15, 128.06, 127.8, 127.6, 127.5, 127.3, 127.1, 89.2, 80.6, 75.1, 74.8, 73.1, 73.0, 72.9, 72.2, 71.0, 69.4, 50.3, 45.8, 34.5, 31.6, 25.1, 22.6, 22.3, 21.3, 17.7, 17.62, 17.60, 15.8, 13.6, 13.4; IR (thin film, cm^{-1}) 3029, 2951, 2866; HRMS (ESI) *m/z* calculated for $[M+NH_4]^+$ 828.4688, found 828.4689.

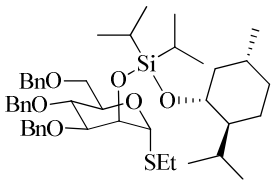

Sugar silane 57 and menthol (compound 68). Following the general procedure, diisopropyl sugar silane **57** (64 mg, 0.105 mmol), (1*R*, 2*S*, 5*R*)-menthol (16 mg, 0.1 mmol), and one third of

the catalyst solution prepared from CuCl (1.5 mg, 0.015 mmol), IMes·HCl (5 mg, 0.015 mmol), and NaO*t*Bu (3 mg, 0.03 mmol) were used. Column chromatography (SiO_2, 7.5 % ethyl acetate/ hexanes) gave 67 mg (84 %) of the desired product as a colorless oil. ^{1}H NMR (500 MHz) δ 7.35-7.24 (m, 13H) 7.19-7.18 (m, 2H) 5.28 (d, *J* = 1.5 Hz, 1H) 4.85 (d, *J* = 10.5 Hz) 4.72 (d, *J* = 11.5 Hz, 1H) 4.63 (d, *J* = 12.0 Hz, 1H) 4.61 (d, *J* = 12.0 Hz, 1H) 4.53 (d, *J* = 12.0 Hz, 1H) 4.52 (d, *J* = 12.0 Hz, 1H) 4.41 (app. t, *J* = 2.0 Hz, 1H) 4.13 (ddd, *J* = 9.9, 4.9, 1.6 Hz, 1H) 3.97 (t, *J* = 9.5 Hz, 1H) 3.79-3.75 (m, 2H) 3.72 (dd, *J* = 11.0, 2.0 Hz, 1H) 3.66 (td, *J* = 10.3, 4.3 Hz, 1H) 2.65 (dq, *J* = 12.8, 7.4 Hz, 1H) 2.57 (dq, *J* = 13.0, 7.5 Hz, 1H) 2.31 (septet of d, *J* = 7.0, 2.4 Hz, 1H) 2.05-2.03 (m, 1H) 1.62-1.54 (m, 2H) 1.38-1.30 (m, 1H) 1.27 (t, *J* = 7.5 Hz, 3H) 1.18-1.12 (m, 1H) 1.09-0.94 (m, 15 H) 0.92-0.83 (m, 1H) 0.89 (d, *J* = 7.0 Hz, 3H) 0.88 (d, *J* = 7.0 Hz, 3H) 0.75 (d, *J* = 6.5 Hz, 3H); ^{13}C NMR (125 MHz) δ 138.7, 138.6, 138.5, 128.25, 128.17, 128.15, 128.0, 127.8, 127.4, 127.3, 85.6, 80.7, 75.0, 74.9, 73.1, 72.9, 72.4, 72.1, 71.0, 69.5, 50.4, 45.8, 34.5, 31.7, 25.2, 25.1, 22.7, 22.3, 21.4, 17.71, 17.67, 17.62, 15.9, 15.1, 13.6, 13.5; IR (thin film, cm^{-1}) 3031, 2952, 2927, 2868; HRMS (ESI) *m/z* calculated for $[M+NH_4]^+$ 780.4688, found 780.4685, calculated for $[M+Na]^+$ 785.4242, found 785.4239.

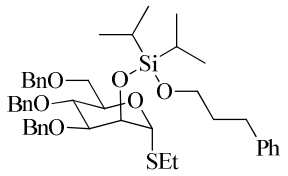

Sugar silane 57 and 3-phenylpropan-1-ol (compound 69). Following the general procedure, diisopropyl sugar silane **57** (67 mg, 0.11 mmol), 3-phenylpropan-1-ol (14 μL, 0.1 mmol), and one third of the catalyst solution prepared from CuCl (1.5 mg, 0.015 mmol), IMes·HCl (5 mg, 0.015 mmol), and NaO*t*Bu (3 mg, 0.03 mmol) were used. Column chromatography (SiO_2, 5 % ethyl acetate/ hexanes) gave 40 mg (55 %) of the desired product. ^{1}H NMR (500 MHz) δ 7.37-7.25 (m, 15H) 7.20-7.16 (m, 5H) 5.32 (d, *J* = 1.5 Hz, 1H) 4.85 (d, *J* = 10.5 Hz, 1H) 4.73 (d, *J* =

11.5 Hz, 1H) 4.65 (d, *J* = 12.0 Hz, 1H) 4.63 (d, *J* = 11.5 Hz, 1H) 4.52 (d, *J* = 12.0 Hz, 2H) 4.41 (t, *J* = 2.3 Hz, 1H) 4.14 (ddd, *J* = 10.0, 4.5, 1.5 Hz, 1H) 4.02 (t, *J* = 9.5 Hz, 1H) 3.82-3.75 (m, 4H) 3.72 (dd, *J* = 11.0, 1.5 Hz, 1H) 2.70-2.63 (m, 3H) 2.59 (dq, *J* = 13.0, 7.7 Hz, 1H) 1.85-1.80 (m, 2H) 1.28 (t, *J* = 7.5 Hz, 3H) 1.10-1.02 (m, 14H); ^{13}C NMR (125 MHz) δ 142.2, 138.6, 136.5, 128.4, 128.3, 128.18, 128.17, 128.0, 127.6, 127.5, 127.42, 127.39, 127.3, 125.7, 85.6, 80.6, 75.0, 74.7, 73.0, 72.3, 72.0, 71.1, 69.3, 62.3, 34.4, 32.0, 25.3, 17.41, 17.37, 15.1, 12.6, 12.5; IR (thin film, cm^{-1}) 3028, 2942, 2865; HRMS (ESI) *m/z* calculated for $[M+NH_4]^+$ 760.4062, found 760.4058.

6.4.3 Glycosylations

General glycosylation procedure.

The silyl acetal starting material (1 equiv.) was dissolved in dry CH_2Cl_2 (0.02 M) and cooled to -40 °C. NIS (1.3 equiv.) and 2,6-DTBMP (2.0 equiv.) were added and the reaction was stirred for ~5 min, followed by addition of TMSOTf (1.2 equiv.). The reaction was stirred at -40 °C for 15-20 min, then warmed to 0 °C and stirred until all starting material was consumed, as judged by TLC analysis. The reaction was then warmed to room temperature and TBAF (5 equiv., 1 M in THF) was added and the reaction was stirred overnight. The reaction was quenched with sat. aq. Na_2SO_3, extracted with ethyl acetate, washed with sat. aq. NH_4Cl, dried over $MgSO_4$, filtered, and concentrated. The product was purified by column chromatography.

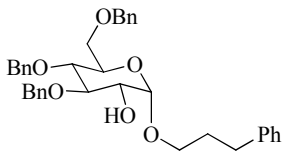

α-Glucoside 70. Following the general procedure, silyl acetal **59** (41 mg, 0.055 mmol), NIS (16 mg, 0.072 mmol), 2,6-DTBMP (23 mg, 0.11 mmol), TMSOTf (12 μL, 0.066 mmol), and TBAF

(0.3 mL, 1M in THF) were employed to give 26 mg (81 %) of the glycosylated product as a colorless oil. ^{1}H NMR (700 MHz) δ 7.41-7.40 (m, 2H) 7.36-7.28 (m, 13H) 7.21-7.19 (m, 3H) 7.17-7.16 (m, 2H) 4.95 (d, *J* = 11.2 Hz, 1H) 4.88 (d, *J* = 3.5 Hz, 1H) 4.85 (d, *J* = 10.5 Hz, 1H) 4.83 (d, *J* = 10.5 Hz, 1H) 4.63 (d, *J* = 11.9 Hz, 1H) 4.51 (d, *J* = 11.9 Hz, 1H) 4.50 (d, *J* = 10.5 Hz, 1H) 3.79-3.69 (m, 5H) 3.66-3.62 (m, 2H) 3.50 (dt, *J* = 13.3, 6.5 Hz, 1H) 2.74 (quint, *J* = 7.2 Hz, 1H) 2.68 (quint, *J* = 7.4 Hz, 1H) 2.00-1.96 (m, 3H); ^{13}C NMR (175 MHz) δ 141.5, 138.7, 138.2, 137.9, 128.40, 128.37, 128.36, 127.92, 127.90, 127.87, 127.71, 127.68, 127.64, 125.9, 98.4, 83.5, 77.4, 75.3, 75.0, 73.5, 73.1, 70.5, 68.5, 67.6, 32.5, 30.9; IR (thin film, cm^{-1}) 3469, 3029, 2919; HRMS (ESI) *m/z* calculated for $[M+NH_4]^+$ 586.3163, found 586.3165.

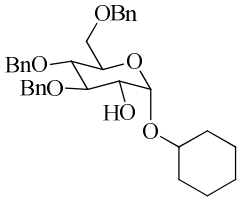

α-Glucoside 71. Following the general procedure, silyl acetal **61** (56 mg, 0.079 mmol), NIS (23 mg, 0.10 mmol), 2,6-DTBMP (32 mg, 0.16 mmol), TMSOTf (17 μL, 0.095 mmol), and TBAF (0.4 mL, 1M in THF) were employed to give 39 mg (93 %) of the glycosylated product as a white solid after purification by column chromatography (SiO_2, 20 % ethyl acetate/ hexanes). ^{1}H NMR (700 MHz) δ 7.39 (d, *J* = 7.7 Hz, 2H) 7.34-7.30 (m, 6H) 7.28-7.25 (m, 5H) 7.14 (d, *J* = 7.0 Hz, 2H) 5.02 (d, *J* = 3.5 Hz, 1H) 4.97 (d, *J* = 10.5 Hz, 1H) 4.824 (d, *J* = 11.2 Hz, 1H) 4.818 (d, *J* = 11.2 Hz, 1H) 4.63 (d, *J* = 11.9 Hz, 1H) 4.49 (d, *J* = 11.2 Hz, 1H) 4.48 (d, *J* = 10.5 Hz, 1H) 3.88-3.87 (m, 1H) 3.76 (dd, *J* = 10.5, 3.5 Hz, 1H) 3.73 (t, *J* = 8.9 Hz, 1H) 3.69 (td, *J* = 9.3, 4.2 Hz, 1H) 3.66-3.60 (m, 3H) 2.03 (d, *J* = 9.8 Hz, 1H) 1.90-1.88 (m, 2H) 1.72-1.70 (m, 2H) 1.53-1.41 (m, 1H) 1.41-1.36 (m, 1H) 1.33-1.17 (m, 4H); ^{13}C NMR (125 MHz) δ 138.8, 138.2, 138.0, 128.4, 128.3, 127.9, 127.8, 127.7, 127.6, 127.5, 96.8, 83.8, 77.3, 76.1, 75.3, 75.1, 73.5, 73.0,

70.5, 68.5, 33.4, 31.7, 25.5, 24.1, 23.9; IR (thin film, cm^{-1}) 3490, 3031, 2932, 2857; HRMS (ESI) *m/z* calculated for $[M+NH_4]^+$ 550.3163, found 550.3161; mp = 92-94 °C.

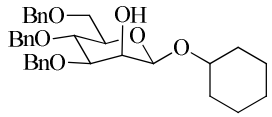

β-Mannoside 72. Following the general procedure, silyl acetal **64** (61 mg, 0.086 mmol), NIS (25 mg, 0.11 mmol), 2,6-DTBMP (35 mg, 0.17 mmol), TMSOTf (19 μL, 0.10 mmol), and TBAF (0.4 mL, 1M in THF) were employed to give 43 mg (93 %) of the glycosylated product as a colorless oil after purification by column chromatography (SiO_2, 25 % ethyl acetate/ hexanes). ^1H NMR (500 MHz) δ 7.40-7.39 (m, 2H) 7.36-7.25 (m, 11H) 7.24-7.23 (m, 2H) 4.91 (d, *J* = 11.0 Hz, 1H) 4.79 (d, *J* = 12.0 Hz, 1H) 4.68 (d, *J* = 12.0 Hz, 1H) 4.63 (d, *J* = 12.0 Hz, 1H) 4.59-4.55 (m, 3H) 4.08 (d, *J* = 3.0 Hz, 1H) 3.86 (t, *J* = 9.3 Hz, 1H) 3.79 (dd, *J* = 10.8, 1.3 Hz, 1H) 3.74 (tt, *J* = 9.3, 3.7 Hz, 1H) 3.70 (dd, *J* = 11.0, 6.0 Hz, 1H) 3.58 (dd, *J* = 9.0, 3.5 Hz, 1H) 3.44 (ddd, *J* = 9.6, 5.6, 1.9 Hz, 1H) 2.50 (br. s.) 2.02-2.00 (m, 1H) 1.90-1.87 (m, 1H) 1.77-1.73 (m, 2H) 1.56-1.54 (m, 1H) 1.50-1.42 (m, 1H) 1.36-1.17 (m, 4H); ^{13}C NMR (125 MHz) δ 138.3, 138.2, 137.8, 128.4, 128.3, 128.2, 128.1, 127.8, 127.74, 127.67, 127.5, 97.3, 81.7, 76.6, 75.2, 75.1, 74.3, 73.4, 71.2, 69.3, 68.8, 33.4, 31.6, 25.5, 24.1, 23.9; IR (thin film, cm^{-1}) 3346, 3031, 2933, 2857; HRMS (ESI) *m/z* calculated for $[M+NH_4]^+$ 550.3163, found 550.3170.

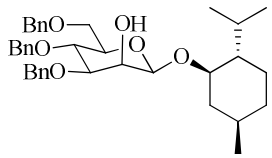

β-Mannoside 73. Following the general procedure, silyl acetal **67** (35 mg, 0.043 mmol), NIS (13 mg, 0.056 mmol), 2,6-DTBMP (18 mg, 0.086 mmol), TMSOTf (10 μL, 0.052 mmol), and TBAF (0.2 mL, 1M in THF) were employed to give 13 mg (52 %) of the glycosylated product as a white solid after purification by column chromatography (SiO_2, 20 % ethyl acetate/ hexanes).

^{1}H NMR (700 MHz) δ 7.40-7.39 (m, 2H) 7.35-7.25 (m, 13H) 4.91 (d, *J* = 11.2 Hz, 1H) 4.80 (d, *J* = 11.9 Hz, 1H) 4.69 (d, *J* = 11.9 Hz, 1H) 4.62 (d, *J* = 11.9 Hz, 1H) 4.59 (d, *J* = 10.5 Hz, 1H) 4.55 (d, *J* = 11.9 Hz, 1H) 4.53 (s, 1H) 4.03 (d, *J* = 2.8 Hz, 1H) 3.87 (t, *J* = 9.5 Hz, 1H) 3.75 (dd, *J* == 10.9, 1.8 Hz, 1H) 3.71 (dd, *J* = 11.2, 5.6 Hz, 1H) 3.59 (td, *J* = 10.7, 4.2 Hz, 1H) 3.58 (dd, *J* = 9.1, 2.8 Hz, 1H) 3.41 (ddd, *J* = 9.8, 5.3, 1.8 Hz, 1H) 2.37 (s, 1H) 2.29 (septet of d, *J* = 6.9, 2.2 Hz, 1H) 2.00-1.98 (m, 1H) 1.67-1.64 (m, 2H) 1.39-1.34 (m, 1H) 1.31-1.26 (m, 2H) 1.03-0.97 (m, 1H) 0.92 (d, *J* = 6.3 Hz, 3H) 0.91 (d, *J* = 6.3 Hz, 3H) 0.89-0.86 (m, 1H) 0.83 (d, *J* = 7.0 Hz, 3H); ^{13}C NMR (175 MHz) δ 138.4, 138.3, 138.0, 128.44, 128.36, 128.30, 128.2, 127.81, 127.75, 127.72, 127.69, 127.5, 96.1, 81.9, 76.5, 75.3, 75.2, 74.4, 73.6, 71.2, 69.7, 69.2, 47.7, 40.4, 34.3, 31.3, 25.3, 23.1, 22.3, 21.0, 15.8; IR (thin film, cm^{-1}) 3478, 3031, 2923, 2868; HRMS (ESI) *m/z* calculated for $[M+NH_4]^+$ 606.3789, found 606.3797; mp = 103-106 °C.

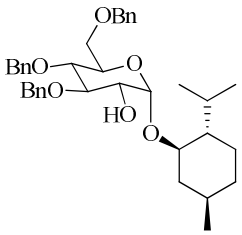

α-Glucoside 74. Following the general procedure, silyl acetal **65** (57 mg, 0.07 mmol), NIS (21 mg, 0.09 mmol), 2,6-DTBMP (29 mg, 0.14 mmol), TMSOTf (15 μL, 0.08 mmol), and TBAF (0.35 mL, 1M in THF) were employed to give 34 mg (82 %) of the glycosylated product after purification by column chromatography (SiO_2, 10 % ethyl acetate/ hexanes to 20 % ethyl acetate/ hexanes). ^{1}H NMR (700 MHz) δ 7.39-7.38 (m, 2H) 7.34-7.25 (m, 11H) 7.15-7.14 (m, 2H) 4.97 (d, *J* = 4.2 Hz, 1H) 4.95 (d, *J* = 11.2 Hz, 1H) 4.83 (d, *J* = 11.2 Hz, 1H) 4.82 (d, *J* = 11.2 Hz, 2H) 4.64 (d, *J* = 11.9 Hz, 1H) 4.49 (d, *J* = 11.9 Hz, 1H) 4.47 (d, *J* = 1.05 Hz, 1H) 3.39 (ddd, *J* = 10.2, 3.9, 2.1 Hz, 1H) 3.75 (dd, *J* = 10.5, 4.2 Hz, 1H) 3.72 (t, *J* = 9.1 Hz, 1H) 3.69 (td, *J* = 9.5, 3.7 Hz, 1H) 3.65 (dd, *J* = 10.9, 1.8 Hz, 1H) 3.60 (dd, *J* = 9.8, 8.4 Hz, 1H) 3.39 (td, *J* = 10.7, 4.4 Hz, 1H)

2.21-2.18 (m, 1H) 2.13 (septet of d, J = 7.0, 2.7 Hz, 1H) 1.95 (d, J = 9.8 Hz, 1H) 1.63-1.61 (m, 2H) 1.39-1.35 (m, 1H) 1.30-1.25 (m, 1H) 1.02-0.93 (m, 2H) 0.91 (d, J = 7.0 Hz, 3H) 0.85 (d, J = 6.3 Hz, 3H) 0.84-0.78 (m, 1H) 0.77 (d, J = 7.0 Hz, 3H); ^{13}C NMR (175 MHz) δ 138.8, 138.2, 138.0, 128.4, 128.3, 127.95, 127.91, 127.8, 127.7, 127.64, 127.59, 100.0, 83.5, 81.1, 77.4, 75.2, 75.0, 73.6, 73.5, 70.6, 68.6, 48.7, 42.9, 34.2, 31.6, 25.5, 22.8, 22.2, 21.2, 15.7; IR (thin film, cm^{-1}) 3473, 3030, 2922; HRMS (ESI) *m/z* calculated for $[M+NH_4]^+$ 606.3789, found 606.3791.

6.5 ^{1}H and ^{13}C NMR Spectra

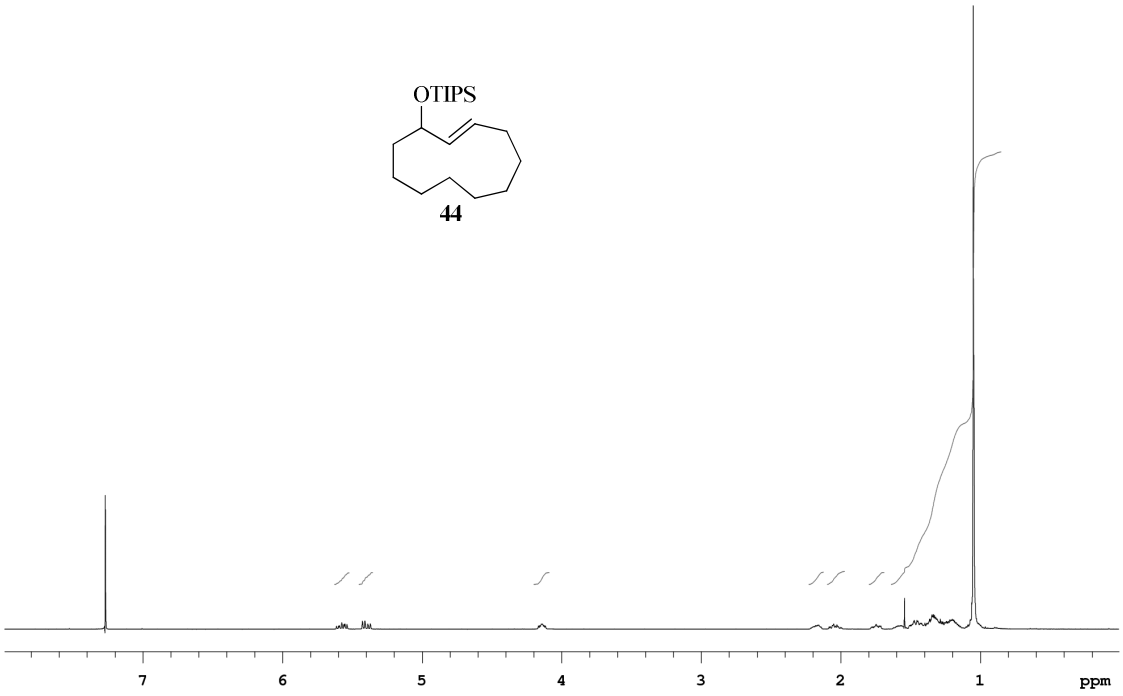

44

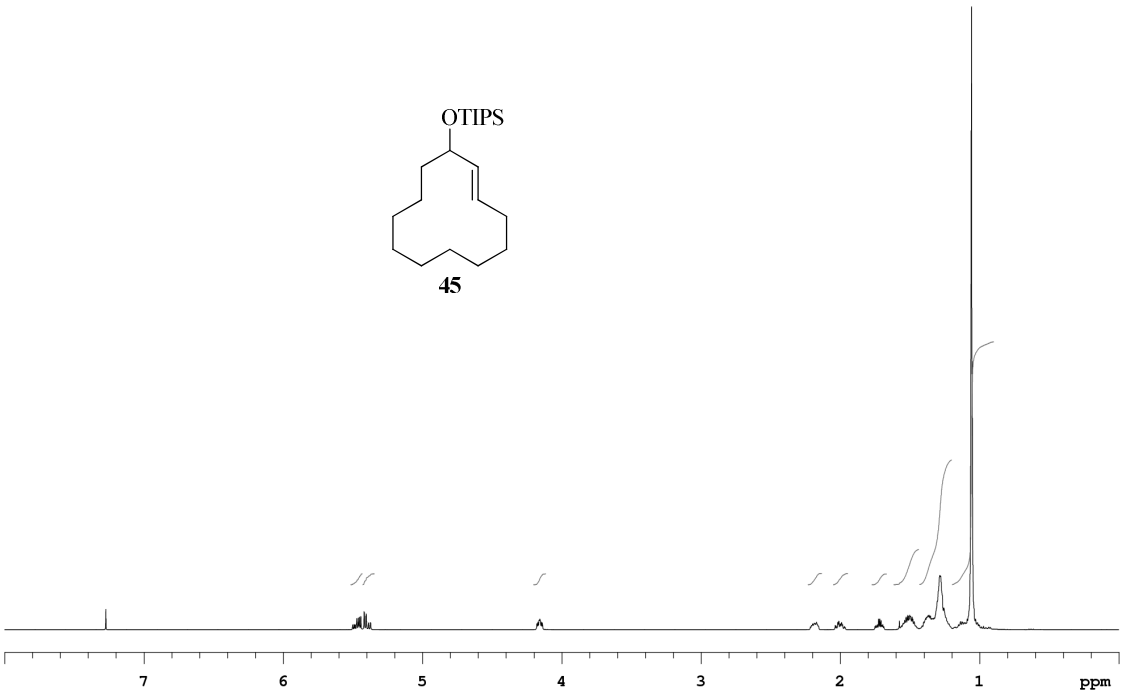

45

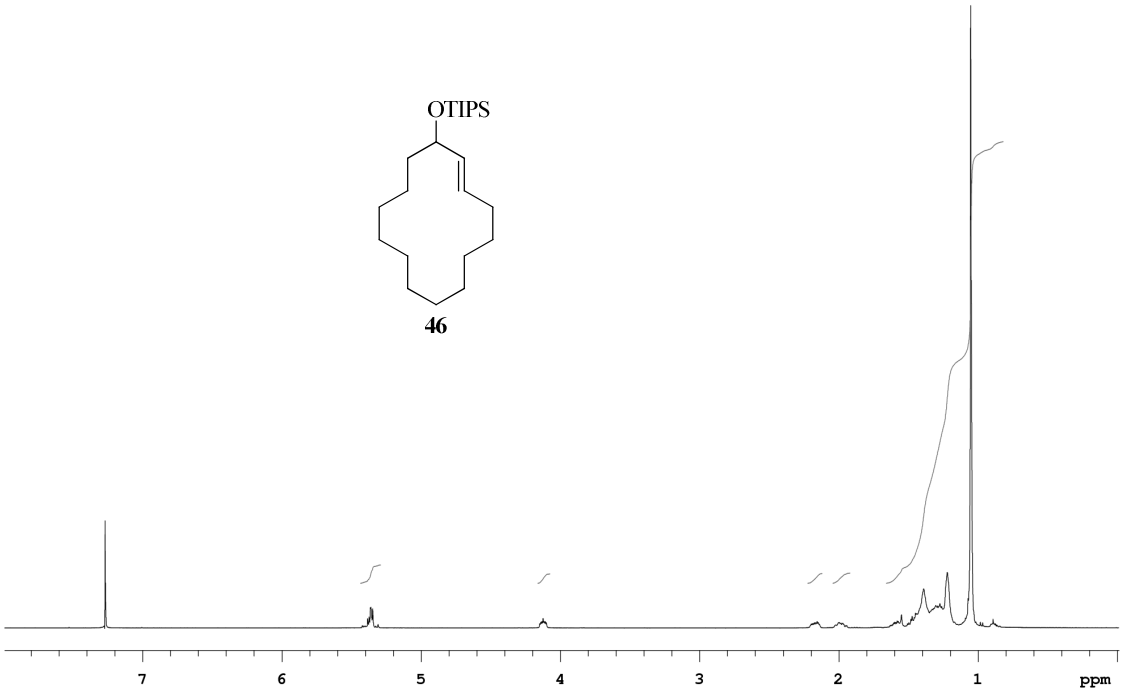

46

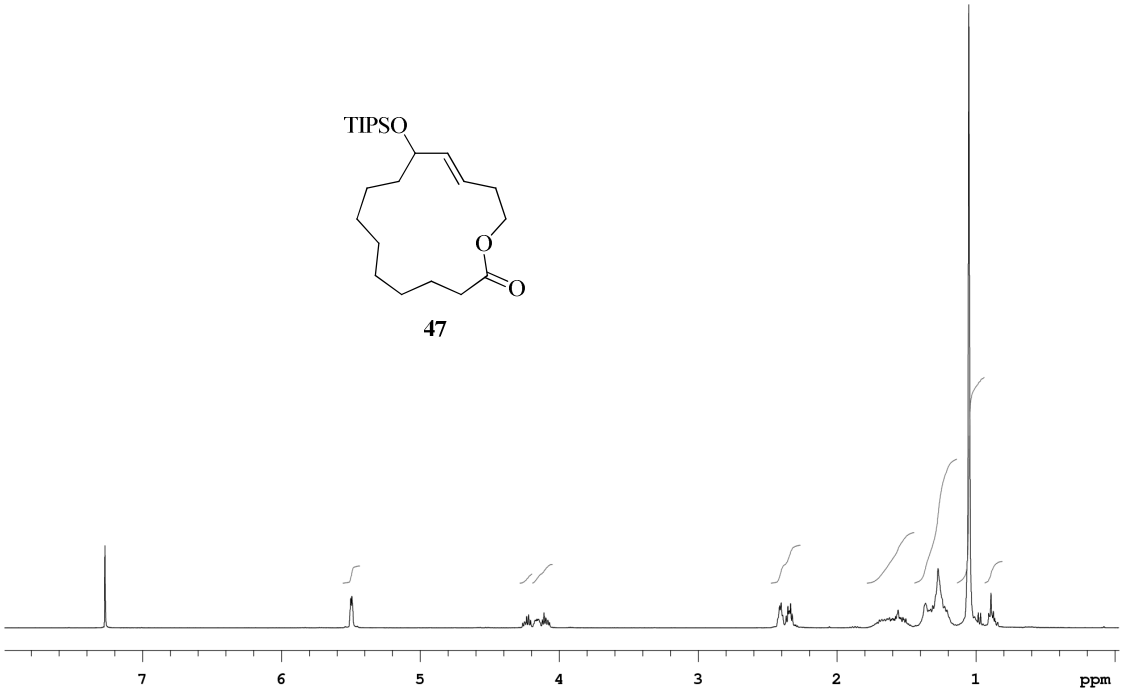

47

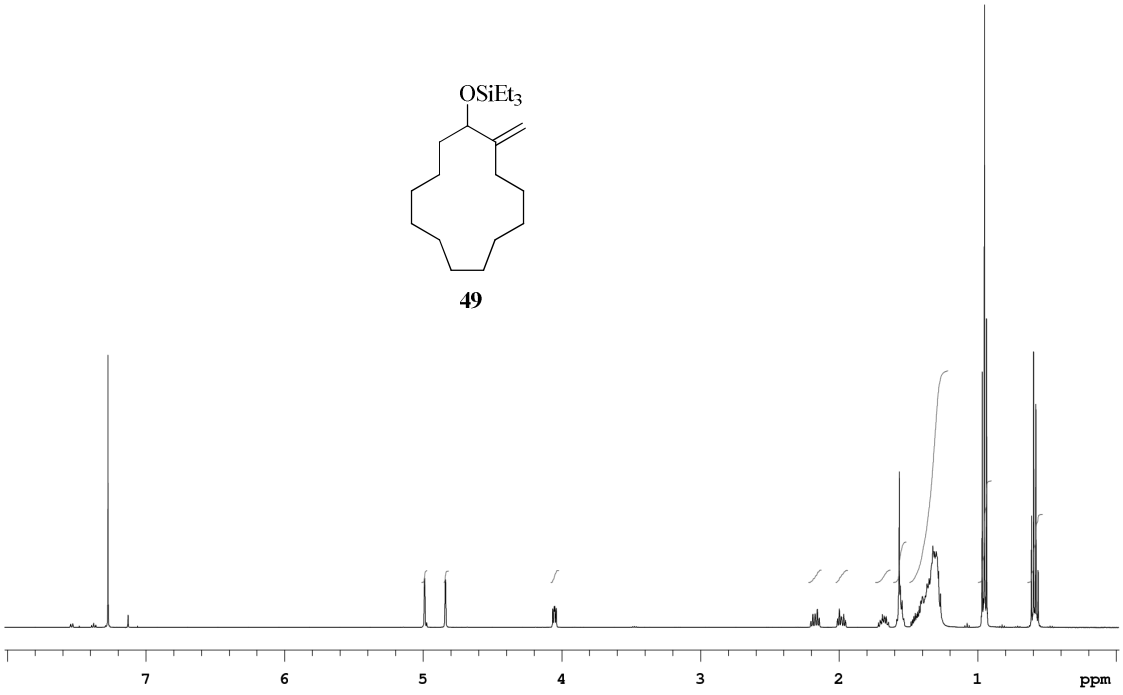

49

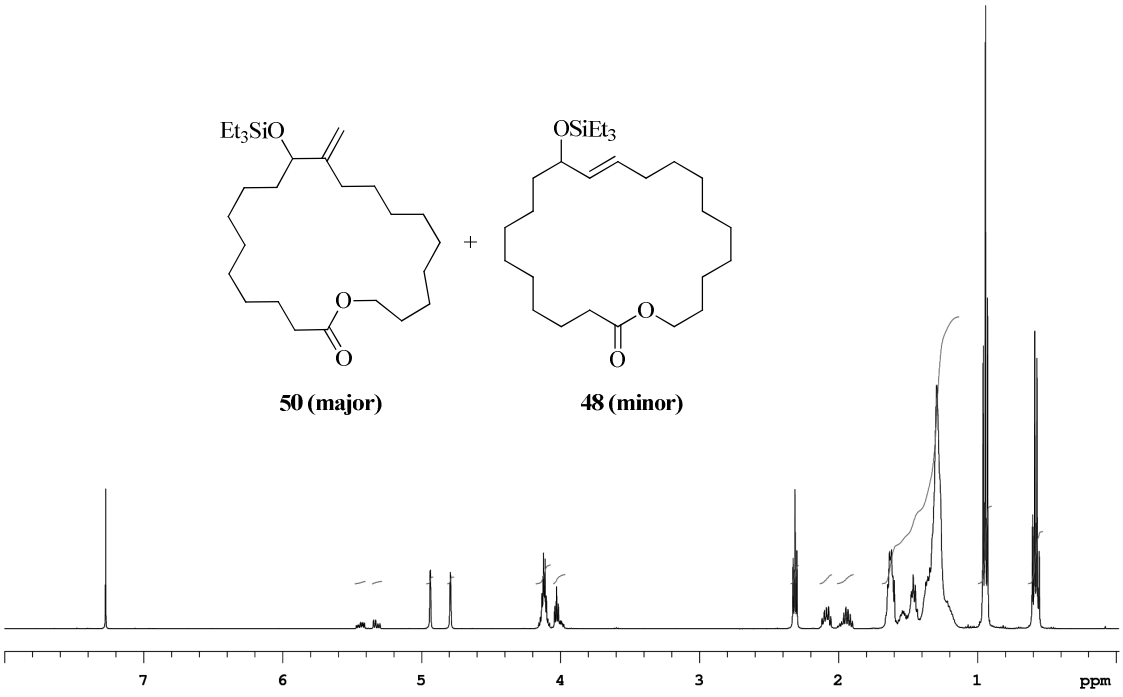

50 (major) **48 (minor)**

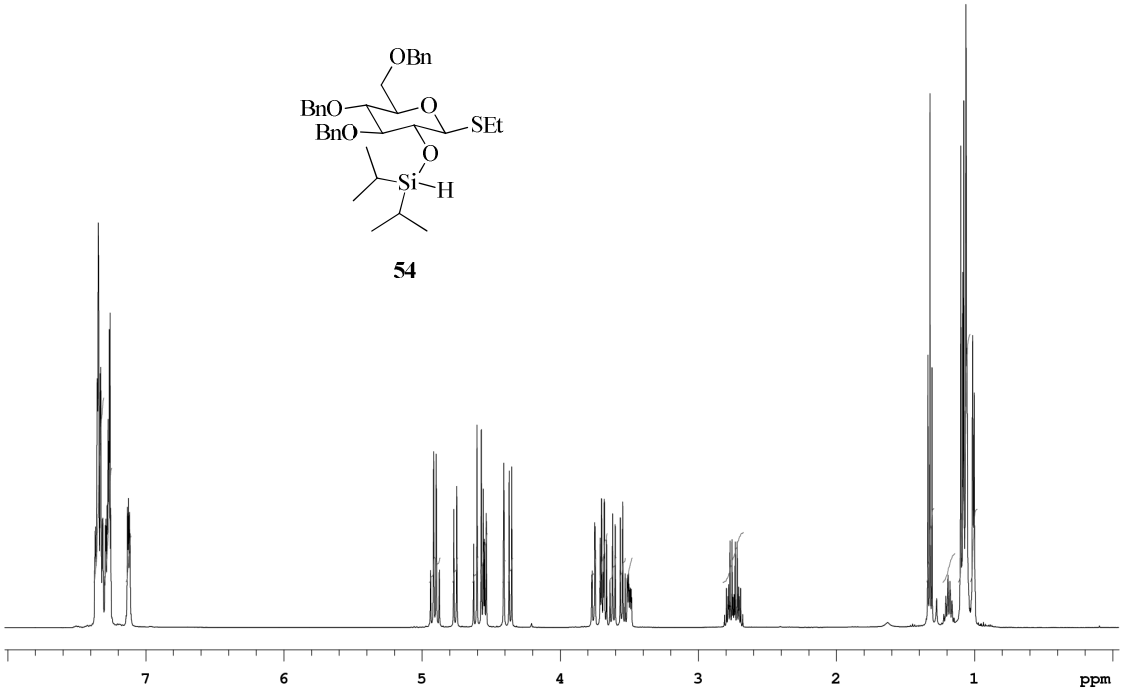
OBn
BnO
BnO
O
SEt
O
Si
H
7
6
5
4
3
2
1
ppm

54

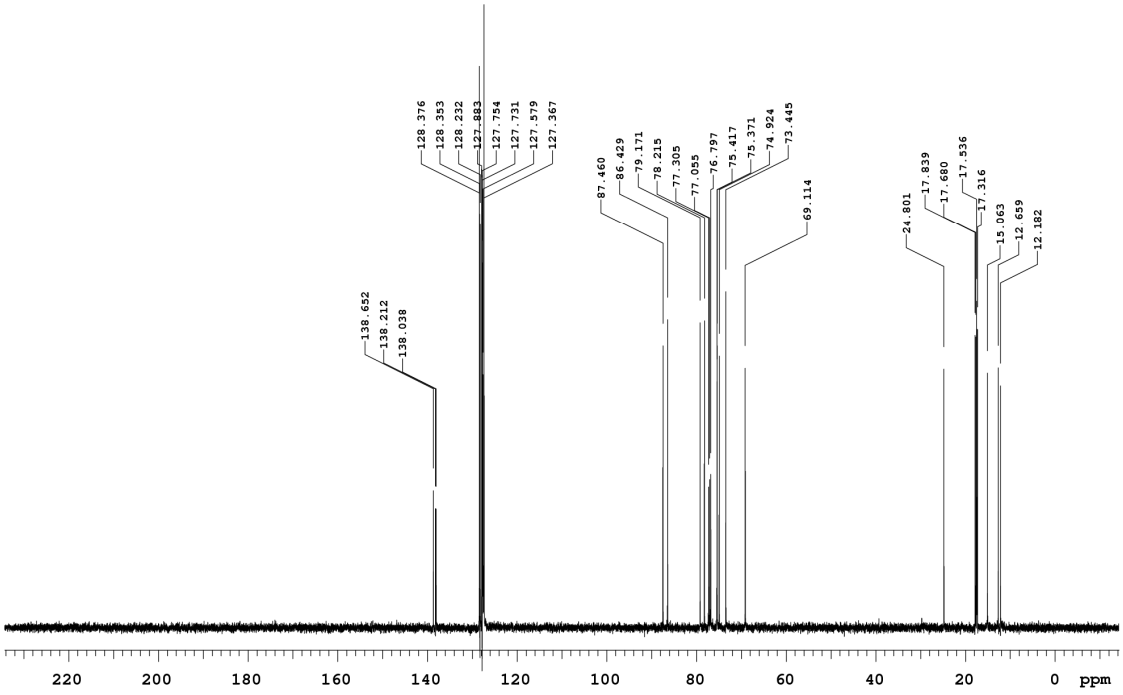
128.376
128.353
128.232
127.883
127.754
127.731
127.579
127.367
87.460
86.429
79.171
78.215
77.305
77.055
76.797
75.417
75.371
74.924
73.445
69.114
138.652
138.212
138.038
24.801
17.839
17.680
17.536
17.316
15.063
12.659
12.182
220
200
180
160
140
120
100
80
60
40
20
0
ppm

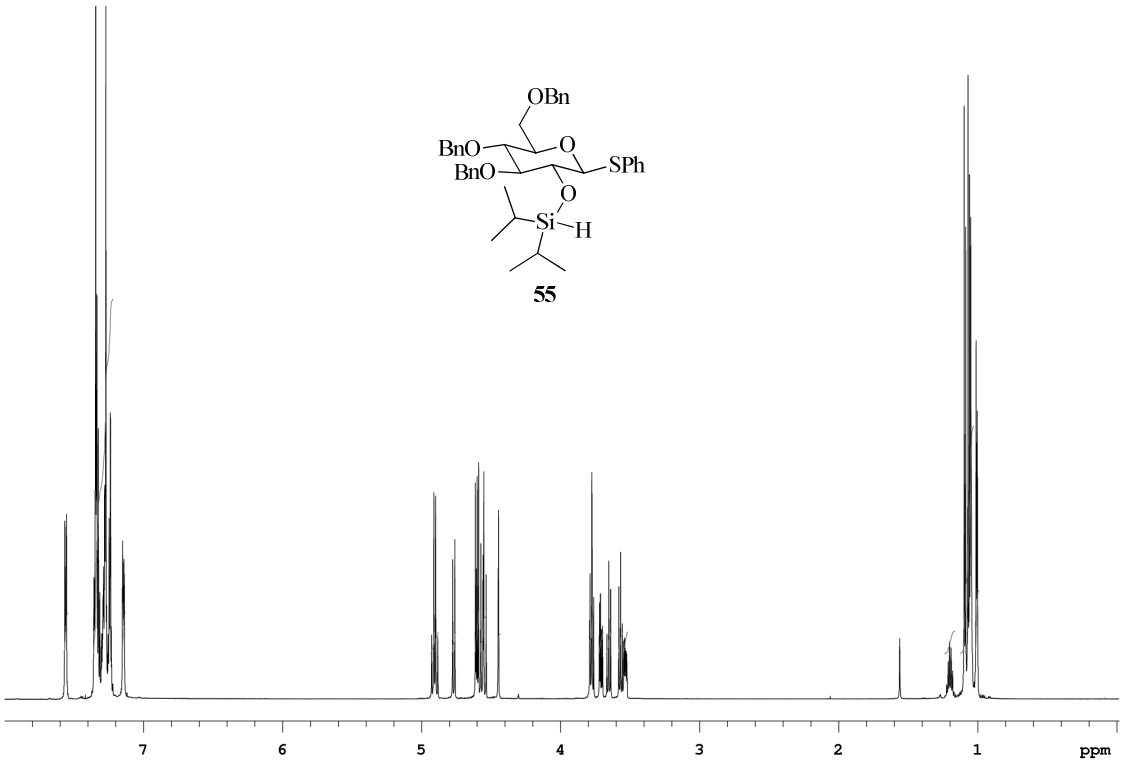
OBn
BnO
O
SPh
BnO
O
Si
H
7
6
5
4
3
2
1
ppm

55

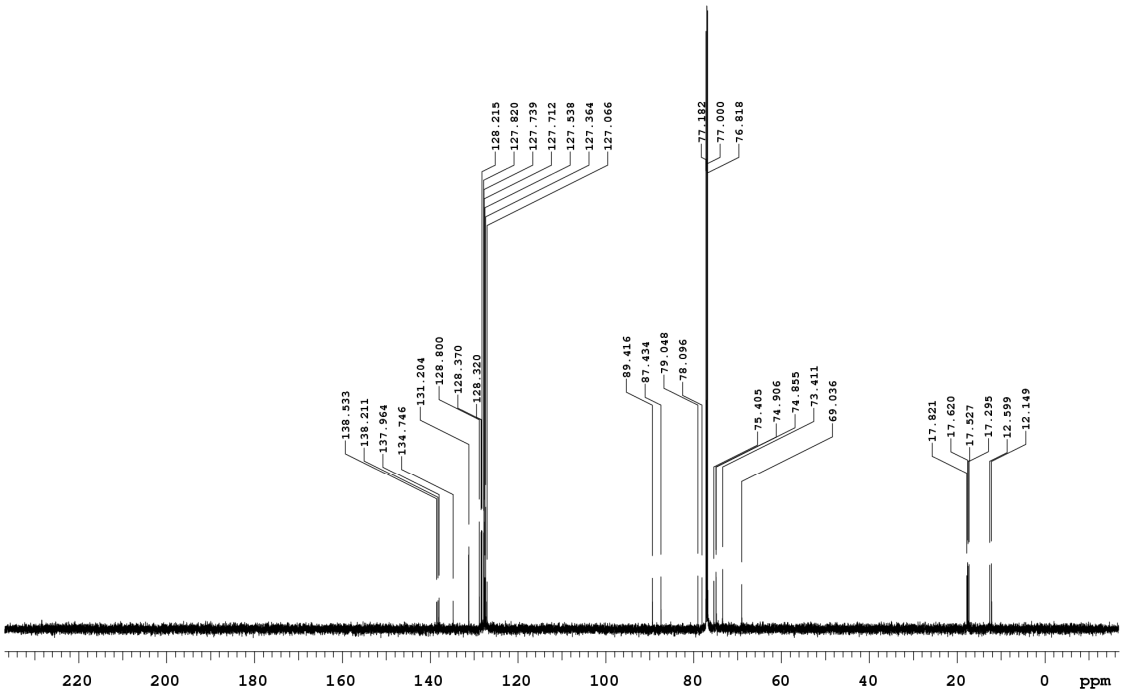
128.215
127.820
127.739
127.712
127.538
127.364
127.066
77.182
77.000
76.818
138.533
138.211
137.964
134.746
131.204
128.800
128.370
128.320
89.416
87.434
79.048
78.096
75.405
74.906
74.855
73.411
69.036
17.821
17.620
17.527
17.295
12.599
12.149
220
200
180
160
140
120
100
80
60
40
20
0
ppm

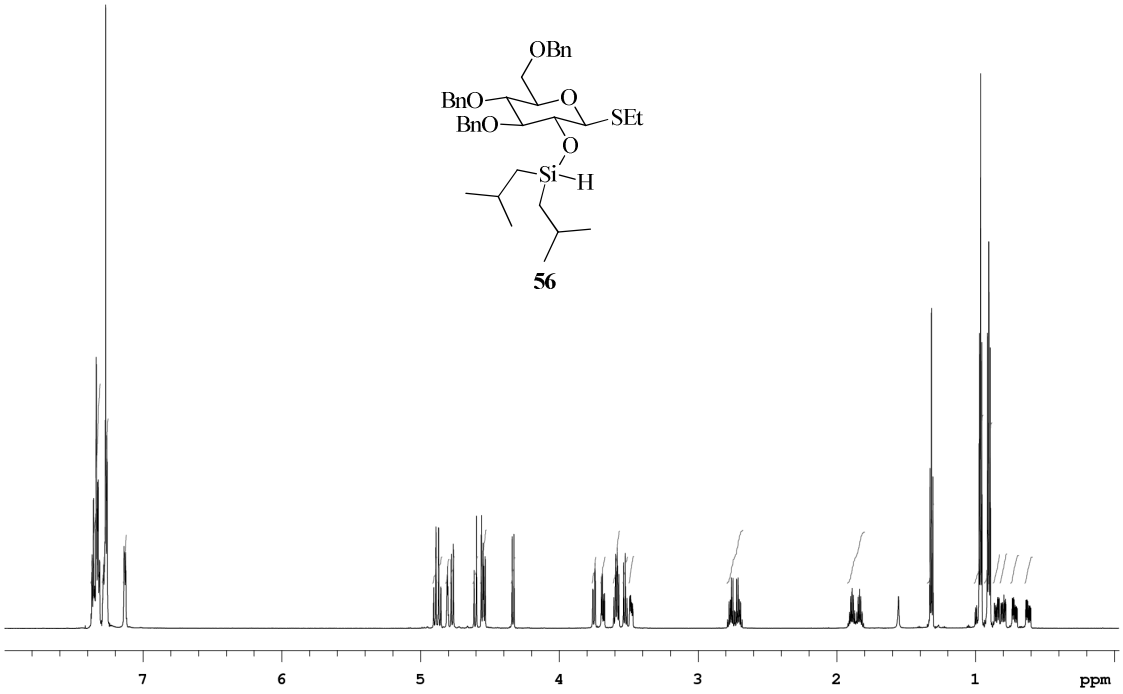
OBn
BnO
BnO
O
SEt
O
Si
H
7
6
5
4
3
2
1
ppm

56

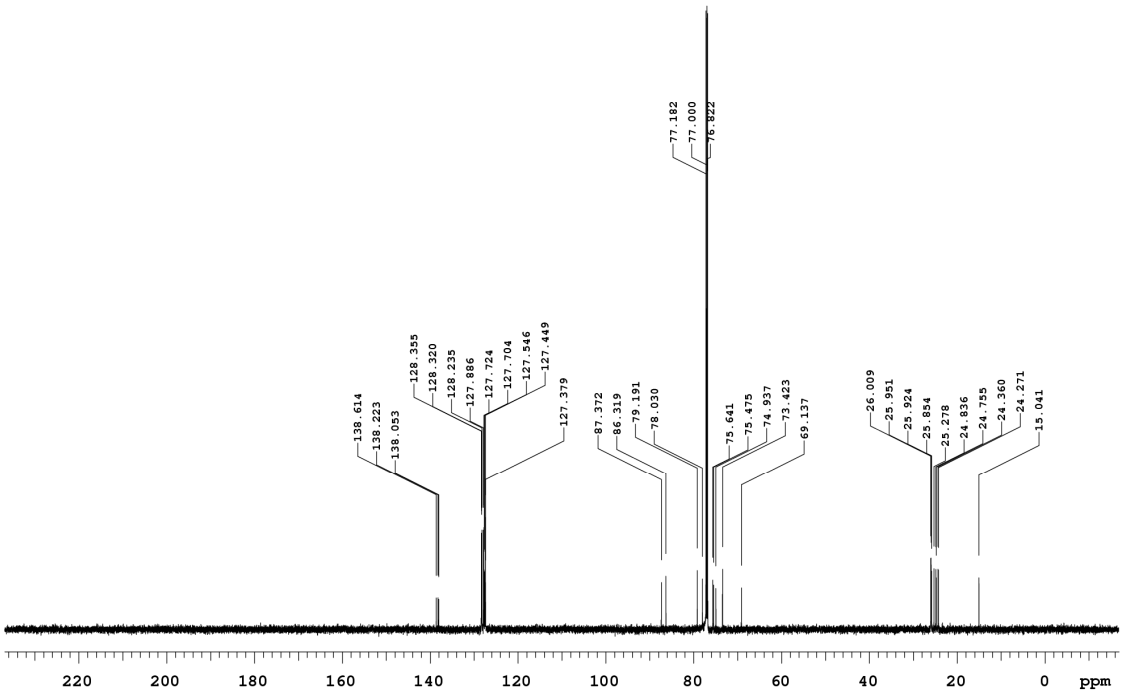
77.182
77.000
76.822
128.355
128.320
128.235
127.886
127.724
127.704
127.546
127.449
127.379
138.614
138.223
138.053
87.372
86.319
79.191
78.030
75.641
75.475
74.937
73.423
69.137
26.009
25.951
25.924
25.854
25.278
24.836
24.755
24.360
24.271
15.041
220
200
180
160
140
120
100
80
60
40
20
0
ppm

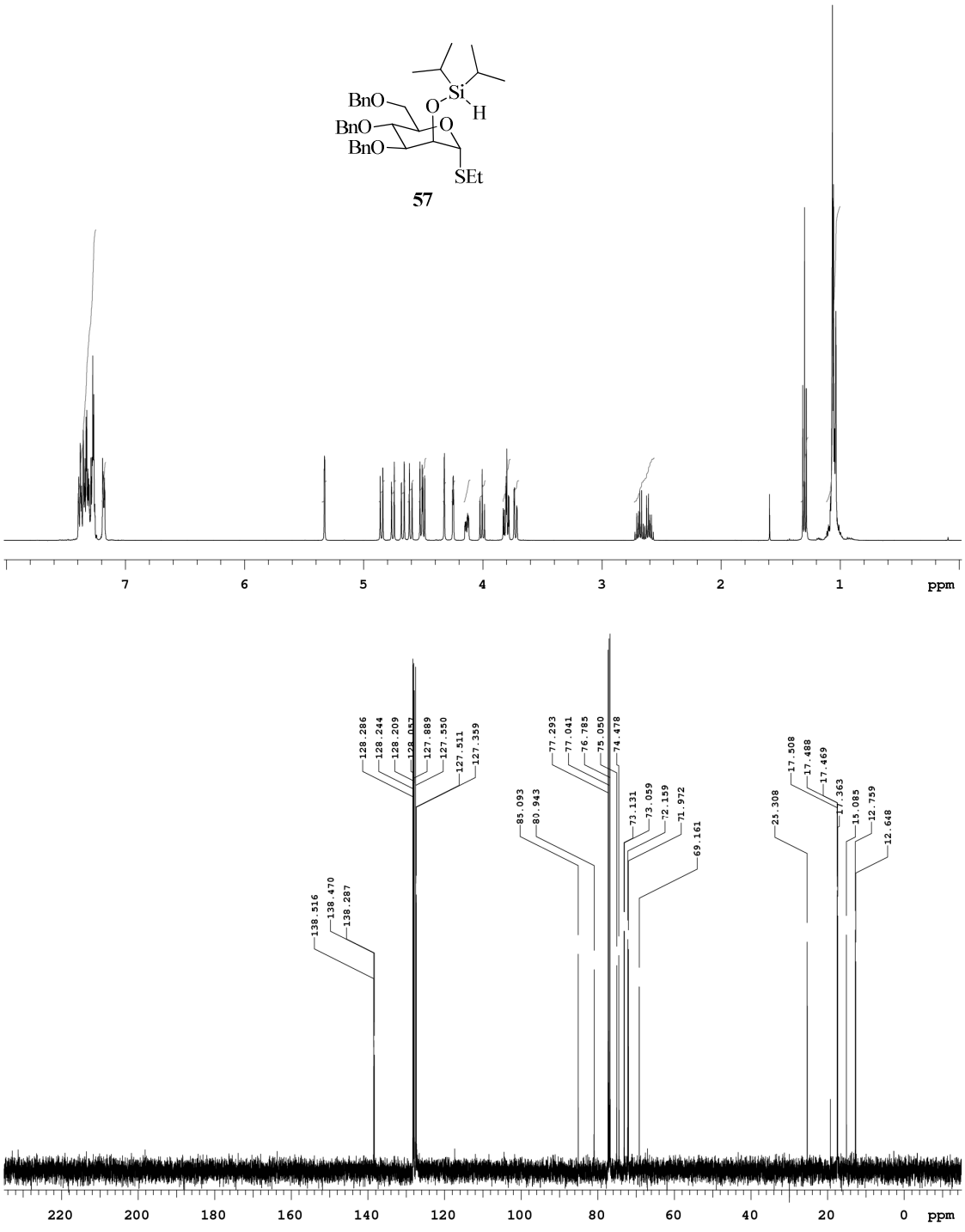
BnO
BnO
BnO
O
Si
H
O
SEt
7
6
5
4
3
2
1
ppm
128.286
128.244
128.209
128.057
127.889
127.550
127.511
127.359
138.516
138.470
138.287
77.293
77.041
76.785
75.050
74.478
85.093
80.943
73.131
73.059
72.159
71.972
69.161
25.308
17.508
17.488
17.469
17.363
15.085
12.759
12.648
220
200
180
160
140
120
100
80
60
40
20
0
ppm

57

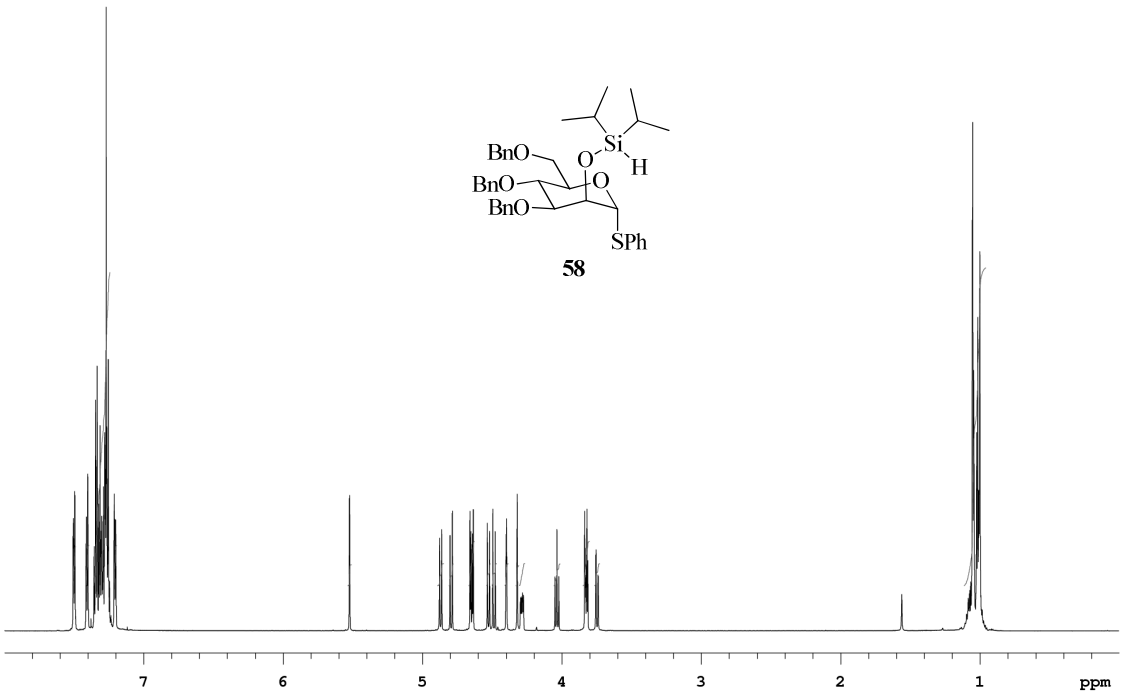
BnO
BnO
BnO
O
Si
H
O
SPh
7
6
5
4
3
2
1
ppm

58

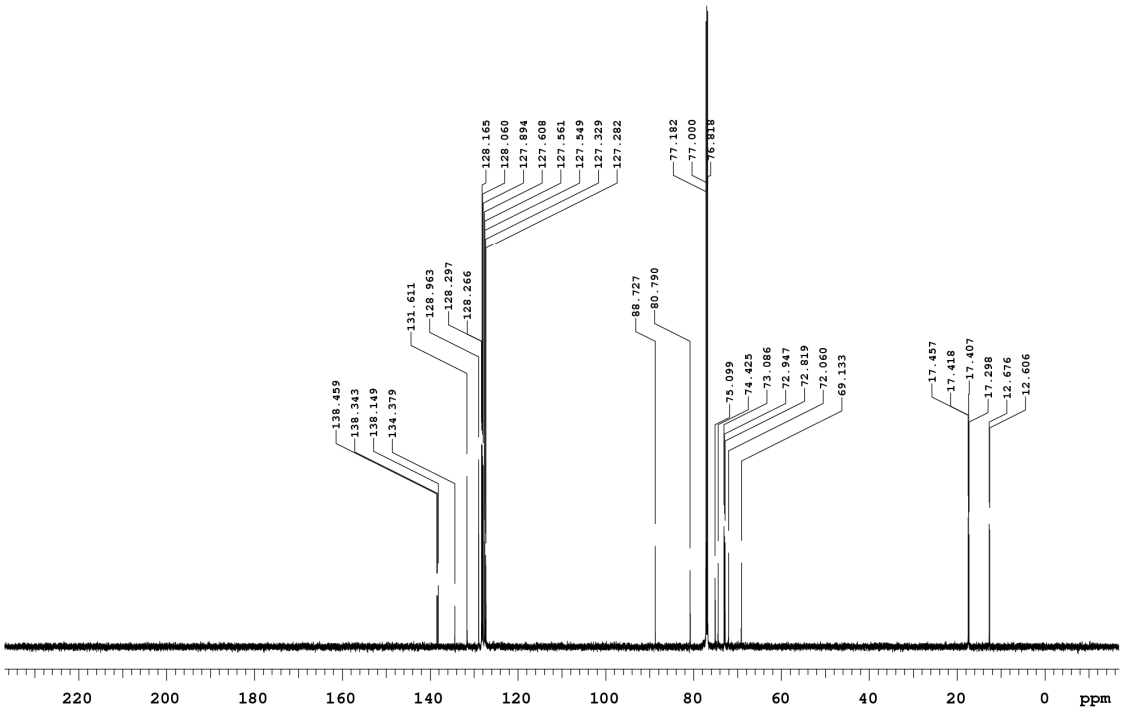
138.459
138.343
138.149
134.379
131.611
128.963
128.297
128.266
128.165
128.060
127.894
127.608
127.561
127.549
127.329
127.282
88.727
80.790
77.182
77.000
76.818
75.099
74.425
73.086
72.947
72.819
72.060
69.133
17.457
17.418
17.407
17.298
12.676
12.606
220
200
180
160
140
120
100
80
60
40
20
0
ppm

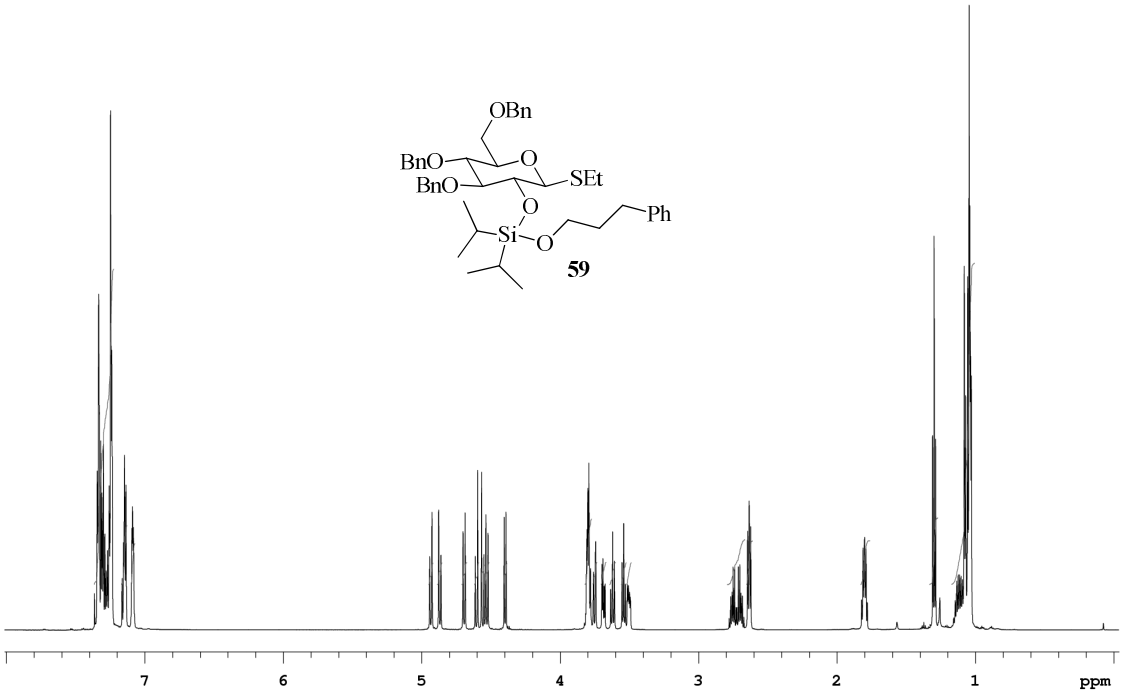
OBn
BnO
BnO
O
SEt
O
Si
O
Ph
59
7
6
5
4
3
2
1
ppm

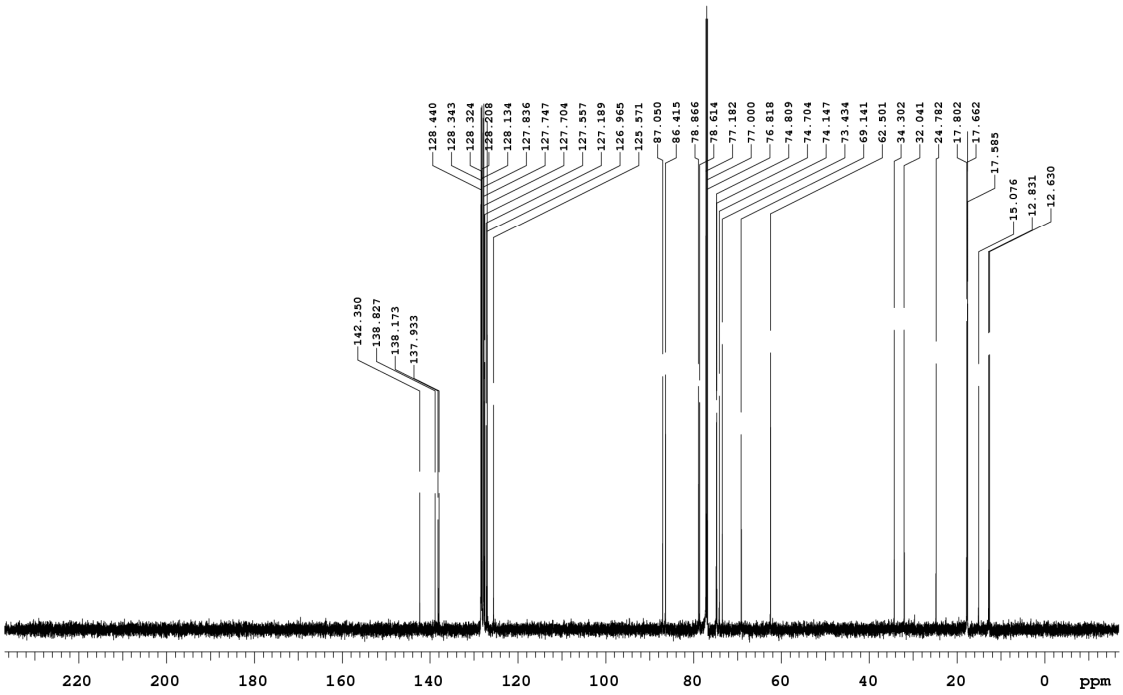
128.440
128.343
128.324
128.208
128.134
127.836
127.747
127.704
127.557
127.189
126.965
125.571
87.050
86.415
78.866
78.614
77.182
77.000
76.818
74.809
74.704
74.147
73.434
69.141
62.501
34.302
32.041
24.782
17.802
17.662
17.585
15.076
12.831
12.630
142.350
138.827
138.173
137.933
220
200
180
160
140
120
100
80
60
40
20
0
ppm

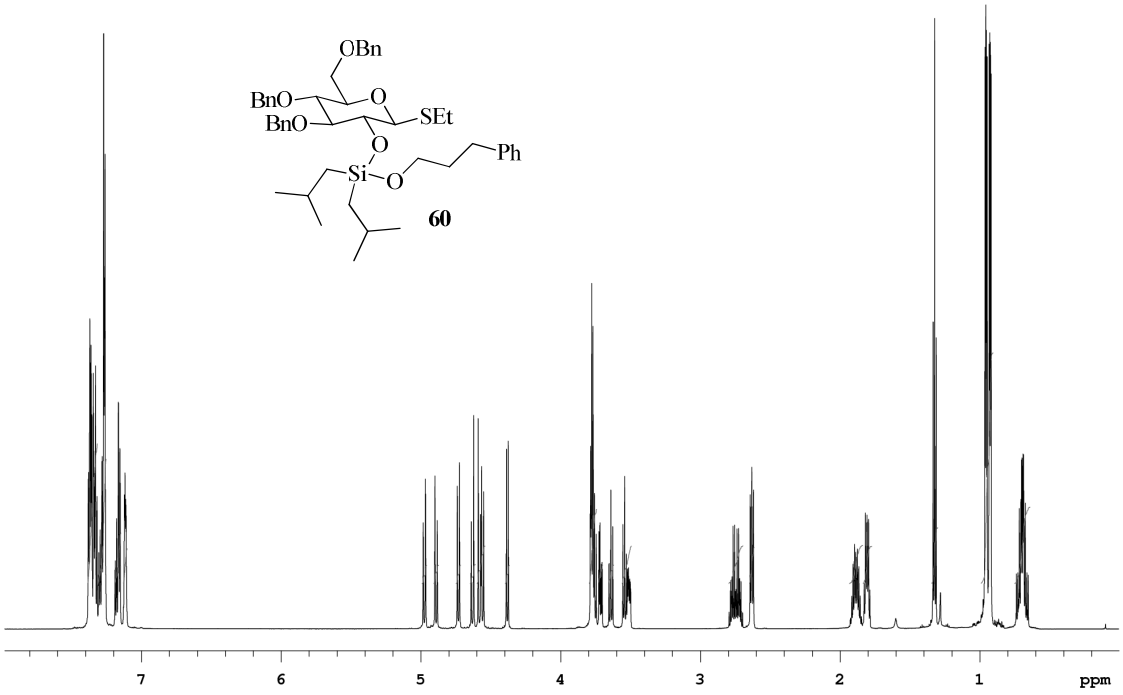
OBn
BnO
BnO
O
SEt
O
Si
O
Ph
60
7
6
5
4
3
2
1
ppm

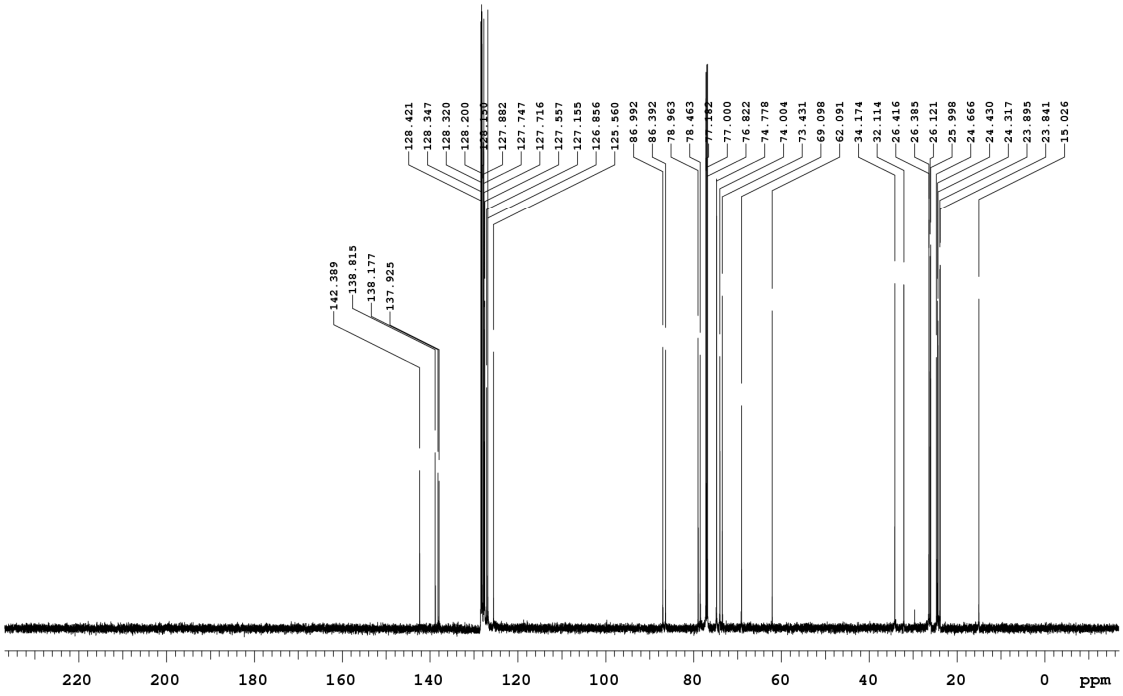
128.421
128.347
128.320
128.200
128.130
127.882
127.747
127.716
127.557
127.155
126.856
125.560
86.992
86.392
78.963
78.463
77.182
77.000
76.822
74.778
74.004
73.431
69.098
62.091
34.174
32.114
26.416
26.385
26.121
25.998
24.666
24.430
24.317
23.895
23.841
15.026
142.389
138.815
138.177
137.925
220
200
180
160
140
120
100
80
60
40
20
0
ppm

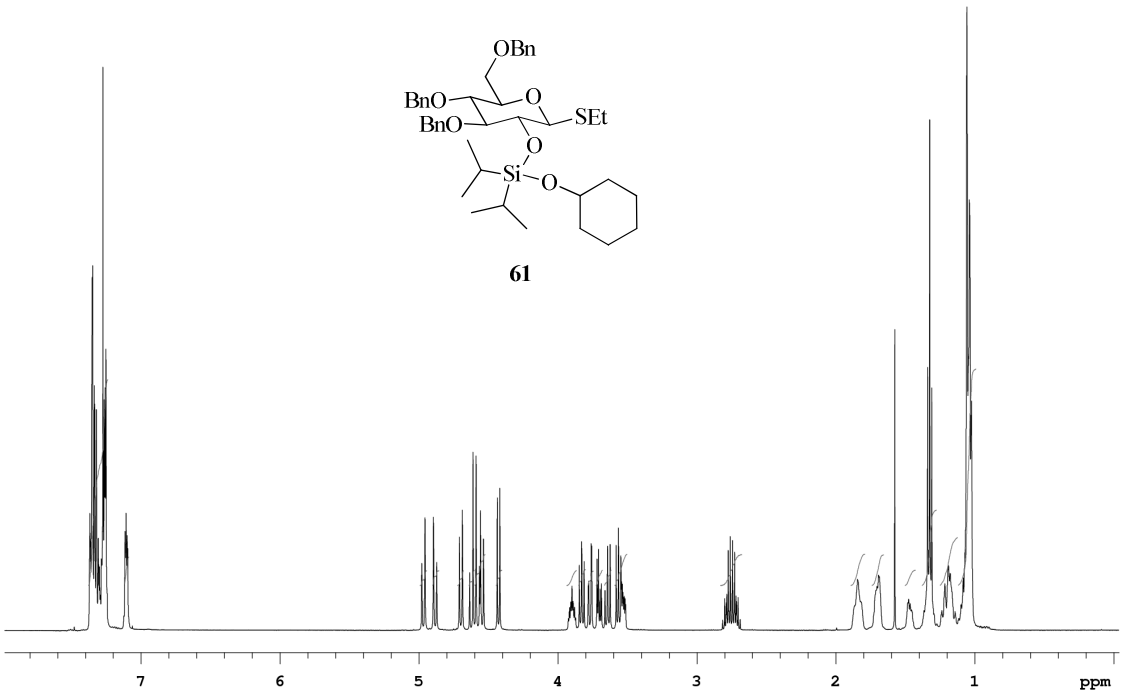
OBn
BnO
O
SEt
BnO
O
Si
O
7
6
5
4
3
2
1
ppm

61

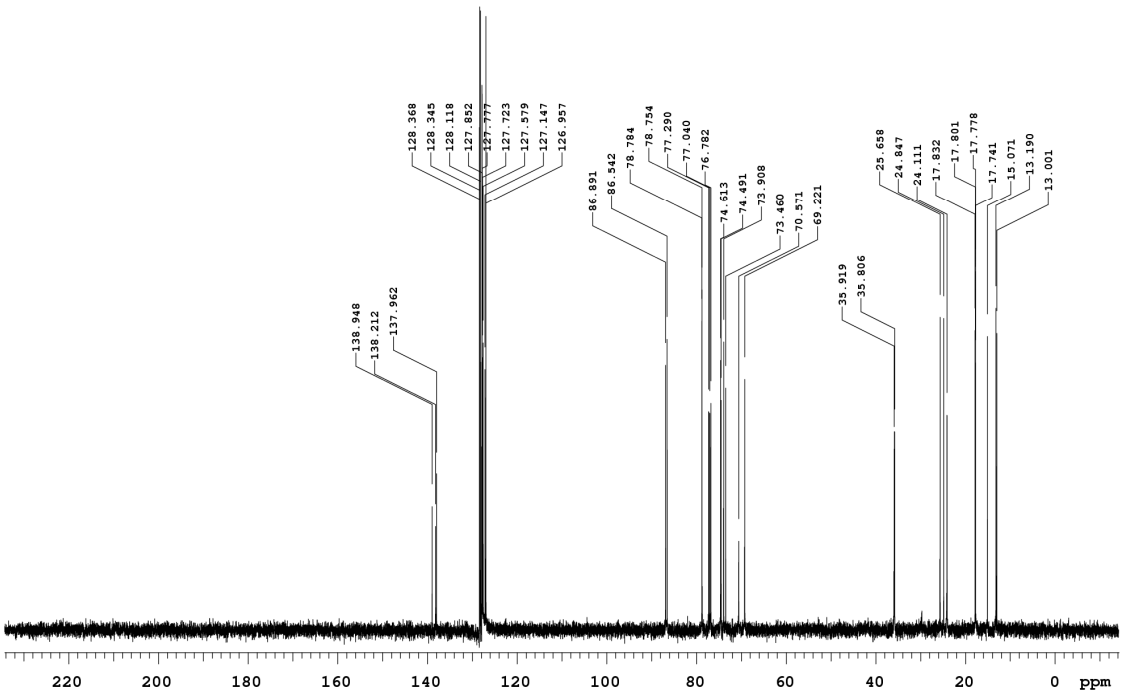
128.368
128.345
128.118
127.852
127.777
127.723
127.579
127.147
126.957
86.891
86.542
78.784
78.754
77.290
77.040
76.782
74.613
74.491
73.908
73.460
70.571
69.221
138.948
138.212
137.962
35.919
35.806
25.658
24.847
24.111
17.832
17.801
17.778
17.741
15.071
13.190
13.001
220
200
180
160
140
120
100
80
60
40
20
0
ppm

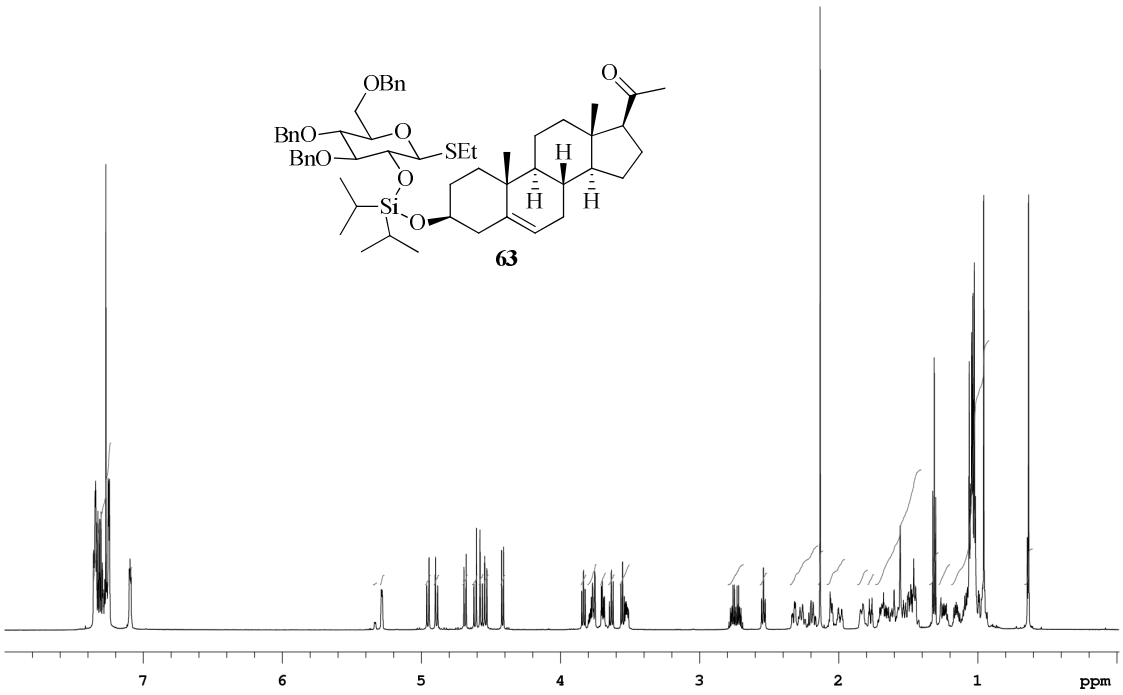
OBn
BnO
BnO
O
SEt
O
Si
O
O
H
H
H
63
7
6
5
4
3
2
1
ppm

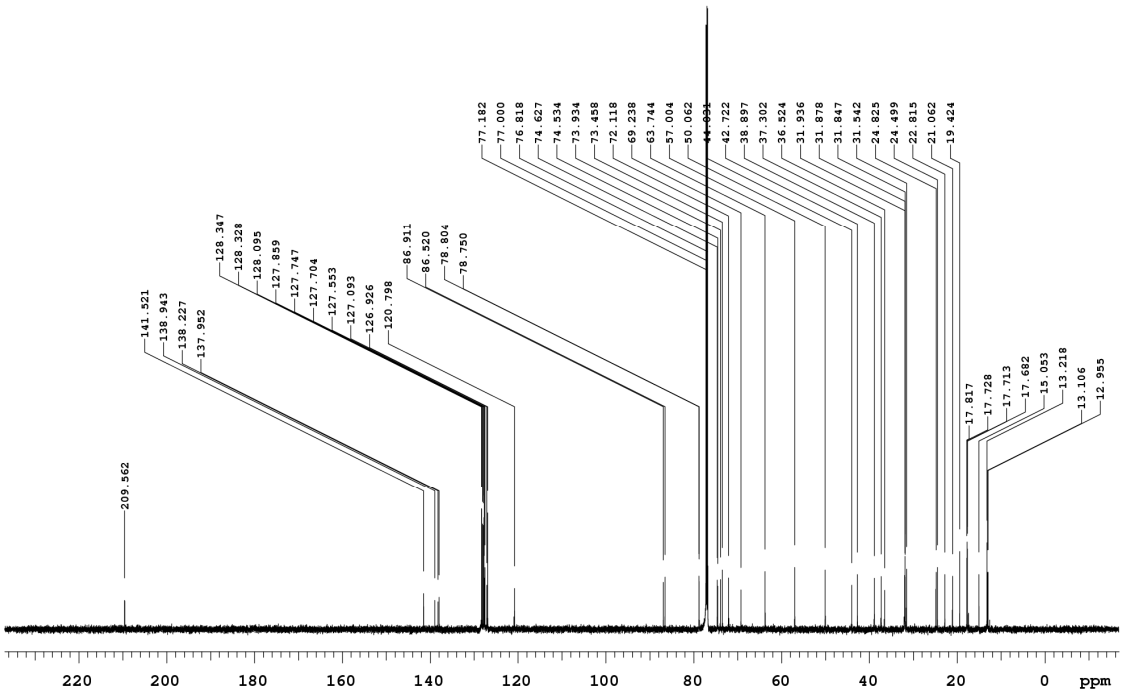
77.182
77.000
76.818
74.627
74.534
73.934
73.458
72.118
69.238
63.744
57.004
50.062
42.722
38.897
37.302
36.524
31.936
31.878
31.847
31.542
24.825
24.499
22.815
21.062
19.424
128.347
128.328
128.095
127.859
127.747
127.704
127.553
127.093
126.926
120.798
86.911
86.520
78.804
78.750
141.521
138.943
138.227
137.952
209.562
17.817
17.728
17.713
17.682
15.053
13.218
13.106
12.955
220
200
180
160
140
120
100
80
60
40
20
0
ppm

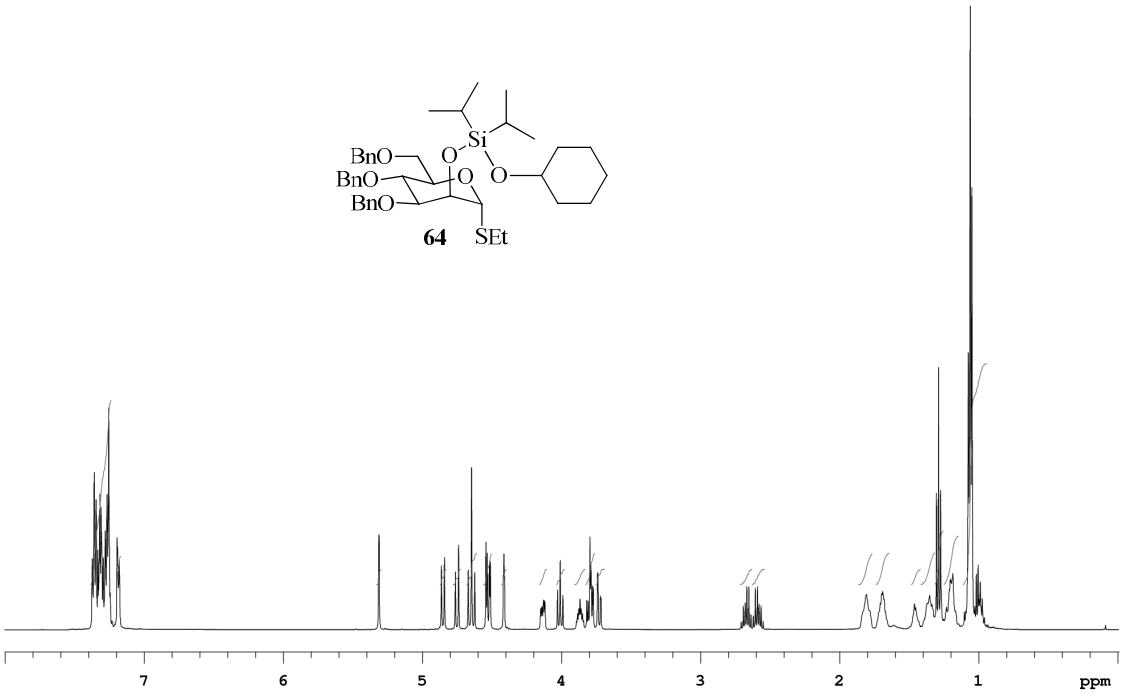
BnO
BnO
BnO
O
Si
O
O
64
SEt
7
6
5
4
3
2
1
ppm

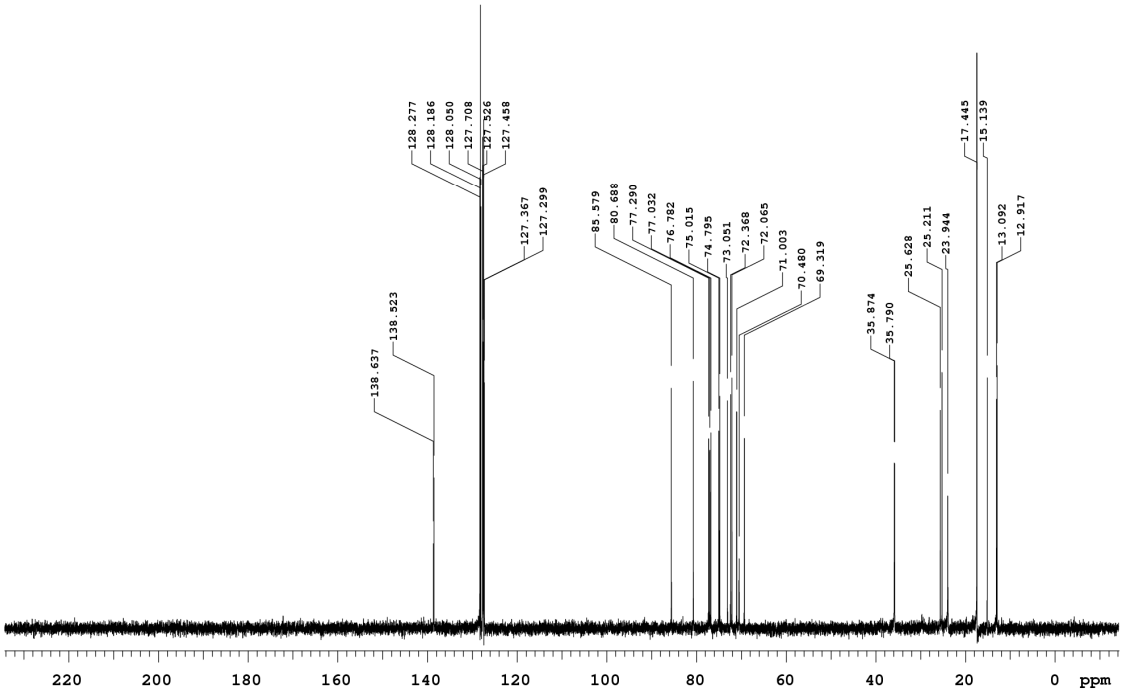
128.277
128.186
128.050
127.708
127.526
127.458
127.367
127.299
138.637
138.523
85.579
80.688
77.290
77.032
76.782
75.015
74.795
73.051
72.368
72.065
71.003
70.480
69.319
35.874
35.790
25.628
25.211
23.944
17.445
15.139
13.092
12.917
220
200
180
160
140
120
100
80
60
40
20
0
ppm

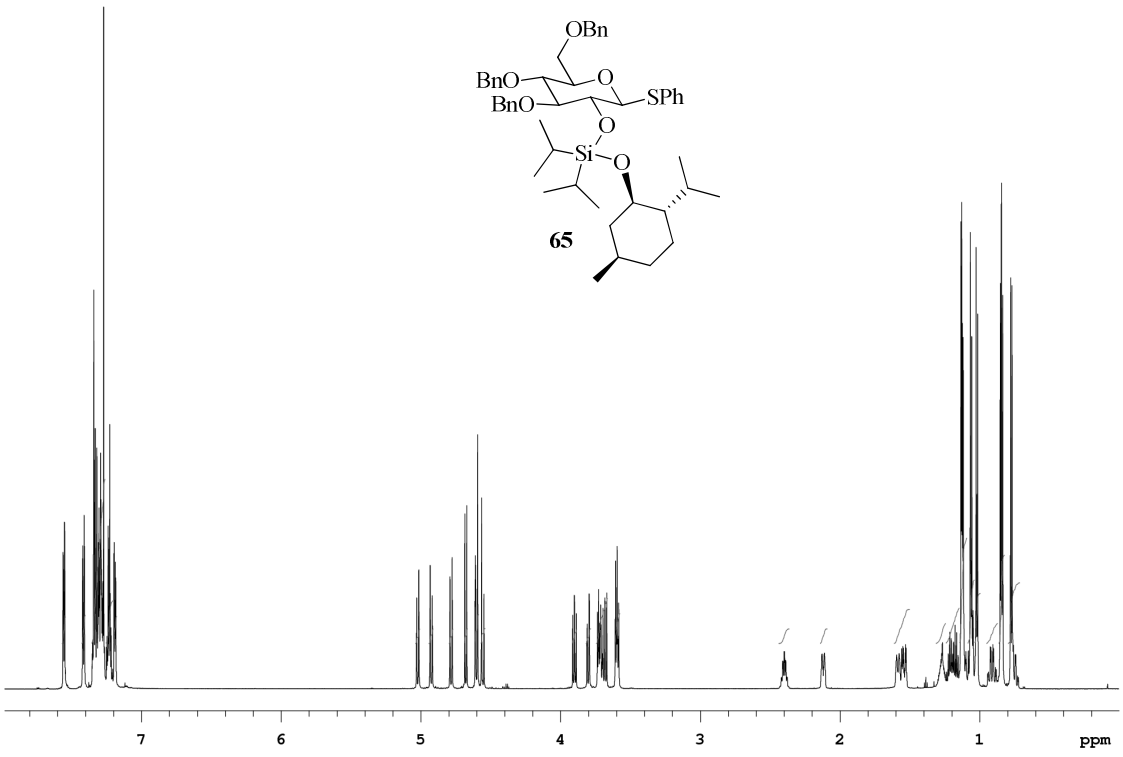
OBn
BnO
BnO
O
SPh
O
Si
O
65
7
6
5
4
3
2
1
ppm

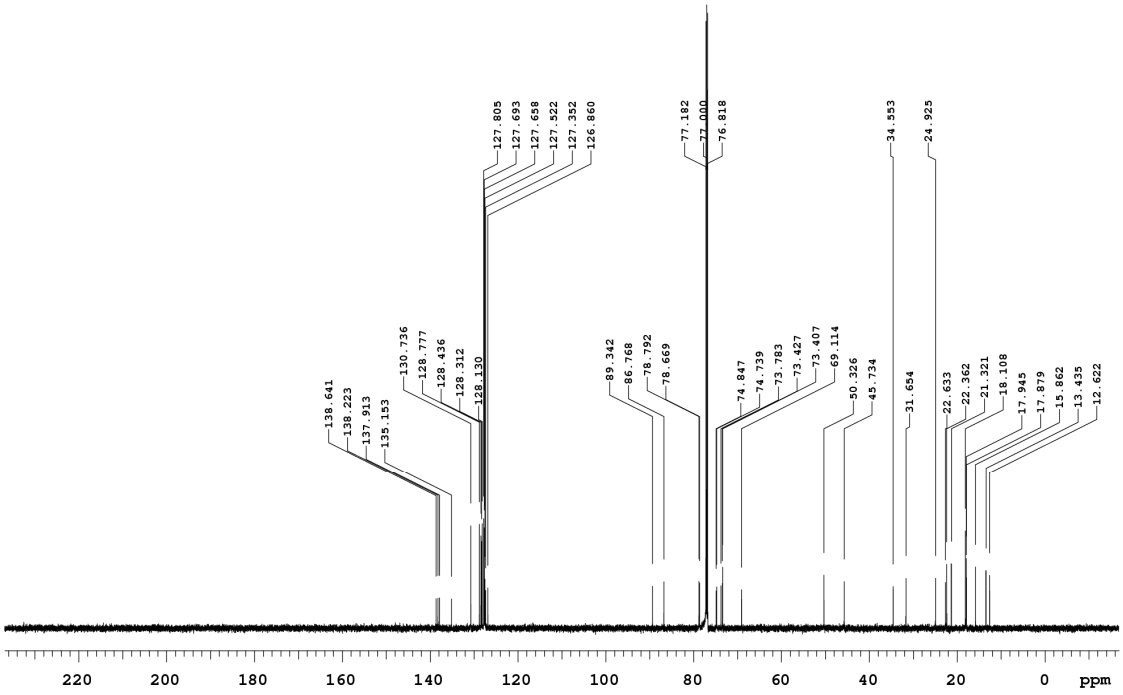
127.805
127.693
127.658
127.522
127.352
126.860
77.182
77.000
76.818
34.553
24.925
138.641
138.223
137.913
135.153
130.736
128.777
128.436
128.312
128.130
89.342
86.768
78.792
78.669
74.847
74.739
73.783
73.427
73.407
69.114
50.326
45.734
31.654
22.633
22.362
21.321
18.108
17.945
17.879
15.862
13.435
12.622
220
200
180
160
140
120
100
80
60
40
20
0
ppm

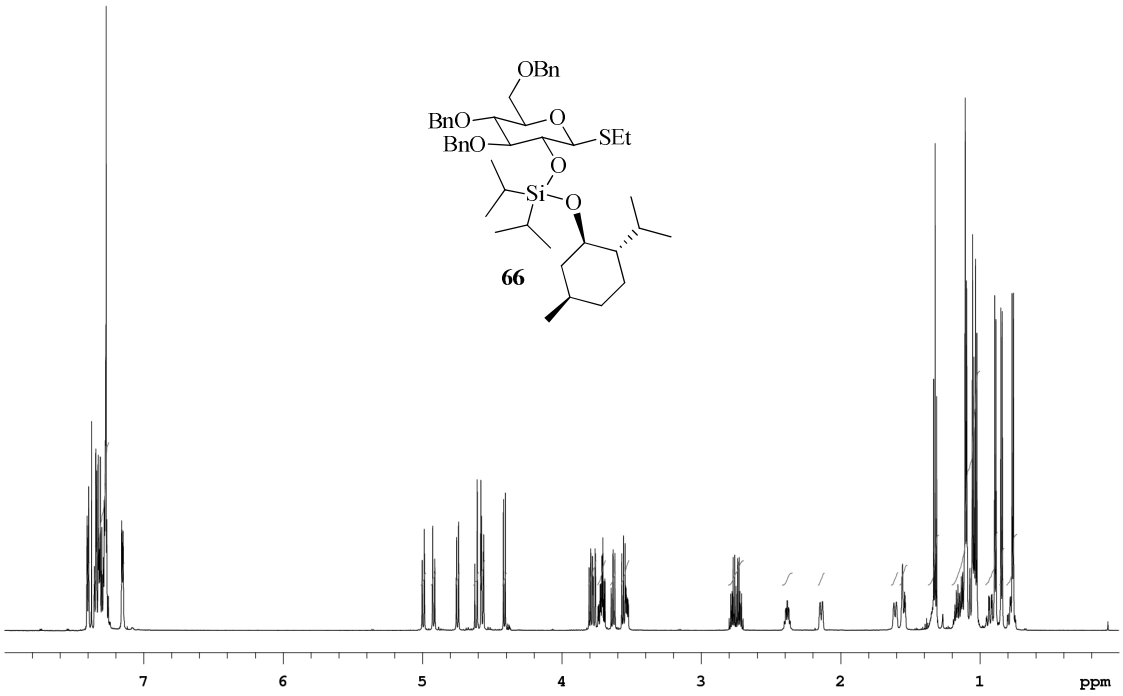
OBn
BnO
BnO
O
SEt
O
Si
O
66
7
6
5
4
3
2
1
ppm

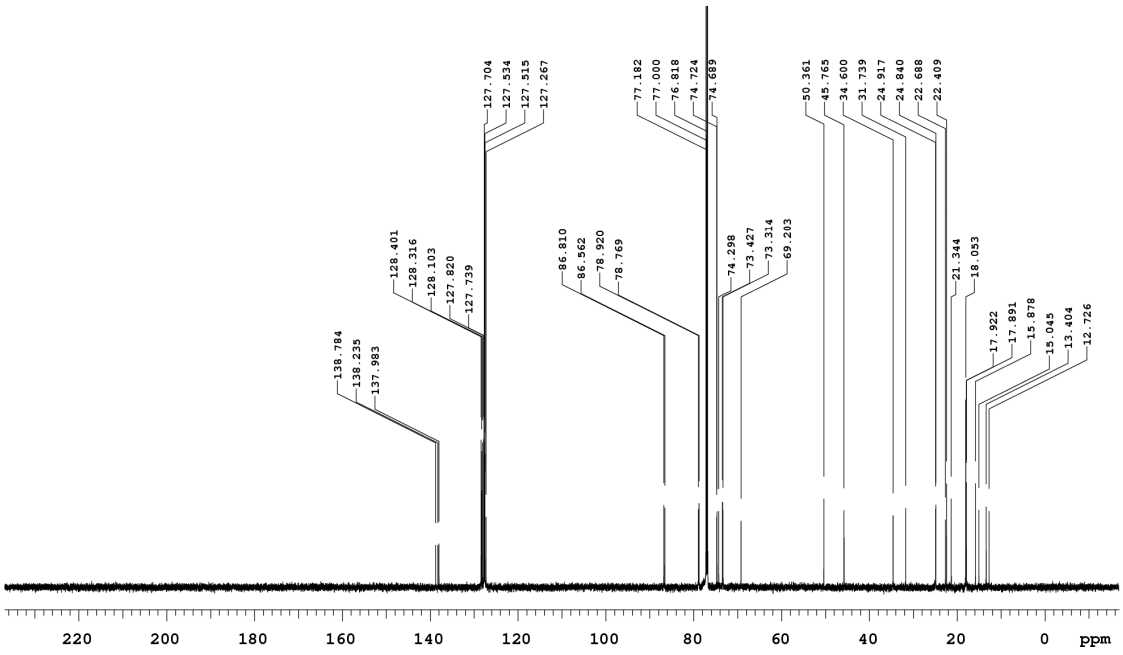
127.704
127.534
127.515
127.267
128.401
128.316
128.103
127.820
127.739
138.784
138.235
137.983
77.182
77.000
76.818
74.724
74.689
86.810
86.562
78.920
78.769
74.298
73.427
73.314
69.203
50.361
45.765
34.600
31.739
24.917
24.840
22.688
22.409
21.344
18.053
17.922
17.891
15.878
15.045
13.404
12.726
220
200
180
160
140
120
100
80
60
40
20
0
ppm

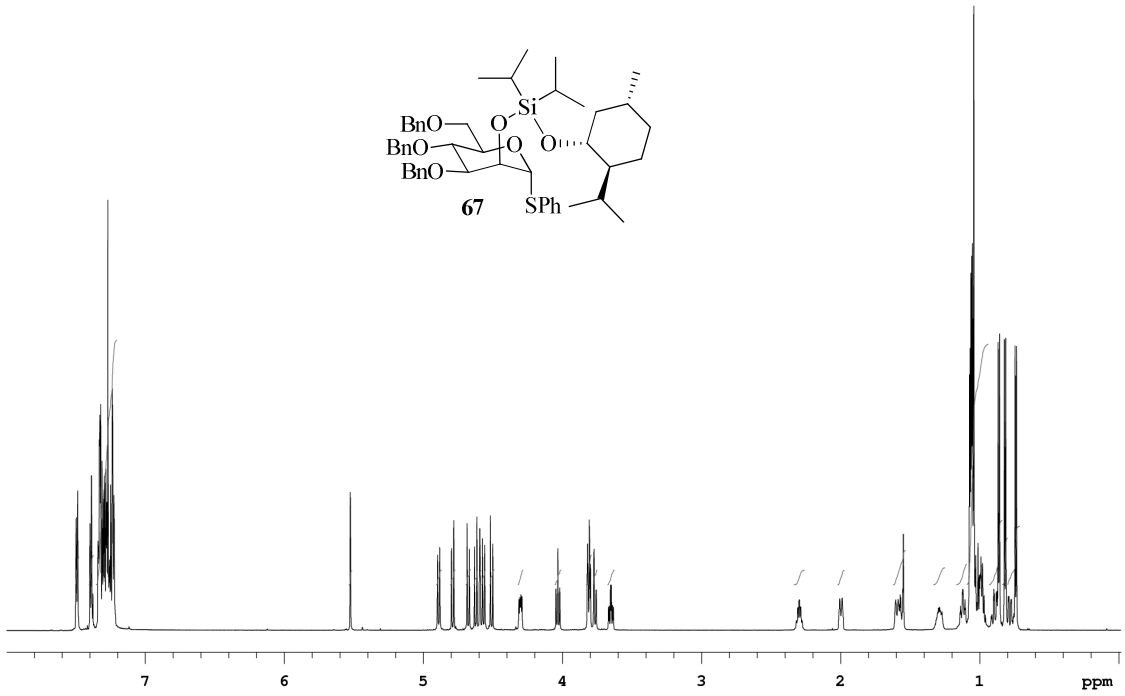
BnO
BnO
BnO
O
Si
O
O
SPh
7
6
5
4
3
2
1
ppm

67

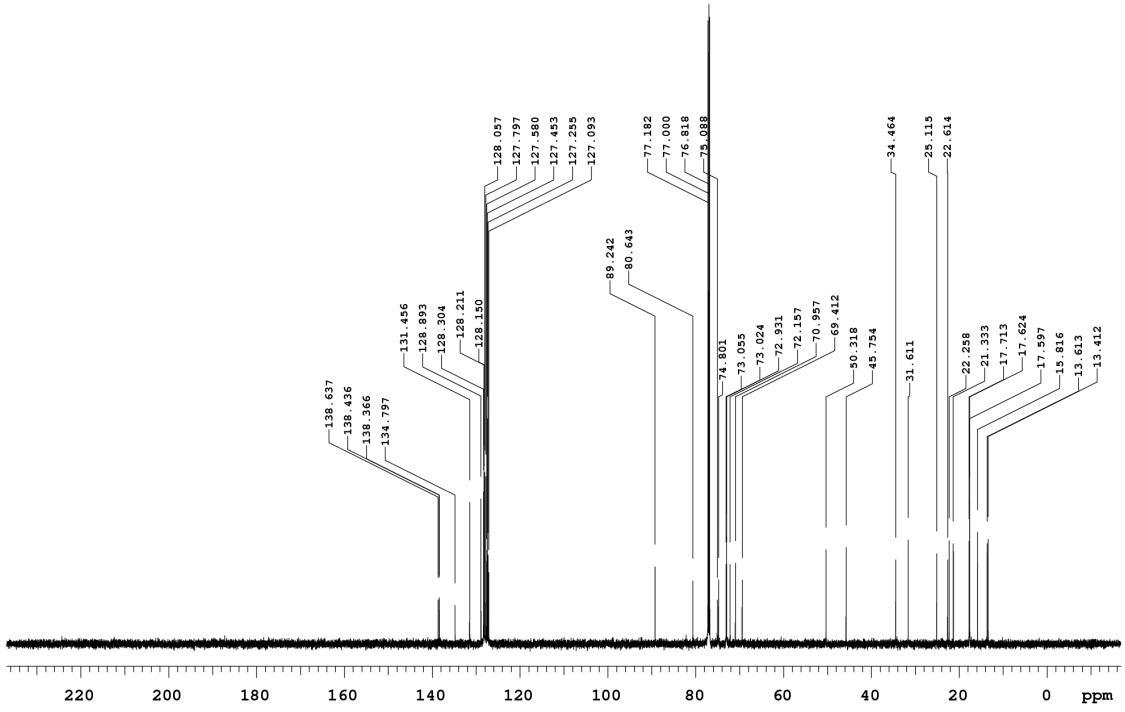
128.057
127.797
127.580
127.453
127.255
127.093
77.182
77.000
76.818
75.088
34.464
25.115
22.614
89.242
80.643
131.456
128.893
128.304
128.211
128.150
74.801
73.055
73.024
72.931
72.157
70.957
69.412
50.318
45.754
31.611
22.258
21.333
17.713
17.624
17.597
15.816
13.613
13.412
138.637
138.436
138.366
134.797
220
200
180
160
140
120
100
80
60
40
20
0
ppm

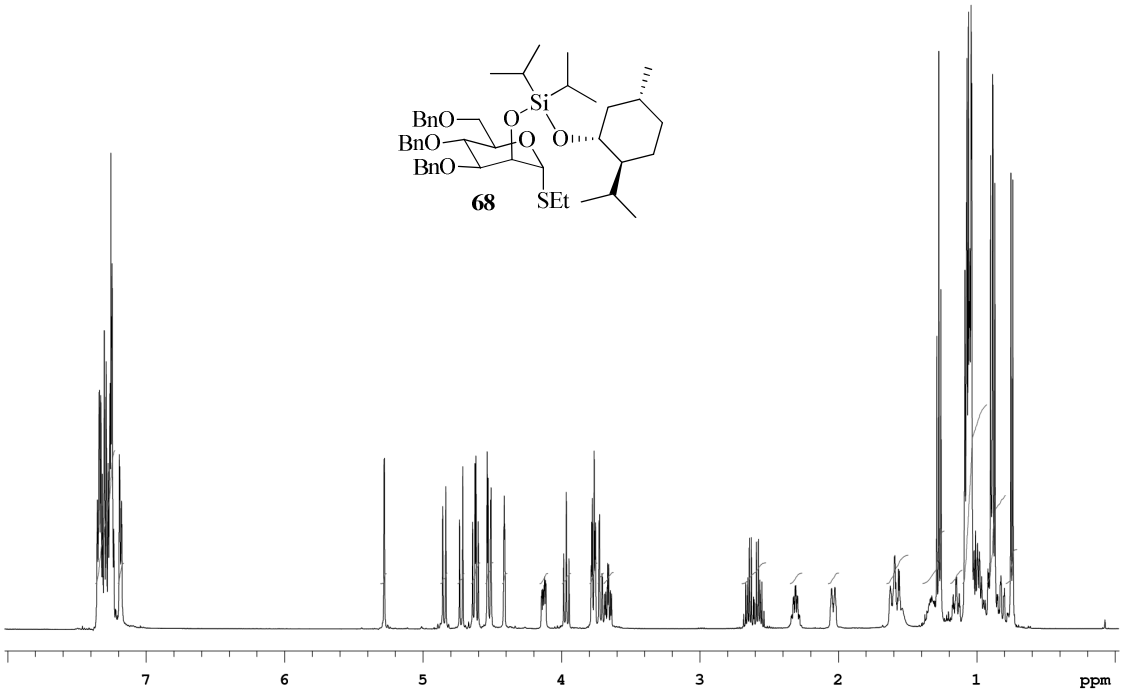
BnO
BnO
BnO
O
Si
O
O
SEt
68
7
6
5
4
3
2
1
ppm

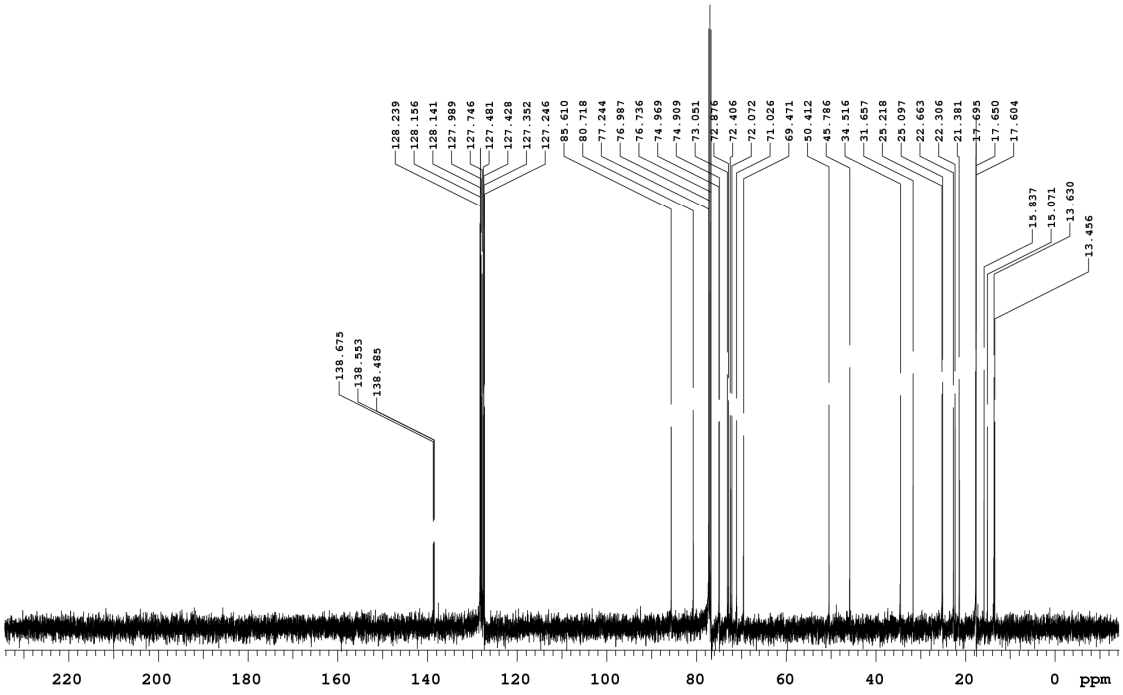
128.239
128.156
128.141
127.989
127.746
127.481
127.428
127.352
127.246
85.610
80.718
77.244
76.987
76.736
74.969
74.909
73.051
72.876
72.406
72.072
71.026
69.471
50.412
45.786
34.516
31.657
25.218
25.097
22.663
22.306
21.381
17.695
17.650
17.604
15.837
15.071
13.630
13.456
138.675
138.553
138.485
220
200
180
160
140
120
100
80
60
40
20
0
ppm

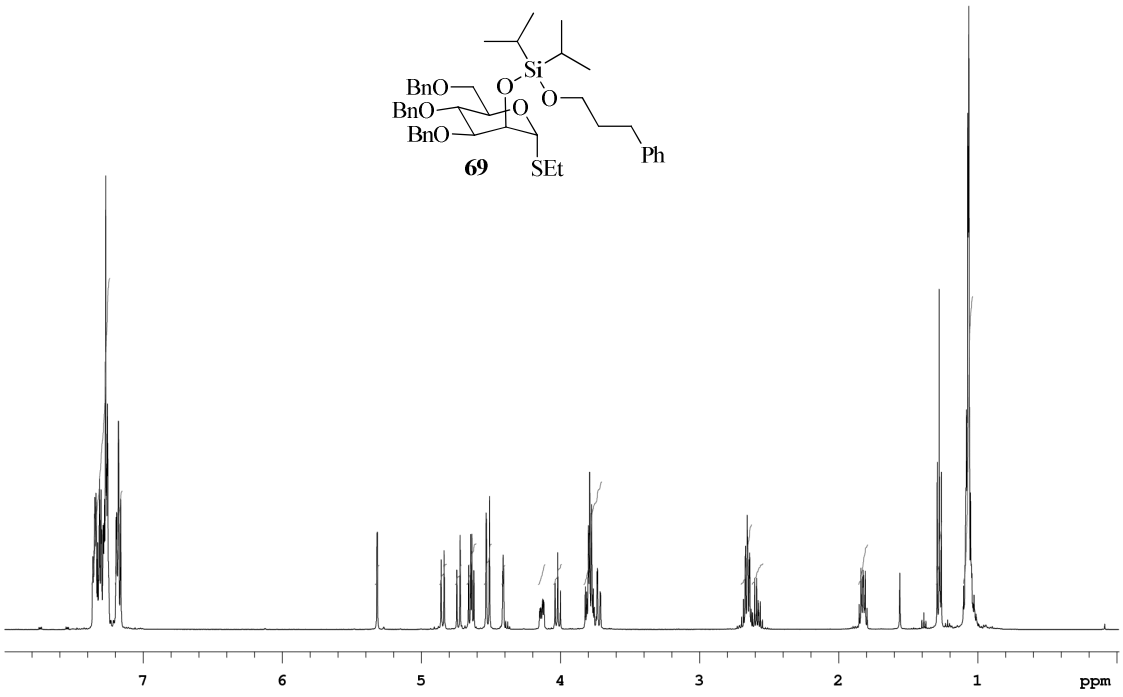
BnO
BnO
BnO
O
Si
O
O
Ph
SEt
69
7
6
5
4
3
2
1
ppm

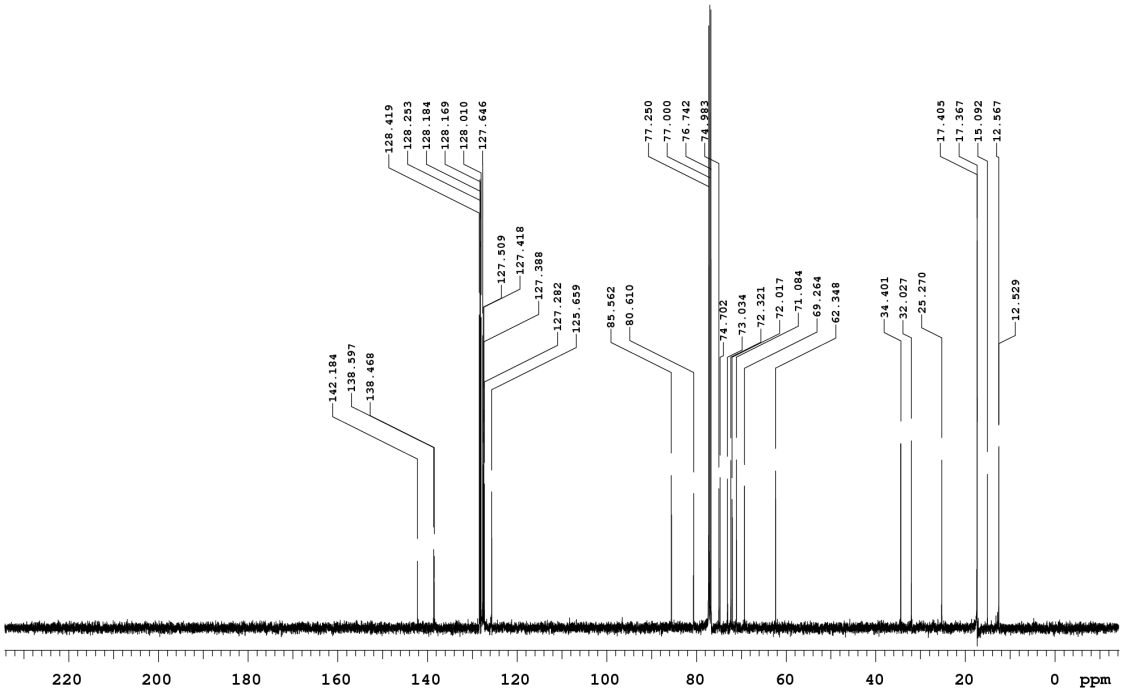
128.419
128.253
128.184
128.169
128.010
127.646
127.509
127.418
127.388
127.282
125.659
142.184
138.597
138.468
85.562
80.610
77.250
77.000
76.742
74.883
74.702
73.034
72.321
72.017
71.084
69.264
62.348
34.401
32.027
25.270
17.405
17.367
15.092
12.567
12.529
220
200
180
160
140
120
100
80
60
40
20
0
ppm

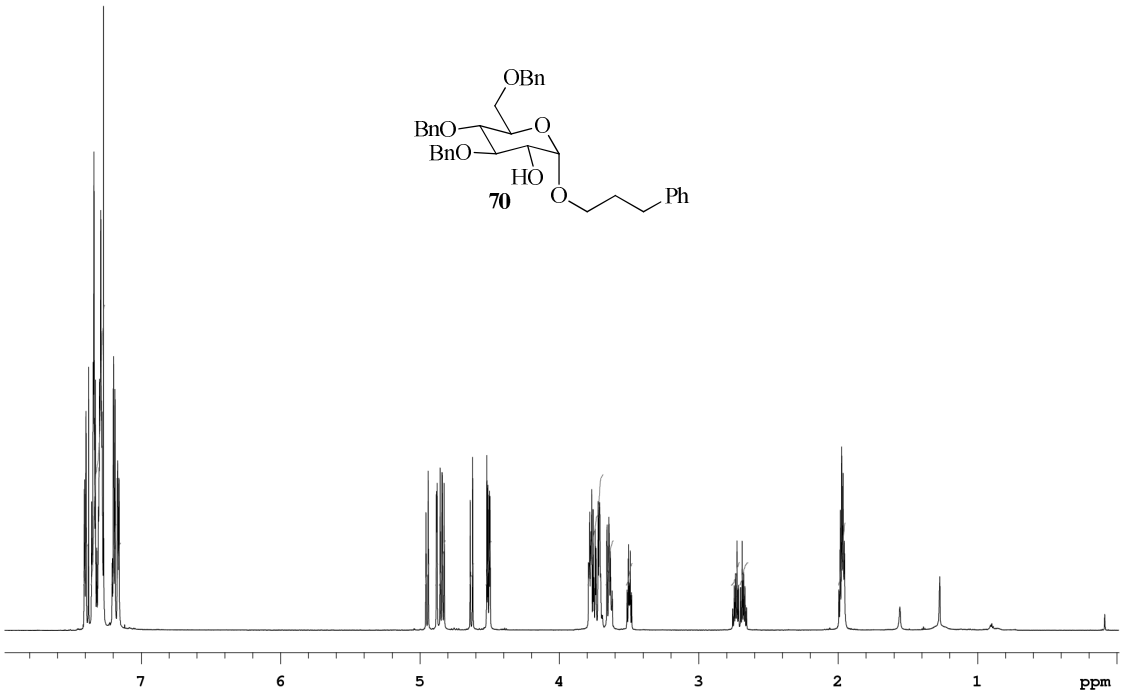
OBn
BnO
O
BnO
HO
O
Ph
70
7
6
5
4
3
2
1
ppm

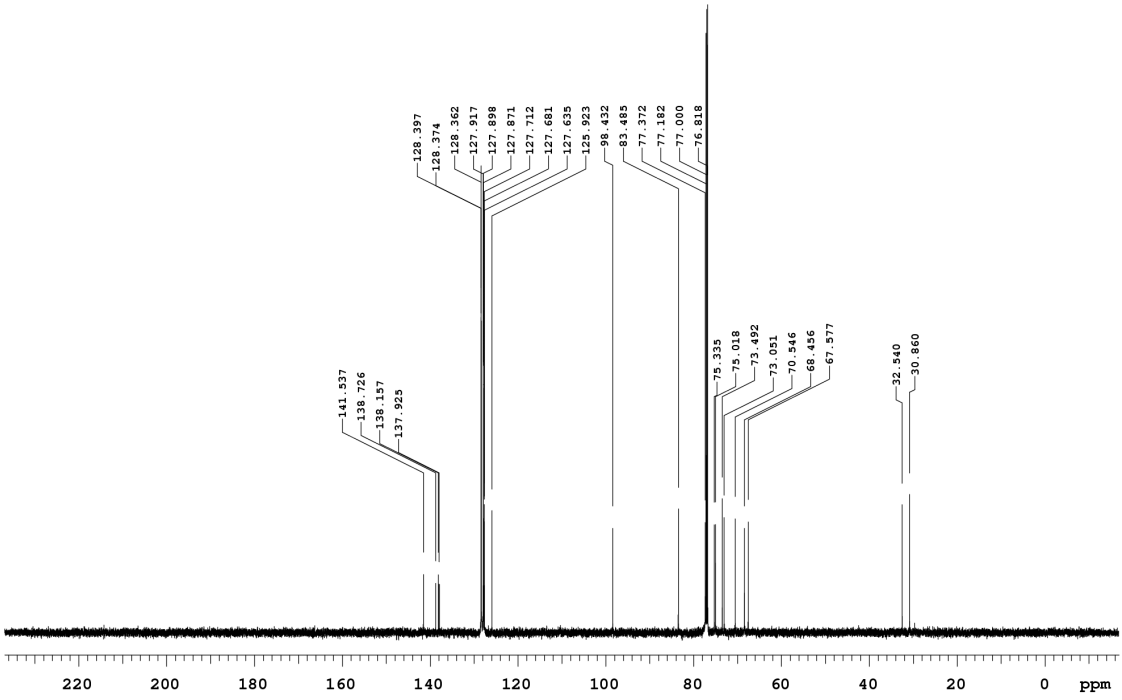
128.397
128.374
128.362
127.917
127.898
127.871
127.712
127.681
127.635
125.923
98.432
83.485
77.372
77.182
77.000
76.818
75.335
75.018
73.492
73.051
70.546
68.456
67.577
32.540
30.860
141.537
138.726
138.157
137.925
220
200
180
160
140
120
100
80
60
40
20
0
ppm

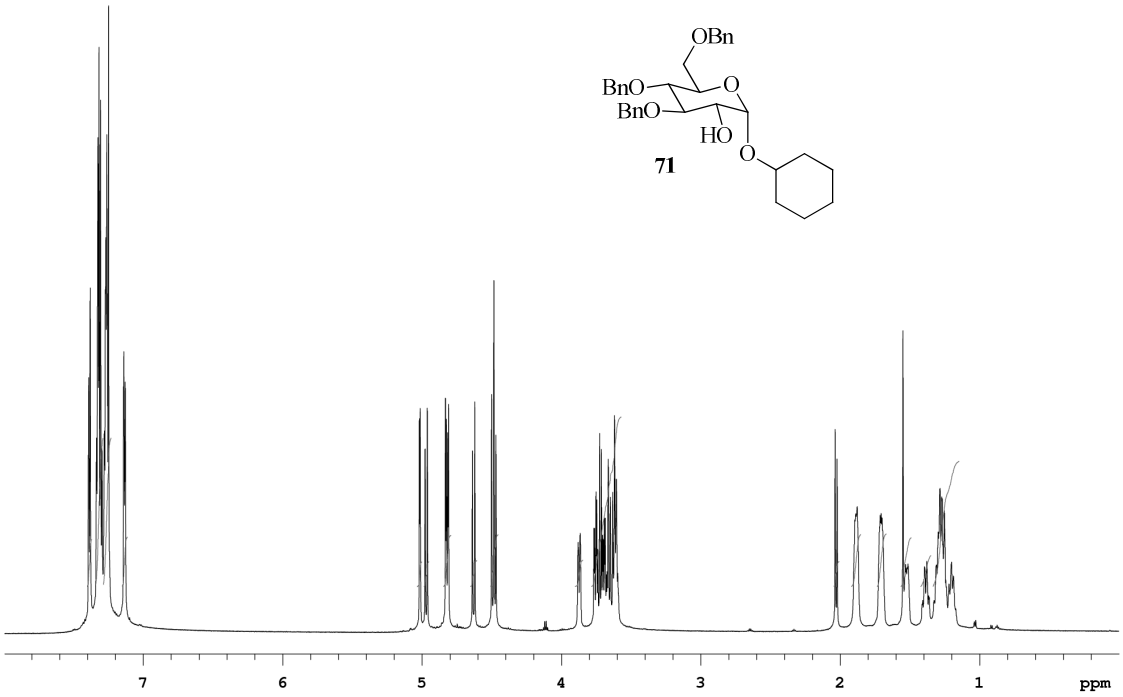
OBn
BnO
O
BnO
HO
O
71
7
6
5
4
3
2
1
ppm

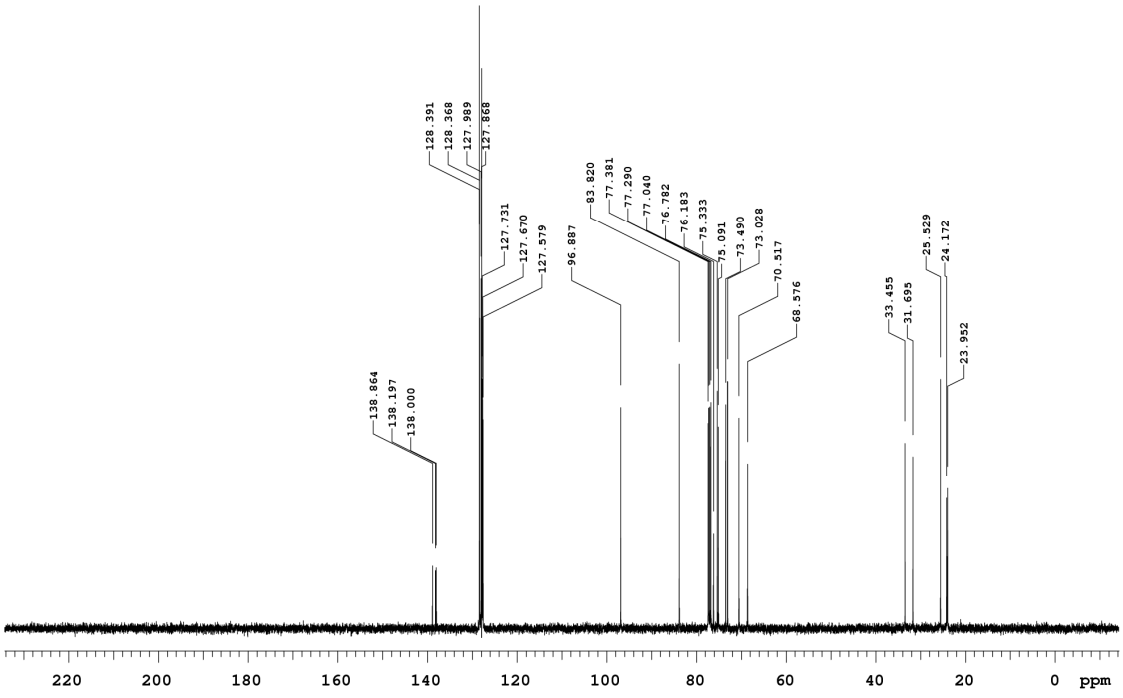
128.391
128.368
127.989
127.868
127.731
127.670
127.579
96.887
83.820
77.381
77.290
77.040
76.782
76.183
75.333
75.091
73.490
73.028
70.517
68.376
138.864
138.197
138.000
33.455
31.695
25.529
24.172
23.952
220
200
180
160
140
120
100
80
60
40
20
0
ppm

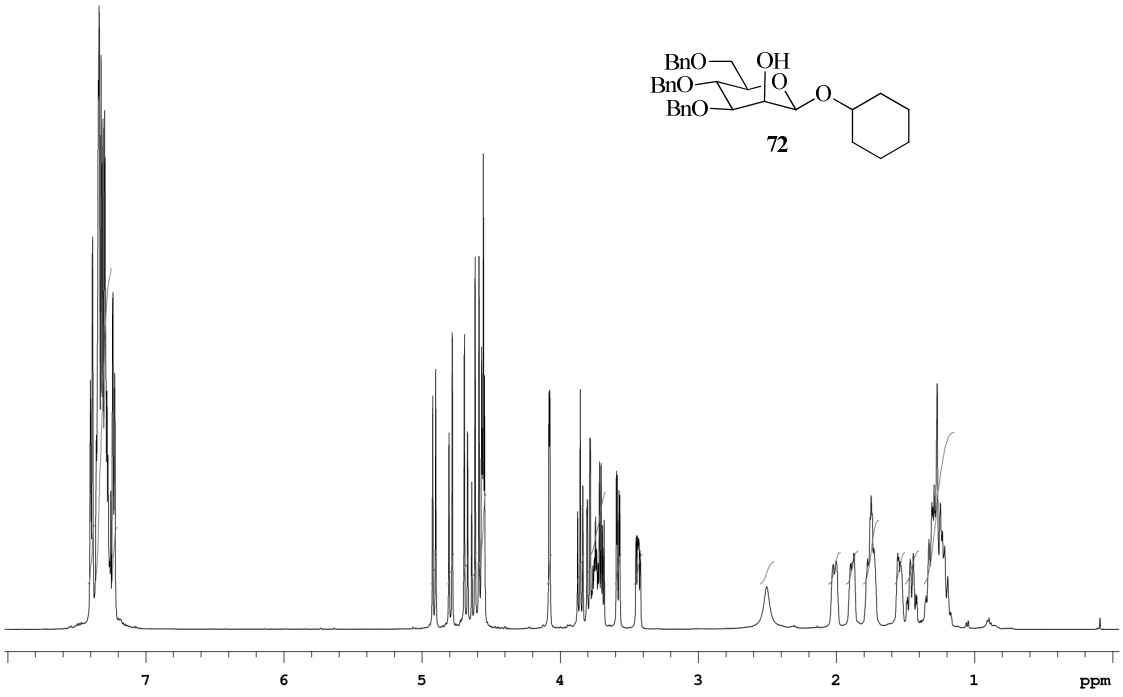
BnO
OH
BnO
O
O
BnO
72
7
6
5
4
3
2
1
ppm

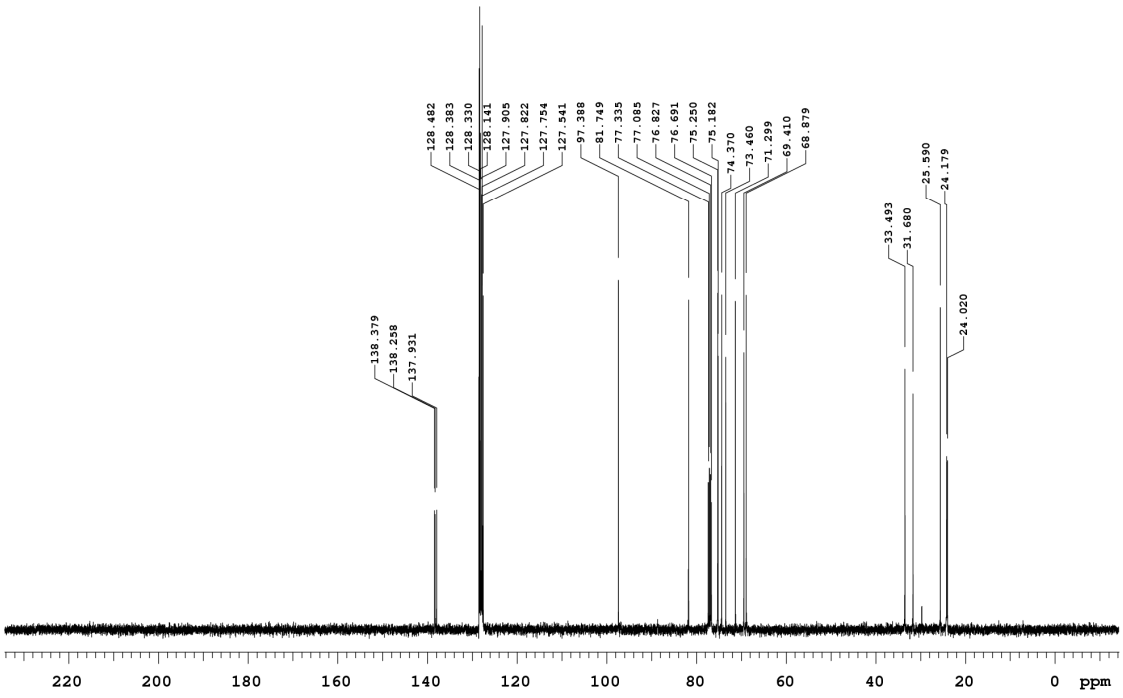
128.482
128.383
128.330
128.141
127.905
127.822
127.754
127.541
97.388
81.749
77.335
77.085
76.827
76.691
75.250
75.182
74.370
73.460
71.299
69.410
68.879
138.379
138.258
137.931
33.493
31.680
25.590
24.179
24.020
220
200
180
160
140
120
100
80
60
40
20
0
ppm

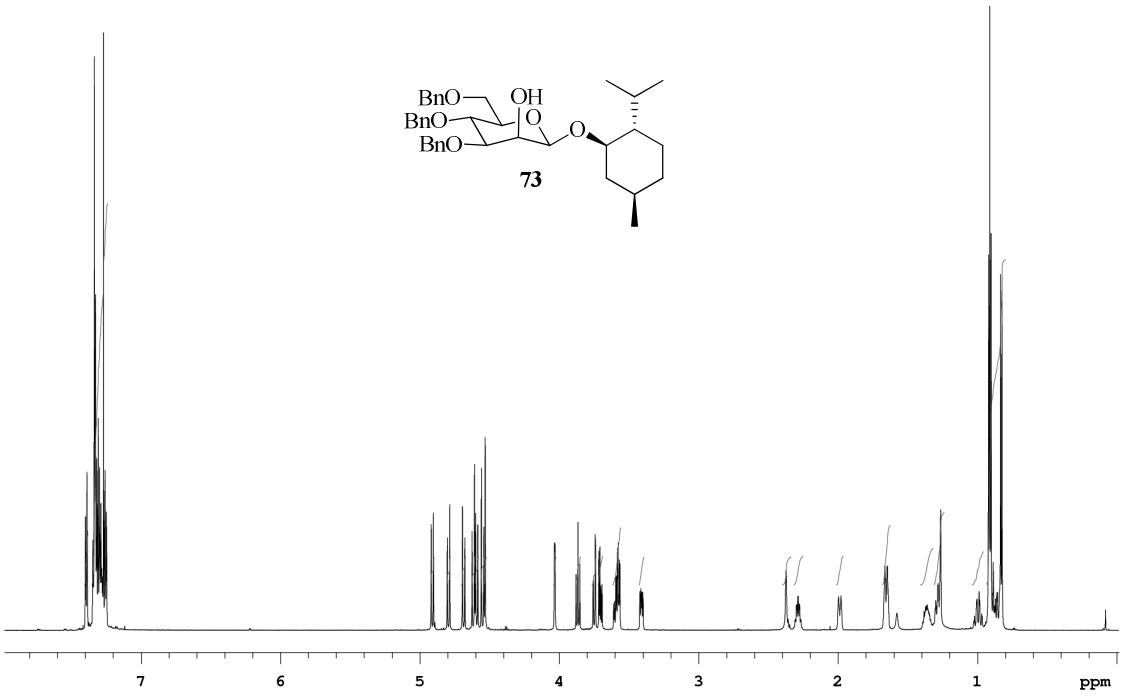
BnO
BnO
BnO
OH
O
O
73
7
6
5
4
3
2
1
ppm

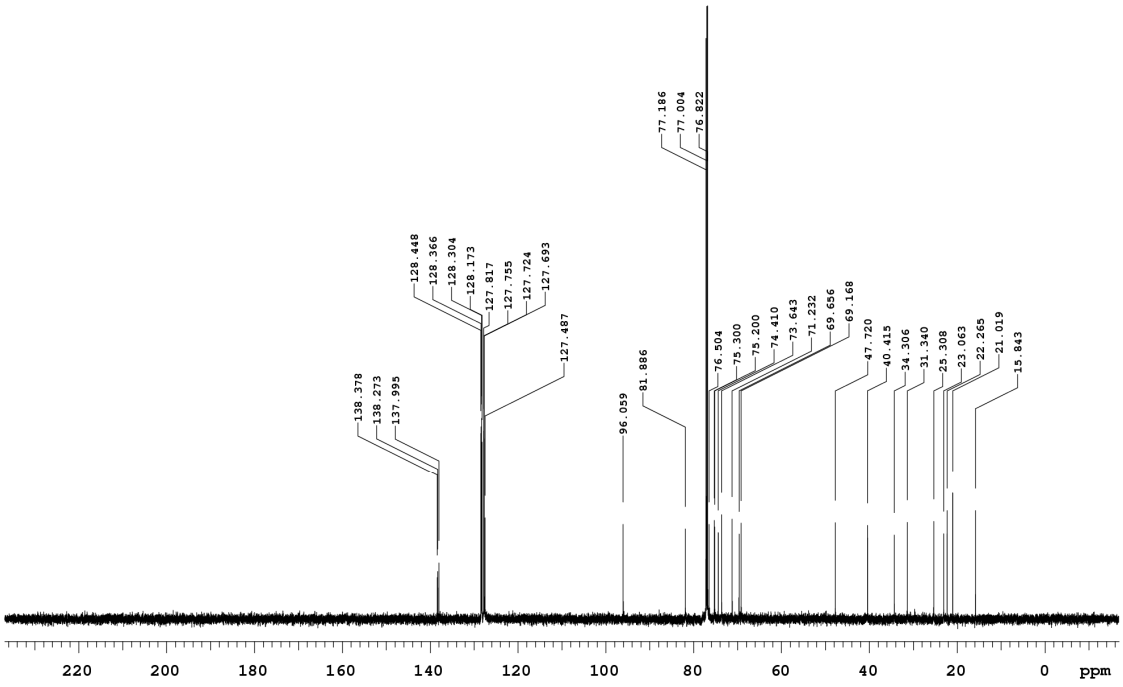
77.186
77.004
76.822
128.448
128.366
128.304
128.173
127.817
127.755
127.724
127.693
127.487
138.378
138.273
137.995
96.059
81.886
76.504
75.300
75.200
74.410
73.643
71.232
69.656
69.168
47.720
40.415
34.306
31.340
25.308
23.063
22.265
21.019
15.843
220
200
180
160
140
120
100
80
60
40
20
0
ppm

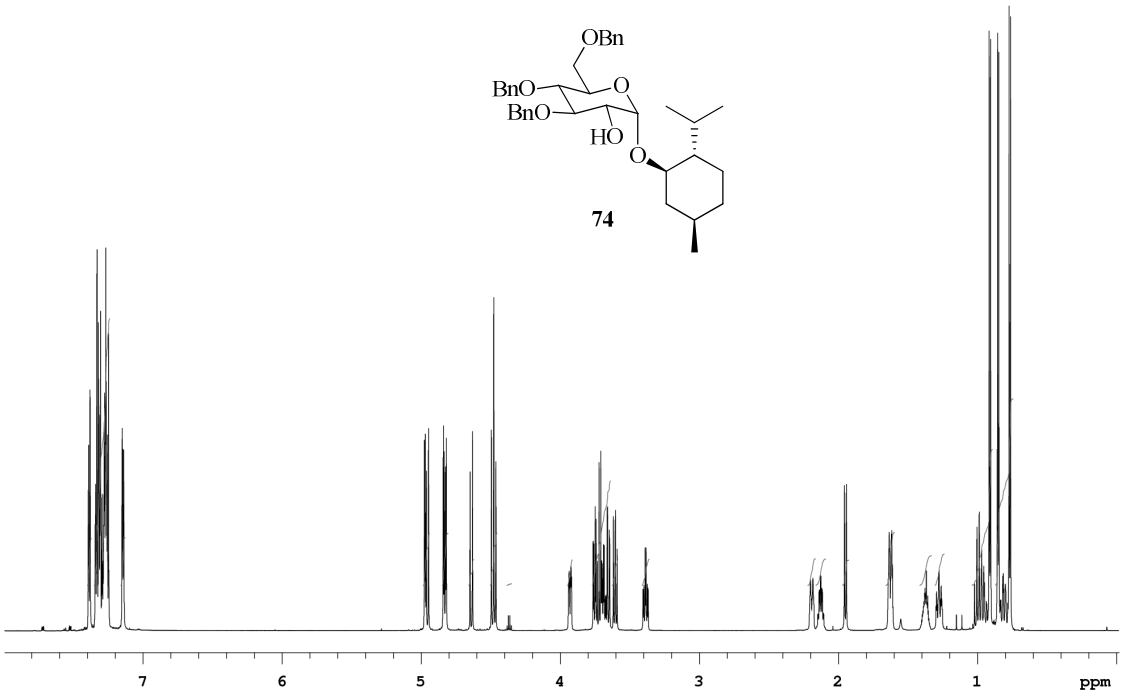
OBn
BnO
O
BnO
HO
O
74
7
6
5
4
3
2
1
ppm

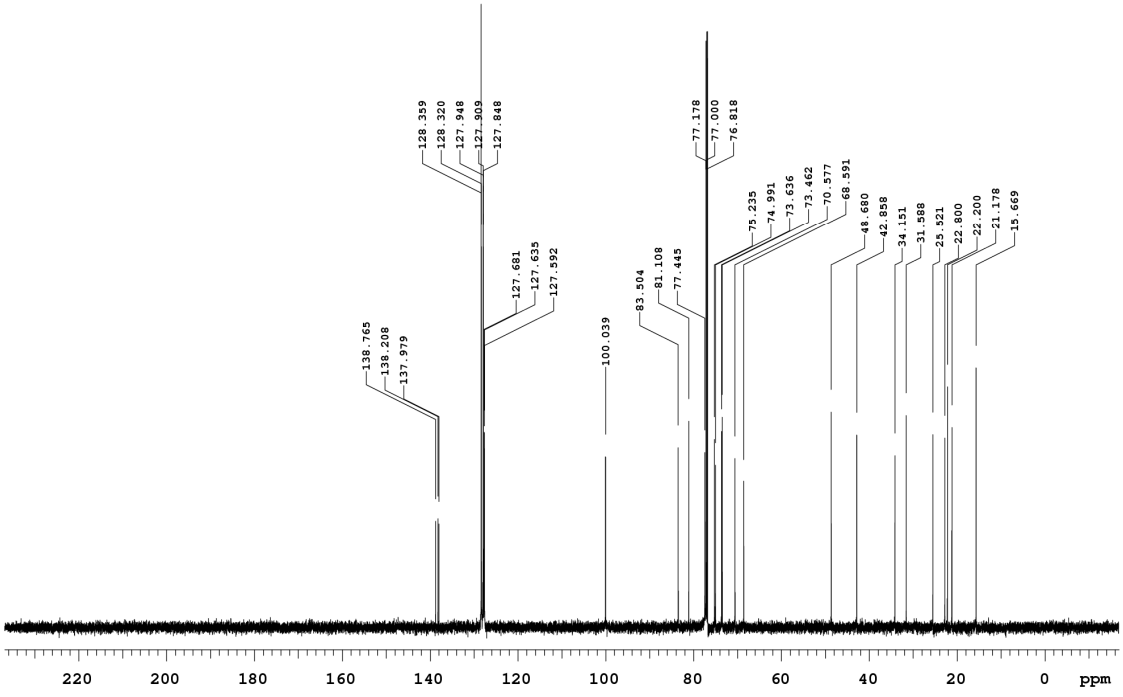
128.359
128.320
127.948
127.909
127.848
127.681
127.635
127.592
138.765
138.208
137.979
100.039
83.504
81.108
77.445
77.178
77.000
76.818
75.235
74.991
73.636
73.462
70.577
68.591
48.680
42.858
34.151
31.588
25.521
22.800
22.200
21.178
15.669
220
200
180
160
140
120
100
80
60
40
20
0
ppm

References

(1) *Natural Products in Chemical Biology*; Civjan, N., Ed.; Wiley, 2012.

(2) Butler, M. S. Natural products to drugs: natural product derived compounds in clinical trials. *Nat. Prod. Rep.* **2005**, *22*, 162–195.

(3) Butler, M. S.; Newman, D. J. Mother Nature's gifts to diseases of man : the impact of natural products on anti-infective, anticholestemics and anticancer drug discovery. In *Natural Products as Drugs Vol. I*; 2008; Vol. 65, pp. 2–44.

(4) Mallinson, J.; Collins, I. Macrocycles in new drug discovery. *Future Med. Chem.* **2012**, *4*, 1409–38.

(5) Marsault, E.; Peterson, M. L. Macrocycles are great cycles: applications, opportunities, and challenges of synthetic macrocycles in drug discovery. *J. Med. Chem.* **2011**, *54*, 1961–2004.

(6) Obrecht, D.; Robinson, J. A.; Bernardini, F.; Bisang, C.; DeMarco, S. J.; Moehle, K.; Gombert, F. O. Recent progress in the discovery of macrocyclic compounds as potential anti-infective therapeutics. *Curr. Med. Chem.* **2009**, *16*, 42–65.

(7) Driggers, E. M.; Hale, S. P.; Lee, J.; Terrett, N. K. The exploration of macrocycles for drug discovery--an underexploited structural class. *Nat. Rev. Drug Discovery* **2008**, *7*, 608–24.

(8) Wessjohann, L. A.; Ruijter, E.; Garcia-Rivera, D.; Brandt, W. What Can a Chemist Learn from Nature′s Macrocycles? A Brief, Conceptual View. *Mol. Diversity* **2005**, *9*, 171–186.

(9) Katz, L.; Ashley, G. W. Translation and protein synthesis: macrolides. *Chem. Rev.* **2005**, *105*, 499–528.

(10) Staunton, J.; Weissman, K. J. Polyketide biosynthesis: a millennium review. *Nat. Prod. Rep.* **2001**, *18*, 380–416.

(11) Schwarzer, D.; Finking, R.; Marahiel, M. A. Nonribosomal peptides: from genes to products. *Nat. Prod. Rep.* **2003**, *20*, 275.

(12) Mortison, J. D.; Sherman, D. H. Frontiers and opportunities in chemoenzymatic synthesis. *J. Org. Chem.* **2010**, *75*, 7041–51.

(13) Kren, V.; Rezanka, T. Sweet antibiotics - the role of glycosidic residues in antibiotic and antitumor activity and their randomization. *FEMS Microbiol. Rev.* **2008**, *32*, 858–89.

(14) Blanchard, S.; Thorson, J. S. Enzymatic tools for engineering natural product glycosylation. *Curr. Opin. Chem. Biol.* **2006**, *10*, 263–71.

(15) Griffith, B. R.; Langenhan, J. M.; Thorson, J. S. "Sweetening" natural products via glycorandomization. *Curr. Opin. Biotechnol.* **2005**, *16*, 622–30.

(16) Jung, S. T.; Lauchli, R.; Arnold, F. H. Cytochrome P450: taming a wild type enzyme. *Curr. Opin. Biotechnol.* **2011**, *22*, 809–17.

(17) Lamb, D. C.; Waterman, M. R.; Kelly, S. L.; Guengerich, F. P. Cytochromes P450 and drug discovery. *Curr. Opin. Biotechnol.* **2007**, *18*, 504–12.

(18) Bernhardt, R. Cytochromes P450 as versatile biocatalysts. *J. Biotechnol.* **2006**, *124*, 128–45.

(19) Auerbach, T.; Bashan, A.; Yonath, A. Ribosomal antibiotics: structural basis for resistance, synergism and selectivity. *Trends Biotechnol.* **2004**, *22*, 570–6.

(20) Schlünzen, F.; Zarivach, R.; Harms, J.; Bashan, a; Tocilj, a; Albrecht, R.; Yonath, a; Franceschi, F. Structural basis for the interaction of antibiotics with the peptidyl transferase centre in eubacteria. *Nature* **2001**, *413*, 814–21.

(21) Auerbach, T.; Mermershtain, I.; Bashan, A.; Davidovich, C.; Rozenberg, H.; Sherman, D. H.; Yonath, A. Structural basis for the antibacterial activity of the 12-membered-ring mono-sugar macrolide methymycin. *Biotechnologia* **2009**, 24–35.

(22) Aldrich, C. C.; Beck, B. J.; Fecik, R. A.; Sherman, D. H. Biochemical investigation of pikromycin biosynthesis employing native penta- and hexaketide chain elongation intermediates. *J. Am. Chem. Soc.* **2005**, *127*, 8441–52.

(23) Borisova, S. A.; Liu, H.-W. Characterization of glycosyltransferase DesVII and its auxiliary partner protein DesVIII in the methymycin/picromycin biosynthetic pathway. *Biochemistry* **2010**, *49*, 8071–84.

(24) Borisova, S. A.; Zhao, L.; Melançon III, C. E.; Kao, C.-L.; Liu, H.-W. Characterization of the glycosyltransferase activity of desVII: analysis of and implications for the biosynthesis of macrolide antibiotics. *J. Am. Chem. Soc.* **2004**, *126*, 6534–5.

(25) Que, L.; Tolman, W. B. Biologically inspired oxidation catalysis. *Nature* **2008**, *455*, 333–40.

(26) Talsi, E. P.; Bryliakov, K. P. Chemo- and stereoselective C-H oxidations and epoxidations/cis-dihydroxylations with H2O2, catalyzed by non-heme iron and manganese complexes. *Coord. Chem. Rev.* **2012**, *256*, 1418–1434.

(27) Newhouse, T.; Baran, P. S. If C-H bonds could talk: selective C-H bond oxidation. *Angew. Chem., Int. Ed.* **2011**, *50*, 3362–74.

(28) Cook, B. R.; Reinert, T. J.; Suslick, K. S. Shape-selective alkane hydroxylation by metalloporphyrin catalysts. *J. Am. Chem. Soc.* **1986**, *108*, 7281–7286.

(29) Desai, L. V; Hull, K. L.; Sanford, M. S. Palladium-catalyzed oxygenation of unactivated sp3 C-H bonds. *J. Am. Chem. Soc.* **2004**, *126*, 9542–3.

(30) Dick, A. R.; Hull, K. L.; Sanford, M. S. A highly selective catalytic method for the oxidative functionalization of C-H bonds. *J. Am. Chem. Soc.* **2004**, *126*, 2300–1.

(31) Neufeldt, S. R.; Sanford, M. S. O-Acetyl Oximes as Transformable Directing Groups for Pd-Catalyzed C-H Bond Functionalization. *Org. Lett.* **2010**, *12*, 532–535.

(32) Stowers, K. J.; Kubota, A.; Sanford, M. S. Nitrate as a redox co-catalyst for the aerobic Pd-catalyzed oxidation of unactivated sp3-C-H bonds. *Chem. Sci.* **2012**, *3*, 3192–3195.

(33) Chen, M. S.; White, M. C. A predictably selective aliphatic C-H oxidation reaction for complex molecule synthesis. *Science* **2007**, *318*, 783–7.

(34) Vermeulen, N. A.; Chen, M. S.; White, M. C. The Fe(PDP)-catalyzed aliphatic C–H oxidation: a slow addition protocol. *Tetrahedron* **2009**, *65*, 3078–3084.

(35) Chen, M. S.; White, M. C. Combined effects on selectivity in Fe-catalyzed methylene oxidation. *Science* **2010**, *327*, 566–71.

(36) Bigi, M. a; Reed, S. a; White, M. C. Directed metal (oxo) aliphatic C-H hydroxylations: overriding substrate bias. *J. Am. Chem. Soc.* **2012**, *134*, 9721–6.

(37) Das, S.; Brudvig, G. W.; Crabtree, R. H. High turnover remote catalytic oxygenation of alkyl groups: how steric exclusion of unbound substrate contributes to high molecular recognition selectivity. *J. Am. Chem. Soc.* **2008**, *130*, 1628–37.

(38) Das, S.; Incarvito, C. D.; Crabtree, R. H.; Brudvig, G. W. Molecular recognition in the selective oxygenation of saturated C-H bonds by a dimanganese catalyst. *Science* **2006**, *312*, 1941–3.

(39) Lee, S.; Fuchs, P. L. Chemospecific chromium[VI] catalyzed oxidation of C-H bonds at -40 °C. *J. Am. Chem. Soc.* **2002**, *124*, 13978–9.

(40) Brodsky, B. H.; Du Bois, J. Oxaziridine-mediated catalytic hydroxylation of unactivated 3° C-H bonds using hydrogen peroxide. *J. Am. Chem. Soc.* **2005**, *127*, 15391–3.

(41) Moreira, R. F.; Wehn, P. M.; Sames, D. Highly Regioselective Oxygenation of C-H Bonds : Diamidomanganese Constructs with Attached Substrates as Catalyst Models. *Angew. Chem., Int. Ed.* **2000**, *39*, 1618–1621.

(42) Sherman, D. H.; Li, S.; Yermalitskaya, L. V; Kim, Y.; Smith, J. A.; Waterman, M. R.; Podust, L. M. The structural basis for substrate anchoring, active site selectivity, and product formation by P450 PikC from Streptomyces venezuelae. *J. Biol. Chem.* **2006**, *281*, 26289–97.

(43) Li, S.; Ouellet, H.; Sherman, D. H.; Podust, L. M. Analysis of transient and catalytic desosamine-binding pockets in cytochrome P-450 PikC from Streptomyces venezuelae. *J. Biol. Chem.* **2009**, *284*, 5723–30.

(44) Li, S.; Podust, L. M.; Sherman, D. H. Engineering and analysis of a self-sufficient biosynthetic cytochrome P450 PikC fused to the RhFRED reductase domain. *J. Am. Chem. Soc.* **2007**, *129*, 12940–1.

(45) Li, S.; Chaulagain, M. R.; Knauff, A. R.; Podust, L. M.; Montgomery, J.; Sherman, D. H. Selective oxidation of carbolide C-H bonds by an engineered macrolide P450 mono-oxygenase. *Proc. Natl. Acad. Sci. U. S. A.* **2009**, *106*, 18463–8.

(46) Parenty, A.; Moreau, X.; Campagne, J.-M. Macrolactonizations in the Total Synthesis of Natural Products. *Chem. Rev.* **2006**, *106*, 911–39.

(47) Parenty, A.; Moreau, X.; Niel, G.; Campagne, J.-M. Update 1 of : Macrolactonizations in the Total Synthesis of Natural Products. *Chem. Rev.* **2012**.

(48) Daly, E. M.; Taylor, R. E. Recent Applications of the Nozaki-Hiyama-Kishi Reaction in Natural Product Synthesis. *Chemtracts* **2007**, *20*, 1–8.

(49) Tang, B.; Bray, C. D.; Pattenden, G. Total synthesis of (+)-intricarene using a biogenetically patterned pathway from (-)-bipinnatin J, involving a novel transannular [5+2] (1,3-dipolar) cycloaddition. *Org. Biomol. Chem.* **2009**, *7*, 4448–57.

(50) Roethle, P. A.; Trauner, D. Expedient synthesis of (+/-)-bipinnatin J. *Org. Lett.* **2006**, *8*, 345–7.

(51) Zhu, W.; Jimenez, M.; Jung, W.-H.; Camarco, D. P.; Balachandran, R.; Vogt, A.; Day, B. W.; Curran, D. P. Streamlined Syntheses of (-)-Dictyostatin, 16-Desmethyl-25,26-dihydrodictyostatin, and 6-epi-16-Desmethyl-25,26-dihydrodictyostatin. *J. Am. Chem. Soc.* **2010**, *132*, 9175–9187.

(52) Mohapatra, D. K.; Das, P. P.; Pattanayak, M. R.; Gayatri, G.; Sastry, G. N.; Yadav, J. S. Protecting-Group Directed Stereoselective Intramolecular Nozaki-Hiyama-Kishi Reaction: A Concise and Efficient Total Synthesis of Amphidinolactone A. *Eur. J. Org. Chem.* **2010**, *2010*, 4775–4784.

(53) Venkatraman, L.; Aldrich, C. C.; Sherman, D. H.; Fecik, R. A. Formal total synthesis of the polyketide macrolactone narbonolide. *J. Org. Chem.* **2005**, *70*, 7267–72.

(54) Venkatraman, L.; Salomon, C. E.; Sherman, D. H.; Fecik, R. A. Total Synthesis of Narbonolide and Biotransformation to Pikromycin. *J. Org. Chem.* **2006**, *71*, 9853–9856.

(55) Gradillas, A.; Perez-Castells, J. Synthesis of Natural Products Containing Macrocycles by Alkene Ring-Closing Metathesis. In *Metathesis in Natural Product Synthesis*; 2010; pp. 149–182.

(56) Gradillas, A.; Pérez-Castells, J. Macrocyclization by ring-closing metathesis in the total synthesis of natural products: reaction conditions and limitations. *Angew. Chem., Int. Ed.* **2006**, *45*, 6086–101.

(57) Kanada, R. M.; Itoh, D.; Nagai, M.; Niijima, J.; Asai, N.; Mizui, Y.; Abe, S.; Kotake, Y. Total synthesis of the potent antitumor macrolides pladienolide B and D. *Angew. Chem., Int. Ed.* **2007**, *46*, 4350–5.

(58) Day, J.; Blake, A.; Moody, C. An Improved Synthesis of Resorcylic Acid Macrolactone Inhibitors of Hsp90. *Synlett* **2009**, *2009*, 1567–1570.

(59) Day, J. E. H.; Sharp, S. Y.; Rowlands, M. G.; Aherne, W.; Workman, P.; Moody, C. J. Targeting the Hsp90 chaperone: synthesis of novel resorcylic acid macrolactone inhibitors of Hsp90. *Chem. Eur. J.* **2010**, *16*, 2758–63.

(60) Yu, M.; Wang, C.; Kyle, A. F.; Jakubec, P.; Dixon, D. J.; Schrock, R. R.; Hoveyda, A. H. Synthesis of macrocyclic natural products by catalyst-controlled stereoselective ring-closing metathesis. *Nature* **2011**, *479*, 88–93.

(61) Oppolzer, W.; Radinov, R. N. Synthesis of (R)-(-)-muscone by an asymmetrically catalyzed macrocyclization of an ω-alkynal. *J. Am. Chem. Soc.* **1993**, *115*, 1593–1594.

(62) Colby, E. A.; O'Brien, K. C.; Jamison, T. F. Total Syntheses of Amphidinolides T1 and T4 via Catalytic, Stereoselective, Reductive Macrocyclizations. *J. Am. Chem. Soc.* **2005**, *127*, 4297–4307.

(63) Knapp-Reed, B.; Mahandru, G. M.; Montgomery, J. Access to macrocyclic endocyclic and exocyclic allylic alcohols by nickel-catalyzed reductive cyclization of ynals. *J. Am. Chem. Soc.* **2005**, *127*, 13156–7.

(64) Malik, H. A.; Baxter, R. D.; Montgomery, J. Nickel-Catalyzed Reductive Couplings and Cyclizations. In *Catalysis without Precious Metals*; 2010; pp. 181–212.

(65) Chrovian, C. C.; Knapp-Reed, B.; Montgomery, J. Total synthesis of aigialomycin D: surprising chemoselectivity dependence on alkyne structure in nickel-catalyzed cyclizations. *Org. Lett.* **2008**, *10*, 811–814.

(66) Malik, H. A.; Sormunen, G. J.; Montgomery, J. A general strategy for regiocontrol in nickel-catalyzed reductive couplings of aldehydes and alkynes. *J. Am. Chem. Soc.* **2010**, *132*, 6304–5.

(67) Mahandru, G. M.; Liu, G.; Montgomery, J. Ligand-dependent scope and divergent mechanistic behavior in nickel-catalyzed reductive couplings of aldehydes and alkynes. *J. Am. Chem. Soc.* **2004**, *126*, 3698–9.

(68) Malik, H. A.; Chaulagain, M. R.; Montgomery, J. Cooperativity of regiochemistry control strategies in reductive couplings of propargyl alcohols and aldehydes. *Org. Lett.* **2009**, *11*, 5734–7.

(69) Liu, P.; Montgomery, J.; Houk, K. N. Ligand Steric Contours To Understand the Effects of N-Heterocyclic Carbene Ligands on the Reversal of Regioselectivity in Ni-Catalyzed Reductive Couplings of Alkynes and Aldehydes. *J. Am. Chem. Soc.* **2011**, *133*, 6956–6959.

(70) Shareef, A.-R.; Sherman, D. H.; Montgomery, J. Nickel-Catalyzed Regiodivergent Approach to Macrolide Motifs. *Chem. Sci.* **2012**, *3*, 892–895.

(71) Chong, J.; Heuft, M.; Rabbat, P. Solvent effects on the monobromination of α,ω-diols: A convenient preparation of ω-bromoalkanols. *J. Org. Chem.* **2000**, *65*, 5837–8.

(72) Rossi, R. Highly Stereoselective Synthesis of (Z)-9,11-Dodecadien-1-yl Acetate; A Sex Pheromone Component of Diparopsis castanea Hmps. *Synthesis* **1981**, 359–361.

(73) Green, N.; Jacobson, M.; Henneberry, T. J.; Kishaba, A. N. Insect Sex Attractants. VI. 7-Dodecen-1-ol Acetates and Congeners. *J. Med. Chem.* **1967**, *10*, 533–535.

(74) Baxter, R. D.; Montgomery, J. Mechanistic study of nickel-catalyzed ynal reductive cyclizations through kinetic analysis. *J. Am. Chem. Soc.* **2011**, *133*, 5728–31.

(75) Galli, C.; Mandolini, L. The Role of Ring Strain on the Ease of Ring Closure of Bifunctional Chain Molecules. *Eur. J. Org. Chem.* **2000**, 3117–3125.

(76) Illuminati, G.; Mandolini, L. Ring Closure Reactions of Bifunctional Chain Molecules. *Acc. Chem. Res.* **1981**, *14*, 95–102.

(77) Liebman, J. F.; Greenberg, A. A Survey of Strained Organic Molecules. *Chem. Rev.* **1976**, *76*, 311–365.

(78) Casadei, M. A.; Calli, C.; Mandolini, L. Ring-Closure Reactions. 22. Kinetics of Cyclization of Diethyl (ω-Bromoalkyl)malonates in the Range of 4- to 21-Membered Rings. Role of Ring Strain. *J. Am. Chem. Soc.* **1984**, *106*, 1051–1056.

(79) Hansen, E. C.; Lee, D. Ring closing enyne metathesis: control over mode selectivity and stereoselectivity. *J. Am. Chem. Soc.* **2004**, *126*, 15074–80.

(80) Nicolaou, K. C.; Hale, C. R. H.; Ebner, C.; Nilewski, C.; Ahles, C. F.; Rhoades, D. Synthesis of macroheterocycles through intramolecular oxidative coupling of furanoid β-ketoesters. *Angew. Chem., Int. Ed.* **2012**, *51*, 4726–30.

(81) Dwek, R. A. Glycobiology: Toward Understanding the Function of Sugars. *Chem. Rev.* **1996**, *96*, 683–720.

(82) Langenhan, J. M.; Griffith, B. R.; Thorson, J. S. Neoglycorandomization and Chemoenzymatic Glycorandomization: Two Complementary Tools for Natural Product Diversification. *J. Nat. Prod.* **2005**, *68*, 1696–1711.

(83) Hong, J. S. J.; Park, S. H.; Choi, C. Y.; Sohng, J. K.; Yoon, Y. J. New olivosyl derivatives of methymycin/pikromycin from an engineered strain of Streptomyces venezuelae. *FEMS Microbiol. Lett.* **2004**, *238*, 391–9.

(84) Langenhan, J. M.; Peters, N. R.; Guzei, I. A.; Hoffmann, F. M.; Thorson, J. S. Enhancing the anticancer properties of cardiac glycosides by neoglycorandomization. *Proc. Natl. Acad. Sci. U. S. A.* **2005**, *102*, 12305–10.

(85) Kazunobu, T.; Tatsuta, K. Recent Progress in O-Glycosylation Methods and Its Application to Natural Products Synthesis. *Chem. Rev.* **1993**, *93*, 1503–1531.

(86) Koenigs, W.; Knorr, E. Ueber einige Derivate des Traubensuckers und der Galactose. *Ber. Dtsch. Chem. Ges.* **1901**, *34*, 957–981.

(87) Crich, D.; Sun, S. Formation of β-Mannopyanosides of Primary Alcohols Using the Sulfoxide Method. *J. Org. Chem.* **1996**, *61*, 4506–4507.

(88) Crich, D.; Sun, S. Are Glycosyl Triflates Intermediates in the Sulfoxide Glycosylation Method? A Chemical and 1H , 13C , and 19F NMR Spectroscopic Investigation. *J. Am. Chem. Soc.* **1997**, *119*, 11217–11223.

(89) Jung, K.-H.; Müller, M.; Schmidt, R. R. Intramolecular O-Glycoside Bond Formation. *Chem. Rev.* **2000**, *100*, 4423–4442.

(90) Barresi, F.; Hindsgaul, O. Synthesis of β-Mannopyranosides by Intramolecular Aglycon Delivery. *J. Am. Chem. Soc.* **1991**, *113*, 9376–9377.

(91) Barresi, F.; Hindsgaul, O. Improved Synthesis of β-Mannopyranosides by Intramolecular Aglycon Delivery. *Synlett* **1992**, 759–761.

(92) Ito, Y.; Ohnishi, Y.; Ogawa, T.; Nakahara, Y. Highly Optimized β-Mannosylation via p-Methoxybenzyl Assisted Intramolecular Aglycon Delivery. *Synlett* **1998**, 1102–1104.

(93) Bols, M. Intramolecular Glycosidation: Stereocontrolled Synthesis of α-Glucosides from a 2-O-Alkoxysilyl Thioglucoside. *Acta Chem. Scand.* **1993**, *47*, 829–834.

(94) Bols, M. Stereocontrolled synthesis of α-glucosides by intramolecular glycosidation. *J. Chem. Soc., Chem. Commun.* **1992**, 913.

(95) Bols, M. Application of intramolecular glycosidation to the stereocontrolled synthesis of disaccharides containing α-gluco and α-galacto linkages. *J. Chem. Soc., Chem. Commun.* **1993**, 791.

(96) Bols, M. Efficient stereocontrolled glycosidation of secondary sugar hydroxyls by silicon tethered intramolecular glycosidation. *Tetrahedron* **1993**, *49*, 10049–10060.

(97) Bols, M. Synthesis of Kojitriose using Silicon-Tethered Glycosidation. *Acta Chem. Scand.* **1996**, *50*, 931–937.

(98) Stork, G.; Kim, G. Stereocontrolled synthesis of disaccharides via the temporary silicon connection. *J. Am. Chem. Soc.* **1992**, *114*, 1087–1088.

(99) Stork, G.; La Clair, J. J.; Clair, J. J. La Stereoselective Synthesis of β-Mannopyranosides via the Temporary Silicon Connection Method. *J. Am. Chem. Soc.* **1996**, *118*, 247–248.

(100) Lorenz, C.; Schubert, U. An Efficient Catalyst for the Conversion of Hydrosilanes to Alkoxysilanes. *Chem. Ber.* **1995**, *128*, 1267–1269.

(101) Ito, H.; Watanabe, A.; Sawamura, M. Versatile dehydrogenative alcohol silylation catalyzed by Cu(I)-phosphine complex. *Org. Lett.* **2005**, *7*, 1869–71.

(102) Fujihara, T.; Semba, K.; Terao, J.; Tsuji, Y. Copper-catalyzed hydrosilylation with a bowl-shaped phosphane ligand: preferential reduction of a bulky ketone in the presence of an aldehyde. *Angew. Chem., Int. Ed.* **2010**, *49*, 1472–6.

(103) Lipshutz, B. H.; Noson, K.; Chrisman, W.; Lower, A. Asymmetric Hydrosilylation of Aryl Ketones Catalyzed by Copper Hydride Complexed by Nonracemic Biphenyl Ligands. *J. Am. Chem. Soc.* **2003**, *125*, 8779–8789.

(104) Appella, D. H.; Moritani, Y.; Shintani, R.; Ferreira, E. M.; Buchwald, S. L. Asymmetric Conjugate Reduction of α,β-Unsaturated Esters Using a Chiral Phosphine-Copper Catalyst. *J. Am. Chem. Soc.* **1999**, *121*, 9473–9474.

(105) Jurkauskas, V.; Sadighi, J. P.; Buchwald, S. L. Conjugate Reduction of α,β-Unsaturated Carbonyl Compounds Catalyzed by a Copper Carbene Complex. *Org. Lett.* **2003**, *5*, 2417–20.

(106) Mankad, N. P.; Laitar, D. S.; Sadighi, J. P. Synthesis, Structure, and Alkyne Reactivity of a Dimeric (Carbene)copper(I) Hydride. *Organometallics* **2004**, *23*, 3369–3371.

(107) Díez-González, S.; Nolan, S. P. Copper, Silver, and Gold Complexes in Hydrosilylation Reactions. *Acc. Chem. Res.* **2008**, *41*, 349–358.

(108) Kaur, H.; Zinn, F. K.; Stevens, E. D.; Nolan, S. P. (NHC)Cu1 (NHC = N-Heterocyclic Carbene) Complexes as Efficient Catalysts for the Reduction of Carbonyl Compounds. *Organometallics* **2004**, *23*, 1157–1160.

(109) Díez-González, S.; Kaur, H.; Zinn, F. K.; Stevens, E. D.; Nolan, S. P. A simple and efficient copper-catalyzed procedure for the hydrosilylation of hindered and functionalized ketones. *J. Org. Chem.* **2005**, *70*, 4784–96.

(110) Diez-Gonzalez, S.; Scott, N. M.; Nolan, S. P. Cationic Copper(I) Complexes as Efficient Precatalysts for the Hydrosilylation of Carbonyl Compounds. *Organometallics* **2006**, *25*, 2355–2358.

(111) Díez-González, S.; Stevens, E. D.; Scott, N. M.; Petersen, J. L.; Nolan, S. P. Synthesis and characterization of [Cu(NHC)2]X complexes: catalytic and mechanistic studies of hydrosilylation reactions. *Chem. Eur. J.* **2008**, *14*, 158–168.

(112) Sirol, S.; Courmarcel, J.; Mostefai, N.; Riant, O. Efficient Enantioselective Hydrosilylation of Ketones Catalyzed by Air Stable Copper Fluoride−Phosphine Complexes. *Org. Lett.* **2001**, *3*, 4111–4113.

(113) Anzai, Y.; Li, S.; Chaulagain, M. R.; Kinoshita, K.; Kato, F.; Montgomery, J.; Sherman, D. H. Functional analysis of MycCI and MycG, cytochrome P450 enzymes involved in biosynthesis of mycinamicin macrolide antibiotics. *Chem. Biol.* **2008**, *15*, 950–9.

(114) Kobierski, M. E.; Kim, S.; Murthi, K. K.; Iyer, R. S.; Salomon, R. G. Synthesis of a Pyrazole Isostere of Pyrroles Formed by the Reaction of the ε-Amino Groups of Protein Lysyl Residues with Levuglandin E2. *J. Org. Chem.* **1994**, *59*, 6044–6050.

(115) Shim, S. C.; Hwang, J.-T. Intramolecular Reductive Cyclization of Aldehydes and Ketones with Alkynes Promoted by Samaraium(II) Iodide. *Tetrahedron Lett.* **1990**, *31*, 4765–4768.

(116) Csuk, R.; Niesen, A.; Tschuch, G.; Moritz, G. Synthesis of a natural insect repellent isolated from thrips. *Tetrahedron* **2004**, *60*, 6001–6004.

(117) Oppolzer, W.; Radinov, R. N.; El-Sayed, E. Catalytic asymmetric synthesis of macrocyclic (E)-allylic alcohols from omega-alkynals via intramolecular 1-alkenylzinc/aldehyde additions. *J. Org. Chem.* **2001**, *66*, 4766–70.

(118) Takagi, R.; Igata, N.; Yamamoto, K.; Kojima, S. Zirconium-catalyzed chemoselective methylalumination of ethers, amines, and sulfides bearing two terminal alkenyl groups. *J. Organomet. Chem.* **2011**, *696*, 1556–1564.

(119) Hopf, H.; Krueger, A. Synthesis of Cyclo-1,3,-dien-5-ynes. *Chem. Eur. J.* **2001**, *7*, 4378–4385.

(120) Yang, P.-Y.; Liu, K.; Ngai, M. H.; Lear, M. J.; Wenk, M. R.; Yao, S. Q. Activity-based proteome profiling of potential cellular targets of Orlistat--an FDA-approved drug with anti-tumor activities. *J. Am. Chem. Soc.* **2010**, *132*, 656–66.

(121) Callam, C. S.; Lowary, T. L. Synthesis and Conformational Investigation of Methyl 4α-Carba- D -arabinofuranosides. *J. Org. Chem.* **2001**, *66*, 8961–8972.

(122) Düffels, A.; Green, L. G.; Ley, S. V; Miller, A. D. Synthesis of high-mannose type neoglycolipids: active targeting of liposomes to macrophages in gene therapy. *Chem. Eur. J.* **2000**, *6*, 1416–30.